Functional characterisation of the ClpP1P2/Clp-ATPase complex of the ADEP producer *Streptomyces hawaiiensis* NRRL 15010 *in vitro* and elucidation of the self-resistance mechanism

Dissertation

der Mathematisch-Naturwissenschaftlichen Fakultät

der Eberhard Karls Universität Tübingen

zur Erlangung des Grades eines

Doktors der Naturwissenschaften

(Dr. rer. nat.)

vorgelegt von

Frau Laura Reinhardt

aus Böblingen

Tübingen

2021

Gedruckt mit Genehmigung der Mathematisch-Naturwissenschaftlichen Fakultät der Eberhard Karls Universität Tübingen.

Tag der mündlichen Qualifikation:	15.06.2021
Dekan:	Prof. Dr. Thilo Stehle
1. Berichterstatter:	Prof. Dr. Heike Brötz-Oesterhelt
2. Berichterstatter:	Prof. Dr. Karl Forchhammer

TABLE OF CONTENT

Summary

The caseinolytic protease Clp, highly conserved in eubacteria and eukaryotes, degrades misfolded proteins as well as short-lived regulatory factors by targeted proteolysis. The Clp degradation machinery consists of two stacked heptameric rings, forming the secluded degradation chamber and hexameric Clp-ATPases, which regulate proteolysis by recognising, unfolding and translocating substrates into the proteolytic chamber (Yu and Houry, 2007). The proteolytic core ClpP is tightly regulated by its cognate Clp-ATPases, thereby protecting the cells from unspecific, Clp-ATPase-independent protease activity. Acyldepsipeptides (ADEPs), produced by *Streptomyces hawaiiensis* NRRL 15010 (Thomy et al., 2019), dysregulate ClpP in a dual mode of action. ADEPs bind to the same hydrophobic pockets as the Clp-ATPases on the one hand, inhibiting the physiological functions of ClpP and on the other hand conferring an independent protease activity to the tetradecameric barrel of the peptidase by opening the axial pores and allosterically activating the catalytic triads (Kirstein et al., 2009, Lee et al., 2010, Li et al., 2010, Gersch et al., 2015, Famulla et al., 2016, Pan et al., 2019, Sass et al., 2011, Silber et al., 2020b). In the current PhD project the *Streptomyces hawaiiensis* housekeeping Clp peptidase was studied and found to consist of a heteromeric ClpP1P2 complex with distinct but complementary functions. The ADEP-sensitive ClpP1 is the main propeptide processor of itself and ClpP2 and confers activity to the mixed ClpP1P2 complex. Contrariwise, the ADEP-insensitive ClpP2 is proteolytically inactive but interacts with the Clp-ATPases ClpX, ClpC1 and ClpC2 for the degradation of the natural substrates ClgR and PopR, as well as the model substrates casein (ß- and fluorogenic α-casein) and GFP-ssrA. In the presence of ADEP1, the Clp-ATPase mediated degradation of natural and model substrates is not abrogated, but even stimulated, revealing a third mechanism of ADEP action by the concomitant binding of ADEP1 and the Clp-ATPases to opposite sides of the ClpP1P2 barrel. Thus, the physiological function of the *Streptomyces* Clp protease in the presence of ADEP1 is not inhibited. Rather, the data indicate that unspecific protease activity by homomeric ClpP1 and heteromeric ClpP1P2 complexes are the ADEP mode of killing in *Streptomyces*. Previously, a sixth *clpP* gene was discovered downstream of the ADEP-biosynthetic gene cluster, designated $clpP_{ADEP}$, which encodes a Clp peptidase that functions as an ADEP resistance factor (Thomy et al., 2019). The current PhD project reveals molecular

insights, how a Clp peptidase mediates producer self-protection against ADEP. *In vitro* substrate degradation experiments in combination with interaction studies revealed a dual mechanism of resistance mediated by $ClpP_{ADEP}$. To protect the cells from unspecific, Clp-ATPase-independent protease activity by ADEP-activated ClpP1 and/or ClpP1P2, $ClpP_{ADEP}$ interacts with ClpP1 and forms lower oligomeric complexes (presumably dimers and/or trimers), thereby inhibiting the formation of ClpP1 homo-tetradecamers and ClpP1P2 hetero-tetradecamers.

Given that ClpP is essential for viability in *Streptomyces* (Viala et al., 2000), the physiological function of the housekeeping ClpP1P2 protease has to be replaced. Experiments employing the two ADEP-insensitive Clp peptidases $ClpP_{ADEP}$ and ClpP2 in Clp-ATPase mediated substrate degradation experiments illustrated that $ClpP_{ADEP}P2$ in association with ClpX can degrade the natural substrates ClgR and PopR. Additionally, $ClpC1P_{ADEP}P2$ successfully hydrolysed the model substrate ß-casein, demonstrating the formation of active ClpC1/ClpX-$P_{ADEP}P2$ complexes *in vitro*. Furthermore, the ClpP2 mutant proteins $ClpP2_{S131A}$ and $ClpP2_{hp}$ were utilised in combination with wild-type $ClpP_{ADEP}$ for the ClpC1-mediated degradation of ß-casein, analysing the catalytic activity and Clp-ATPase/ClpP interactions of the $ClpP_{ADEP}P2$ complex. Those experiments indicate that $ClpP_{ADEP}$ exhibits proteolytic activity in the $ClpP_{ADEP}P2$ complex, thereby functioning as an ADEP-insensitive replacement of the ADEP-sensitive ClpP1, whereas ClpP2 remains the sole interaction partner for the Clp-ATPases.

Zusammenfassung

Die caseinolytische Protease Clp ist in Pro-und Eukaryonten hoch-konserviert und für den gezielten Abbau von fehlgefalteten Proteinen sowie spezifischen Transkriptionsfaktoren zuständig. Clp besteht aus zwei Komponenten: der Peptidase ClpP, die für die katalytische Aktivität des Komplexes verantwortlich ist sowie den Clp-ATPasen, welche eine regulatorische Funktion durch das Erkennen, Entfalten und Einfädeln der Substrate in die proteolytische Kammer von ClpP ausüben. Die Clp Peptidase besteht aus zwei heptameren Ringen, die sich zu einer einer tetradekameren Fassstruktur assemblieren, in deren Inneren sich die 14 katalytischen Triaden (Ser-His-Asp) befinden (Yu and Houry, 2007). Die Clp-ATPasen kontrollieren die proteolytische Aktivität von ClpP, um einen selektiven Proteinabbau zu gewährleisten und so die

Zelle zu schützen. Acyldepsipeptide, die von *Streptomyces hawaiiensis* NRRL 15010 produziert werden (Thomy et al., 2019), deregulieren ClpP durch einen dualen Wirkmechanismus. Zum einen binden ADEPs an die gleichen hydrophoben Bindestellen wie die Clp-ATPasen, wodurch die physiologische Funktion der Clp Protease inhibiert wird (Kirstein et al., 2009, Gersch et al., 2015, Famulla et al., 2016, Pan et al., 2019). Zum anderen verleiht die Bindung von ADEP der Clp Peptidase eine Clp-ATPasen-unabhängige proteolytische Aktivität durch das Öffnen der Eingangsporen zur proteolytischen Kammer und einer allosterische Aktivierung der katalytischen Triaden (Lee et al., 2010, Li et al., 2010, Sass et al., 2011, Gersch et al., 2015, Pan et al., 2019, Silber et al., 2020b). In *Streptomyces hawaiiensis* besteht der physiologisch aktive, proteolytische Komplex aus den beiden ClpP Isoformen ClpP1 und ClpP2, und kann nach Assoziation mit den Partner-Clp-ATPasen ClpX, ClpC1 und ClpC2 *in vitro* sowohl natürliche Substrate, wie ClgR und PopR, als auch Modellsubstrate wie Casein und GFP-ssrA abbauen. Beide ClpP Isoformen besitzen im heteromeren ClpP1P2 Komplex unterschiedliche und sich ergänzende Funktionen. Während ClpP1 dem gemischten Komplex proteolytische Aktivität verleiht und sowohl sich selbst als auch ClpP2 prozessiert, ist ClpP2 proteolytisch inaktiv und für die Interaktion mit den Partner Clp-ATPasen ClpX, ClpC1 und ClpC2 zuständig. In Anwesenheit von ADEP1 wird der Clp-ATPasen vermittelte Substratabbau von ClpP1P2 nicht inhibiert, sondern eher stimuliert, wodurch ein neuartiger, dritter Wirkmechanismus von ADEP entdeckt werden konnte. Dieser Wirkmechanismus kann durch die gleichzeitige Bindung von ADEP1 und den Clp-ATPasen an gegenüberliegende Seiten des ClpP1P2 Komplexes erklärt werden. Somit wird die physiologische Funktion von ClpP in Streptomyzeten in Anwesenheit von ADEP1 nicht inhibiert. Insgesamt deutet die Datenlage daraufhin, dass ein unspezifischer Proteinabbau durch ADEP-aktivierte ClpP1 Homo-Tetradekamere und/oder ClpP1P2 Hetero-Tetradekamere für den ADEP-vermittelten bakteriziden Effekt in ADEP-sensitiven Streptomyzeten verantwortlich ist. Im Vorfeld dieser Studie konnte ein sechstes *clpP*, welches sich in der Nähe des ADEP Biosyntheseclusters befindet, als Resistenzfaktor gegen ADEP identifiziert werden (Thomy et al., 2019). Im Zuge dieser Arbeit wurde der Resistenzmechanismus von $ClpP_{ADEP}$ auf molekularer Ebene untersucht und es zeigte sich, dass er aus zwei komplementären Funktionen besteht.

Mit Hilfe von Substratabbau-Experimenten und Interaktionsstudien konnte gezeigt werden, dass $ClpP_{ADEP}$ mit ClpP1 interagiert und niedrig-oligomere Komplexe bildet (Dimere und/oder Trimere) um die ADEP-induzierte Assemblierung von ClpP1 Homo-Tetradekameren und ClpP1P2 Hetero-Tetradekameren zu verhindern. Letzteres konnte durch die $ClpP_{ADEP}$-vermittelte Inhibierung des ADEP-induzierten Abbaus von ß-Casein durch ClpP1P2 gezeigt werden. ClpP ist jedoch für die Lebensfähigkeit von Streptomyzeten essentiell (Viala et al., 2000), wodurch sich die Frage ergibt, wie die physiologische Funktion von ClpP1P2 ersetzt werden kann. *In vitro* Substratabbau-Experimente zeigten einen ClpX-vermittelten Abbau der natürlichen Substrate ClgR und PopR durch $ClpP_{ADEP}P2$ sowie eine ClpC1-abhängige Hydrolyse von ß-Casein durch $ClpP_{ADEP}P2$, womit die Rekonstitution eines physiologisch aktiven $ClpP_{ADEP}P2$ Komplexes nachgewiesen werden konnte. Außerdem konnte mit Hilfe der ClpP2 Mutanten $ClpP2_{S131A}$ und $ClpP2_{hp}$ in Kombination mit wildtypischem $ClpP_{ADEP}$ die proteolytische Aktivität sowie Clp-ATPase/ClpP Interaktionen des $ClpP_{ADEP}P2$ Komplexes in ß-Casein-Abbauexperimenten analysiert werden. Diese deuten darauf hin, dass $ClpP_{ADEP}$ als ADEP-insensitiver Ersatz von ClpP1 fungiert und für die proteolytische Aktivität des $ClpP_{ADEP}P2$ Komplexes zuständig ist. Währenddessen bleibt ClpP2 als alleiniger Interaktionspartner für die Clp-ATPasen bestehen.

1. Introduction

1.1 The caseinolytic protease Clp

In all living cells, proteins are constantly produced and degraded in order to maintain protein homoeostasis. The removal of abberant proteins and specific regulatory factors is conferred by proteases such as Clp, Lon and FtsH which are present in eukaryotic and prokaryotic cells (Sauer and Baker, 2011). In bacterial cells, the majority (~80 %) of proteolytic activities is performed by the Clp and Lon protease combined (Goldberg et al., 1994). The caseinolytic protease Clp is composed of the proteolytic core ClpP, a 14-mer barrel, and hexameric Clp-ATPases, which recognise, unfold and thread substrates into the proteolytic chamber under ATP consumption (Olivares et al., 2016). The degradation chamber is located within the tetradecamer, shielded from the cytoplasm. Clp-ATPases, like ClpA or ClpX in *Escherichia coli*, bind to either one or both sides of the barrel, creating a funnel-shaped, tightly regulated access to the proteolytic chamber (Kessel et al., 1995, Grimaud et al., 1998). Bacteria possess a set of different Clp-ATPases that interact with the peptidase ClpP in order to fulfil its physiological function, like ClpX and ClpA in *E. coli*, or ClpX and ClpC1 in *Mycobacterium tuberculosis*, yielding ClpXP, ClpAP or ClpC1P complexes, respectively.

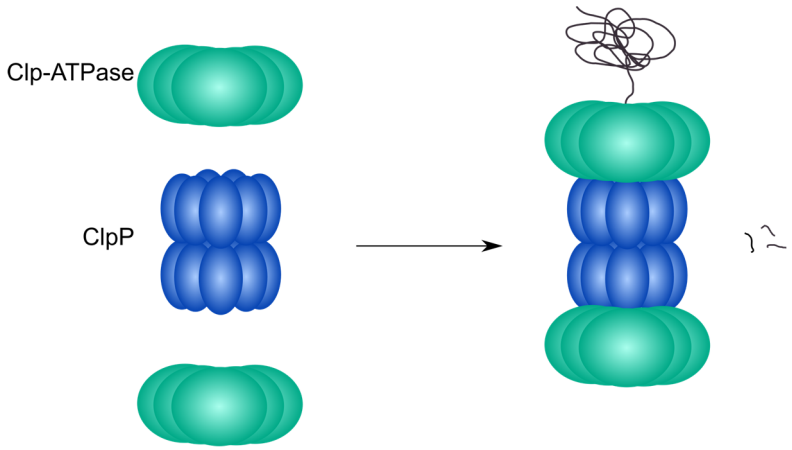

Figure 1.1: **Model of substrate degradation by the caseinolytic protease**. Clp-ATPases recognise, unfold and translocate polypeptide chains into the internal degradation chamber of ClpP in an ATP-dependent manner.

Substrates of the Clp protease machinery are involved in metabolic activities, cell division, damage repair and regulation of transcription. For a substrate analysis, tagged inactive EcClpP was employed as a trap in an *in vivo* experiment and 60 different proteins could be identified as potential ClpXP substrates involved in starvation and oxidative stress responses, transcriptional activation and metabolic activities (Flynn et al., 2003). Despite the broad range of substrates, a deletion of ClpP or Clp-ATPases in *E. coli* merely resulted in a weak phenotype (Maurizi et al., 1990a), which is due to overlapping substrate recognition domains of the Clp and Lon protease (Smith et al., 1999). In *Bacillus subtilis*, Clp substrates were identified by the use of 2D-PAGE analysis of the wild type and a Δ*clpP* deletion mutant. Those substrates included metabolic enzymes, aminoacyl-tRNA synthetases and enzymes of certain biosynthetic pathways like IlvB (large subunit of the acetolactate synthase), involved in the synthesis of the amino acids isoleucine, leucine and valine, and GlmS that is part of the hexosamine metabolism and thus involved in peptidoglycan synthesis (Kock et al., 2004). A lack of ClpP in *B. subtilis* leads to a severe pleiotropic phenotype impairing motility, sporulation, genetic competence, heat tolerance and late stationary phase adaptive responses (Msadek et al., 1998). Although substrates of the caseinolytic protease differ between species, the discovery of substrates in distinct model organisms illustrates that the Clp system has a significant impact on the regulation of the bacterial proteome. Additionally, Clp is involved in virulence and pathogenesis in several bacteria, such as *M. tuberculosis* and *Legionella pneumophila* (Raju et al., 2012, Zhao et al., 2016). In *Staphylococcus aureus*, a deletion of the proteolytic core *clpP* or the Clp-ATPase *clpX* leads to attenuated virulence in skin abscesses of mice. In those mutants the amount of, e.g., α-haemolysin (*hla*) was significantly reduced. By analysing *hla* expression, low α-haemolysin amounts could be observed at the transcriptional level, which is controlled by the *agr* locus. In Δ*clpP* and Δ*clpX* mutants, transcription of the *agr* effector molecule, the RNA polymerase III as well as the activity of the autoinducing peptide (AIP) was strongly decreased, suggesting that ClpP and ClpX control the activity of major virulence factors (Frees et al., 2003).

In the pathogenic bacterium *M. tuberculosis*, ClpP is essential for viability, in contrast to *B. subtilis* or *S. aureus*, where the Clp protease is dispensable for growth under non-stressing *in vitro* conditions (Msadek et al., 1998, Raju et al., 2012, Raju et al., 2014, Frees et al., 2003). This

pathogen is the cause of tuberculosis, leading to millions of deaths every year. In contrast to most eubacteria which contain only one *clpP* gene, *M. tuberculosis* carries two *clpP* genes, *clpP1* and *clpP2*, whose ClpP proteins form the ClpP1P2 proteolytic core of the caseinolytic protease (Akopian et al., 2012, Schmitz et al., 2014). A functional ClpP1P2 complex is not only essential for growth but for infection by the pathogen as well (Raju et al., 2012). The essential transcriptional repressor WhiB was identified as substrate of *M. tuberculosis* ClpP1P2 in proteomic analyses employing a conditional ClpP1P2 mutant compared to the wild type. The stabilisation of WhiB by blocking its ClpP1P2-dependent degradation resulted in cell death illustrating the necessity of a regulatory check of WhiB levels mediated by the Clp system (Raju et al., 2014).

1.1.1 The proteolytic core ClpP

The proteolytic core ClpP is a self-compartmentalised serine peptidase, which assembles into two stacked heptameric rings forming a tetradecameric barrel with the proteolytic chamber enclosing 14 Ser-His-Asp catalytic triads, well hidden from the cytoplasm. The structure of ClpP is highly conserved among eubacteria and was intensively studied in the model organisms *S. aureus*, *B. subtilis* and *E. coli* (Liu et al., 2014). Each ClpP monomer comprises an N-terminal domain that forms entrance pores on the apical surface of the tetradecameric cylinder, a head domain, representing the main part of the barrel and a handle region, which is essential for oligomerisation and allosteric activation of the catalytic triads (Wang et al., 1997). ClpP from different organisms could be crystallised in three distinct conformational states, namely the active extended, inactive compact and inactive compressed state (Wang et al., 1997, Geiger et al., 2011, Gersch et al., 2012, Ye et al., 2013, Liu et al., 2014). All three conformations vary in the height of the barrel and the alignment of the catalytic triads. Figure 1.2 illustrates the extended and compressed state of *S. aureus* ClpP protomers. In the extended conformation, the α5 helix, which is part of the handle region, is straight and thus responsible for stabilising ring-ring interactions of two opposing ClpP protomers by forming hydrogen bonds (Lee et al., 2011). In contrast, the α5-handle in the compressed conformation is kinked and stabilised by hydrogen bonds within its own subunit (Ye et al., 2013). Additionally, the extended conformation of ClpP protomers is the only state, in which the three amino acid residues of the catalytic triad (Ser98, His123 & Asp172

in SaClpP) were found to be located in close proximity to each other, able to form hydrogen bonds (Fig. 1.2).

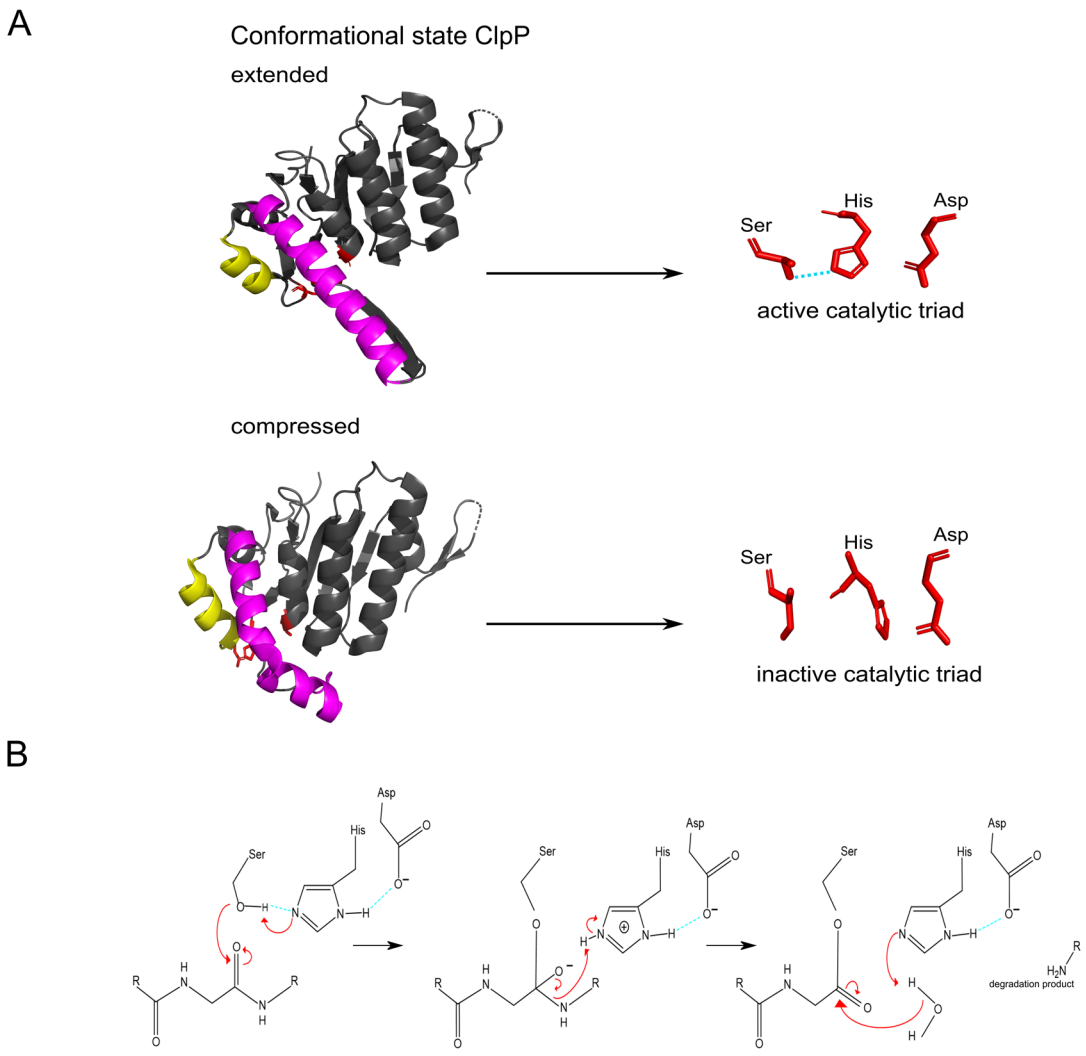

Figure 1.2: **Crystal structure of a SaClpP protomer in the extended (PDB: 3V5E) and compressed (PDB: 3qwd) conformation. A:** SaClpP is shown in dark grey, with the handle region composed of α5 and α6 highlighted in magenta and yellow. The three amino acid residues of the catalytic triad (Ser97, His121, Asp171) are depicted in red. In the active extended conformation, the amino acid residues of the catalytic triad are aligned in close proximity, able to form hydrogen bonds. In the compressed conformation, the catalytic triads are arranged with an increased distance from each other, preventing the formation of hydrogen bonds. **B:** Schematic representation of peptide bond cleavage mediated by the catalytic triad. The formation of hydrogen bonds is depicted in a dashed blue line.

In the extended conformation, the nucleophilic serine residue attacks the electron deficient carbonyl carbon of the peptide bond to form an acyl-ester intermediate, where the proton of the serine residue is withdrawn by the imidazole ring of the histidine residue. The positive charge of the histidine residue in turn is stabilised by the negative charge of the carboxyl group of the aspartate residue. Subsequently, the acyl-ester intermediate is hydrolysed and the serine residue is regenerated. The formation of hydrogen bonds between the positively charged imidazole ring of the histidine and the negatively charged hydroxyl group of the serine residue enhances its nucleophilicity in the catalysis competent conformation of the catalytic triad. In the compressed conformation, the imidazole ring of the histidine residue is rotated away from the hydroxyl group of the serine residue, preventing the formation of hydrogen bonds (see Figure 1.2). Figure 1.3 represents the crystal structure of the tetradecameric SaClpP barrel in the extended conformation.

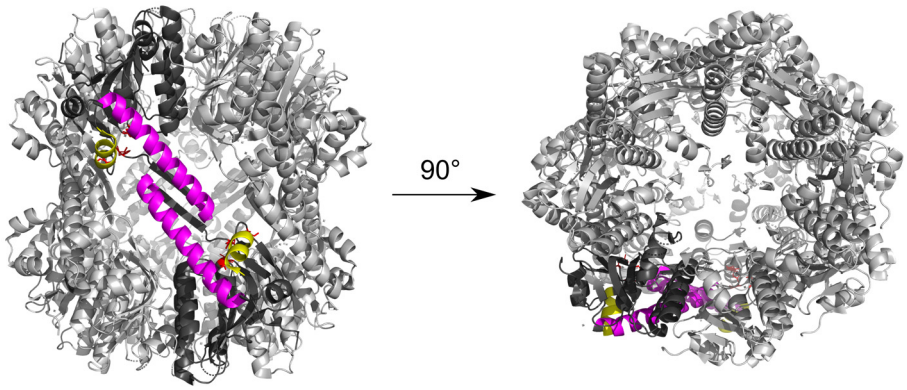

Figure 1.3: **Crystal structure of the SaClpP 14-mer barrel in the extended active conformation (PDB: 3V5E)**. Two opposing protomers are coloured in dark grey with the handle domain composed of α5 and α6 in magenta and yellow. The entrance pore located at the apical side of ClpP could be visualised by a 90° rotation of the crystal structure.

In this conformation, the handle regions of opposing subunits interact with each other, stabilising the interface of two heptameric rings. Surprisingly, a deletion of the handle region did not lead to the dissociation of the tetradecamer into two heptameric rings but instead resulted in inactive barrels, highlighting the significance of the handle region for catalytic competence (Gribun et al., 2005). Instead, charge-charge interactions of amino acid residues located in the head domain were suggested to be responsible for the stabilisation of the tetradecameric barrel (Ingvarsson et al., 2007).

According to molecular dynamic simulations, the compact conformational state was suggested to be a stable intermediate between the extended and compressed state (Ye et al., 2013). Additionally, calculating collective motions of proteins by normal mode analysis indicated that the extended conformation, which is essential for the proteolytic activity of the complex, switches into an inactive compact conformation for product release (Kimber et al., 2010). Furthermore, quantitative NMR spectroscopy studies strongly suggested that degradation products may exit the proteolytic chamber through transient equatorial pores rather than through the axial pores of the proteolytic chamber (Sprangers et al., 2005). All three conformations, the active extended, inactive compact and inactive compressed state seem to be significant snapshots reflecting the strict regulation of ClpP function as part of a protection system in the cell, preventing un-controlled access to the highly unspecific catalytic triads whose catalytic competence is dependent on the conformation of the handle regions of the tetradecameric barrel.

The ClpP barrel itself is only capable of degrading short peptides up to five amino acid residues in length which diffuse through entrance pores located on both sides of the peptidase (Woo et al., 1989, Thompson and Maurizi, 1994). In order to degrade proteins, ClpP has to interact with its cognate Clp-ATPases, which recognise, unfold and translocate substrates into the proteolytic chamber. The binding regions for the Clp-ATPases are highly conserved, hydrophobic and located on the apical surface of ClpP. Each hydrophobic binding pocket is formed by two adjacent ClpP monomers resulting in seven binding regions on both apical sides of the barrel, serving as anchors for the Clp-ATPases (Wang et al., 1997, Kim et al., 2001, Joshi et al., 2004). Those hydrophobic pockets contain conserved and solvent-exposed aromatic amino acid residues like Tyr60, Tyr62 and Phe82 of mature *E. coli* ClpP (Wang et al., 1997).

In order to activate ClpP for substrate degradation, different Clp peptidases from various organisms, like e.g., EcClpP and MtClpP1P2, have to cleave off a propeptide sequence which is located at the N-terminus and clogs the pore, preventing access to the proteolytic chamber (Maurizi et al., 1990a, Akopian et al., 2012). In case of *E. coli* ClpP, the first 14 amino acid residues are autocatalytically cleaved off to form the mature peptidase (Maurizi et al., 1990b).

ClpP from different organisms consisting of multiple ClpP isoforms

As mentioned above, ClpP was intensively studied in prototype organisms like *E. coli* and *B. subtilis*, carrying only one *clpP* gene. By investigating more complex model organisms, the co-existence of multiple ClpP isoforms has moved into focus increasingly. In this course, the ClpP organisation in the pathogen *M. tuberculosis* has been analysed, revealing a heteromeric ClpP1P2 complex, which consists of two homo-heptameric ClpP1 and ClpP2 rings (Akopian et al., 2012, Schmitz et al., 2014). While both *clpP* genes are located on the same operon in *M. tuberculosis* (Sherrid et al., 2010), *clpP1* and *clpP2* of the pathogen *Chlamydia trachomatis* are located on separate genetic loci, whose ClpP proteins form a heteromeric ClpP1P2 complex as well, highlighting the diversity of *clpP* organisation and regulation in different species (Pan et al., 2019).

In contrast to the Clp system of *M. tuberculosis* and *C. trachomatis,* which both consist of heteromeric ClpP1P2 complexes, the pathogen *Pseudomonas aeruginosa* seems to form distinct tetradecameric complexes, consisting of either ClpP1 or ClpP2 although a functional ClpP2 homo-tetradecamer could not be reconstituted *in vitro* and the formation of heteromeric ClpP1P2 complexes cannot be ruled out. Both *clpP1* and *clpP2* genes are regulated separately and fulfil different functions in the cell, as it was shown by analysing different Δ*clpP1*, Δ*clpP2* and Δ*clpP1P2* deletion mutants, strongly suggesting the formation of ClpP1 and ClpP2 homo-tetradecamers (Hall et al., 2017). Similar to ClpP1 and ClpP2 of *P. aeruginosa*, the two ClpP isoforms of *Clostridium difficile* seem to form two distinct homomeric complexes as well, with ClpP1 as the main contributor to maintain protein homoeostasis in the cell (Lavey et al., 2019). The formation of ClpP1P2 complexes as a regulatory mechanism was revealed in *Listeria monocytogenes*, where catalytically active ClpP2 homo-tetradecamers as well as heteromeric ClpP1P2 complexes could be reconstituted *in vitro*. In contrast, ClpP1, whose catalytic triad consists of an asparagine instead of an aspartate residue, did not form functional homo-tetradecamers. However, ClpP1 exhibited catalytic activity in complex with ClpP2, highlighting an unprecedented regulatory mechanism of ClpP1P2 complexes, with all 14 catalytic triads aligned (Zeiler et al., 2013, Dahmen et al., 2015). Figure 1.4 summarises a variety of different physiologically active ClpP complexes from various pathogenic organisms harbouring multiple ClpP isoforms, which were investigated *in vitro*.

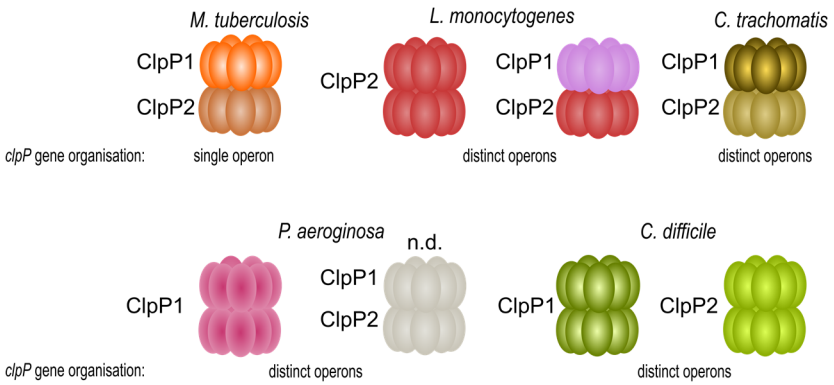

Figure 1.4: **Schematic representation of distinct tetradecameric complexes of organisms, harbouring multiple ClpP isoforms, which were studied *in vitro*.** *M. tuberculosis* and *C. trachomatis* exclusively form heteromeric complexes, whereas *L. monocytogenes* is able to form two distinct tetradecameric complexes composed of homomeric ClpP2 or heteromeric ClpP1P2. Additionally, functional ClpP1 homo-tetradecamers of *P. aeruginosa*, as well as functional ClpP1 and ClpP2 homo-tetradecamers of *C. difficile* could be achieved *in vitro*. A functional ClpP1P2 heteromeric complex of *P. aeruginosa* has not been determined (n.d.) so far (Akopian et al., 2012, Zeiler et al., 2013, Schmitz et al., 2014, Dahmen et al., 2015, Hall et al., 2017, Pan et al., 2019, Lavey et al., 2019).

Considering the existence of multiple ClpP isoforms forming heteromeric complexes, questions arise regarding their functionality and specific role they have to fulfil in those complexes. In *M. tuberculosis*, ClpP2 is the sole interaction partner for its cognate Clp-ATPases ClpX and ClpC1, whereas ClpP1 is the main propetide processor of both peptidases (Leodolter et al., 2015). Another example is ClpP1P2 of *L. monocytogenes*, in which ClpP2 exclusively interacts with the Clp-ATPase ClpX (Gatsogiannis et al., 2019, Fux et al., 2019).

1.1.2 Clp-ATPases

Clp-ATPases, which form together with the peptidase ClpP the caseinolytic complex Clp, belong to the Clp/Hsp100 family of AAA+ proteins (ATPase associated with diverse cellular activities). Members of the AAA+ superfamily are divided into subgroups according to their structural similarities. ClpA, ClpC, ClpE, ClpB and Hsp104 belong to class I of the AAA+ superfamily, which harbour two nucleotide binding domains, consisting of canonical Walker A and B motifs (Schirmer et al., 1996, Ingmer et al., 1999). While ClpA, ClpC and ClpE interact with the peptidase ClpP for substrate degradation, ClpB and its orthologue in yeast Hsp104 rescue misfolded and aggregated proteins independent of ClpP in an ATP-dependent manner (Schirmer et al., 1996, Gerth et al., 2004, Haslberger et al., 2010). In contrast, ClpX belongs to class II of the Clp/Hsp100 family, which

consist of only one nucleotide binding domain (Schirmer et al., 1996). The catalytic triads of the Clp peptidase are highly unspecific, thus substrate specificity is conferred by the different Clp-ATPases, which tightly regulate access to the proteolytic chamber of ClpP. Clp-ATPases recognise substrates by inherent or added degradation tags which are either accessible or exposed in a partially unstructured protein (Flynn et al., 2003). An intensively studied degradation tag, which is recognised by ClpX and ClpA in *E. coli* is the C-terminal ssrA-tag, which is added to nascent polypeptide chains that are stalled at the ribosome. The ssrA-tag (small stable RNA), which functions as both a t-and mRNA, encodes a small peptide that is added during translation and is recognised as substrate by ClpXP or ClpAP (Gottesman et al., 1998). Specifically the last three amino acid residues of this tag sequence are recognised by ClpX, consisting of either LAA or VAA in a variety of bacterial species (Flynn et al., 2001).

To form a functionally active Clp complex, two different kinds of interactions are necessary: First, loop-structures of the Clp-ATPases consisting of a well-conserved tripeptide motif, the (I/L/V)-G-(F/L) loops, bind to conserved hydrophobic grooves on the apical surface of ClpP, setting the general positions of the Clp-ATPase on the tetradecameric barrel of ClpP. Second, pore-2 loops of the Clp-ATPases interact with N-terminal loops of ClpP to enable dynamic, nucleotide-dependent transactions as it is represented in Figure 1.5 (Wang et al., 1997, Kim et al., 2001, Martin et al., 2007). Essential for Clp-ATPase/ClpP interaction is the binding but not hydrolysis of ATP by the Clp-ATPases (Grimaud et al., 1998, Joshi et al., 2004, Hersch et al., 2005).

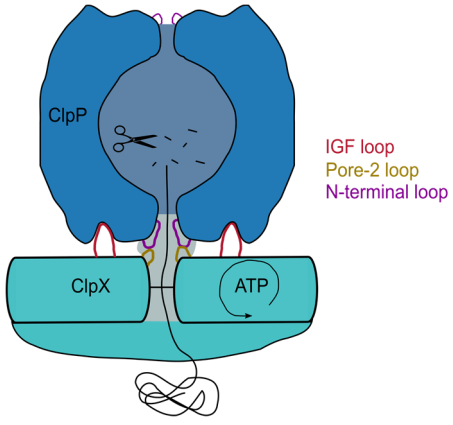

Figure 1.5: **Schematic model of Clp-ATPase/ClpP interaction during substrate degradation.** IGF-loops of the ATPase ClpX bind to conserved hydrophobic grooves located on the apical surface of

the ClpP barrel. Additionally, Pore-2 loops of ClpX interact with N-terminal loops of the peptidase ClpP, enabling transient and nucleotide-dependent transactions (Martin et al., 2007, modified).

While ATP binding is essential for the formation of the Clp protease, the degradation of substrates is fueled by ATP hydrolysis to ADP, which generates a mechanical force translocating an unstructured degron, like the ssrA-tag, towards the entrance pore (Sauer and Baker, 2011, Cordova et al., 2014). As a folded substrate is hindered in passaging the entrance pore of the complex, the translocation of the recognition tag towards the entrance pore drags on the folded portion of the protein and thereby unfolds it, applying mechanical denaturation on the substrate for subsequent translocation of the unfolded peptide chain into the degradation chamber of ClpP, illustrated in Figure 1.6 (Cordova et al., 2014).

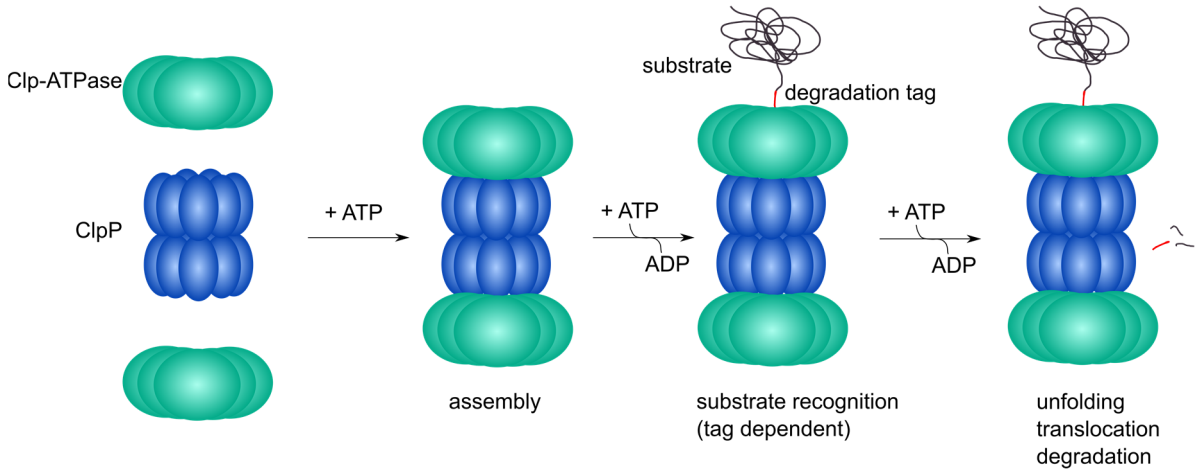

Figure 1.6: **Substrate degradation by the caseinolytic complex Clp is dependent on the recognition of unstructured degrons (red) and the unfolding and translocation of structural elements near the degradation tag.** Mechanical denaturation of the folded substrate is conducted by pulling the folded protein towards the entrance pore, thereby denaturing it in an ATP-dependent manner. Subsequently, the unfolded peptide chain is spooled into the degradation chamber of ClpP (Cordova et al., 2014).

To elucidate the mechanisms underlying substrate degradation by the Clp protease complex in detail, the ClpXP degradation machinery of *E. coli* was intensively studied, serving as a paradigm for other protease complexes like ClpAP and ClpCP. Furthermore, crystallisation attempts using ClpA or ClpC are challenging because of its increased conformational heterogeneity harbouring two nucleotide binding sites, thereby shifting the attention to ClpX. Nevertheless, crystallisation

is still challenging, leaving a lot of questions unanswered due to missing high-resolution ClpXP structures. Particularly the interaction of ClpXP in relation to the symmetry mismatch of the hexameric Clp-ATPases and the heptameric ring of ClpP remained elusive for many years. The Clp-ATPase ClpX of *E. coli* comprises an N-terminal zinc-binding domain (ZBD) and an AAA + module (Baker and Sauer, 2012). The ZBD domain is responsible for the recognition and engagement of several substrates and forms dimers, each stabilised by a zinc atom (Banecki et al., 2001, Wojtyra et al., 2003, Donaldson et al., 2003). The AAA+ module is composed of a large and small domain harbouring one nucleotide binding site which consists of a characteristic Walker A and B motif (Baker and Sauer, 2012). Furthermore, the large and small AAA+ domain of ClpX function together to build a cleft, enabling ATP or ADP to bind (Kim and Kim, 2003, Glynn et al., 2009). This cleft is mostly composed of well conserved sequence motifs such as box II, the Walker A and B motifs, the arginine finger and sensor two arginine (Neuwald et al., 1999, Erzberger and Berger, 2006). The Walker A sequence motif is known to be responsible for ATP binding, whereas ATP hydrolysis is conducted by Walker B (Walker et al., 1982). Additionally, the amino acid residues of box II (Val78 & Ile79 of EcClpX) are involved in ATP binding and hydrolysis (Joshi et al., 2003, Fei et al., 2020). The arginine finger is suggested to be required for ATP hydrolysis, although the functional role that conserved residues have to fulfil may differ in a broad range of AAA+ family members (Wendler et al., 2012). Furthermore, the conserved arginine sensor II is proposed to link ATP binding to conformational changes, which are necessary for substrate binding to ClpP (Joshi et al., 2004). Not only the N-terminal domain of ClpX but also flexible loops, which are located around the entrance pore and contain the RKH sequence, are involved in tag recognition of protein substrates (Baker and Sauer, 2012). Figure 1.7 represents a scheme of linear ClpX where the localisation of those conserved motifs are depicted. The turquoise colour of the pore-1 and 2 loops and the RKH-sequence illustrates the ssrA-tag binding region, whereas the conserved sequences necessary for ATP binding and hydrolysis are represented in white. Regions, which are known to interact with the peptidase ClpP, like the IGF-loop and the pore-1 and -2 loops are shown in purple and turquoise.

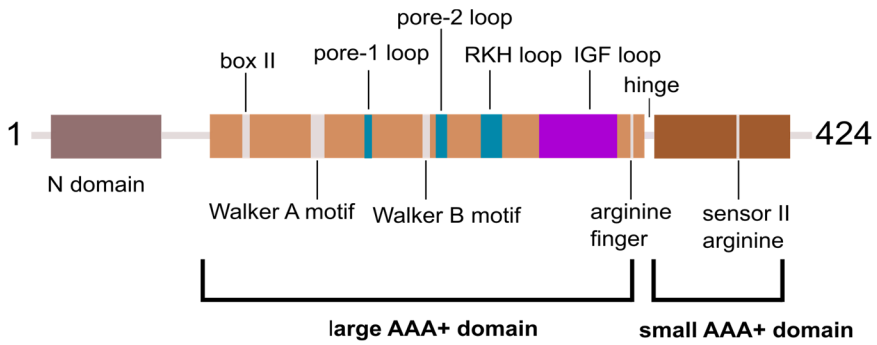

Figure 1.7: **Schematic representation of the different functional domains with respect to the linear amino acid sequence of EcClpX**. Turquoise: ssrA-tag binding; white: ATP binding and hydrolysis; purple: ClpP binding regions. The N-terminal pore-1 and 2 loops depicted in turquoise are also involved in ClpP binding (Baker and Sauer, 2012, Fei et al., 2020, modified).

A recently published cryo-EM structure of ClpXP1P2 of *L. monocytogenes* revealed that highly flexible interactions of the ClpX IGF-loops and the binding pockets of ClpP heptamers allow the interaction of the symmetry mismatched partners. LmClpX, which binds to its main interaction partner LmClpP2, showed a tilted hexameric ring towards LmClpP2 with one stretched IGF-loop, leaving one of the hydrophobic pockets empty, see Figure 1.8 (Gatsogiannis et al., 2019).

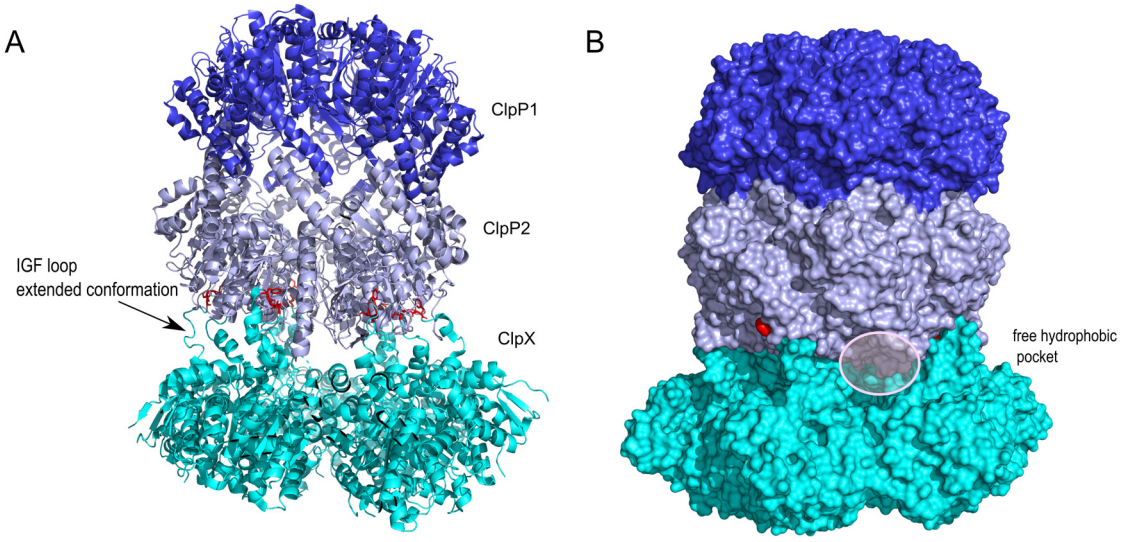

Figure 1.8: **Cryo-EM structure of LmClpXP1P2 visualising the symmetry mismatch of hexameric LmClpX (PDB: 6SFW) binding to the heptameric surface of LmClpP2 of the heteromeric LmClpP1P2 complex (PDB: 6SFX).** One IGF-loop is captured in an extended conformation, leaving one hydrophobic pocket unoccupied. **A:** LmClpXP1P2 is represented in dark blue (ClpP1), light blue (ClpP2) and cyan (ClpX), visualised as cartoon. The conserved amino acid residues of the IGF-loop are coloured in red and shown as sticks. **B**: The LmClpXP1P2 cryo-EM structure is depicted in a surface fill model representation, revealing one unoccupied hydrophobic pocket of LmClpP2.

Of note, the entrance pore of ClpP2 was captured closed, with the N-termini in the “up”-conformation (Gatsogiannis et al., 2019). In this conformation the N-termini of ClpP are moving out of the pore and thereby closing it (Bewley et al., 2006). However, in contrast to LmClpXP1P2, a cryo-EM structure of EcClpXP revealed a widened entrance pore of EcClpP from 10 Å (closed state) to ~30 Å (Fei et al., 2020). Furthermore, the cryo-EM structure of ClpXP of the Gram-negative *Neisseria meningitis* presented a similar widened entrance pore of ~23 Å on the ClpX bound apical side of ClpP (Ripstein et al., 2020). In contrast to the cryo-EM structure of LmClpXP1P2, both EcClpXP and NmClpXP structures were captured during substrate degradation. Although it is commonly suggested that the translocation forces which are generated by the Clp-ATPases underlie a general mechanism, differences across species concerning substrate recognition and Clp-ATPase/ClpP interactions are to be expected. While the cryo-EM structure of EcClpXP revealed multiple substrate contacts involving the pore-2 loop and the RKH-loop, no engagement of the pore-2 loops or RKH-loops of NmClpX with the substrate could be observed (Fei et al., 2020, Ripstein et al., 2020). In addition, EcClpP cryo-EM structures showed that the axial tunnel is filled with only one polypeptide chain, raising questions how two or more cross-linked polypeptide chains can be translocated simultaneously as it was shown previously in biochemical assays (Burton et al., 2001, Fei et al., 2020). Besides, studies on the stability of substrates, which were degraded by EcClpXP using the ssrA-tag at different geometric positions, strongly indicated that the stability of local elements attached to the recognition site, determines the degradation rate of the protein by the protease complex rather than the global thermodynamic stability of the substrate (Kenniston et al., 2004). Thus, analyses of more cryo-EM substrate-bound ClpXP structures combined with biochemical studies on a variety of different Clp substrates are needed to understand how ClpXP can denature and translocate an enormous set of different proteins, enabling it to function in protein quality control.

1.2 The proteolytic machinery Clp as a drug target

The caseinolytic complex Clp has a significant impact on the regulation of the bacterial proteome, thus compounds that target Clp-ATPases or ClpP are considered to be attractive antibacterial agents which could be used to combat pathogenic bacteria like *Staphylococcus aureus*, *Listeria monocytogenes* or *Pseudomonas aeruginosa* in bacterial infections (Moreno-Cinos et al., 2019).

Compounds that selectively target ClpP, thereby affecting virulence of a number of pathogens, represent a promising alternative to conventional antibiotics, considering the rising threat to public health by the increasing development of multi-drug resistant bacteria. In this project, the natural product ADEP1 was employed, which targets the tetradecameric barrel ClpP (Michel and Kastner, 1985, Brötz-Oesterhelt et al., 2005b) as it is described in the following chapter.

1.3 Targeting ClpP by acyldepsipeptides (ADEPs)

The A54556 complex, comprising eight closely related acyldepsipeptides, was produced by aerobic fermentation of *Streptomyces hawaiiensis* NRRL 15010 and isolated, described and published in 1985 by Michel and Kastner (Michel and Kastner, 1985) . The main component of this complex is factor A, also named as ADEP1, which exhibits antibacterial activity against Gram-positive bacteria like vancomycin-resistant enterococci, penicillin-resistant streptococci and methicillin-resistant *S. aureus* (MRSA) strains (Brötz-Oesterhelt et al., 2005b). In contrast to Gram-positive bacteria, Gram-negative bacteria are not affected by acyldepsipeptides since passaging across the outer membrane is hampered (Brötz-Oesterhelt et al., 2005b). Hence, when referring to acyldepsipeptides as a class of antibiotics consisting of the natural product ADEP1 and its derivatives, the shortened term ADEP is used. Figure 1.9 displays the structure of six components of the A54556 complex, named factor A (ADEP1), B, C, D, E and H, whose physical and spectral properties have been described by Michel and Kastner, see Figure 1.9.

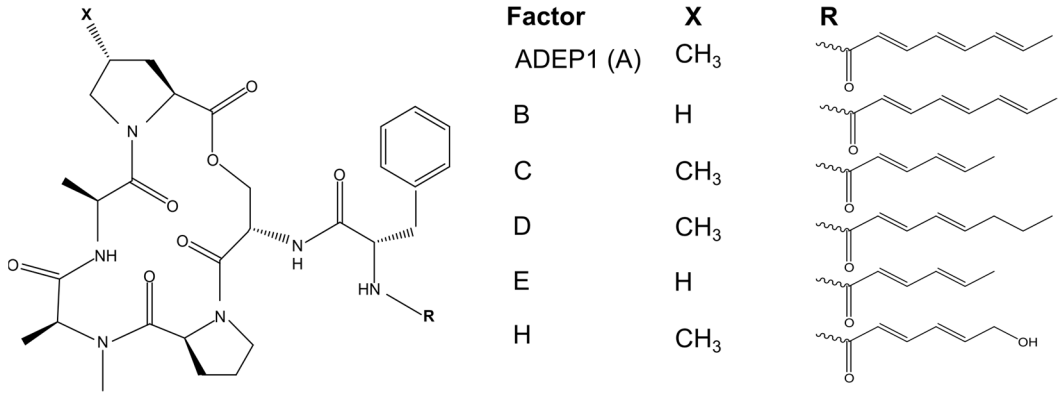

Figure 1.9: **Structure of the ADEP core and its factor specific residues consisting of factor A, B, C, D, E & H (Michel and Kastner, 1985, Hinzen et al., 2006).**

ADEP1 comprises a peptidolactone core which is linked via an N-acylphenylalanine moiety to an aliphatic side chain. Furthermore, important structural elements of this natural product are the aliphatic side chain, which is temperature and light sensitive, the phenylalanine linker, a methylated proline moiety, as well as an N-methylalanine residue (Michel and Kastner, 1985, Brötz-Oesterhelt et al., 2005b, Hinzen et al., 2006). Figure 1.10 A and B illustrate the natural product ADEP1 with its important structural elements coloured respectively in which Fig. 1.10 **B** represents the 3D structure of ADEP1 as sticks extracted from the EcClpP-ADEP1 crystal structure (PDB: 3MT6).

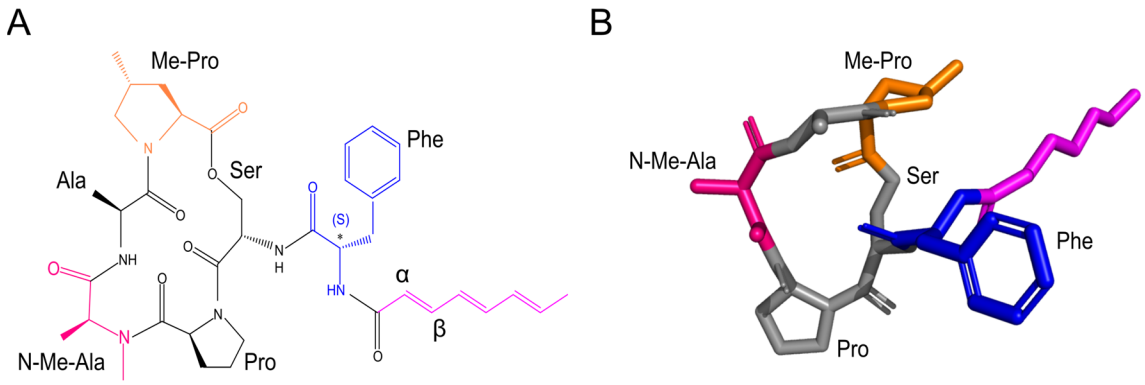

Figure 1.10: **ADEP1 with its important structural elements coloured such as the aliphatic side chain (purple), the N-acylphenylalanine linker (blue), a methyl-proline moiety (orange) and a methylated alanine residue (pink). A**: Schematic representation of ADEP1. **B**: The 3D-structure of ADEP1 was extracted from the EcClpP-ADEP1 structure (PDB: 3MT6) and is depicted as sticks.

Crystallised ADEP-bound EcClpP and BsClpP complexes revealed the binding site of this natural product as the same hydrophobic pockets located on the apical surface of ClpP serving as anchors for the Clp-ATPases (Lee et al., 2010, Li et al., 2010). The tetradecameric barrel of EcClpP bound to ADEP1 was captured in the extended, active conformation with the α5-handles straight and the catalytic triads aligned. In BsClpP, the N-terminal loops formed ß-hairpins moving out of the pore comparable to the “up”-conformation but with an enlarged axial pore, described as the open-gate conformation (Lee et al., 2010).

Figure 1.11 represents the closed entrance pore of an apo-EcClpP crystal structure (Wang et al., 1997) as well as the opened entrance pore of an EcClpP-ADEP1 structure (Li et al., 2010). However, ADEP binding does not only lead to the opening of the entrance pore, but also exhibits

conformational control over the whole ClpP barrel: It stabilises ClpP in the active extended state, thereby allosterically activating the catalytic centers of the peptidase, leading to an accelerated substrate degradation (Gersch et al., 2015). Without ADEP, protein substrate degradation is only possible in the presence of Clp-ATPases which form the physiologically active Clp protease complex together with ClpP. In the ADEP-bound state, the tetradecameric barrel of ClpP is able to degrade proteins like the model substrate casein independently from its cognate Clp-ATPases. Proteins with loosely folded structural domains or nascent polypeptide chains, which do not fit through the closed entrance pores of ClpP, are able to diffuse through the opened entrance pores of ADEP-bound ClpP, resulting in un-controlled proteolysis (Brötz-Oesterhelt et al., 2005b, Kirstein et al., 2009, Lee et al., 2010, Li et al., 2010).

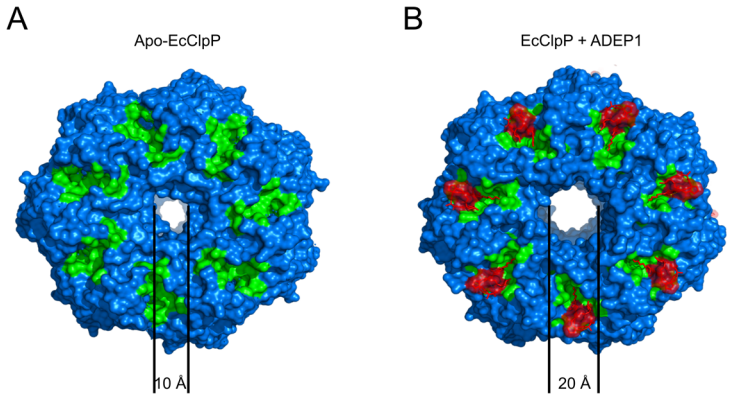

Figure 1.11: **Binding of ADEP1 to EcClpP leads to the widening of the entrance pore**. **A**: Apo crystal structure of EcClpP (PDB: 1TYF) with a closed entrance pore of ~10 Å in diameter (Wang et al., 1997). **B**: Crystal structure of EcClpP in complex with ADEP1 (PDB: 3MT6) captured with a widened entrance pore of ~20 Å in diameter (Li et al., 2010). Both crystal structures are shown as surface models with the hydrophobic pockets coloured in green and ADEP1 shown as sticks and illustrated in red.

Furthermore, proteomic studies using dormant methicillin-resistant *S. aureus* cells, which were treated with the ADEP1 derivative ADEP4, showed a significant decrease in their protein abundance with over 400 affected proteins compared to an untreated negative control (Conlon et al., 2013). Additionally, ADEP-treatment of *S. aureus*, *B. subtilis* and *Wolbachia* sp. led to the inhibition of cell division, caused by the ClpP-ADEP induced degradation of FtsZ, a tubulin homologue in prokaryotes (Sass et al., 2011, Sass and Brötz-Oesterhelt, 2013, Schiefer et al., 2013, Mayer et al., 2019).

To summarise, ADEP binding to the proteolytic core ClpP stabilises the handle region in its straight conformation, thereby aligning the catalytic sites and increasing substrate degradation by the opening of the entrance pores, ultimately leading to un-controlled proteolysis (Kirstein et al., 2009, Lee et al., 2010, Li et al., 2010, Gersch et al., 2015).

1.4 ClpP-ADEP interaction

ADEP1 as well as its synthetic derivative ADEP2 bind to the hydrophobic pockets which are formed by two adjacent ClpP monomers and are located on the apical surface of ClpP (Lee et al., 2010, Li et al., 2010). In order to explain the strong effects ADEP exerts on the conformational state of the ClpP tetradecameric barrel, interactions between ClpP and ADEP within the hydrophobic pocket were analysed in detail. ADEP1, as it is seen in Figure 1.12, fills the hydrophobic pocket in which most amino acid residues are hydrophobic in nature and whose hydrophobic interactions are illustrated as brackets in Figure 1.12 B, (Lee et al., 2010). Specifically, the aliphatic side chain and the benzene ring of the phenylalanine moiety are embedded deeply into the hydrophobic pocket and are responsible for the majority of interactions with the Clp peptidase (Malik and Brötz-Oesterhelt, 2017). Additionally, ADEP1 forms hydrogen bonds with a serine and tyrosine residue (Ser61 & Tyr63) which are represented as dotted lines (Lee et al., 2010). The latter represents a key switch for the ADEP-induced activation of ClpP, revealing a 90° rotation in various ADEP-bound crystal structures of BsClpP, EcClpP and MtClpP1P2-agonist compared to its corresponding apo-crystal structures (Lee et al., 2010, Li et al., 2010, Schmitz et al., 2014, Ni et al., 2016, Malik and Brötz-Oesterhelt, 2017).

As it is seen in Figure 1.12, the tyrosine residue at position 63 in BsClpP forms not only hydrogen bonds with the macrolactone core and the aliphatic side chain, but interacts with the benzene moiety of the phenylalanine residue as well (Lee et al., 2010). Exchanging Tyr63 for an alanine residue in SaClpP led to a gain-of-function mutant, in which the peptide backbone is rotated and capable of degrading protein substrates like casein or FtsZ independently without the addition of ADEP (Ni et al., 2016). While ADEP1 fills the hydrophobic pocket of ClpP completely in the extended conformation, modeling of ADEP1 into the hydrophobic pocket of BsClpP in the compressed conformation would lead to sterical clashes of the aliphatic side chain, explaining

the lack of ADEP-bound ClpP crystal structures in the compressed conformational state by blocking its transition from the active into the inactive state (Malik and Brötz-Oesterhelt, 2017).

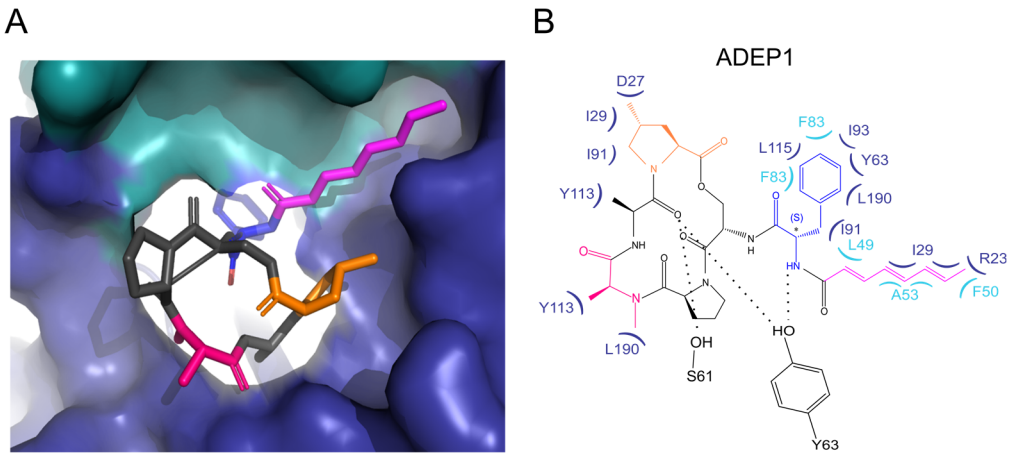

Figure 1.12: **ADEP1 binds to the hydrophobic pocket of BsClpP (PDB: 3KTI), formed by two adjacent ClpP monomers (blue and turquoise) and interacts effectively with BsClpP by hydrophobic interactions (brackets) and the formation of hydrogen bonds (dashed line), (Lee et al., 2010), modified. A:** BsClpP is shown as surface model and ADEP1 as sticks with the aliphatic side chain (purple), the phenylalanine moiety (blue), methyl-proline (orange) and methylalanine (pink) coloured, respectively. **B:** Hydrophobic interactions are shown in brackets, coloured in blue and turquoise corresponding to the two adjacent ClpP monomers, respectively. Numbers shown here are assigned to start methionine in position 1.

1.5 Acyldepsipeptides and their unique mode of action

Acyldepsipeptides deviate from traditional antibiotics that interfere with essential biosynthetic pathways like cell wall, DNA, RNA or protein biosynthesis by their unusual target and dual mode of action. ADEP binding to the hydrophobic pockets of the proteolytic core results in inhibition of complex formation of the peptidase with its cognate Clp-ATPases (1), thereby preventing regulated proteolysis of specific Clp substrates and misfolded proteins (Kirstein et al., 2009, Gersch et al., 2015, Famulla et al., 2016, Amor et al., 2016, Pan et al., 2019). Simultaneously, ADEP binding to the same hydrophobic pockets of the peptidase leads to opening of the entrance pores of ClpP and an allosteric activation of the catalytic triads, thereby resulting in un-controlled proteolysis of nascent polypeptide chains and loosely folded proteins (Kirstein et al., 2009, Lee et al., 2011, Li et al., 2010, Sass et al., 2011, Alexopoulos et al., 2013, Gersch et al., 2015, Pan et al., 2019, Silber et al., 2020b). Figure 1.13 summarises the two distinct ADEP mechanisms of

action, which consist of the inhibition of Clp-ATPase/ClpP interactions (1) and an overactivation of the ClpP barrel (2).

The ability of ADEP to inhibit Clp-ATPase/ClpP interactions was demonstrated by measuring ADEP affinities to ClpP which are much higher in comparison to the Clp-ATPases and one ADEP molecule is able to replace an assembled ClpX hexamer (Gersch et al., 2015).

However, bactericidal effects of ADEP deviate in Firmicutes and Actinobacteria.

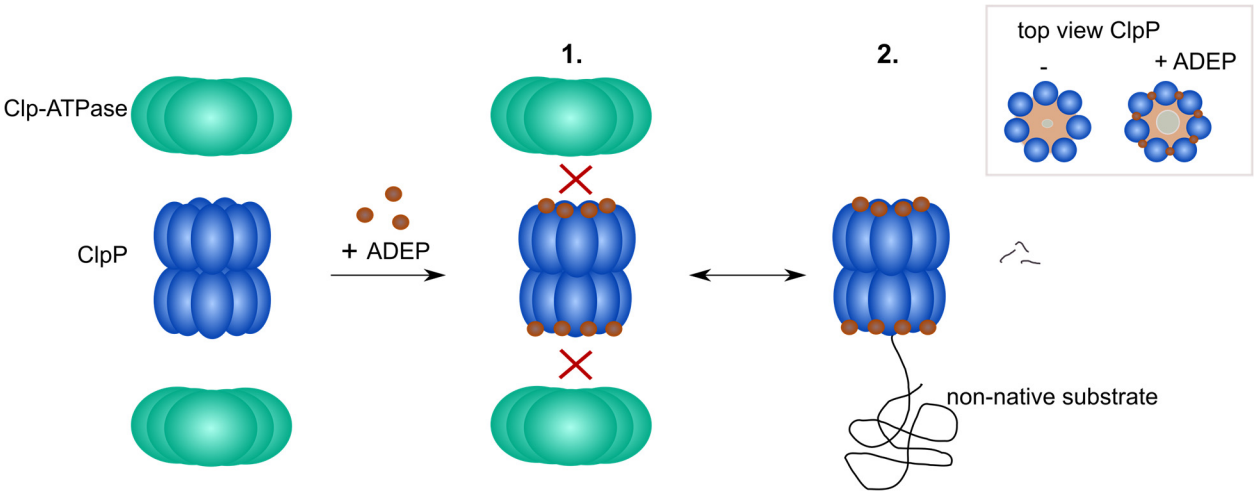

Figure 1.13: **ADEP affects the caseinolytic complex Clp in a dual mode of action. 1**: ADEP binding to the ClpP barrel inhibits Clp complex formation, abrogating the physiological function of the Clp protease. **2:** Furthermore, the binding of ADEP to the hydrophobic pockets of ClpP leads to the opening of the entrance pores and an allosteric activation of the catalytic triads, resulting in un-controlled, ATPase-independent degradation of non-native substrates (Kirstein et al., 2009, Lee et al., 2010, Li et al., 2010, Sass et al., 2011, Alexopoulos et al., 2013, Gersch et al., 2015, Amor et al., 2016, Famulla et al., 2016, Pan et al., 2019, Silber et al., 2020b).

The ADEP mode of killing in Firmicutes and Actinobacteria

In Firmicutes such as *B. subtilis* or *S. aureus*, which harbour non-essential ClpP proteins, preventing Clp-ATPase/ClpP interactions in *in vitro* experiments under non-stressing conditions did not lead to cell death, as exemplified by *S. aureus clpP* and *clpX* deletion mutants (Sass and Brötz-Oesterhelt, 2013, Brötz-Oesterhelt and Sass, 2014, Frees et al., 2014). Consequently, the ADEP mode of killing in Firmicutes is the un-controlled proteolysis of nascent polypeptide chains

and loosely folded proteins (Brötz-Oesterhelt et al., 2005b, Kirstein et al., 2009). In contrast, ClpP is essential in Actinobacteria and the cause of cell death does not originate from un-controlled proteolysis but from preventing Clp-ATPase/ClpP interactions (Famulla et al., 2016). The construction of a conditional *clpP1clpP2* knock-down mutant of *Mycobacterium bovis* surprisingly led to an increased ADEP susceptibility under down-regulation of ClpP1P2, strongly indicating that inhibited Clp protease functions are the ADEP mode of killing in mycobacteria (Famulla et al., 2016). On the contrary, reduced levels of ClpP in *B. subtilis* increased ADEP resistance. In contrast to Firmicutes like *B. subtilis* and *S. aureus*, ADEP failed to overactivate mycobacterial ClpP1P2 on its own, only in the presence of peptide agonists like carboxybenzyl-leucyl-leucine (Z-LL), the model substrate casein could be degraded by ADEP-bound MtClpP1P2. Besides, the physiologically active Clp complex MtClpC1P1P2 revealed a much stronger casein degradation rate compared to ADEP-activated MtClpP1P2 (Famulla et al., 2016). Although ADEP alone failed to overactivate MtClpP1P2, it efficiently inhibited MtClpX and MtClpC1 interactions with the heteromeric MtClpP1P2 proteolytic core (Schmitz et al., 2014, Famulla et al., 2016).

1.6 Streptomycetes and their complex Clp system

Considering the increasing development of multi-drug resistant bacteria and the lack of new antibiotics, it is an urgent need to discover new compounds to ensure the treatment of bacterial infectious diseases, preventing the development of a global health crisis. This global health crisis is expected to come true in the 21th century, stated by the world health organisation (WHO) in their report on global antimicrobial resistance, published in 2014 (World Health Organization, 2014). Microbial natural compounds represent a promising source of unprecedented lead structures which often act by novel mechanisms, inhibiting bacterial growth. Furthermore, those natural products can be used for the synthesis of optimised derivatives to combat drug resistances against established antibiotic drugs that interfere with metabolic pathways like cell wall, protein or DNA synthesis. For decades, bacteria have been known as an abundant source of antibiotic compounds, especially actinomycetes which provide the progenitors of 80% of all clinically applied antibiotics (Watve et al., 2001). Specifically the *Streptomyces* genus is known to produce a variety of bioactive compounds that affect bacterial growth, but also molecules with anti-fungal, anti-protozoal and anti-viral activity (Procopio et al., 2012). Streptomycetes are

filamentous soil-dwelling bacteria that undergo a complex differentiation cycle, which represents the hallmark of actinomycetes. They are ubiquitous in nature and develop spores out of vegetative hyphae, thereby facilitating the colonisation of the soil and their persistence. Spores are a semi-dormant stage in the complex differentiation cycle and can survive low nutrient and water availability. Under favourable conditions, germ tubes arise by tip extension and subsequent branch formation, building a substrate mycelium (Flärdh and Buttner, 2009). Subsequently, an aerial mycelium starts to grow, which involves the activation of numerous *bld* genes (McCormick and Flärdh, 2012). Aerial hyphae emerge from the colony surface, grow into the air and develop spores, thereby starting a new cycle of differentiation (Flärdh and Buttner, 2009) as it is seen in Figure 1.14.

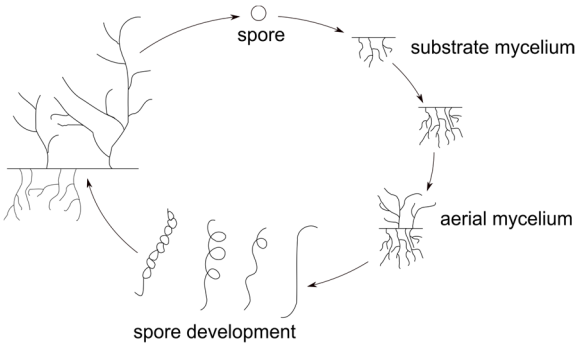

Figure 1.14: **Schematic representation of the complex life cycle of streptomycetes (Flärdh and Buttner, 2009, modified).**

Streptomyces mutants, which fail to form aerial hyphae and are thus blocked in early stages of differentiation, are called *bld* mutants (McCormick and Flärdh, 2012). These mutants are known to have multiple defects, e.g., with regard to the production of antibiotic compounds, catabolite repression and cell-cell signaling (Champness, 1988, Willey et al., 1993, Pope et al., 1996). For instance, studies on a *bldB* mutant of *Streptomyces coelicolor* revealed that *bldB* encodes a small protein which is necessary for cell morphogenesis and antibiotic production (Pope et al., 1998).

ClpP in streptomycetes

Whereas most eubacteria contain only one or two *clpP* genes, *Streptomyces* species mostly encode five ClpP homologues, which are organised in one monocistronic and two bicistronic operons, representing a ClpP system with a considerably increased complexity (de Crecy-Lagard et al., 1999, Viala et al., 2000). However, the ClpP system of streptomycetes was never studied

in vitro, leaving significant questions concerning the composition of the physiologically active Clp complex unanswered. Regulation of transcription of the different *clpP* genes in *S. lividans* and *Streptomyces coelicolor* was analysed in detail, see Figure 1.15.

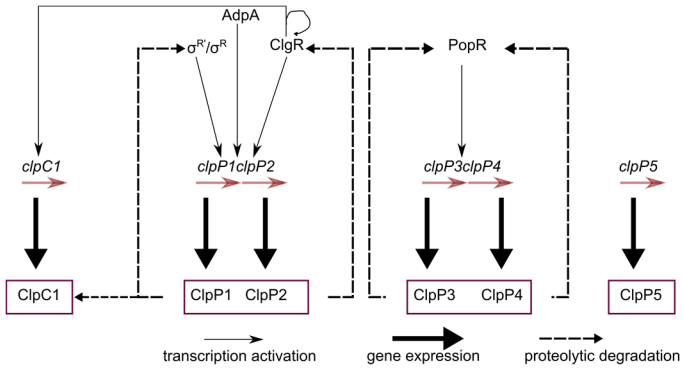

Figure 1.15: ***ClpP* gene organisation and regulation in *S. lividans* and *Streptomyces coelicolor*** (Viala et al., 2000, Viala and Mazodier, 2002, Bellier and Mazodier, 2004, Bellier et al., 2006, Kim et al., 2009, Gominet et al., 2011, Guyet et al., 2013).

The *clpP1clpP2* bicistronic operon is inducible by three different transcriptional activators $\sigma^{R'}$, AdpA and ClgR. $\sigma^{R'}$, an unstable isoform of σ^{R}, is a stress sigma factor and the thiol-status is sensed by its cognate anti-sigma factor RsrA (Paget et al., 1998). The pleiotropic regulator AdpA is involved in primary and secondary metabolism as well as in regulation and cell development in *S. lividans* and activates the expression of *clpP1clpP2* (Guyet et al., 2013, Guyet et al., 2014). ClgR, the *clpP* and *lon* gene regulator, controls the expression of *clpP1clpP2*, the ATPase-encoding *clpC1* gene, *lon*, another protease gene, and itself (Bellier and Mazodier, 2004). ClpP1P2 control their own expression by degrading their transcriptional activators $\sigma^{R'}$ and ClgR in negative feedback loops (Bellier et al., 2006, Kim et al., 2009). In wild-type *S. lividans* cells, the bicistronic operon *clpP1clpP2* is induced, whereas the *clpP3clpP4* genes remain silent. The corresponding ClpP3 and ClpP4 proteins can only be detected using specific antibodies in a *clpP1* knock-out mutant, where PopR, the transcriptional activator of the bicistronic operon *clpP3clpP4* cannot be degraded anymore by ClpP1P2, resulting in *clpP3clpP4* gene expression. PopR, the *clpP3* operon regulator, a paralogue of ClgR, is considered to recruit the RNA polymerase for *clp3clpP4* expression and is recognised by ClpP1P2 as a substrate (Viala et al., 2000). Additionally, analyses of PopR degradation by ClpP1P2 demonstrated that the last two alanine residues located at the C-terminus of PopR are essential for the recognition and subsequent degradation by ClpP1P2.

Exchanging those two alanine residues by aspartate residues increased the stability of PopR significantly (Viala and Mazodier, 2002). In *S. lividans*, *popR* was discovered to be located downstream from *clpP3P4* in the opposite orientation (Viala et al., 2000). ClgR and PopR, the transcriptional activators of the *clpP1P2* and the *clpP3clpP4* operons, both serve as substrates of ClpP1P2. Additionally, PopR can be degraded by ClpP3P4, monitoring their own synthesis in a negative feedback loop, similar to the degradation of ClgR by ClpP1P2 (Viala and Mazodier, 2002, Bellier and Mazodier, 2004). Contrariwise to the regulation of *clpP1P2* and *clpP3P4*, *clpP5* expression is constitutive, independent of ClgR and PopR and cannot replace the physiological function of ClpP1P2 or ClpP3P4 (Gominet et al., 2011). Besides, in *S. lividans* at least one functional copy of either *clpP1clpP2* or *clpP3clpP4* is necessary for cell viability (Viala et al., 2000). Furthermore, Mazodier and collegues discovered four distinct Clp-ATPases in *S. coelicolor*, ClpX and three ClpC proteins (Bellier and Mazodier, 2004). Specifically ClpC1 was suggested to be essential (Bellier and Mazodier, 2004), whereas ClpX is non-essential and located downstream from the *clpP1P2* operon (de Crecy-Lagard et al., 1999, Viala and Mazodier, 2002).

1.7 $ClpP_{ADEP}$ confers ADEP resistance in *S. hawaiiensis* NRRL 15010

By analysing the ADEP biosynthetic gene cluster, Thomy and co-workers discovered an additional sixth *clpP* gene which is located downstream of the ADEP biosynthetic gene cluster and represents the so far missing ADEP resistance factor in the producer strain *S. hawaiiensis*, see Fig. 1.16. This additional Clp peptidase was named $ClpP_{ADEP}$ (Thomy et al., 2019).

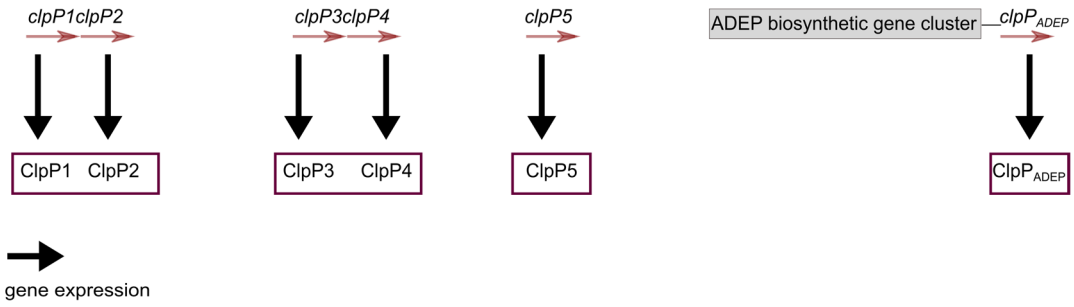

Figure 1.16: **An additional *clpP* is located in close proximity to the ADEP-biosynthetic gene cluster of *S. hawaiiensis*, which is named $clpP_{ADEP}$ (Thomy, 2019, modified).**

Moreover, biosynthetic gene clusters for secondary metabolites with intracellular targets often harbour genes that encode for transporters, exporting the respective molecules out of the cell.

However, Thomy *et al.* did not detect genes encoding a putative ADEP transporter within or in close proximity to the cluster borders (Thomy et al., 2019).

The heterologous expression of $clpP_{ADEP}$ in *S. lividans*, *S. coelicolor* and *Streptomyces griseus* clearly confirms the sixth Clp peptidase as resistance determinant against ADEP (Thomy et al., 2019). All three wild-type strains were not able to grow near the ADEP producer strain *S. hawaiiensis* on agar because of the release of ADEP into the medium. Exclusively under $clpP_{ADEP}$ expression, cells of all three *Streptomyces* strains grew in close proximity to *S. hawaiiensis*, in contrast to *S. lividans/S. coelicolor/S. griseus* wild-type cells and the empty plasmid control (Fig. 1.17).

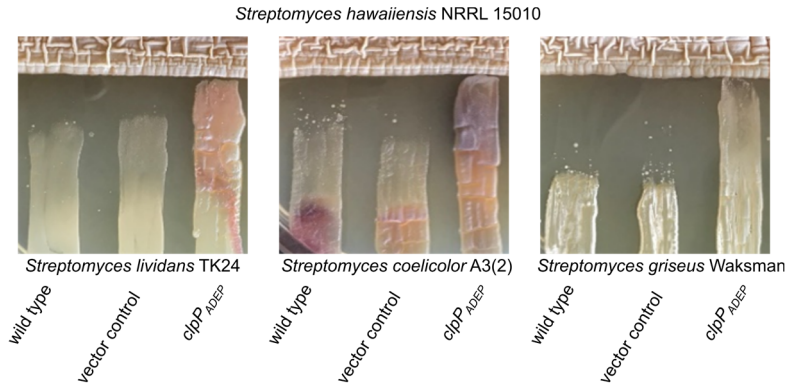

Figure 1.17: **Heterologous expression of $clpP_{ADEP}$ in *S. lividans*, *S. coelicolor* & *S. griseus* mediates ADEP resistance.** Reprinted with permission by (Thomy et al., 2019).

Nucleotide and amino acid sequence alignments of the different *clpP* genes and their respective ClpP proteins from *S. lividans* and *S. hawaiiensis* were performed, revealing high sequence identities on the gene and protein level [shown in %], which is illustrated in Figure 1.18. Previous work by Dr. Dhana Thomy revealed the same *clpP1-5* gene organisation in one monocistronic and two bicistronic operons in *S. hawaiiensis* (Thomy, 2019) compared to the *clpP* gene organisation in *S. lividans* (de Crecy-Lagard et al., 1999, Viala et al., 2000), see Figure 1.18.

These observations suggested that *clpP* genes of *S. hawaiiensis* underlie the same gene regulation as in *S. lividans,* given that in Western blot experiments ClpP1, but not ClpP3 was detected in the ADEP producer strain, implying that ClpP1P2 prevent *clpP3P4* expression by degrading their transcriptional activator PopR (Gominet et al., 2011).

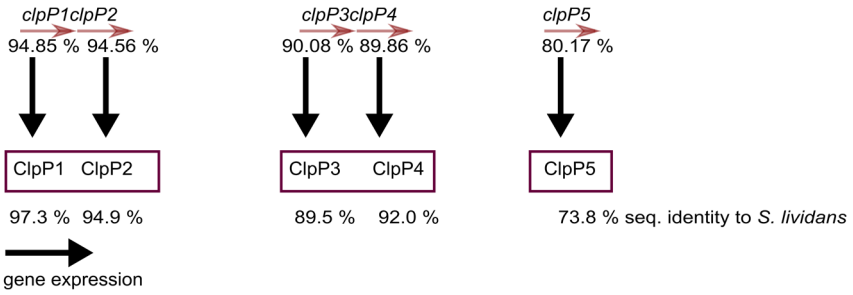

Figure 1.18: ***ClpP* gene organisation in *S. hawaiiensis* (Thomy, 2019). *ClpP* gene and amino acid sequence identities of the ClpP proteins from *S. hawaiiensis* compared to *S. lividans* are shown [%].** Similar to *S. lividans*, the *clpP1clpP2* and *clpP3clpP4* genes of *S. hawaiiensis* are organised in two bicistronic operons. Additionally, clpP5 is organised in one monocistronic operon (Thomy, 2019). The nucleotide and amino acid sequences of *SlclpP1-clpP5* and *ShclpP1-clpP5* were aligned and the sequence identity in % was calculated using Nucleotide and Protein BLAST (https://blast.ncbi. nlm.nih.gov/Blast.cgi?PAGE_TYPE=BlastSearch, https://blast.ncbi. nlm.nih.gov/Blast.cgi?PAGE =Proteins).

As a following step, a detailed amino acid sequence alignment was performed from ClpP homologues from *S. hawaiiensis* and *S. lividans* with the catalytic triads indicated by asterisks, see Figure 1.19. Figure 1.19 illustrates that only ClpP1, ClpP2 and ClpP3 of *S. hawaiiensis* and *S. lividans* comprise a catalytic triad consisting of a serine, histidine and aspartate residue.

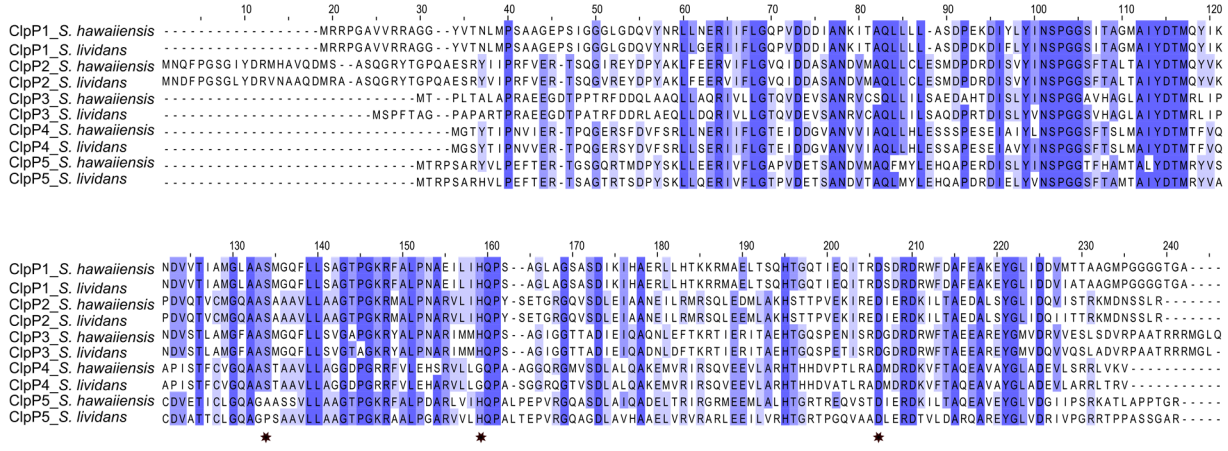

Figure 1.19: **Amino acid sequence alignment of ClpP homologues from *S. hawaiiensis* and *S. lividans***. The conserved amino acid residues of the catalytic triad are marked as asterisks. The alignment was generated using protein sequences of *S. lividans* TK24 (NZ_CP009124.1) and *S. hawaiiensis* NRRL 15010 (CP021978.1) and the online tool clustalΩ (https ://www.ebi. ac.uk/Tools/msa/clustalo/). ClpP sequence identities were computed using Jalview Software (Waterhouse et al., 2009). In each column, the percentage of amino acid residues that agree with the consensus sequence are visualised from dark blue (> 80 %) to marine (> 60 %) to pale blue (> 40 %).

Contrariwise, ClpP4 from *S. hawaiiensis* and *S. lividans* do not contain a canonical catalytic triad, given that the histidine residue is replaced by a glycine residue, strongly implying that ClpP4 could be catalytically inactive. In addition, ClpP5 from both organisms (*S. hawaiiensis* and *S. lividans*) show a non-typical spacing of the catalytic triad, suggesting that ClpP5 could be a catalytically inactive Clp peptidase.

1.8 Aims

Considering the unique dual mode of action of ADEP and the necessity of a vital Clp system in streptomycetes, questions arise, how the ADEP producer strain *S. hawaiiensis* protects itself during the production of ADEP and answering this question would provide essential knowledge on ADEP resistance mechanisms. In addition, studies on complex Clp systems are rare and *in vitro* data of streptomycetes ClpP proteins are lacking completely. By focusing on the ADEP producer strain *S. hawaiiensis* and its complex Clp system, two aims were followed in this study:

- **First**, a detailed *in vitro* investigation on *Streptomyces* Clp complex formation to provide insights into the composition of physiologically active Clp complexes, thereby focusing on the Clp peptidases ClpP1 and ClpP2 which are considered to be housekeeping peptidases based on previous *in vivo* experiments by Mazodier and colleagues (Gominet et al., 2011), see chapter 1.7, and high sequence homologies on the gene and protein level of ClpP proteins from *S. hawaiiensis*, including the same *clpP* gene organisation (Thomy, 2019), compared to the well-studied Clp peptidases from *S. lividans* (Viala and Mazodier, 2002).
- **Second**, an analysis of this Clp system in the presence of ADEP1 to elucidate the self-resistance mechanism of the ADEP producer strain *S. hawaiiensis* NRRL 15010.

To achieve this aims, the housekeeping Clp complex of *S. hawaiiensis* was reconstituted *in vitro* and a detailed biochemical study was conducted including substrate degradation experiments, interaction and functional studies, as well as oligomeric analyses in the absence and presence of the natural product ADEP1. Thereby this dissertation project aimed not only to reveal the composition of the main *Streptomyces* Clp complex but to elucidate, how a single protein like $ClpP_{ADEP}$ is able to avert the multi-layered destructive potential of ADEP, revealing a novel mechanism of producer strain survival.

2. Materials and methods

2.1 Materials

2.1.1 Equipment

Table 2.1: Equipment, software and services

Name	Type	Company/manufacturer
Äkta Pure	Chromatography system	GE-Healthcare
Chromas	Software	Technelysium Pty Ltd
ChemDraw 19.0	Software	PerkinElmer
CLC Sequence Viewer	Software	Qiagen
Ecotron HT	Shaker	Infors AG
EndNote X8	Software	Clarivate Analytics
Innova 44	Shaker	New Brunswick Scientific
GraphPad Prism 6	Software	GraphPad Software
Heraeus Multifuge X3R	Centrifuge	Thermo Fisher Scientific
Microcentrifuge 5418	Centrifuge	Eppendorf
Microcentrifuge 5418R, coolable	Centrifuge	Eppendorf
ImageLabs	Software	Bio-Rad Laboratories
In110	Incubator	Memmert
Inkscape	Software	Free Software Foundation
IrfanView 64	Software	Irfan Skiljan
Jalview	Software	Geoff Barton's Group, University of Dundee
LGC Genomics	Services (Sanger sequencing)	LGC Genomics
Microsoft Office	Software	Microsoft
Milli-Q Advantage A10	Water purification system	Merck Millipore
Mini Gel Tank	SDS gel electrophoresis	Thermo Fisher
Mini PROTEAN® Tetra Cell System	chamber	Bio-Rad Laboratories
Nanodrop	Photometer	Nanodrop Technologies
Perfect Blue Gelsystem	Agarose gel electrophoresis chamber	Peqlab/VWR
Perfect Blue Semi-Dry Blotter, Sedec	Western blot	Peqlab
SerialCloner 2.6.1	Software	SerialBasics
SnapGene Viewer	Software	GSL Biotech LLC
Sorvall LYNX 4000	Centrifuge	Thermo Fisher Scientific
peqStar 2X gradient	Thermal cycler	VWR
Peq Power E300	Power supply	Peqlab Biotechnology GmbH
PowerPac Universal		Bio-Rad Laboratories
Precellys Evolution	Homogenizer	Bertin Technologies
PyMol	Software	DeLano Scientific LLC
Quantity One	Software	Bio-Rad Laboratories

Quantum ST5	UV/VIS-Imager	Vilber
Gel Doc XR+		Bio-Rad Laboratories
REAX 2000	Mixer	Heidolph
Safe 2020	Biological safety cabinet	Thermo Fisher Scientific
TB2 Thermoblock	Heating block	Biometra
TECAN i-control	Software	Tecan Group
TECAN infinite M200/Spark	Spectrofluorometer	Tecan Group
Unicorn 6.3	Software	GE Healthcare

2.1.2 Chemicals, enzymes, kits and antibodies

Table 2.2: Chemicals and other materials

Name	Company
Adenosin triphosphate (ATP)	Sigma-Aldrich
ADEP1	Dhana Thomy
Agar	Applichem
Agarose	Peqlabs
Amersham™ ECL prime Western blotting detection reagent	GE Healthcare
Amersham Hybond-ECL nitrocellulose blotting membrane 0.45 µm	GE Healthcare
Amicon® Ultracel® -10 K/ -30 K	Merck KgaA
Ampicillin	Roth GmbH
Bolt™ Bis-Tris Plus Gel 12 % , 12 well	Thermo Fisher Scientific
Bolt™ Bis-Tris Plus Gel 4-12% , 15 well	Thermo Fisher Scientific
Bolt™Native Tris-Glycine Gel 4-12 % , 10 well	Thermo Fisher Scientific
Bolt™ MOPS SDS Running Buffer 20×	Thermo Fisher Scientific
Bolt™ MES SDS Running Buffer 20×	Thermo Fisher Scientific
Bolt™ LDS sample buffer 4×	Thermo Fisher Scientific
Bradford protein assay dye reagent concentrate	Bio-Rad Laboratories
Bovine serum albumin (BSA)	Sigma-Aldrich
BS3 chemical cross-linker	Thermo Fisher Scientific
ß-casein (bovine)	Sigma-Aldrich
FITC-casein (α-casein)	Sigma-Aldrich
Chloramphenicol	Sigma-Aldrich
Coomassie brilliant Blue G250	Merck KgaA
Creatine phosphokinase (rabbit)	Sigma-Aldrich
Creatine phosphate	Sigma-Aldrich
Deoxynucleotide triphosphate (dNTP) set 100 mM solutions	Thermo Fisher Scientific
Dimethylsulfoxide (DMSO)	Roth GmbH
1,4-Dithiothreitol (DTT)	Sigma-Aldrich
Ethanol, p.a.	Sigma-Aldrich
Ethanol, denaturated	Sigma-Aldrich
Ethidium bromide	Sigma-Aldrich
Glass beads (Ø150-212 µM)	Sigma-Aldrich
Glycerin	Roth GmbH
H_2O, HPLC-grade	Sigma-Aldrich

HEPES (4-(2-hydroxyethyl)-1-piperazine-ethanesulfonic acid)	Roth GmbH
HiTrap™ Q XL 1 ml column	GE Healthcare
HiTrap™ Q XL 5 ml column	GE Healthcare
HisPur™ Ni-NTA Resin	Thermo Fisher Scientific
Hydrochloric acid (HCl)	Central chemical warehouse, University of Tuebingen
Isopropyl-ß-D-thiogalactopyranoside (IPTG), Dioxane-free	Sigma-Aldrich
Imidazole	Sigma-Aldrich
InstantBlue™ Protein Stain	Expedeon
Kanamycin	Sigma-Aldrich
Magnesium chloride ($MgCl_2$)	Merck KgaA
Membrane filter (0.45 µM)	Sarstedt
Methanol, p.a.	Sigma-Aldrich
Amersham™ Portran™ Nitrocellulose membrane	Cytiva
Pierce™ Unstained Protein MW Marker	Thermo Fisher
Potassium chloride	Merck KgaA
Potassium di hydrogen phosphate (KH_2PO_4)	Merck KgaA
(Di) Potassium hydrogen phosphate tri hydrate ($K_2HPO4 \times 3 H_2O$)	Roth GmbH
Polypropylene column	Thermo Fisher
PD-10 Sephadex™ G-25 desalting column	GE Healthcare
PVDF Transfer membrane	Merck KgaA
Skim Milk Powder	Sigma-Aldrich
Sodium chloride	Sigma-Aldrich
Sodium dodecyl sulfate (SDS)	Roth GmbH
Sodium-di-hydrogen phosphate (NaH_2PO_4)	Merck KgaA
(Di) Sodium hydrogen phosphate (Na_2HPO_4)	Sigma-Aldrich
Sodium hydroxide (NaOH)	Sigma-Aldrich
Succinyl-Leu-Tyr-AMC (Suc-LY-AMC)	Enzo
Superdex™ 200 10 300	GE Healthcare
Superdex™ 200 Increase 3.2 300	GE Healthcare
Tris (hydroxymethyl) aminomethane (Tris)	Sigma-Aldrich
Tris (hydroxymethyl) aminomethane-HCl (Tris-HCl)	Sigma-Aldrich
Tryptone	Sigma-Aldrich
Tween 20	Roth GmbH
Yeast extract	Sigma-Aldrich

Table 2.3: Restriction enzymes and polymerases

Name	Company
*Bam*HI-HF®	NEB
*Dpn*I	NEB
*Hind*III-HF®	NEB
*Kpn*I-HF®	NEB
*Nco*I-HF®	NEB

*Nde*I	NEB
*Xho*I	NEB
Phusion™ High fidelity DNA polymerase	Thermo Fisher Scientific
Q5® high fidelity DNA polymerase	NEB
ReproFast polymerase	Genaxxon

Table 2.4: Enzymes

Name	Company
Antarctic Phosphatase	NEB
cOmplete™ mini, EDTA free, Protease Inhibitor Cocktail	Roche
DNAase I, RNAse-free	Thermo Fisher Scientific
Lysozyme, chicken egg	Thermo Fisher Scientific
Proteinase K	Analytik Jena
T4 DNA Ligase	NEB/ Thermo Fisher Scientific

Table 2.5: Kits

Name	Company
GeneJet Plasmid Miniprep Kit	Thermo Fisher Scientific
innuPREP Bacteria DNA Kit	Analytik Jena
innuPREP DOUBLEpure Kit	Analytik Jena
Quick Change II Site directed mutagenesis Kit	Agilent Technologies

Table 2.6: Antibodies

Name	Company/manufacturer
Rabbit anti-*Streptomyces* ClpP1 antibody, polyclonal	Philippe Mazodier
Rabbit anti-PopR antibody, polyclonal	Philippe Mazodier
Goat anit-Rabbit IgG Secondary antibody, HRP-conjugate	Pierce
Mouse anti-6×Histidine mAB	IBA
Rabbit anti-mouse pAp, HRP-conjugate	IBA

2.1.3 Strains, plasmids and oligonucleotides

Table 2.7: Strains

Name	Genotype	Source/References
Escherichia coli - K12 JM109	*endA1 glnV44 thi-1 relA1 gyrA96 recA1 mcrB+ Δ(lac-proAB) e14- [F' traD36 proAB+ lacIq lacZΔM15] hsdR17(rK-mK+)*	AiCuris GmbH & Ko. KG (Yanisch-Perron et al., 1985)

Escherichia coli DH5α	*Δ(argF-lac)169*, ϕ80d*lacZ58*(M15), *ΔphoA8*, *glnX44*(AS), *λ-*, *deoR481*, *rfbC1*, *gyrA96*(NalR), *recA1*, *endA1*, *thiE1*, *hsdR17*	Thermo Fisher Scientific
Escherichia coli XL1-Blue	*recA1 endA1 gyrA96 thi-1 hsdR17 supE44 relA1 lac pr B lacIqZΔM15 Tn10 (Tetr)]*	Agilent GmbH
Escherichia coli SG1146a	BL21(DE3) *ClpP::cam*	(Maurizi et al., 1990a)
Streptomyces hawaiiensis NRRL 15010		Eric Cheng, Wisconsin (Michel and Kastner, 1985)

Table 2.8: Plasmids

Plasmids	Relevant characteristics	Source
pET11a	vector for the expression of native proteins T7 *lac* promoter, lacI repressor, Amp^R	Novagen
pET22b	vector for the expression of C-terminal His_6-fusion proteins T7 *lac* promoter, lacI repressor, Amp^R	Novagen
pETDUET-1	vector for the co-expression of two target genes Two T7 *lac* promoters, lacI repressor, Amp^R	Novagen
pET28aShclpP1	pET28a + ORF CEB94_14110 (*S. hawaiiensis clpP1*)	Gift from J. Ortega
pET21bShclpP2	pET21b + ORF CEB94_14105 (*S. hawaiiensis clpP2*)	Gift from J. Ortega
pET11aShclpP1$_{ATG2}$	pET11a + ORF CEB94_14110 (*S. hawaiiensis clpP1*)	This study
pET22bShclpP1$_{ATG2\text{-}His6}$	pET11a + ORF CEB94_14110 (*S. hawaiiensis clpP1*)	This study
pET11aShclpP2	pET11a + ORF CEB94_14105 (*S. hawaiiensis clpP2*)	This study
pET22b*_Nco_I-ShclpP2$_{\text{-}His6}$	pET22b*_Nco_I + ORF CEB94_14105 (*S. hawaiiensis clpP2*)	This study
pET11aShclpP2$_{ATG2}$	pET11a + ORF CEB94_14105 (*S. hawaiiensis* clpP2)	This study
pET22b*_Nco_I-ShclpP2$_{ATG2\text{-}His6}$	pET22b*_Nco_I + ORF CEB94_14105 (*S. hawaiiensis clpP2*)	This study
pET22bShclpP1*$_{\text{-}His6}$	pET22b + ORF CEB94_14110 (*S. hawaiiensis clpP1*)	This study
pET22b*_Nco_I-ShclpP2*$_{\text{-}His6}$	pET22b + ORF CEB94_14105 (*S. hawaiiensis clpP2*)	This study
pET11aShclgR$_{\text{-}N\text{-}His6}$	pET11a + ORF CEB94_30145 (*S. hawaiiensis clgR*)	This study
pET11aShpopR$_{\text{-}N\text{-}His6}$	pET11a + MT943519 (*S. hawaiiensis popR*)	This study
pETDUETShclpP1$_{ATG2}$clpP2$_{\text{-}His6}$	pETDUET-1 + ORF CEB94_14110 + 14105 (*S. hawaiiensis clpP1+P2*)	This study
pET22b*_Nco_I-ShclpX$_{\text{-}His6}$	pET22b*_Nco_I + ORF CEB94_14100 (*S. hawaiiensis clpX*)	Janna Hauser
pET22b*_Nco_I-ShclpC1$_{\text{-}His6}$	pET22b*_Nco_I + ORF CEB94_23085 (*S. hawaiiensis clpC1*)	Janna Hauser
pET22bShclpC2$_{\text{-}His6}$	pET22b + ORF CEB94_33910 (*S. hawaiiensis clpC2*)	D. Latifovic
pET22bShclpP1$_{S113A}$	pET22bShclpP1$_{\text{-}His6}$ carrying aa mutation S113A in the *S. hawaiiensis clpP1* gene	This study
pET22b*_Nco_I-ShclpP2$_{S131A}$	pET22b*_Nco_I-ShclpP2$_{\text{-}His6}$ carrying aa mutation S131A in the *S. hawaiiensis clpP2* gene	This study
pET22b*_Nco_I-ShclpP2$_{S131A\text{-}ATG2}$	pET22b*_Nco_I-ShclpP2$_{ATG2\text{-}His6}$ carrying aa mutation S131A in the *S. hawaiiensis clpP2* gene	This study
pET11aShclpP1$_{hp}$	pET11aShclpP1 carrying aa mutation Y76V, Y78V, Y98V in the *S. hawaiiensis clpP1* gene	This study
pET22b*_Nco_I-ShclpP2$_{hp}$	pET22b*_Nco_I-ShclpP2$_{ATG2\text{-}His6}$ carrying aa mutation S94A, Y96V, Y116V in the *S. hawaiiensis clpP2* gene	This study
pET11aShclpP1$_{Y76SATG2\text{-}His6}$	pET11aShclpP1 carrying aa mutation Y76S in the *S. hawaiiensis clpP1* gene	This study
pET22b*_Nco_I-ShclpP2$_{S94YATG2\text{-}His6}$	pET22b*_Nco_I-ShclpP2$_{ATG2\text{-}His6}$ carrying aa mutation S94Y in the *S. hawaiiensis clpP2* gene	This study
pET22bShclpP$_{ADEP\text{-}His6}$	pET22b + $_{clpADEP\text{-}His6}$ expressing aa 1-206	This study
pET22bShclpP$_{ADEP\text{-}short\text{-}His6}$	pET22b + *clpP$_{ADEP\text{-}short\text{-}His6}$* expressing aa 16-206	This study

Table 2.9: Synthetic Oligonucleotides: Restriction sites are underlined

Plasmids		Forward (F)/Reverse (R) oligo (5'- 3' direction)	Template
pET11aShclpP1$_{ATG2}$		F: aaacatatgacgaatctgatgccctcagc (ClpP1_fw_*Nde*I) R: aaaggatcctcaggccccggtgccgc (ClpP1_rev_*Bam*HI)	pET28ShclpP1
pET22bShclpP1$_{ATG2\text{-}His6}$		F: aaacatatgacgaatctgatgccctcagc (ClpP1_fw_*Nde*I) R: taaactcgagggccccggtgccgcc (ClpP1_rev_*Xho*I)	pET28aShclpP1
pET11aShclpP2		F: aaacatatgaaccagttccccggcag (ClpP2_long_*Nde*I) R: aaaggatcctcagcgcaggctcgagttgtc (ClpP2_rev_*Bam*HI)	*S. hawaiiensis* genomic DNA
pET22b**Nco*I-ShclpP2$_{\text{-}His6}$		F: aaacatatgaaccagttccccggcag (ClpP2_long_*Nde*I) R: aaaccatgggcgcaggctcgagttgtc (ClpP2_rev_*Nco*I)	*S. hawaiiensis* genomic DNA
pET11aShclpP2$_{ATG2}$		F: aaacatatgagcgcctcccagggc (ClpP2_fw_*Nde*I) R: aaaggatcctcagcgcaggctcgagttgtc (ClpP2_rev_*Bam*HI)	pET21bShclpP2
pET22b**Nco*I-ShclpP2$_{ATG2\text{-}His6}$		F: aaacatatgagcgcctcccagggc (ClpP2_fw_*Nde*I) R: aaaccatgggcgcaggctcgagttgtc (ClpP2_rev_*Xho*I)	pET21bShclpP2
pET22bShclpP1*$_{\text{-}His6}$		F: aaacatatgccttccatcggtggtggcctcggt (ClpP1_*Nde*_MS) R: taaactcgagggccccggtgccgcc (ClpP1_rev_*Xho*I)	pET22bShclpP1$_{\text{-}His6}$
pET22b**Nco*I-ShclpP2*$_{\text{-}His6}$		F: aaacatatgcgctacatcattccccgcttc (ClpP2_*Nde*_MS) R: aaaccatgggcgcaggctcgagttgtc (ClpP2_rev_*Nco*I)	pET22b**Nco*I-ShclpP2$_{\text{-}His6}$
pET11aShclgR$_{\text{-}N\text{-}His6}$		F: aaacatatgcaccaccaccaccaccacattctgctccgtcgcctgctgggtgacgtg (ClgR*Nde*I) R: taaggatcctcacgcggcgacgacgtccactgc (ClgR*Bam*HIrev)	*S. hawaiiensis* genomic DNA
pET11aShpopR$_{\text{-}N\text{-}His6}$		F: aaacatatgcaccaccaccaccaccacaccagccacctgccgaacgaagcccgagtc (PopR_*Nde*_His_fw) R: taaggatcctcaggcggccaggcacattccgtcgtg (PopR_*Bam*HI)	*S. hawaiiensis* genomic DNA
pETDUETShclpP1clpP2$_{\text{-}His6}$	clpP1	F: aaacatatgacgaatctgatgccctcagc (ClpP1_fw_*Nde*I)	pET11aShclpP1$_{ATG2}$
		R: aaaggtacctcaggccccggtgcc (ClpP1_*Kpn*I)	pET22b**Nco*I-ShclpP2$_{\text{-}His6}$
	clpP2	F: aaaccatgggaaaccagttccccggcagcg (ClpP2_long_*Nco*I)	
		R: aaaaagctttcagtggtggtggtggtggcgcaggctcgagttgtccatcttcc (ClpP2_long_His_HindIII)	
pET22bShclpC2$_{\text{-}His6}$		F: aaacatatgagcagcggcttcaccagc (ClpC2_*Nde*_fw) R: taaactcgagtcggggcacggtactgaacg (ClpC2_long_*Xho*I) F: gagtaccgccggatcgagaaggac → for sequencing (ClpC2seqfw)	*S. hawaiiensis* genomic DNA
pET22bShclpP1$_{S113A}$		F: gggcctggcagccgcgatgggccagttc (ClpP1S113A_fw) R: gaactggcccatcgcggctgccaggccc (ClpP1S113A_rev)	pET22bShclpP1$_{\text{-}His6}$
pET22bShclpP2$_{S131A}$		F: ccaggcggccgccgccgccgccgtc (ClpP2S131A_fw) R: gacggcggcggcggcggccgcctgg (ClpP2S131A_rev)	pET22b**Nco*I-ShclpP2$_{\text{-}His6}$

pET11aShclpP1$_{hp}$	F: gacggcggcggcggccgcctgg (ClpP1hp_fw) R: cctcttcctgtagcaggaccagtagttgtcggggccg (ClpP1hp_rev) F: gacaccatgcaggtcatcaagaacgac (ClpP1Y98V_fw) R: gtcgttcttgatgacctgcatggtgtc (ClpP1Y98V_rev)	pET11aShclpP1$_{ATG2}$
pET22bShclpP2$_{hp}$	F: cgaccgtgacatcgcggtggtcatcaacagccccggc (ClpP2hp_fw) R: gctggcactgtagcgccaccagtagttgtcggggccg (ClpP2hp_rev) F: gacacgatgcaggtcgtgaagccggac (ClpP2Y116V_fw) R: gtccggcttcacgacctgcatcgtgtc (ClpP2Y116V_rev)	pET22b*_Nco_I-ShclpP2$_{ATG2\text{-}His6}$
pET11aShclpP1$_{Y76S}$	F: gagaaggacatctccctgtacatcaacag (ClpP1$_{Y76S}$fw) R: ctgttgatgtacagggagatgtccttctc (ClpP1$_{Y76S}$rev)	pET11aShclpP1$_{ATG2}$
pET22bShclpP2$_{S94YATG2\text{-}His6}$	F: gaccgtgacatctacgtgtacatcaac (ClpP2$_{S94Y}$fw) R: gttgatgtacacgtagatgtcacggtc (ClpP2$_{S94Y}$rev)	pET22b*_Nco_I-ShclpP2$_{ATG2\text{-}His6}$
pET22bShclpP$_{ADEP\text{-}His6}$	F: aaacatatgaaggacattaaggaactgacgg (ClpP$_{ADEP}$_fw_NdeI) R: taaactcgagcttcgctgccccgatattg (ClpP$_{ADEP}$_rev_XhoI)	*S. hawaiiensis* genomic DNA
pET22bShclpP$_{ADEP\text{-}short\text{-}His6}$	F: taacatatgcggtggaacctgaacgaccag (ClpP$_{ADEP}$_*Nde*I_RWN) R: taaactcgagcttcgctgccccgatattg (ClpP$_{ADEP}$_rev_*Xho*I)	pET22bShclpP$_{ADEP\text{-}His6}$

2.1.4 Media

Liquid media:

LB medium (Lysogeny-Broth) (Bertani, 1951)

Substance	Final concentration	Amount per 1 L
Tryptone	1 %	10 g
Yeast extract	0.5 %	5 g
NaCl	1 %	10 g

Add 1 L Milli-Q® water → pH 7.3 → sterilize

TB medium (Terrific Broth)

900 ml TB medium + 100 ml 10 × TB salts

Substance	Final concentration	Amount per 1 L
Tryptone	1.2 %	12 g
Yeast extract	2.4 %	24 g

Glycerin	0.5 %	5 g

→ add 900 ml Milli-Q® water

10 × TB salts

Substance	Final concentration	Amount per 100 ml
KH_2PO_4	0.17 M	2.3 g
K_2HPO_4	0.72 M	12.5 g

→ add 100 ml Milli-Q® water and autoclave seperatively

TSB medium (Tryptic Soy Broth)

Substance	Final concentration	Amount per 1 L
Tryptic Soy Broth	30 %	30 g

→ add 1 L Milli-Q® water, sterilize

TYM medium (Tryptone-Yeast-Magnesium)

Substance	Final concentration	Amount per 1 L
Tryptone	2 %	20 g
Yeast extract	0.5 %	5 g
NaCl	0.584 %	5.84 g
Magnesium sulfate	0.246 %	2.46 g

→ add 1 L Milli-Q® water, sterilize

Solid media:

LB agar

Substance	Final concentration	Amount per 1 L
Tryptone	1 %	10 g
Yeast extract	0.5 %	5 g
NaCl	1 %	10 g
Agar	1.5 %	15 g

→ add 1 L Milli-Q®, pH 7.3 → sterilize

2.1.5 Markers

Table 2.10: Markers

Name	Company
GeneRuler™ 1 kb	Thermo Fisher Scientific
GeneRuler™ DNA ladder mix	Thermo Fisher Scientific
Pierce™ Unstained Protein MW marker	Thermo Fisher Scientific
PageRuler™ Unstained Protein ladder	Thermo Fisher Scientific
PageRuler™Plus Prestained Protein ladder	Thermo Fisher Scientific
Colour Prestained Protein Standard, Broad Range	NEB
Native Marker, Liquid Mix for BN/CN	Serva

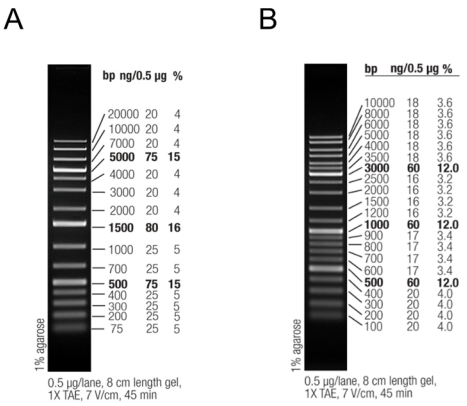

Figure 2.1: **GeneRuler™ 1 kb DNA ladder and GeneRuler™ DNA ladder mix**. DNA bands are visualised on a 1 % TAE agarose-gel.

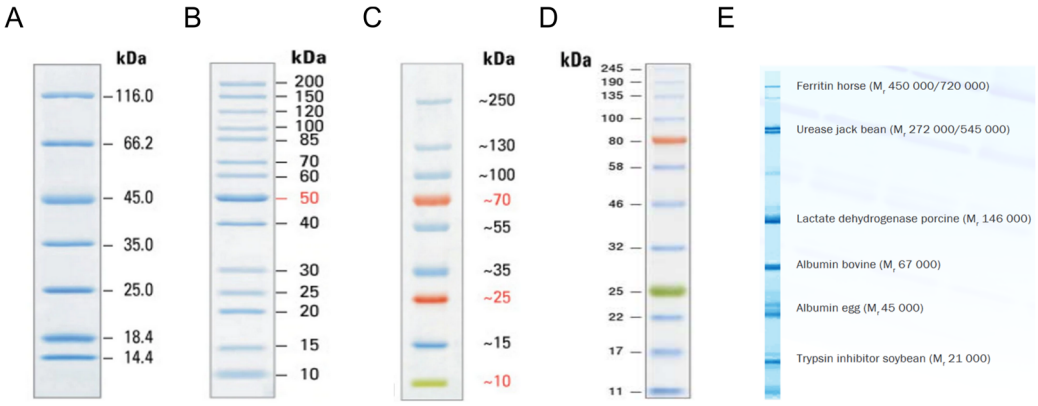

Figure 2.2: **Protein ladder, unstained and prestained. A**: Pierce™ Unstained Protein MW marker visualised on a 12 % Tris-Glycine gel after coomassie blue staining. **B**: PageRuler™ Unstained Protein ladder on a 8-16 % Tris-Glycine gel, stained with coomassie blue. **C**: PageRuler™Plus Prestained Protein ladder (10 – 250 kDa) on a 4-20% Tris-Glycine gel. **D**: Colour Prestained Protein Standard, Broad Range on a 10-20 % Tris-Glycine gel. **E:** Serva Native Marker Liquid Mix for BN/CN PAGE on Serva*Gel*™ N 4-16 %.

2.1.6 Internet sources

Table 2.11: Internet sources

Programmeme/tool	Application	Source
BLAST	Basic Local Alignment Search Tool; Comparison of nucleotide or amino acid sequences with data bases	https://blast.ncbi.nlm.nih.gov/Blast.cgi
Clustal omega	Alignment of nucleotide or amino acid sequences	http://www.ebi.ac.uk/Tools/msa/clustalo
ExPasy Translate	Translastion of nucleotide sequences into amino acid sequences	https://web.expasy.org/translate/
protparam	Computation of various physical and chemical parameters of proteins	https://web.expasy.org/protparam/
Uniprot	Protein data base	https://www.uniprot.org/
Ncbi (National Center for Biotechnology Information)	Database for biomedical and genomic information	https://www.ncbi.nlm.nih.gov/
pI/MW tool expasy	Computation of the theoretical pI and MW of proteins	https://web.expasy.org/compute_pi/
Protein Calculator v3.4	Computation of estimated charge of proteins over pH range, pI, etc.	http://protcalc.sourceforge.net/

2.2 Methods

2.2.1 Cultivation and conservation of bacterial strains

For the cultivation of bacterial strains, LB medium was supplemented with the respective antibiotic and the cells were grown over night at 37°C, 180 rpm, see table 2.12. To conserve bacterial strains, 500 µl or 1 ml of bacterial overnight cultures were added to equal volumes (v/v: 1:1) of 60 % glycerin and subsequently mixed and stored at -80°C.

Table 2.12: Cultivation of bacterial strains

Strain	With Plasmid	Solid/Liquid media
Escherichia coli JM109	-	-
	pET11a	LB + ampicillin (200 µg/ml final concentration)
	pET22b	LB + ampicillin (200 µg/ml)
Escherichia coli DH5α	-	-
	pET11a	LB + ampicillin (200 µg/ml)
	pET22b	LB + ampicillin (200 µg/ml)
Escherichia coli XL-1 *Blue*	-	-
	pET11a	LB + ampicillin (200 µg/ml)
	pET22b	LB + ampicillin (200 µg/ml)
	pETDUET-1	LB + ampicillin (200 µg/ml)
Escherichia coli SG1146a	-	LB + chloramphenicol (30 µg/ml)
	pET11a	LB + ampicillin (200 µg/ml)
	pET22b	LB + ampicillin (200 µg/ml)
	pETDUET-1	LB + ampicillin (200 µg/ml)

2.2.2 Measuring bacterial growth

Bacterial growth was determined by measuring the optical density at 600 nm (OD_{600}). Therefor, 1 ml of a bacterial liquid culture was transferred into a plastic cuvette (layering thickness: 1 cm) similarly to the reference which consists of pure liquid medium.

2.2.3 Isolation of genomic DNA

Genomic DNA of *Steptomyces hawaiiensis* NRRL 15010 was isolated using the innuPrep bacterial DNA Kit (Analytik Jena) according to the manufacturer's protocol. Previously, 20 ml TSB medium was inoculated with 5 µl of *S. hawaiiensis* spores and incubated for approx. 48 h at 30°C. However, the amount of added lysozyme to the bacterial culture was adjusted to ensure sufficient hydrolysis of the *Streptomyces* mycelium using 10 µl of lysozyme (50 mg/ml) for at least 2 h at 37°C.

2.2.4 DNA amplification via polymerase chain reaction (PCR)

For the amplification of the respective gene of interest, a polymerase chain reaction (PCR) was performed employing a heat-stabile DNA-polymerase such as phusion or Q5 polymerase in a reaction mixture consisting of DNA as template (plasmid or genomic DNA), primer and nucleotides. After the initial denaturation of the double-stranded DNA molecule at 95-98°C (according to the respective polymerase), primer anneal with complementary parts of the single stranded DNA template at 50-70°C, which are elongated at 72°C by the polymerase. Via repetition of the denaturing, annealing and elongation step, the respective gene of interest can be amplified and visualised via agarose gel electrophoresis. Annealing temperatures were calculated using the NEB Tm calculator, or by employing a temperature gradient. The Phusion or Q5 polymerase was utilised in this study with the respective protocols:

Table 2.13: PCR protocol Phusion/ Q5 polymerase

Ingredients	Volume	Stock concentration	Final concentration
Phusion HF / Q5 buffer	10 µl	5 ×	1 ×
dNTPs	1 µl	10 mM	200 µM
Fw primer	2.5 µl	10 µM	0.5 µM
Rev primer	2.5 µl	10 µM	0.5 µM
Template DNA	Conc. dependent	variable	Up to 100 nM
DMSO/ Q5 high GC enhancer	1.5 µl / 10 µl	100 % / 5×	3 % / 1 ×
Phusion® DNA polymerase/ Q5® DNA polymerase	0.5 µl	2000 U/ml	0.02 U/µl

→ add 50 µl Milli-Q®

Table 2.14: PCR programme utilising phusion/Q5 polymerase

	Temperature Phusion/Q5	Duration Phusion/Q5	Number of cycles
Initial denaturation	98	3/1 min	1
Denaturation	98	10/30 sec	
Annealing	variable	30/30 sec	30
Elongation	72	20/30 s per kb	

Final Elongation	72	10/2 min	1

2.2.5 Site-directed mutagenesis

In order to mutate plasmid DNA, a site-directed mutagenesis was performed with two complementary primers, which contain the desired mutation in the middle and are used to amplify the entire plasmid. The primers were designed according to the protocol of the Site-directed mutagenesis Kit II (Agilent). The reaction was performed according to the following protocol:

Table 2.15: Site-directed mutagenesis protocol

Components	Final concentration	volume
DNA	200 ng	variable
Primer fw (10 µM)	0.1 µM	1 µl
Primer rev (10 µM)	0.1 µM	1 µl
dNTPs (10 mM)	250 µM	1.25 µl
Reprofast buffer	10 ×	5 µl
Reprofast polymerase	5 U	1 µl

→ add 50 µl Milli-Q®

Table 2.16: Site-directed mutagenesis programme

	Temperature	Duration	Number of cycles
Initial denaturation	95 °C	3 min	1
Denaturation	95 °C	1 min	
Annealing	50 °C	1 min	19
Elongation	68°C	20 min	
Final Elongation	68°C	10 min	1

In order to digest the methylated, non-mutated template DNA, 1 µl DpNI was added to the reaction mixture as well as 5 µl of 10 × cutsmart® buffer and incubated at 37°C over night. Afterwards, 10 µl of the reaction was transformed in chemically competent *E. coli* cells.

2.2.6 Agarose gel electrophoresis

DNA samples can be separated via agarose gel electrophoresis in which the negatively charged DNA runs towards the positive pole in the agarose gel matrix by generating an electric current on the agarose gel which is covered in TAE × buffer. PCR products or plasmids are separated according to their size and the size of the pores within the agarose matrix. The pore size of the agarose gel is determined by the applied concentration of agarose, a polysaccharide consisting of D-galactose and 3, 6-anhydro-L-galactose.

In this study, 0.8 and 1 (w/v) % agarose gels were used. Therefor, the agarose was dissolved in the appropriate amount of TAE buffer by shortly boiling the mixture in a microwave oven and then casted in a gel tray, which was covered by TAE-buffer, once it hardened. DNA samples were mixed with 6× Gel Loading Dye (NEB) or 10 × Fast Digest Green Buffer (Thermo Fisher Scientific) (v/v: 3:1) and applied to the different wells in the gel. Additionally, a size marker (GeneRuler™ 1 kb ladder or GeneRuler™ ladder mix (Thermo Fisher Scientific)) was applied to the gel as well. Electrophoresis was performed for 30-120 min at 80-120 V depending on the gel size and the required resolution. After finishing the electrophoresis, DNA bands could be visualised by incubating the agarose gel in a solution of 0.0004 % w/v ethidium bromide, which intercalates the DNA, thereby increases fluorescence emission upon UV irradiation.

50 × TAE-buffer

Subtance	Amount per 500 ml
EDTA-Disodium	9.31 g
Tris	121.14 g
Pure acetic acid	27 ml

→ add 500 ml Milli-Q® water, pH 8

Before usage, 50 × TAE buffer was dissolved (v/v: 1/49) with Milli-®Q water.

2.2.7 Purification of DNA fragments

Amplified PCR products were purified using the innuPrep DOUBLEpure Kit (Analytik Jena) according to the manufacturer's protocol "Purification and concentration of PCR products".

Isolated DNA, which was cut out of the agarose gel, was purified according to the protocol “DNA extraction from agarose gel slices”.

2.2.8 Determination of DNA concentration

Concentrations of DNA were calculated by measuring the absorption at 260 nm utilising a spectrophotometer (Nano-drop 2000c, Thermo Fisher Scientific). Since proteins absorb light at 280 nm, the purity of DNA samples can be determined by analysing the coefficient of A260/A80 nm. DNA samples, whose A260/A280 values are located within the range of 1.8-2 can be considered as pure.

2.2.9 Restriction enzyme digestion and dephosphorylation

PCR products and plasmids were digested utilising high fidelity restriction endonucleases (NEB), which are listed in table 2.3. The restriction enzymes used belong to type II of restriction endonucleases that cleave within or near their recognition sequences and create sticky or blunt ends. For the digestion of plasmids and PCR products, the DNA concentration was adjusted to 1 µg in 50 µl reaction volumes. Additionally, plasmids were dephosphorylated by adding the Antarctic phosphatase to the reaction mixture.

Table 2.17: Protocol for restriction enzyme digestion

	Plasmids	PCR products
DNA	Adjusted to 1 µg	Adjusted to 1 µg
Enzyme 1	1 µl	1 µl
Enzyme 2	1 µl	1 µl
Cutsmart® buffer (10 ×)	5 µl	5 µl
Antarctic Phosphatase	1 µl	-
Antarctic Phosphatase buffer	1 µl	-
Milli-Q® water	add 50 µl	add 50 µl

The reaction mixture was incubated for at least two hours or over night at 37°C. Subsequently, the PCR products or plasmids were purified using the innuPrep DOUBLEpure Kit protocol

"Purification and Concentration of PCR products" or alternatively when isolated via agarose gel electrophoresis according to the protocol "DNA extraction from agarose gel slices". For the analysis of plasmids, control digestions were carried out in smaller 20 µl volumes for 2 h at 37°C and lower DNA concentrations.

2.2.10 Ligating DNA fragments

Ligation of digested DNA fragments was carried out employing the T4 ligase (Thermo Fisher Scientific or NEB) which catalyses the formation of phosphodiester bonds of the digested double stranded DNA under ATP-consumption. Typically, a threefold excess of the DNA insert was added to the linearized vector in 10 µl reaction volumes. Therefor, 70 ng of the digested vector was used and the amount of insert was calculated by the following formula:

$$\text{Insert [ng]: } \frac{70\ \text{ng} * (\text{size of digested insert [kb]})}{\text{size of digested vector [kb]}} * 3$$

If needed, the calculated amount of DNA insert was increased up to a sixfold excess which was added to the linearized vector in 10 or 20 µl reaction volumes.

Table 2.18: Protocol for ligating DNA fragments

components	10 µl (reaction volume)	20 µl
T4 DNA ligase	1 µl	1 µl
10 × T4 DNA buffer	1 µl	2 µl
DNA insert	variable	variable
Linearized vector	70 ng	70 ng
Milli-Q®	Add 10 µl	Add 20 µl

The reaction was carried out over night at 22°C (Thermo Fisher Scientific) or 16°C (NEB). Afterwards 10 µl of the samples were transformed into chemically competent *E. coli* JM109, XL-1 Blue or DH5α cells.

2.2.11 Transformation of chemically competent *E. coli* cells

For the transformation of chemically competent cells, 1 µl of plasmid DNA or 10 µl of reaction mixture was incubated with 50 µl thawed cells for 30 min on ice. A heat shock was performed for

90 sec at 42°C, allowing the DNA to enter the cells. After a 5 min incubation on ice, 500 µl LB medium was added to the reaction mixture and incubated for 1 h at 37°C, 180 rpm. In case of transforming a ligation mixture, the samples were centrifuged for 3 min at 10 847 g (9 000 rpm) and the pellet resuspended in 150 µl LB medium and plated onto an antibiotic containing LB-agar plate. If plasmid DNA was transformed, 150 µl of the samples were plated on antibiotic containing LB-agar plates and incubated over night at 37°C.

2.2.12 Preparation of chemically competent *E. coli* cells

For the preparation of chemically competent cells, 50 ml TYM medium was inoculated (1:100) with an overnight culture of the respective *E. coli* strain of interest and incubated at 37°C, 180 rpm until an OD_{600}: 0.5 – 0.7 was reached. The cells were centrifuged for 10 min at 4 098.7 g (4 000 rpm), 4 °C and the pellet resuspended on ice in 5 ml cold TFBI medium. Afterwards, another centrifugation step was performed and the pellet resuspended in 2.5 ml cold TFBII medium. The cells were shock frozen with liquid nitrogen in 50 ml aliquots and stored at -80°C.

TFBI:

Substance	Final concentration	Amount per 50 ml
Potassium acetate (5M)	30 mM	0.3 ml
MnCl2	50 mM	495 mg
KCl (2 M)	100 mM	2.5 ml
CaCl2 (1 M)	10 mM	0.5 ml
Glycerin	15 %	7.5 ml

→ add 50 ml Milli-Q® water

TFBII:

Substance	Final concentration	Amount per 50 ml
MOPS (2 M), pH7	10 mM	2.5 ml
CaCl2 (1 M)	75 mM	3.7 ml
KCl (2 M)	10 mM	250 µl
Glycerin	15 %	7.5 ml

→ add 50 ml Milli-Q® water

2.2.13 Isolation of plasmid DNA from bacterial cultures

The isolation of plasmid DNA from *E. coli* strains was carried out according to the protocol of the GeneJET Plasmid Miniprep Kit (Thermo) with 4 ml of overnight culture.

2.2.14 Protein purification

In this study, native as well as C-terminally His_6-tagged proteins were purified either via anion exchange chromatography or immobilised metal ion affinity chromatography (IMAC).

2.2.14.1 Protein expression

Before the respective proteins of interest were expressed for subsequent protein purification, the expression of the protein was analysed by inducing the cells in the exponential growth phase (OD_{600}: 0.5-0.6) with 1 mM IPTG for 4 h at 37°C. Before and after induction of protein expression, 1 ml cell culture was centrifuged for 1 min at 16 873 g (14 000 rpm) and the cell pellet was resuspended in lysis buffer pH 7.7, see 2.2.15. For an SDS-PAGE analysis, 10 µl of the resuspended cell pellet was mixed with 4× Bolt™ LDS sample buffer, consisting 100 mM DTT and loaded on an SDS-PAGE gel, see 2.2.16.

For the purification of the proteins used in this study, the following conditions were applied:

Table 2.19: Protein expression conditions

Protein	Temp. after induction	Expression time after induction	Medium	Volume	IPTG final conc.
ClpP1	30 °C	3-4 h	LB	1 L	1 mM
ClpP2	30 °C	5 h /16 h	LB	1 L	0.5 mM
ClpX	30 °C	4-5 h	LB	4 L	0.5 mM
ClpC1	30°C	4-5 h	LB	3 L	0.5 mM
ClpC2	30°C	4-5 h	LB	3 L	0.5 mM
ClgR	16°C	16 h	LB	1 L	0.5 mM
PopR	30°C	4-5 h	LB	1 L	0.5 mM
$ClpP_{ADEP}$	20°C	4-5 h	LB	8 L	0.08 mM

$ClpP_{ADEP\text{-}short}$	20°C	16 h	TB	4 L	0.1 mM

Wild-type, as the mutant proteins of ClpP1 and ClpP2, were expressed under similar conditions. As a following step, the cells were harvested for 30 min at 17 568 g, 4°C with the Sorvall LYNX 4000 centrifuge or for at least 45 min at 4 816 g, 4°C with the Heraeus Multifuge X3R. Subsequently the cell pellets were stored at -20°C.

2.2.14.2 Cell disruption

The previously harvested cells were resuspended in the appropriate buffer (10 ml buffer per 1 L harvested cells) and disrupted utilising 0.5 g glass beads (150-212 µm) in 15 ml tubes with a precellys homogenizer and the following programme:

3 × 20 sec at 6 500 rpm, 15 sec pause in between each run.

This programme was repeated for four times in order to ensure a complete disruption of the cells which were cooled on ice in between each run for at least 10 min. As a following step, the disrupted cells were centrifuged for 30 min at 4 816 g (Heraeus Multifuge X3R) and further processed depending on different purification procedures for native (anion exchange chromatography) and His_6-tagged proteins (immobilised nickel ion affinity chromatography).

2.2.14.3 Anion exchange chromatography

Anion exchange chromatography was performed in order to purify native ClpP1, ClpP2 as well as the mutant proteins $ClpP1_{hp}$ and $ClpP1_{Y76S}$. This method is based on purifying native proteins according to its negative charge at a certain pH, which then can bind to positively charged Q sepharose columns, such as HiTrap™ Q XL with 1 or 5 ml column volumes (GE Healthcare). Therefor, the cells are resuspended in buffer A and applied to the column, whereas unspecifically and weakly bound proteins are washed off the column. As a following step, the column-bound protein of interest can then be eluted by displacing it, utilising negatively charged chloride ions which are present in buffer B.

Buffer A, pH 8: 20 mM Tris **Buffer B, pH 8:** 20 mM Tris, 1 M NaCl

To ensure that both ClpP homologues are negatively charged at pH 8, a calculation of the protein charge at the respective pH was done by using the protein calculator v3.4, see table 2.11. After resuspending the cells in buffer A, a cell disruption was performed, followed by a centrifugation step, see 2.2.14.2. Subsequently, the supernatant was applied to the Äkta Pure chromatography system. For the anion exchange chromatography, a HiTrap™ Q XL column was used, either with 1 or 5 ml column volume, see table 2.20.

Table 2.20: Biochemical properties of HiTrap™ Q XL columns

column	Column volume (CV)	Flow rate	Pressure limit
HiTrap™ Q XL	0.962 ml	1 ml/min	0.3 mPa
HiTrap™ Q XL	5.027 ml	5 ml/min	0.3 mPa

According to the column volume, different programmes were used, as it is seen in table 2.21:

Table 2.21: Anion exchange chromatography programme for 1/5 ml HiTrap™ Q XL columns

Method settings	1 ml column	5 ml column
Prime and equilibration	5 CV	5 CV
Sample application	variable	variable
Wash out unbound	20 CV	10 CV
Elution and fractionation	Linear gradient elution: Start with 0 % B Target % B Volume Concentration 100.0 30 CV Step gradient elution: 100.0 5 CV	Linear gradient elution: Start with 5 % B Target % B Volume Concentration 100.0 20 CV Step gradient elution: 100.0 1 CV
Prime and equilibration	5 CV	5 CV

The elution was performed in 0.5 ml (HiTrap™ Q XL column, 1 ml) or 1 ml (HiTrap™ Q XL column, 5 ml) fractions.

To purify ClpP1 and the mutant proteins $ClpP1_{hp}$ and $ClpP1_{Y76S}$, both HiTrap™ Q XL columns with 1 and 5 ml column volumes were utilised whereas for ClpP2, only the HiTrap™ Q XL column, 5 ml was applied.

According to the absorption spectrum at A280 nm as well as an SDS-PAGE analysis, the fractions consisting of the highest amount of the protein of interest, were pooled and the volume of the protein solution was decreased in centrifugal filters (Amicon®Ultracel®-10 K, Merck) by performing multiple centrifugation steps (5-10 min, 4 098.7 g, 4°C) to reach a required volume of 2.5 ml. As a following step, a buffer exchange was performed, applying a PD-10 Sephadex™ G-25 desalting column (GE Healthcare). The buffer exchange was performed according to the gravity protocol and the protein was eluted in 3.5 ml activity buffer pH 7.5.

Activity buffer, pH 7.5:
50 mM HEPES, KOH
150 mM KCl
20 mM $MgCl_2$
10 % glycerin

Next, the volume of the protein solution was decreased again using centrifugal filters in multiple centrifugation steps as described previously. The protein concentration was determined using a Bradford assay with BSA as reference. Aliquots, consisting of 25-30 µl purified protein, were shock frozen and stored at -80°C.

2.2.14.4 Determination of protein concentration via Bradford

In order to determine the concentration of a purified protein, BSA was used as a reference in a Bradford assay (Bradford, 1976). This assay is based upon an absorbance shift of the dye Coomassie Brilliant Blue G-250, which absorbs light differently depending on its protonated (red, A_{max}=470 nm), neutral (green, A_{max}= 650 nm) or deprotonated (blue, A_{max}= 595 nm) state (Compton and Jones, 1985). Under acidic conditions, the protonated red cationic form binds to proteins mainly to basic and aromatic amino acid residues (Compton and Jones, 1985), thereby forming a stable unprotonated blue form which can be measured at A_{max} = 595 nm (Reisner et al., 1975, Fazekas de St Groth et al., 1963, Sedmak and Grossberg, 1977). For calculating the concentration of purified proteins, the reference BSA (1 mg/ml) was diluted (v/v: 1:100) in Milli-

Q® and then mixed with 900 µl 1 × Bradford reagent, yielding a concentration range from 1 – 7 µg/ml BSA, see table 2.22.

Table 2.22: Bradford assay, utilising BSA as protein standard.

Reference	1 mg/ml BSA [µl]	Milli-Q® [µl]	Bradford (1 ×) [µl]
1	1	99	900
2	2	98	900
3	3	97	900
4	4	96	900
5	5	95	900
6	6	94	900
7	7	93	900

As a following step, 1-4 µl of the purified protein was mixed with 99-96 µl Milli-Q® water and added to 900 µl of Bradford protein dye. The absorbance of the different samples was measured at A_{595} and the protein concentration was calculated using duplicates or triplicates.

2.2.14.5 Immobilised nickel ion affinity chromatography

For the purification of Histidine-tagged proteins, an immobilised nickel ion affinity chromatography (IMAC) was performed. This method is based on the high binding affinity of the histidine-tag of the protein to nickel ions, thereby purifying the protein of interest, which can be eluted by adding high concentrations of imidazole (250-500 mM), thereby displacing the Ni-NTA-bound protein. Therefor, the following buffers were used:

Lysis buffer, pH 7.7: 50 mM NaH_2PO_4
300 mM NaCl
10 mM Imidazole

Wash buffer, pH 7.7: 50 mM NaH_2PO_4
300 mM NaCl
20 mM Imidazole

Elution buffer, pH 7.7: 50 mM NaH_2PO_4
300 mM NaCl
500 mM Imidazole

The previously harvested cells, see 2.2.14.1, were resuspended in lysis buffer and disrupted with glass beads and a precellys homogenizer, followed by a centrifugation step (see 2.2.14.2). Afterwards, 10 µl DNAse I was added to the supernatant which was centrifuged again for 30 min at 32 000 g, 4°C using the Sorvall LYNX centrifuge. Before the Ni-NTA resin was added to the supernatant, the resin was washed in three centrifugation steps (3 min, 10 847 g (9 000 rpm)) and resuspended in lysis buffer. Afterwards, 500-700 µl Ni-NTA resin was added to the supernatant and incubated for at least two hours (or overnight) on a rotation wheel at 4-6°C. Next, an immobilised nickel ion affinity chromatography was performed at 4-6 °C with a previously prepared polypropylene column. Then, the supernatant was applied to the column, allowing the Ni-NTA resin to settle. The column was washed two times with 10-12 ml of lysis and wash buffer and the flow-through, as the washing steps, were collected in 50 or 15 ml falcons. As a following step, the protein was eluted in 10 × 250 µl fractions with elution buffer. Samples of the flow-through, the washing steps, the pellet (after centrifugation of the supernatant at 32 000 g, 30 min) and the elution fractions were taken according to the following protocol:

Table 2.23: Sample preparation for SDS-PAGE analysis

Name	Sample [µl]	Milli-Q® [µl]	4×Bolt™ LDS sample buffer + 100 mM DTT [µl]
Flow-through	1	9	5
Wash I	2	8	5
Wash II	10	-	5
Elution fractions 1-10	10	-	5

The samples were applied to Bolt™ Bis-Tris gels (Thermo Fisher Scientific) for subsequent SDS-PAGE analysis. Furthermore, the elution fractions were pooled and a buffer exchange was performed, employing the PD-10 Sephadex™ G-25 desalting column (GE Healthcare), according

to the gravity protocol. Therefor, the activity buffer pH 7.5 was applied, see 2.2.14.3. To achieve a satisfying concentration of the purified protein, the volume of the protein solution was decreased by using centrifugal filters in multiple centrifugation steps (3-10 min at 2 049.4 – 4 098.7 g (2 000 - 4 000 rpm), Hereaus centrifuge X3R). The protein concentration was determined via a Bradford assay, see 2.2.14.4.

2.2.15 Size exclusion chromatography

Size exclusion chromatography was performed, to further purify proteins employing a Superdex^{TM} 200 10 300 column (GE Healthcare) with a column volume ~ 24 ml, a flow rate: 0.5 ml/min and a pressure limit of 1.5 mPa. Therefor, 500 µl of a protein solution was centrifuged for 2 min at 16 873 g (14 000 rpm) to remove precipitates. Before the protein sample was applied to the Äkta Pure chromatography system, the column was washed with at least two column volumes of filtered Milli-Q® water and activity buffer. As a next step, the sample was injected via a 500 µl loop and eluted in activity buffer pH 7.5. An isocratic elution was performed comprising 1.5 CV with a fractionation of the eluted proteins starting after 0.2 CV in 0.5 ml samples. Subsequently, the column was washed again with filtered Milli-Q® water and filtered 20 % ethanol. The fractions, which contained the highest amount of the protein of interest, were further processed utilising centrifugal filters in multiple centrifugation steps, as described in 2.2.14.5, to decrease the volume of the protein solution. The protein concentration was determined via a Bradford assay, see 2.2.14.4.

2.2.16 SDS gel electrophoresis

Proteins can be separated by SDS-PAGE (sodium-dodecyl sulfate polyacryl amide gel electrophoresis) according to its molecular weight. The addition of SDS in polyacryl amide gels denatures and negatively charges the proteins, thereby eliminating influences of the charge and the structure of the proteins in combination with DTT, a strong reducing agent, which is added to the 4 × loading dye and mixed with the protein samples prior to the sample application. By generating an electric current, the negatively charged proteins wander from the cathode side to the anode side in the gel matrix, in which smaller proteins migrate faster in the SDS-polyacryl amide gel. In this study, Bolt^{TM}4-12 % and 12 % Bis-Tris gels (Thermo Fisher Scientific) were used

in combination with MOPS-buffer (Thermo Fisher Scientific). Samples, which were applied to the SDS-PAGE gel were mixed with 4× Bolt™ LDS sample buffer + 100 mM DTT (v/v: 2:1) and cooked for 10 min at 70°C. Additionally, a protein marker (5-8 µl), see 2.1.5, was applied to the gel. The gels were run for 60-90 min at 150-200 V and afterwards stained with InstantBlue™ Protein Stain (Expedeon) or directly employed in semi-dry Western-blotting.

2.2.17 Protein transfer: Semi-dry Western blot

For the detection of proteins with specific antibodies, a semi-dry Western blot was performed to transfer the proteins from a gel onto a nitrocellulose or PVDF membrane. Therefor, the following buffers were used:

10 × PBS buffer, pH 7.4: 1.4 M NaCl
27 mM KCl
101 mM Na_2HPO_4
18 mM KH_2PO_4

1 × PBS-T buffer (1L): 100 ml 10 × PBS + 900 µl Milli-Q® + 1 ml Tween 20 (0.01 %)

10 × Transfer buffer: 1.92 M Glycine
0.25 M Tris

1 × Transfer buffer (1L): 100 ml 10 × transfer buffer + 150 ml methanol + 500 µl 20 % SDS
→ add 1 L Milli-Q® water

Whatman filter paper, gel and the nitrocellulose or PVDF membrane were incubated separately in 1 × transfer buffer for at least 15 min. As a following step, a sandwich consisting of in transfer buffer soaked whatman filter-membrane-gel-whatman filter (from bottom to top) was placed on the semi-dry blotter (peqlab). Additionally, air bubbles were removed from the sandwich. An electric current was generated according to the size of the membrane (0.8 mA per cm^2) and the negatively charged proteins migrated from the cathode site to the anode site within 70-120 min. Afterwards, the membrane was blocked for at least two hours, or overnight in blocking buffer.

Blocking buffer: 5 % Skim milk in PBS-T.

As a following step, the membrane was washed three times for 10 min with PBS-T and then incubated with the primary antibody. In this study, three different primary antibodies were used: the anti-ClpP1 antibody (1:2000), anti-PopR antibody (1:2000) or anti-His antibody (1:1000),

which were incubated for 1 h at RT under constant shaking. Next, the membrane was washed again three times for 10 min in PBS-T, before the secondary antibody was applied. The HRP (Horseradish peroxidase)-coupled anti-rabbit (1: 5000) antibody was applied for the detection of ClpP1 and PopR, whereas the HRP-coupled anti-mouse antibody (1: 5000) was employed for the detection of His_6-tagged proteins, for 1 h at RT under constant shaking. Afterwards, the membrane was washed again three times for 10 min in PBS-T and chemiluminescence signals were detected by adding the Amersham ECL prime Western blotting detection reagent. This reagent contains luminol, which can be oxidised by the horseradish peroxidase (HRP) and emits light (425 nm). Chemiluminescence signals were detected with the Molecular Imager ChemiDoc XRS System.

2.2.18 Intact protein mass spectrometry

Intact protein mass spectrometry was performed by Dr. Markus Lakemeyer, AG Sieber, TU munich. High-resolution intact protein mass spectrometry was performed to analyse the processing sites of ClpP1 and ClpP2 of *S. hawaiiensis*. A Dionex Ultimate 3000 HPLC system coupled to an LTQ FT Ultra (Thermo) mass spectrometer with an electrospray ionization source (spray voltage 4.0 kV, tube lens 110 V, capillary voltage 48 V, sheath gas 60 a.u., aux gas 10 a.u., sweep gas 0.2 a.u.) was applied to perform measurements. Prior to the measurements, reaction mixtures, which contained a total of about 1-10 pmol protein, were desalted with a Massprep desalting cartridge (Waters). The mass spectrometer was operated in positive ion mode collecting full scans at high resolution (R = 200,000) from m/z 600 to m/z 2000. The Thermo Xcalibur Xtract algorithm was utilised to deconvolute the protein spectra.

2.2.19 Processing assay

To analyse the N-terminal processing of ClpP1 and ClpP2, 2 µM of ClpP1, ClpP2 and a mixed sample consisting of 2 µM ClpP1 + 2 µM ClpP2 were incubated at 30°C with 10 µM ADEP1 or DMSO in activity buffer, pH 7.5: 50 mM HEPES-KOH, 150 mM KCl, 20 mM MgCl2, 10% glycerin. Samples (20 µl) were taken after 0, 1, and 3 h, mixed with 10 µl of 4× Bolt™ LDS sample buffer (Thermo-Fisher, + 100 mM DTT) and cooked for 10 min at 30°C. Afterwards, 12 µl of each sample was loaded on Bolt™12% Bis-Tris gels (Thermo-Fisher) using MOPS (Thermo Fisher Scientific) as

running buffer. Subsequently, the gels were stained with InstantBlue™ Coomassie protein stain (Expedeon).

2.2.20 Substrate degradation assays

All substrate degradation assays were carried out in 100 µl reaction volumes at 30°C in activity buffer, pH 7.5. All degradation assays employing ClgR, PopR or ß-casein were applied to Bolt™ 12% Bis-Tris gels (Thermo Fisher Scientific) with MOPS as running buffer. Therefor, samples (20 µl) were taken, mixed with 10 µl of 4× Bolt™ LDS sample buffer (Thermo-Fisher, + 100 mM DTT) and cooked for 10 min at 70°C, before 12 µl of each sample was loaded on the gel. All gels were stained with InstantBlue™ Coomassie protein stain (Expedeon).

2.2.20.1 Peptide degradation assay

The peptidolytic activity of ClpP1 and ClpP2 with and without the addition of 10 µM ADEP1 was measured using fluorogenic N-succinyl-Leu-Tyr-7-amido-4-methylcoumarin (Suc-LY-AMC) as substrate in a concentration of 100 µM. A total protein concentration of 4 µM was used for each sample, using equal amounts of ClpP1 and ClpP2 (2 µM each) in a mixed sample. DMSO instead of ADEP1 was added in the control samples. For the analysis of the hydrophobic pocket mutants $ClpP1_{hp}$ and $ClpP2_{hp,}$ a total protein concentration of 8 µM with 30 µM ADEP was used. Before the reaction was started, ClpP in combination with ADEP1/DMSO was pre-incubated for 10 min at 30°C.

Applying $ClpP_{ADEP\text{-}short}$ in Suc-LY-AMC degradation assays, 30 µM ADEP1 was added after the samples were pre-incubated for 24 h at 4°C.

The release of AMC was monitored in black flat-bottom 96 well plates (Sarstedt) in a spectrofluorometer (TECAN Spark®) at an excitation wavelength λ ex: 380 nm and emission wavelength λem: 460 nm. Data shown were obtained using three biological replicates with three technical replicates, respectively. Data employing the hydrophobic pocket mutant proteins ($ClpP1_{hp}$ and $ClpP2_{hp}$) or $ClpP_{ADEP\text{-}short}$, where gained utilising two biological replicates, comprising three technical replicates. P-values were calculated with one-way ANOVA (p-values: ns > 0.05; * ≤ 0.05; ** ≤ 0.01; ***≤ 0.001; ****≤ 0.0001).

2.2.20.2 ClgR and PopR degradation assay

ClgR and PopR degradation assays in the presence of ClpX +/- ADEP1

For the degradation of the natural substrates ClgR and PopR, 3 µM ClpP1, 3 µM ClpP2 and 1.5 + 1.5 µM ClpP12, were used in combination with 1.5 µM ClpX. The transcriptional activators ClgR and PopR were added in a total protein concentration of 3 µM. The degradation of ClgR and PopR was carried out in the presence of 2 mM DTT. In ADEP competition assays, 30 µM ADEP1 or DMSO was added to the samples. Additionally, an artificial ATP regeneration system (4 mM ATP, 8 mM creatine phosphate, and 10 U /ml creatine phosphokinase) was added to the reaction.

For the ClpX-mediated degradation of ClgR and PopR by $ClpP_{ADEP\text{-}short}P2$, 2 µM of each ClpP1, ClpP2, ClpX as well as ClgR or PopR were used in the presence of 2 mM DTT.

ClgR and PopR degradation assays in the presence of ClpC1 or ClpC2 +/- ADEP1:

1.5 µM ClpP1 and ClpP2 were used in combination with the unfoldase ClpC1 or ClpC2 (1.5 µM) to degrade ClgR or PopR (3 µM) with or without the addition of 30 µM ADEP1.

2.2.20.3 Casein degradation assay

FITC-casein degradation assays in the presence of ClpC1 +/-ADEP1

For the ClpC1-mediated degradation of casein fluorescein isothiocyanate (FITC-casein) Type III, a total protein concentration of 8 µM ClpP1, ClpP2 and a mixed sample consisting of 4 µM ClpP1 + 4 µM ClpP2 + 4 µM ClpC1 were used. 6 µM FITC-casein was added to start the reaction. Therefor, a 2 mg/ml FITC-casein stock-solution was prepared in activity buffer pH 7.5. As control, a mixed sample consisting of ClpP1P2 without the addition of ClpC1 was applied side by side. Furthermore, an artificial ATP regeneration system (4 mM ATP, 8 mM creatine phosphate, and 10 U /ml creatine phosphokinase) was added to the reaction as well.

For measuring the ADEP-induced proteolytic activity of ClpP1, ClpP2 and ClpP1P2 in FITC-casein degradation assays, a total protein concentration of 10 µM ClpP1 or ClpP2 was used as well as 5 µM of each in a mixed ClpP1P2 sample. DMSO instead of ADEP1 (30 µM) was applied in the control samples. Before the assay was started with the addition of substrate (6 µM FITC-casein), all ingredients were pre-incubated for 10 min at 30°C.

A FITC-casein competition assay in the presence of ClpC1 and ADEP1 was performed using 4 µM of ClpP1, ClpP2 and ClpC1. An artificial ATP regenerating system was added to the reaction together with 30 µM ADEP1 or DMSO in the control samples.

The hydrolysis of FITC-casein was monitored in black 96-well plates (Sarstedt) in a spectrofluorometer (Tecan Spark®) at excitation wavelength λex = 490 nm and emission wavelength λem = 525 nm. Experiments were performed at least with three biological replicates comprising three technical replicates. Statistics were performed with one-way ANOVA (p-values: ns > 0.05; * ≤ 0.05; ** ≤ 0.01; ***≤ 0.001; ****≤ 0.0001).

ß-casein degradation assays in the presence of ClpC1/ClpC2 +/- ADEP1

Equal amounts of ClpP1, ClpP2 and ClpC2 (1.5 µM each) were used to degrade 10 µM of ß-casein. ClpC1-meditated degradation assays of ß-casein by $ClpP_{ADEP\text{-}short}P2$ were performed with 2.5 µM $ClpP_{ADEP\text{-}short}$, 2.5 µM ClpP2 in combination with equal or double amounts of ClpC1 to degrade 10 µM ß-casein. In ADEP-competition assays, 30 µM ADEP1 was added. Additionally, an artificial ATP regeneration system (4 mM ATP, 8 mM creatine phosphate, and 10 U /ml creatine phosphokinase) was employed. In ADEP competition assays, 30 µM ADEP1 or DMSO as control were applied. Assays were performed in three biological replicates.

2.2.20.4 GFP-ssrA degradation assay in the presence of ClpX +/- ADEP1

The hydrolysis of C-terminally ssrA-tagged GFP (0.36 µM, provided by Dr. Imran Malik) was performed applying 3 µM of ClpP1, ClpP2 and ClpX. ADEP1 (30 µM) or DMSO was added before the reaction was started with substrate. Additionally, the reaction was carried out in the presence of 2 mM DTT. Furthermore, an artificial ATP regeneration system was utilised (4 mM ATP, 8 mM creatine phosphate, and 10 U /ml creatine phosphokinase) and all reaction components were pre-incubated for 10 min at 30°C, without the addition of GFP-ssrA. GFP fluorescence was monitored in white, flat bottom 96-well plates (Greiner) over 120 min at excitation wavelength λ ex = 465 nm and emission at λ em = 535 nm using a spectrofluorometer (TECAN infinite M200 and TECAN Spark®). The data shown are exemplary for three independently performed biological replicates.

2.2.21 Interaction studies

2.2.21.1 Pull-down assay of native ClpP1 with His_6-tagged ClpP2

The pETDUET vector system was applied to co-elute native ClpP1 with His_6-tagged ClpP2. Therefor, both genes were cloned into the pETDUET-1 vector which comprises two multiple cloning sites and two T7 promoters. Protein expression was conducted using the SG1146a strain for 4 h at 30°C, induced with 0.5 mM IPTG. The cells were harvested and disrupted using glass beads and the precellys system, see 2.2.14.2. The supernatant was incubated with 500 µl of Ni-NTA resin for two hours at 4°C under constant shaking. As a next step, an IMAC was performed, identically as described in 2.2.14.5. Samples of the flow-through, wash and the elution fractions were taken, and applied to Bolt™12% Bis-Tris gels (Thermo Fisher Scientific) with MOPS as running buffer. Additionally, a Western blot was performed as described in 2.2.17, employing a nitrocellulose membrane. The shown experiment represents one of three biological replicates.

2.2.21.2 Chemical cross-linking with BS3

To demonstrate ClpP1P2 heteromeric complex formation, the Pierce™ BS3 (bis(sulfo-succ-inimidyl)suberate) cross-linker (Thermo Fisher Scientific) was used to stabilise weak and transient interactions between ClpP1 and ClpP2. BS3 is an amine-to-amine cross linker (MW: 572.43), with a 11.4 Å spacer arm. This cross linker is water soluble and reacts with primary amines (Thermo Fisher Scientific, 2020).

A mixture of ClpP1P2 (6/10 µM each) as wells as two separate samples with ClpP1 or ClpP2 (6/10 µM) were pre-incubated for 30 min at 30°C in activity buffer pH 7.5 (50 mM HEPES-KOH, 150 mM KCl, 20 mM MgCl2, 10% glycerin). 50 × BS3 over the total ClpP concentration (0.6/1 mM BS3 for the mixed P1P2 sample/0.3/0.5 mM BS3 for ClpP1 or ClpP2) was added to the samples after dissolving BS3 in water to a final stock concentration of 100 mM. The samples were incubated for 30 min at 30°C without shaking. Subsequently the reaction was stopped by adding 20 mM Tris to the samples for 15 min at RT. Samples (20 µl) were taken and mixed with native loading dye (10 µl) to apply them (40 µl each or 35 µl for a Western blot) on Novex 4-12% Tris-Glycine gels (Thermo Fisher Scientific) using 1 × native running buffer.

10× native running buffer: Tris 0.25 M, glycine 1.92 M.

Subsequently, the gel was stained with InstantBlue™ Coomassie (Expedeon). Additionally, a Western blot was carried out. Therefor, the native Tris-Glycine gel was incubated in transfer buffer for 1 h at RT and transferred to a PVDF membrane (Merck) via semi-dry protein blotting at 0.8 mA/cm^2 for at least 90 min.

Transfer buffer: 25 mM Tris, 192 mM glycine, 15% v/v methanol, 0.5% w/v SDS.

ClpP1 and ClpP2 were detected specifically using anti-ClpP1 and anti-His antibodies as described previously in chapter 2.2.17.

2.2.21.3 Pull-down assay of native ClpP1 with His_6-tagged $ClpP_{ADEP\text{-}short}$

8 µM ClpP1 and 8 µM $ClpP_{ADEP\text{-}short}$ in a total reaction volume of 500 µl were incubated for 1 h at 4°C in activity buffer, pH 7.5. In the meantime, a polypropylene column was prepared with 50 µl Ni-NTA resin. The Ni-NTA resin was washed three times with lysis buffer pH 7.7, see 2.2.14.5 and applied to the column to settle. As a following step, the sample was applied to the column, which was washed three times with 500 µl lysis buffer, pH 7.7 (1×) and wash buffer, pH 7.7 (2×). The proteins were eluted in 4× 50 µl aliquots with elution buffer, pH 7.7, see 2.2.14.5. Samples (20 µl) were taken from the flow-through, the wash steps and the elution fractions, mixed with 10 µl of 4× Bolt™ LDS sample buffer (Thermo-Fisher, + 100 mM DTT), cooked for 10 min at 70°C and loaded on a Bolt™ 12% Bis-Tris gel (12 µl of each sample) using MOPS (Thermo Fisher Scientific) as running buffer. The gel was stained with InstantBlue™ Coomassie Protein Stain (Expedeon).

2.2.22 Analytical size exclusion chromatography

For analysing the oligomeric state of native ClpP1 and native ClpP2 separately on the gel filtration column in the absence and presence of ADEP1, the Superdex™ 200 Increase 3.2 300 column was employed. Therefor, 80 µM of the proteins were incubated with 200 µM ADEP1 for 30 min at 30°C and applied to the Äkta Pure chromatography system. For the analysis of $ClpP_{ADEP}$ 50 µM was used in combination with 80 µM ADEP1 or DMSO as control.

When $ClpP_{ADEP\text{-}short}$ was applied in combination with ClpP1, as well as the respective control samples, 80 µM of each protein was used in the absence or presence of 320 µM ADEP1. The

samples were applied with or without a 24 h incubation time at 4°C prior to the addition of ADEP1.

As markers thyroglobulin (669 kDa), apoferritin (443 kDa), ß-amylase (200 kDa), alcohol dehydrogenase (150 kDa, yeast), BSA (66 kDa) and carbonic anhydrase (29 kDa, bovine) were applied to the column by Stefan Pan.

The Superdex^{TM} 200 Increase 3.2 300 comprises a column volume of ~2.5 ml, flow rate: 0.075 ml/min and a column pressure: 3.5 mPa. Prior to the samples application, the column was washed and equilibrated with filtered Milli-Q® and activity buffer pH 7.5 with at least 2 CV each. Prior to the sample application, the samples were centrifuged for 2 min at 16 873 g (14 000 rpm) to remove precipitates. An isocratic elution was performed comprising 1.2 or 1.5 CV with activity buffer pH 7.5. Subsequently, the column was washed again with at least two CVs (column volumes) of filtered Milli-Q® water and 20 % ethanol for long-term storage.

3. Results

3.1 *In vitro* studies on *Streptomyces* Clp protease complex formation

According to previous whole cell experiments, confirming the presence of ClpP1 instead of ClpP3 in *S. hawaiiensis* (Gominet et al., 2011), ClpP1 and ClpP2 were considered to be the house-keeping Clp peptidases in the ADEP producer strain *S. hawaiiensis*, similar to *S. lividans* (Viala et al., 2000, Viala and Mazodier, 2002).

For the reconstitution of functional Clp protease complexes *in vitro*, the two ClpP isoforms ClpP1 and ClpP2 as well as the three Clp-ATPases ClpX, ClpC1 and ClpC2 from *S. hawaiiensis* were heterologously expressed and purified.

3.1.1 Purification of ShClpP1 and ShClpP2

In order to analyse the composition of the proteolytic core ClpP of *S. hawaiiensis in vitro*, *clpP1* or *clpP2* were cloned with and without a poly-Histidine-tag into the pET22b and pET11a vector, respectively. The recombinant clones were heterologously expressed in the *E. coli* BL21 derivative SG1146a in which a part of the *E. coli clpP* gene was deleted to prevent the expression of functional EcClpP and thus, a co-purification with the respective Clp peptidase of interest (Maurizi et al., 1990a). In *S. lividans*, both genes, *clpP1* and *clpP2*, have two putative start codons (Viala and Mazodier, 2002). Based on codon usage analyses of *Streptomyces clpPs*, *SlclpP1* was predicted to be expressed from the second start codon, whereas *SlclpP2* was expressed from the first start codon (de Crecy-Lagard et al., 1999). Additionally, previous work confirmed the predicted translation sites of both *clpP1* and *clpP2* genes (Thomy, 2019). Therefore, *ShclpP1* and *ShclpP2* were cloned from the second and from the first start codon, respectively. Figure 3.1 represents an amino acid sequence alignment of ClpP1 and ClpP2 from *S. hawaiiensis* and *S. lividans* with the two putative start codons encoding methionine or valine residues framed in red.

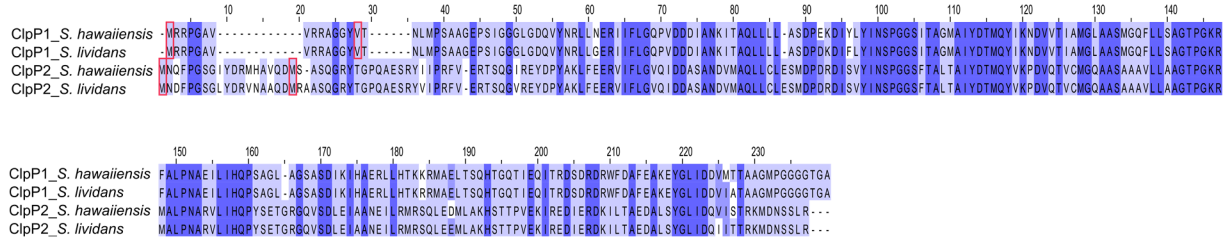

Figure 3.1: **Amino acid sequence alignment of ClpP1 and ClpP2 from *S. hawaiiensis* and *S. lividans* representing the two putative start codons encoding methionine or valine residues framed in red (de Crecy-Lagard et al., 1999, Viala et al., 2000).** The alignment was generated using protein sequences of *S. hawaiiensis* NRRL 15010 (CP021978.1) and *S. lividans* TK24 (NZ_CP009124.1) and the online tool clustalΩ (https ://www.ebi.ac.uk/Tools/msa/clustalo/). ClpP sequence identities were computed using Jalview Software (Waterhouse et al., 2009). In each column, the percentage of amino acid residues that agree with the consensus sequence are visualised from dark blue (> 80 %) to marine (> 60 %) to pale blue (> 40 %).

For most experiments described in this thesis, native ClpP1 and His_6-tagged ClpP2 were employed. However, for both ClpP proteins, the native as well as the His-tagged form was prepared and all four purifications are shown in this chapter. The expression of native and His_6-tagged ClpP1 was carried out for 5 h at 30°C, induced with 1 mM IPTG, respectively. For the purification of ClpP2 (with and without a C-terminally attached His_6-tag), protein expression was induced with 0.5 mM IPTG for 5 or ~16 h at 30°C.

Figure 3.2 depicts the purification of native (A + B, E + F) and His_6-tagged ClpP1 and ClpP2 (C + G). The anion exchange chromatography was performed according to the protocol in section 2.2.14.3. Fraction 10 for ClpP1 and fraction 12 for ClpP2, which comprised the highest amount of protein, defined by the absorption at 280 nm (Figure 3.2 A + E) and an SDS-PAGE analysis of the respective fractions (Figure 3.2 B + F) were further processed, see chapter 2.2.14.3.

Histidine-tagged ClpP1 and ClpP2 were purified according to the protocol in chapter 2.2.14.5. Although samples of only the first four elution fractions of the immobilised nickel ion affinity chromatography of $ClpP1_{His}$ are shown in Figure 3.2, elution fractions 5-10 contained a high amount of $ClpP1_{His}$ as well. Further procedures including reduction of sample volume and subsequent determination of the protein concentration according to Bradford (Bradford, 1976) were performed identically to the purification of native ClpP1 and ClpP2. Additionally, samples

of purified native and His-tagged ClpP1 and ClpP2 were analysed via SDS-PAGE as it is shown in Figure 3.2 D + H.

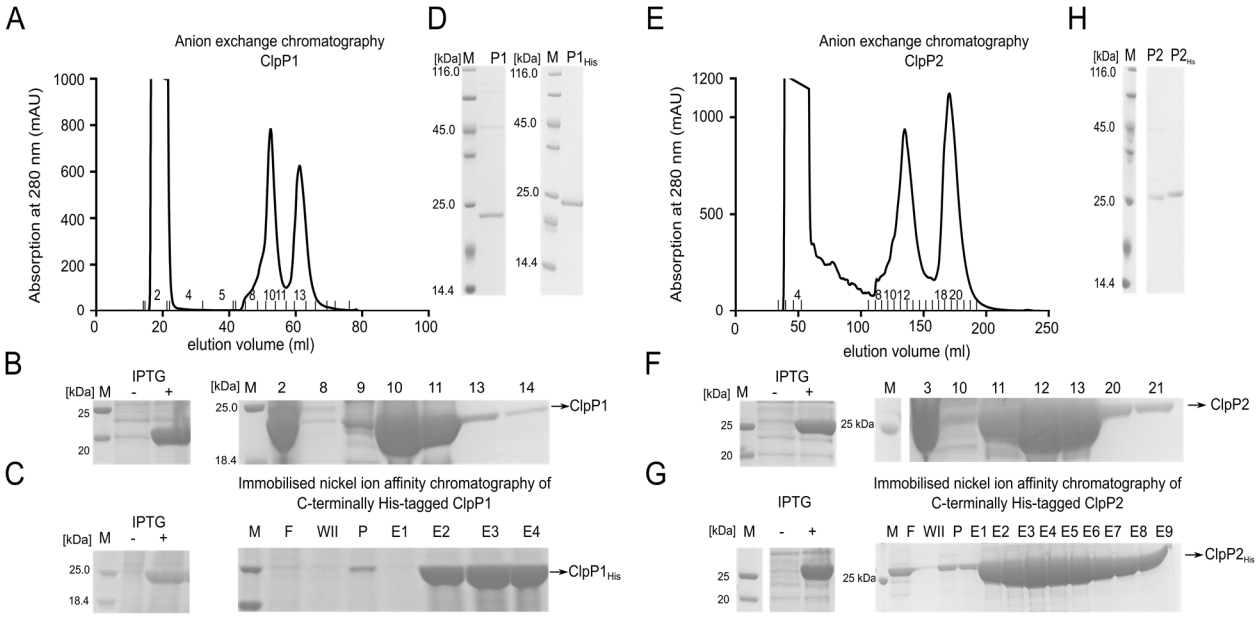

Figure 3.2: **Purification of native and His_6-tagged ShClpP1 and ShClpP2. A + E:** Anion exchange chromatography of native ShClpP1 and ShClpP2 using the 1/5 ml HiTrap™ Q XL column (GE Healthcare). **B + F**: An expression test of native ShClpP1 and ShClpP2 was carried out at 37°C prior to the purification procedure. The cells were induced with 1 mM IPTG and a sample was taken after 4 h at 37°C and loaded on a 12 % Bis-Tris gel with the un-induced control sample. For the purification of native ShClpP1 and ShClpP2, samples of the fractions, which were collected during the anion exchange chromatography, were loaded on a 12% Bis-Tris gel and analysed for elution of the respective Clp peptidase of interest. **C + G:** The expression of $ShClpP1_{His}$ and $ShClpP2_{His}$ was induced with 1 mM IPTG at 37°C for 4 h and whole cell extracts were loaded on a 12% Bis-Tris gel side by side with an un-induced negative control. Furthermore, the purifications of $ShClpP1_{His}$ and $ShClpP2_{His}$ were conducted using a nickel ion affinity chromatography column and the proteins were eluted with 500 mM imidazole. Samples of the flow-through (F), the second wash step (WII), the pellet after centrifugation (P) and samples of the elution fractions (E1-E4 for ShClpP1/E1-E9 for ShClpP2) were loaded on 12 % Bis-Tris gels for SDS-PAGE analysis. **D+H**: Additionally, 2 µM of purified ShClpP1 and $ShClpP1_{His}$ as well as native ShClpP2 together with $ShClpP2_{His}$ were loaded on 12% Bis-Tris gels.

In addition to the constructs pET11ashclpP2 and $pET22bshclpP2_{His}$, which were expressed from the first start codon, a third construct was cloned expressing *clpP2* from the putative second start codon in the BL21 derivative SG1146a (0.5 mM IPTG for 5 or ~ 16 h at 30°C) followed by a nickel ion affinity chromatography, see Figure 3.3.

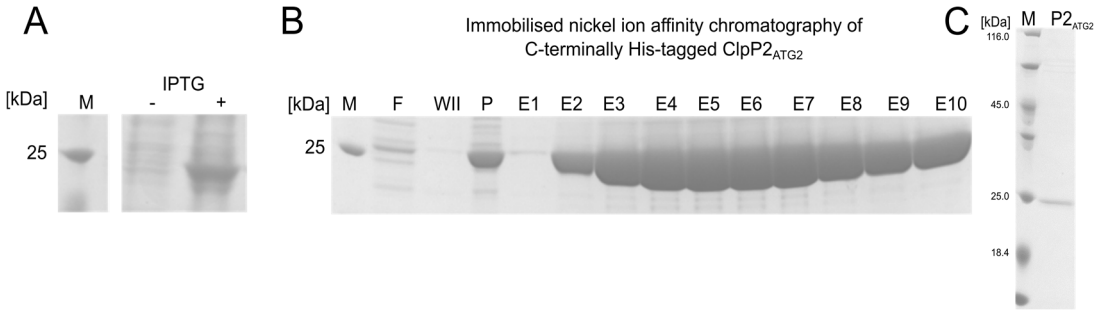

Figure 3.3: **Immobilised nickel ion affinity chromatography of ShClpP2$_{ATG2}$. A**: Analysis of ShClpP2$_{ATG2}$ expression, induced with 1 mM IPTG for 4 h at 37°C. Whole cell extracts (un-induced and induced) were loaded on a 12% Bis-Tris gel. **B**: Samples of the nickel ion affinity chromatography comprising flow-through (F), wash II, pellet after centrifugation (P) and elution fractions E1-E10 were applied to a 12 % Bis-Tris gel. **C**: Purified ShClpP2$_{ATG2}$ (2 µM) was analysed via SDS-PAGE.

The purification was performed identically to the purification of ClpP1$_{His}$ and ClpP2$_{His}$, see chapter 2.2.14.5 and the protein was eluted and stored in activity buffer pH 7.5.

3.1.2 Purification of the Clp-ATPases ShClpX, ShClpC1 & ShClpC2

The genome of *S. hawaiiensis* comprises one *clpX* and four distinct *clpC* genes, namely *clpC1*, *clpC2*, *clpC4* and *clpC5* (Thomy, 2019). However, no gene homologous to *clpC3* of *S. lividans* could be found in the genome of *S. hawaiiensis* (Thomy, 2019). In contrast to *clpC1* and *clpC2*, *clpC4* and *clpC5* encode shortened proteins which do not contain conserved nucleotide binding sites (Walker et al., 1982) which suggests that they are incapable of fulfilling Clp-ATPase activity. Thus, for the reconstitution of physiologically active Clp protease complexes *in vitro*, the Clp-ATPases ClpX, ClpC1 and ClpC2 were heterologously expressed in *E. coli* SG1146a and purified via immobilised nickel ion affinity chromatography, employing a C-terminally attached His$_6$-tag. Protein expression of ClpX, ClpC1 and ClpC2 was induced with 0.5 mM IPTG and performed for 5 h at 30°C, respectively. Analysis of protein expression and purification of the different unfoldases is summarised in Figure 3.4. All three Clp-ATPases were purified according to the protocol in chapter 2.2.14.5, similar to the Clp peptidases ClpP1$_{His}$ and ClpP2$_{His}$. The elution fractions E1-E10 were pooled and a buffer exchange was conducted using the PD-10 desalting column in activity buffer pH 7.5. Prior to the determination of protein concentration via Bradford, the volume of protein solution was decreased by multiple centrifugation steps in Thermo protein concentrators at low rotational speed (2 049-4 098 g, 2 000- 4 000 rpm) for 3-10 min at 4°C, respectively. All

three Clp-ATPases were prone to aggregate during the centrifugation steps, therefore resuspension of the protein solution in between the centrifugation steps was necessary, especially for ClpC2 which was centrifuged for 1-3 min at 2 049 g (2 000 rpm) for a reduction of volume from 3.5 ml to 1 ml of purified protein. Samples of purified ClpX, ClpC1 and ClpC2 were analysed via SDS-PAGE and are presented in Figure 3.4 C.

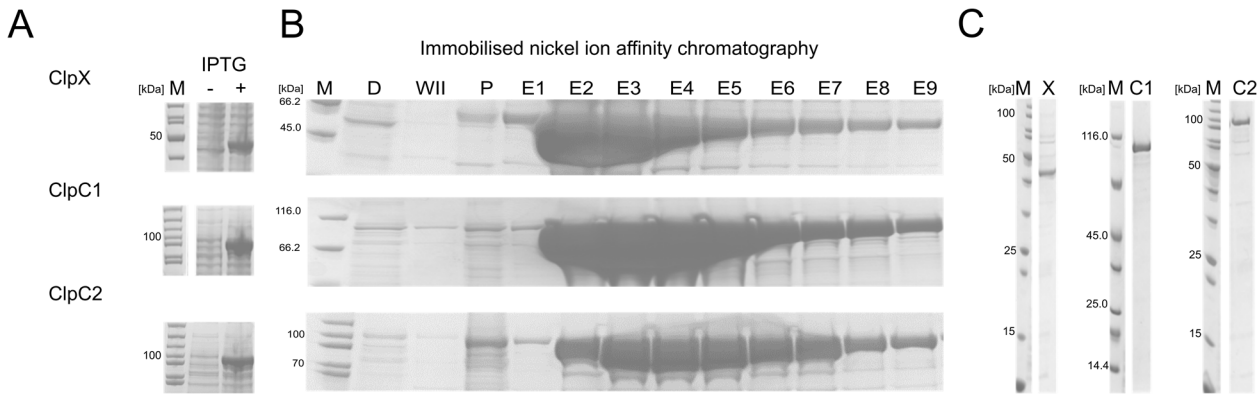

Figure 3.4: **Immobilised nickel ion affinity chromatography of ShClpX, ShClpC1 and ShClpC2. A:** Analysis of protein expression after 4 h at 37°C, induced with 1 mM IPTG. Whole cell extracts (before and after induction) were visualised via SDS-PAGE gels. **B:** Samples of the flow-through, wash II, pellet after centrifugation (P) and elution fractions E1-E9 were applied to 4-12 % Bis-Tris gels. **C**: The purified Clp-ATPases ShClpX, ShClpC1 and ShClpC2 were analysed on 4-12 % Bis-Tris gels.

3.1.3 Purification of the transcriptional activators ShClgR & ShPopR

The *clp* and *lon* gene regulator (ClgR) of the bicistronic operon *clpP1P2* and its paralogue PopR (*clpP3* operon regulator), which activates the expression of *clpP3clpP4,* were shown to be physiological substrates of ClpP1P2 in *S. lividans* in *in vivo* experiments (Viala and Mazodier, 2002, Bellier et al., 2006). As a following step, ClgR and PopR of *S. hawaiiensis* were tested as potential protein substrates for ClpP1P2 in association with either ClpX, ClpC1 or ClpC2 in *in vitro* degradation experiments. Therefore, *clgR* or *popR* were cloned into the pET11a vector, which is usually used for native protein purifications but this time was utilised for the purification via an N-terminal poly-Histidine-tag to ensure the accessibility of the essential C-terminal substrate recognition sequence, consisting of VAA (ClgR) or LAA (PopR). The purification of ClgR and PopR was performed according to the protocol in chapter 2.2.14.5. Protein expression was induced using 0.5 mM IPTG for ~ 16 h at 20°C for ClgR and 5 h at 30°C for PopR. Figure 3.5 summarises

the analysis of protein expression and subsequent isolation of the two transcriptional regulators ClgR and PopR. Regarding the purification of ClgR, a high amount of overexpressed protein could be detected in samples taken from the flow-through and the washing step prior to the protein elution, indicating a complete saturation of the Ni-NTA beads with His-tagged ClgR, see Figure 3.5 B. Furthermore, samples, which were taken during the elution of PopR, revealed two protein bands appearing on SDS-PAGE gels, indicating a putative internal second start codon, leading to the expression of a shorter PopR fragment, named $PopR_{ATG2}$, in addition to the PopR full-length protein. A Western blot analysis of purified PopR could confirm the second detected protein band as a fragment of PopR, since both protein bands were detectable using anti-PopR antibodies. However, anti-His-antibodies only detected the full-length PopR, not the fragment, strongly suggesting that this fragment has a shorter N-Terminus which did not contain the poly-Histidine-tag but was co-purified with full-length PopR. Of note, PopR was found to dimerize in *in vivo* experiments (Viala and Mazodier, 2002), providing a potential explanation for the co-purification of $PopR_{ATG2}$ with the N-terminal His-tagged full-length protein.

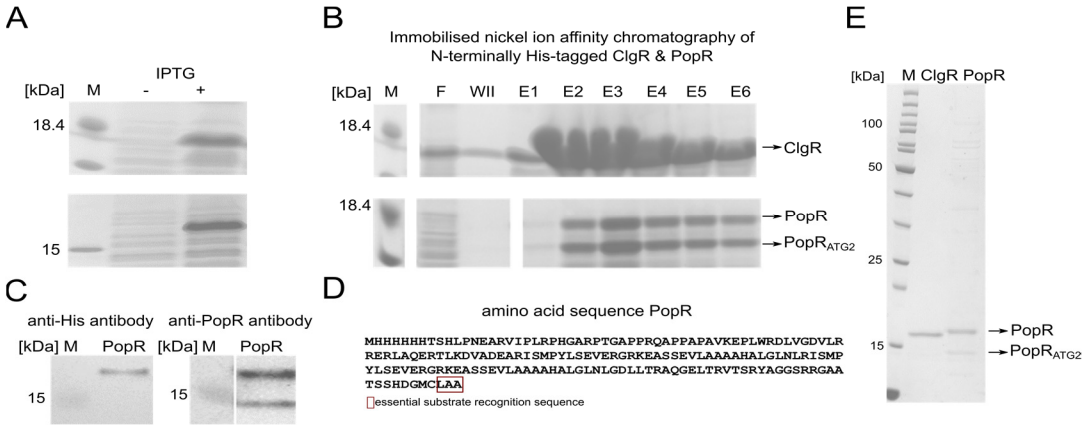

Figure 3.5: **Nickel ion affinity chromatography of ShClgR and ShPopR including Western blot analyses of purified ShPopR employing anti-His and anti-PopR antibodies. A + B:** Analysis of protein expression was carried out for 4 h at 37 °C using 1 mM IPTG and whole cell extracts were loaded on 12 % Bis-Tris gels side by side with corresponding negative controls (**A**). Additionally, samples which were taken during the purification of N-terminally His-tagged ShClgR and ShPopR were visualised on SDS-PAGE gels including the flow-through (F), wash II and the elution fractions E1-E6 (**B**). Besides, purified ShPopR was loaded on a 12 % Bis-Tris gel and blotted on a nitrocellulose membrane for specific detection via primary anti-His and anti-PopR antibodies and HRP-coupled secondary anti-mouse and anti-rabbit antibodies (**C**). **D**: Amino acid sequence of

ShPopR illustrating the essential substrate recoginition sequence LAA in dark red. **E**: Purified ShClgR and ShPopR protein bands detected on SDS-PAGE gels.

Figure 3.5 D represents the amino acid sequence of PopR with the essential substrate recognition sequence framed in dark red. A defined protein concentration of isolated ClgR and PopR (2 µM) was analysed via SDS-PAGE, which can be seen in Figure 3.5 E.

3.1.4 Analysis of ShClp complexes in *in vitro* substrate degradation experiments

To establish an *in vitro* reconstitution system in which *Streptomyces* ClpP proteins form physiologically active Clp complexes, ClpP1, ClpP2 and their cognate Clp-ATPases ClpX, ClpC1 and ClpC2 were employed in degradation experiments to digest a set of different protein substrates such as the potential natural substrates ClgR and PopR as well as the model substrate casein, in an un-tagged (β-casein) or fluorescently labeled form (FITC-casein). All degradation assays were performed utilising native ClpP1 in conjunction with His_6-tagged ClpP2.

Figure 3.6 demonstrates that neither ClpX nor ClpC2 or ClpC1 in association with ClpP1 or ClpP2 were capable of digesting ClgR, PopR or the model substrate casein (β and α-casein). However, both ClpP isoforms (ClpP1 and ClpP2) combined in association with the unfoldases ClpX, ClpC2 or ClpC1 resulted in efficient substrate degradation of ClgR, PopR and casein, strongly pointing towards a joined function of heteromeric ClpP1P2 complexes.

Besides, the two transcriptional regulators ClgR and PopR, which were confirmed as substrates of ClpP1P2 in *S. lividans* in *in vivo* experiments (Viala and Mazodier, 2002, Bellier et al., 2006), could be revealed as substrates of ClpP1P2 *in vitro* in the highly homologous *S. hawaiiensis* as well (Fig. 3.6 A). Regarding the degradation of PopR, the $PopR_{ATG2}$ fragment was observed to be digested by ClpXP1P2, but significantly slower compared to the full-length protein (Fig. 3.6 A). Hence, for the sake of simplicity, the degradation of PopR will only be shown for the full-length protein in further degradation experiments.

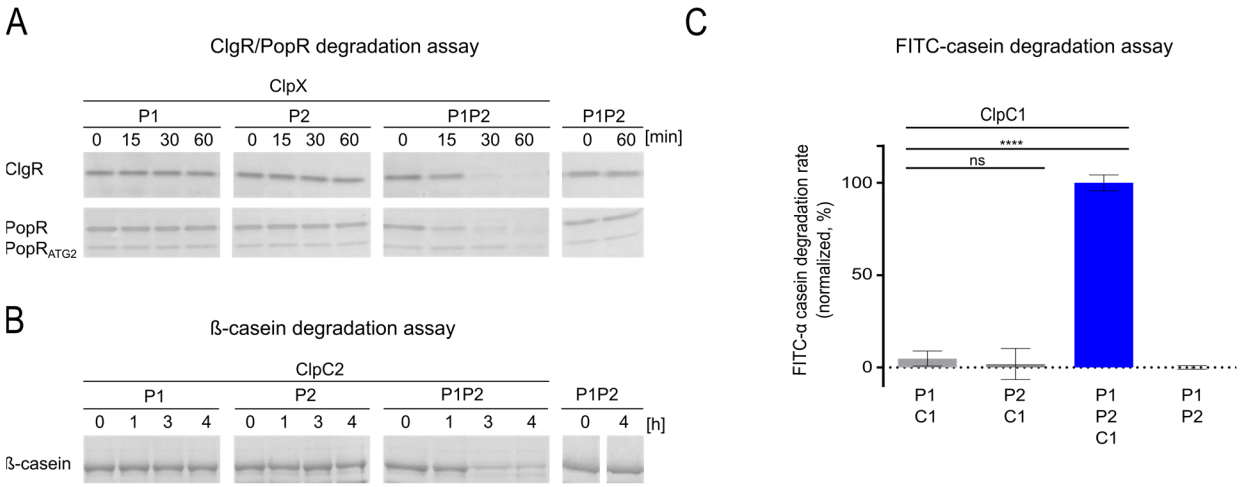

Figure 3.6: ***In vitro*** **degradation experiments utilising the unfoldases ShClpX (A), ShClpC2 (B) and ShClpC1 (C) in combination with ShClpP1, ShClpP2 and ShClpP1P2 to degrade a set of different protein substrates such as ShClgR, ShPopR (A), as well as β-casein (B) and fluorogenic α-casein (C). A:** The Clp-ATPase ShClpX (1.5 µM) was tested with ShClpP1 (3 µM), ShClpP2 (3 µM) and ShClpP1P2 (1.5 + 1.5 µM) yielding ShClpXP1, ShClpXP2 and ShClpXP1P2, respectively to degrade the potential substrates ShClgR (3 µM) and ShPopR (3 µM). Both degradation experiments were conducted at 30°C. Samples were taken at different time points and loaded on 12 % Bis-Tris gels. The presented data are exemplary for at least three independent biological replicates. **B**: A ß-casein (10 µM) degradation assay was performed using the Clp-ATPase ShClpC2 (1.5 µM) in combination with ShClpP1 (3 µM), ShClpP2 (3 µM) and ShClpP1P2 (1.5 + 1.5 µM). The experiment was conducted at 30°C and samples, which were collected after different time points, were analysed via SDS-PAGE. The presented SDS-PAGE gel is exemplary for three biological replicates. **C**: For the degradation of fluorescently labeled α-casein (6 µM), the Clp-ATPase ShClpC1 (4 µM) was used in combination with ShClpP1 (8 µM), ShClpP2 (8 µM) and ShClpP1P2 (4 + 4 µM) and the increase of fluorescence intensity was recorded in a time-dependent manner, resulting in the release of fluorescein isothiocyanate. Mean of initial slopes are given (normalized in %) and error bars indicate corresponding standard deviations. Statistics were calculated with one-way ANOVA by using three biological replicates comprising three technical replicates, respectively; p-values: ns > 0.05; ****≤ 0.0001.

The efficient ClpX-mediated degradation of ClgR and PopR by ClpP1P2 clearly presents both transcriptional activators as substrates of ClpXP1P2. Nevertheless, ClpC1 and ClpC2 were tested in association with ClpP1P2 for the degradation of ClgR and PopR as well. As can be seen in Figure 3.7, both Clp-ATPases recognised ClgR as substrate, however, less effectively than ClpX in association with ClpP1P2, employing similar substrate concentrations. In contrast, PopR could only be hydrolysed by ClpC2P1P2, yet substantially slower compared to ClpXP1P2.

Remarkably, all three Clp-ATPases ClpX, ClpC1 and ClpC2 shared the transcriptional activator ClgR as substrate. In contrast, while the model substrate casein could be degraded by ClpC1 or ClpC2 in association with ClpP1P2 (Figure 3.6), ClpX failed to mediate a ClpP1P2-dependent casein degradation (Figure 3.7 B).

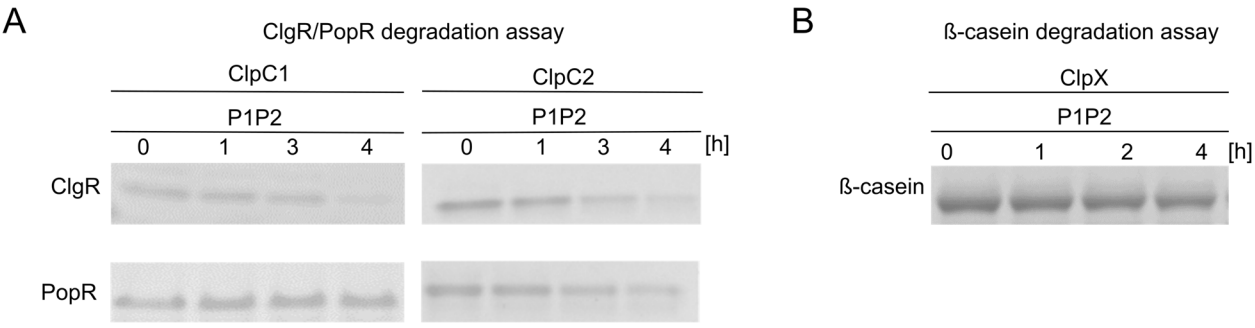

Figure 3.7: **ShClpC1 and ShClpC2-dependent degradation of ShClgR and ShPopR as well as ShClpX-dependent digestion of ß-casein by ShClpP1P2**. Degradation experiments were conducted for 4 h at 30°C. Samples were taken and loaded on 12 % Bis-Tris gels. Similar protein concentrations for ShClpP1P2 (1.5 µM each) as for the Clp-ATPases ShClpX, ShClpC1 and ShClpC2 (1.5 µM each) were used to degrade ShClgR (3 µM), ShPopR and ß-casein (10 µM). Data presented are exemplary for three independent biological replicates.

Nevertheless, to ensure that the C-terminally attached Histidine-tag of ClpP2 did not impair the formation of physiologically active Clp complexes, degradation experiments were performed employing ClpP1P2 and ClpP1P2$_{His}$ side by side in association with either ClpX or ClpC1 for ClgR, PopR and FITC-casein digestion (see Figure 3.8).

Similar proteolytic activities of ClpP1P2 and ClpP1P2$_{His}$ in association with ClpX or ClpC1 demonstrate that the C-terminally attached Histidine-tag of ClpP2 did not affect the formation of physiologically active Clp complexes, see Figure 3.8.

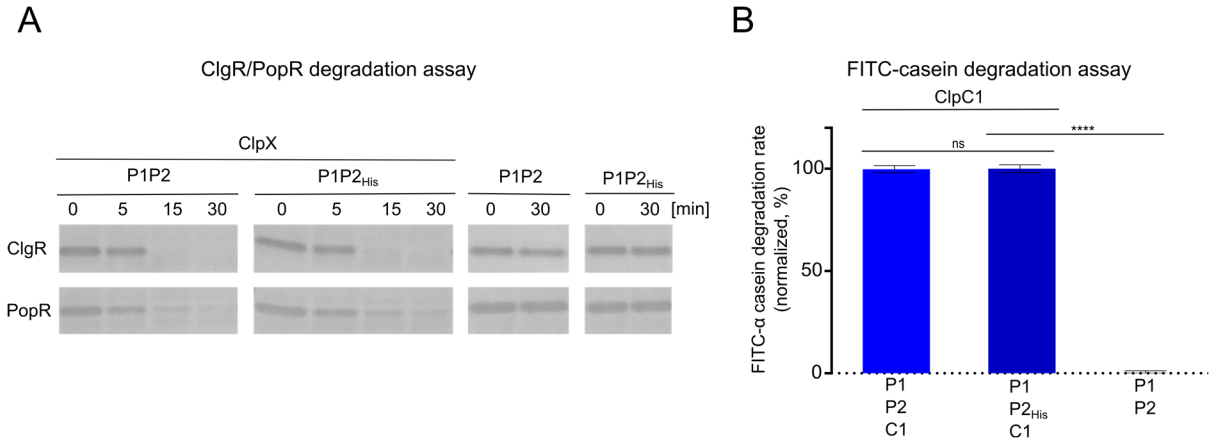

Figure 3.8: **ShClpP1 combined with either native or C-terminally His-tagged ShClpP2 in combination with ShClpX or ShClpC1 were used to degrade ShClgR, ShPopR (A) and FITC-casein (B).** All experiments were performed at 30°C**. A**: Samples were taken after different time points and loaded on 12% Bis-Tris gels. 1.5 µM of ShClpP1, ShClpP2 (native or His_6-tagged) and ShClpX were used to degrade 3 µM ShPopR or ShClgR. The presented gels are exemplary for three independent biological replicates. **B**: FITC-casein (6 µM) degradation by ShClpC1P1P2 and ShClpC1P1$P2_{His}$ (4 µM each) was monitored as an increase in fluorescence intensity (RFUs) over time. Mean of initial slopes are shown, normalized in %. Statistics were performed with one-way ANOVA comprising three biological and three technical replicates, respectively. P-values: ns > 0.05; ****≤ 0.0001. Error bars indicate corresponding standard deviations.

3.1.5 ShClpP1 and ShClpP2 interaction studies: pull-down and cross-linking experiments

To confirm the formation of heteromeric ClpP1P2 complexes, interaction studies of ClpP1 and ClpP2 were performed by means of pull-down and cross-linking experiments. A pull-down experiment was conducted using the pET DUET vector system which comprises two T7 promoters and two multiple cloning sites. Both *clpP1* and *clpP2* genes were inserted into the pETDUET vector with a poly-Histidine-tag attached to *clpP2*. The recombinant clone was transformed into *E. coli* SG1146a and ClpP1 and $ClpP2_{His}$ protein expression was induced by the addition of IPTG. Subsequently, an immobilised nickel ion affinity chromatography of His_6-tagged ClpP2 was performed in order to analyse a potential co-purification of un-tagged ClpP1, thereby indicating a direct interaction between both peptidases. As it is seen in Figure 3.9 A, native ClpP1 could be co-eluted with His-tagged ClpP2, confirmed by Western blot experiments with anti-ClpP1 and anti-His antibodies. Additionally, cross-linking experiments employing the chemical cross-linker

Bissulfosuccinimidyl suberate (BS3) demonstrate the formation of hetero-tetradecamers, visualised on native 4-12 % Tris-Glycine gels and Western blots, see Figure 3.9.B.

Interestingly, co-expression of ClpP1 and ClpP2 resulted in a step-wise processing of ClpP2, yielding mature ClpP2 (Fig. 3.9 A), which is described in section 3.1.10 in detail. Samples of the flow-through, wash and elution fractions contained high amounts of full-length and processed versions of His_6-tagged ClpP2, whereas for co-purified native ClpP1 only faint bands appeared, which can be explained by the different expression levels of ClpP1 and ClpP2 as indicated via whole cell extracts (-/+ IPTG) on SDS-PAGE gels.

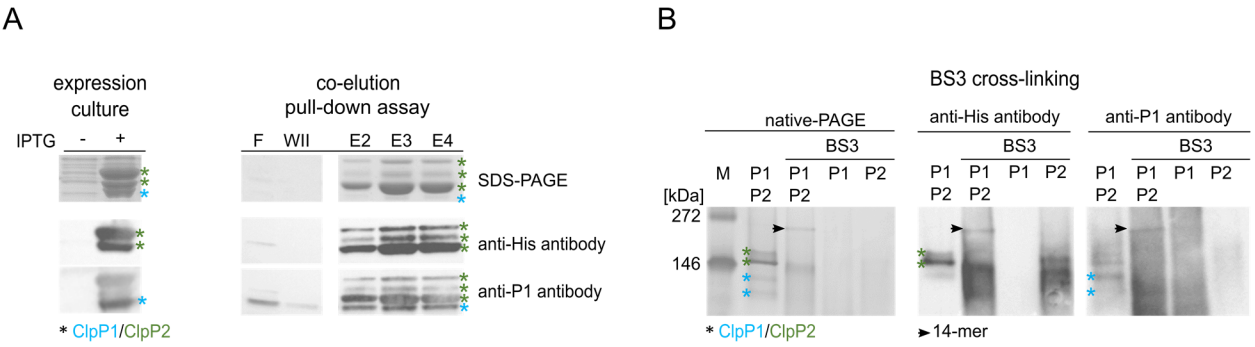

Figure 3.9**: ShClpP1 and ShClpP2 form hetero-tetradecamers. A:** Expression of ShClpP1 and $ShClpP2_{His}$ was tested by loading whole cell extracts (+/- IPTG) on 12 % Bis-Tris gels. Additional Western blot experiments utilising anti-His and anti-ClpP1 antibodies as primary and HRP-coupled anti-mouse and anti-rabbit as secondary antibodies verified the expression of ShClpP1 and $ShClpP2_{His}$. Co-purification of native ShClpP1 with Histidine-tagged ShClpP2 expressed in the pETDUET vector system visualised on 12% Bis-Tris gels. As previously described, Western blot experiments were performed utilising anti-His and anti-ClpP1 antibodies. Samples of the flow-through and wash II indicate the removal of unbound ShClpP1. Full-length and processed bands of $ShClpP2_{His}$ (described in section 3.1.10) are indicated as green asterisks whereas the protein band of ClpP1 is marked with a blue asterisk. **B**: BS3 cross-linking of ClpP1P2 heteromeric complexes (6 µM each) visualised on native 4-12% Tris-Glycine gels**.** Additionally, Western blot experiments were performed, confirming the presence of ShClpP1 and $ShClpP2_{His}$ via anti-ClpP1 and anti-His antibodies. The presented experiments are exemplary for at least three biological replicates.

Furthermore, it is noteworthy to mention that anti-ClpP1 antibodies cross-reacted with ClpP2 as well, due to comparatively high amounts of ClpP2 in the elution fractions, however with a considerably lower affinity as it is shown in Figure 3.9 A.

In order to visualise mixed heteromeric ClpP1P2 complexes on native Tris-Glycine gels, the cross-linker BS3 was used to stabilise potential weak and unstable interactions between ClpP1 and ClpP2. This cross-linker is water soluble and has an 8-carbon spacer arm with one amine-reactive N-hydroxysulfosuccinimide (NHS) ester on each end. It reacts with primary amines of proteins, which are in close proximity to each other and forms stabile covalent amide bonds, thereby releasing the N-hydroxysulfosuccinimide. Usually, proteins contain several primary amines, including lysine residues and the N-terminus of each polypeptide chain (Thermo Fisher Scientific, 2020). The reaction was performed in activity buffer pH 7.5, using native ClpP1 and Histidine-tagged ClpP2 with 6 µm of each peptidase. An excess of BS3 (50 ×) over the total ClpP concentration was used and added to different samples consisting of ClpP1P2, ClpP1 or ClpP2. As negative control, mixed ClpP1P2 was used without the addition of BS3 and treated comparably to the cross-linked samples. As a following step, the samples were loaded on native 4-12% Tris-Glycine gels, see Figure 3.9 and materials and methods chapter 2.2.21.2.

Applying the cross-linked samples on native Tris-Glycine gels revealed tetradecameric complexes (~ 300 kDa) exclusively in samples, consisting of ClpP1 and ClpP2, whereas no tetradecameric species appeared in samples consisting of ClpP1, ClpP2 or mixed ClpP1P2 without BS3. Additionally, both ClpP1 and ClpP2 could be detected in the respective tetradecameric complexes via immunoblotting employing anti-ClpP1 and anti-His antibodies. Lower oligomeric states could be visualised in mixed ClpP1P2 samples as well, corresponding to mostly heptameric species of ClpP1 and ClpP2.

3.1.6 Purification of the mutant proteins ShClpP1$_{S113A}$, ShClpP2$_{S131A}$, ShClpP1$_{hp}$ and ShClpP2$_{hp}$

To investigate the catalytic activity of ClpP1P2 heteromeric complexes, ClpP1$_{S113A}$ and ClpP2$_{S131A}$ catalytic triad knock-out mutant proteins were expressed in which the nucleophilic serine moiety of the catalytic triad was exchanged by an alanine residue, abolishing the catalytic activity of those mutants. Both *clpP1$_{S113A}$* and *clpP2$_{S131A}$* genes contain a C-terminally attached Histidine-tag using the IPTG-inducible pET22b vector. Additionally, Clp-ATPase/ClpP interactions were studied

by constructing hydrophobic pocket mutants of ClpP1 and ClpP2, abrogating the ability of the proteolytic core to interact with its cognate Clp-ATPases. Wang *et al*. 1997 described three solvent-exposed aromatic residues (Y74, Y76, F96) within the hydrophobic pocket of EcClpP, the binding region for the Clp-ATPases, which were assumed to stabilise Clp-ATPase/ClpP interactions (Wang et al., 1997). Besides, the corresponding amino acid residues were previously mutated in ClpP1 and ClpP2 from the homologous *M. tuberculosis* (Leodolter et al., 2015).

Hydrophobic pocket mutant proteins were constructed by aligning amino acid (aa) sequences of EcClpP with amino acid sequences of ShClpP1 and ShClpP2, exchanging the respective residues which correspond to the conserved aromatic amino acid residues in EcClpP. Figure 3.10 depicts an amino acid sequence alignment of ClpP proteins from *B. subtilis*, *E. coli*, *S. hawaiiensis* and *M. tuberculosis*. Additionally, SlClpP1 and SlClpP2 were included in the alignment, illustrating high sequence homologies between amino acid sequences of *S. hawaiiensis* and *S. lividans* ClpP1 and ClpP2.

For ClpP1, Y76V, Y78V and Y98V were exchanged, whereas for ClpP2 S94A, Y96V and Y116V were mutated via site-directed mutagenesis, see 2.2.5. The hydrophilic tyrosine and serine residues were replaced by hydrophobic valine and alanine residues, respectively.

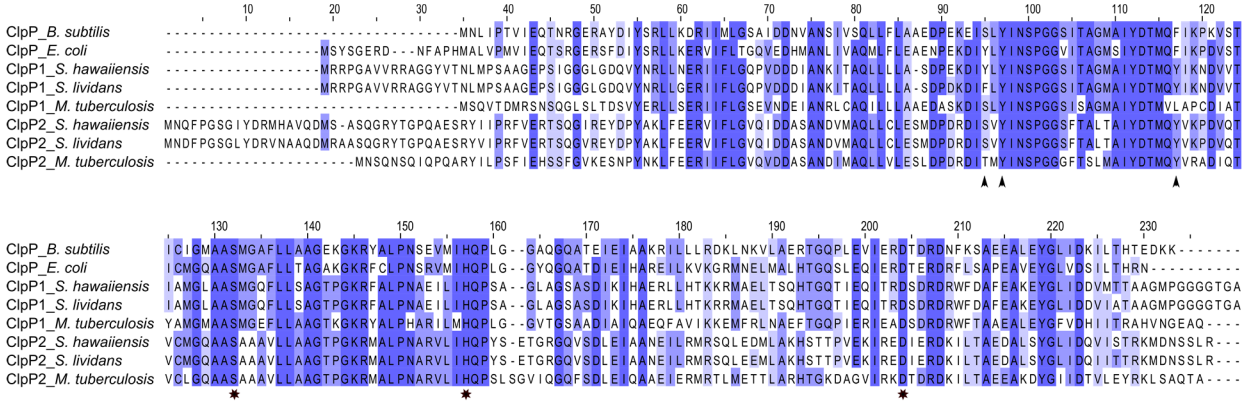

Figure 3.10: **Amino acid sequence alignment of ClpP homologues from *B. subtilis*, *E. coli*, *S. hawaiiensis*, *S. lividans* and *M. tuberculosis***. The three conserved aromatic residues (Y74, Y76 and F96 of unprocessed *E. coli* ClpP) within the hydrophobic pocket of EcClpP are marked as black triangles whereas amino acid residues of the catalytic triad are marked as asterisks. Corresponding amino acid residues were mutated in ClpP1 and ClpP2 of *S. hawaiiensis*. MSA was performed using the online tool clustalΩ (https ://www.ebi.ac.uk/Tools/msa/clustalo/) with ClpP

proteins from *B. subtilis* strain 168 (NC_000964.3), *Escherichia coli* K-12 (U00096.3), *S. hawaiiensis* NRRL 15010 (CP021978.1), *S. lividans* TK24 (NZ_CP009124.1) and *M. tuberculosis* ATCC 25618 (NC_000962.3). Sequence identities were computed using Jalview Software (Waterhouse et al., 2009). In each column, the percentage of amino acid residues that agree with the consensus sequence are visualised from dark blue (> 80 %) to marine (> 60 %) to pale blue (> 40 %). Comparing ClpP1 protein sequences of *S. hawaiiensis* and *S. lividans*, as ClpP2, using BLAST® (https://blast.ncbi.nlm.nih.gov/Blast.cgi) revealed sequence identities of 97.3 % for ClpP1 and 94.9 % for ClpP2 between these species.

While the expression and purification of $ClpP1_{hp}$ resulted in a stable protein preparation, the expression and purification of $ClpP2_{hp}$ yielded mostly insoluble protein aggregates with a minor fraction of soluble protein, which was highly unstable. Therefore, instead of using $ClpP2_{hp}$ expressed from the first start codon, a new $ClpP2_{hp}$ construct was cloned, utilising the putative second start codon as it was previously described for wild-type $ClpP2_{ATG2}$, resulting in a stable protein preparation. For the purification of native $ClpP1_{hp}$ and $ClpP2_{hp}$, the proteins were expressed for 5 h at 30°C respectively, using 1 or 0.5 mM IPTG for induction. Figure 3.11 presents the purification of the catalytic triad knock-out mutant proteins $ClpP1_{S113A}$ and $ClpP2_{S131A}$ and the hydrophobic pocket mutant $ClpP2_{hp}$ via nickel ion affinity chromatography as well as the isolation of $ClpP1_{hp}$ via anion exchange chromatography. Additionally, a pET22bshclpP2$_{S131A\text{-}ATG2\text{-}His}$ construct was cloned, utilising the putative second start codon. However, for the sake of simplicity, only the purification of full-length $ClpP2_{S131A}$ is shown in this chapter.

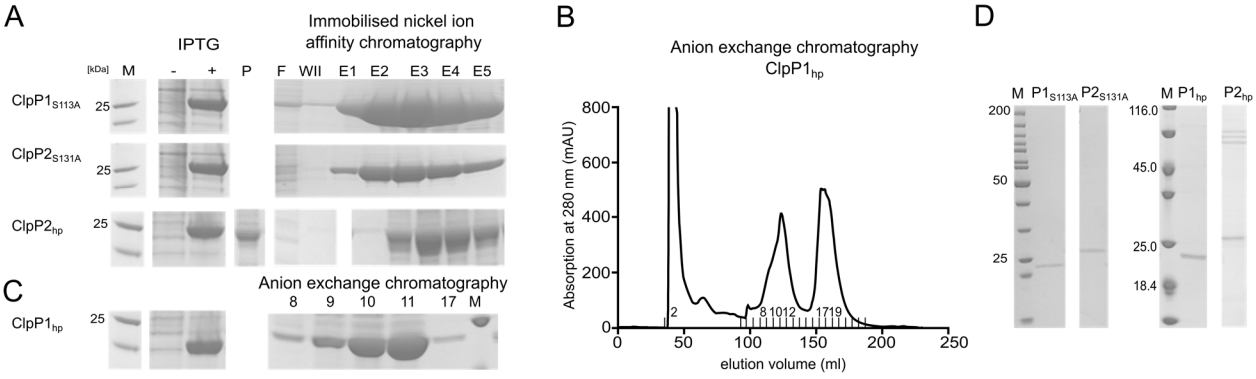

Figure 3.11: **Purification of the catalytic triad knock-out mutant proteins $ShClpP1_{S113A}$, $ShClpP2_{S131A}$ and the hydrophobic pocket mutant $ClpP2_{hp}$ via immobilised nickel ion affinity chromatography. Anion exchange chromatography of $ShClpP1_{hp}$ including analysis of expression of the mutant proteins prior to the purification procedure**. **A**: Test of $ShClpP1_{S113A}$, $ShClpP2_{S131A}$ and $ShClpP2_{hp}$ expression, conducted at 37°C for 4 h, induced with 1 mM IPTG. Whole cell extracts (un-induced + induced) were analysed via SDS-PAGE. Additionally, samples of

the immobilised nickel ion affinity chromatography including the flow-through, wash II and elution fractions E1-E5 are presented on SDS-PAGE images. **B:** Anion exchange chromatography of $ClpP1_{hp}$, monitored at 280 nm. **C**: Expression of $ClpP1_{hp}$ was tested for 4 h at 37°C, loading induced (+ 1 mM IPTG) and un-induced whole cell extracts on 12 % Bis-Tris gels. Additionally, samples, which were taken during anion exchange chromatography, were loaded on 12 % Bis-Tris gels as well. **D:** After the protein purification procedure, 2 µM of $ClpP1_{S113A}$, $ClpP2_{S131A}$, $ClpP1_{hp}$ and $ClpP2_{hp}$ were analysed via SDS-PAGE.

Similarly to the anion exchange chromatography of wild-type ClpP1, the collected fraction, which contained the highest amount of $ClpP1_{hp}$ according to the absorption spectrum at 280 nm and an SDS-PAGE analysis, was further processed identically to the purification of native ClpP1.

Given that the hydrophobic pocket mutant $ClpP2_{hp}$ was expressed from the putative second start codon, wild-type ClpP2 and $ClpP2_{ATG2}$ were applied side by side in combination with ClpP1 or $ClpP1_{hp}$ in those substrate degradation experiments in which the hydrophobic pocket mutant proteins $ClpP1_{hp}$ and $ClpP2_{hp}$ were applied. However, only simplified versions of the substrate degradation experiments are shown in chapter 3 presenting exclusively $ClpP2_{ATG2}$ in combination with ClpP1 or $ClpP1_{hp}$. For the sake of simplicity, $ClpP2_{ATG2}$ is only referred to as ClpP2 in Figure 3.12, 3.13, 3.15 and 3.16. However, the complete degradation experiments utilising ClpP2 and $ClpP2_{ATG2}$ side by side in combination with wild-type ClpP1 or $ClpP1_{hp}$ can be seen in Figure 6.6 in the appendix.

3.1.7 *In vitro* substrate degradation experiments employing the mutant proteins $ShClpP1_{S113A}$, $ShClpP2_{S131A}$, $ShClpP1_{hp}$ and $ShClpP2_{hp}$

ClpC1-mediated FITC-casein degradation experiments employing the catalytic triad knock-out mutant proteins $ClpP1_{S113A}$ and $ClpP2_{S131A}$ were performed in order to examine if both ClpP isoforms equally contribute to the proteolytic activity of ClpP1P2 heteromeric complexes. Similarly, Clp-ATPase/ClpP interactions of ClpP1 and ClpP2 with ClpX, ClpC1 and ClpC2 were analysed employing the hydrophobic pocket mutant proteins $ClpP1_{hp}$ and $ClpP2_{hp}$ in *in vitro* degradation experiments using casein (α and β) and ClgR as substrates, see Fig. 3.12.

Surprisingly, studying the hydrolysis of fluorogenic casein revealed similar proteolytic activities between wild-type ClpP1P2 and ClpP1P2$_{S131A}$, whereas the combinations of ClpP1$_{S113A}$ with either ClpP2 or ClpP2$_{S131A}$ completely abolished FITC-casein degradation. Hence, the proteolytic activity of heteromeric ClpP1P2 complexes is exclusively conferred by ClpP1. Since ClpP2 did not exhibit proteolytic activity in ClpP1P2 heteromeric complexes under the conditions applied here but is essential for the Clp-ATPase-mediated degradation of substrates, see Figure 3.6, it was further speculated that ClpP2 could be the main interaction partner for the Clp-ATPases ClpX, ClpC1 and ClpC2.

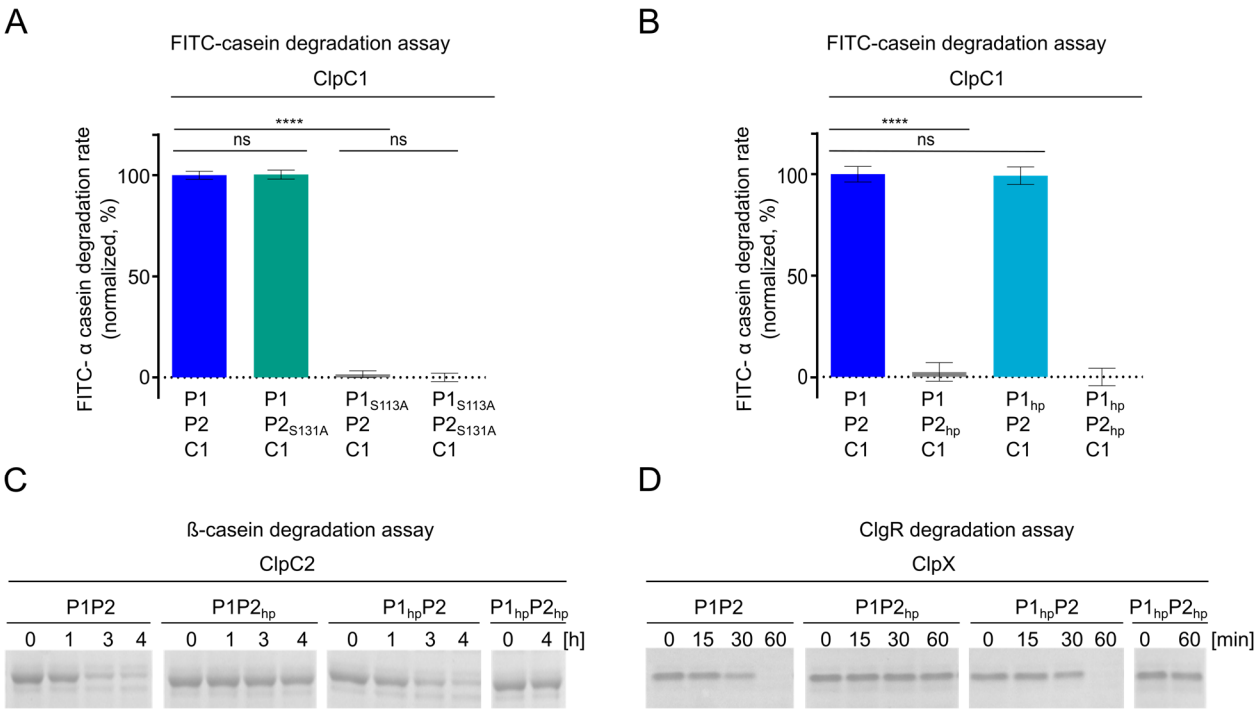

Figure 3.12: **ShClpP1 and ShClpP2 isoforms fulfil distinct but complementary functions in heteromeric ShClpP1P2 complexes. A:** Proteolytic activity of ShClpP1P2 (4 µM each) complexes was analysed in ShClpC1 (4 µM)-mediated FITC-casein (6 µM) degradation assays applying the catalytic triad knock-out mutant proteins ShClpP1$_{S113A}$ and ShClpP2$_{S131A}$ in combination with wild-type ShClpP1 and ShClpP2. **B**: Clp-ATPase/ClpP interactions were examined in ShClpC1 (4 µM)-mediated FITC-casein (6 µM) degradation assays employing the hydrophobic pocket mutant proteins ShClpP1$_{hp}$ and ShClpP2$_{hp}$ in combination with wild-type ShClpP1 and ShClpP2 (4 µM of wild-type and mutant ShClpP1 and ShClpP2 proteins). **A + B**: Time-dependent increase in fluorescence intensity was recorded (RFUs). Mean of initial slopes are given (normalized in %). P-values were calculated using one way ANOVA with three biological comprising three technical replicates, respectively. P-values: ns > 0.05; ****≤ 0.0001. Error bars indicate corresponding standard deviations. **C**: ShClpC2 (1.5 µM)-mediated ß-casein (10 µM) degradation experiments

were performed applying the hydrophobic pocket mutant proteins ShClpP1$_{hp}$ and ShClpP2$_{hp}$ in combination with ShClpP1 and ShClpP2 (1.5 µM each). **D**: Similarly, the natural substrate ShClgR (3 µM) was used in ShClpX-mediated degradation experiments (1.5 µM of ShClpP1, ShClpP2 and ShClpX). **C + D**: Experiments were conducted at 30°C. Samples were taken after different time points and loaded on 12% Bis-Tris gels for subsequent analysis. **B-C**: All degradation experiments employing ShClpP2$_{hp}$ were performed with ShClpP2 and ShClpP2$_{ATG2}$ side by side in combination with ShClpP1 or ShClpP1$_{hp}$. Simplified degradation experiments are shown here and the complete assays are presented in the appendix, see Figure 6.6. The presented gels are exemplary for at least three independent biological replicates.

Fig. 3.12 clearly demonstrates that the ClpC1, ClpC2 and ClpX-mediated degradation of casein and ClgR was completely abolished applying the hydrophobic pocket mutant protein ClpP2$_{hp}$ in combination with wild-type ClpP1. In contrast, the proteolytic activity of ClpP1$_{hp}$P2 was comparable to wild-type ClpP1P2, implying that the Clp-ATPases ClpC1, ClpC2 and ClpX bind to the proteolytic core exclusively via ClpP2, resulting in asymmetrical Clp protease complexes with one Clp-ATPase ring bound to ClpP2. While proteolytic activity is conferred by ClpP1, substrates, which are recognised, unfolded and threaded into the proteolytic chamber by the Clp-ATPases, enter the internal degradation chamber of the peptidase via the Clp-ATPase-bound heptameric ring of ClpP2.

3.1.8 Substrate degradation experiments using ADEP1 as ClpP activator

Considering the fact that *S. hawaiiensis* is the producer of ADEP1, the capability to dysregulate ClpP1 and ClpP2 using this natural product as activator of its peptido- and proteolytic activity was tested in substrate degradation experiments. Therefor, two different model substrates were utilised: a short, fluorescently-labeled dipeptide, named Suc-LY-AMC, and fluorescently-labeled α-casein (FITC-casein). Additionally, the catalytic triad knock-out mutant proteins ClpP1$_{S113A}$ and ClpP2$_{S131A}$ as well as the hydrophobic pocket mutant proteins ClpP1$_{hp}$ and ClpP2$_{hp}$ were applied in combination with wild-type ClpP1 and ClpP2 in Suc-LY-AMC degradation experiments. Fig. 3.13 clearly demonstrates that ClpP1, ClpP2 and a mixture of both ClpP isoforms did not exhibit peptidolytic activity in the absence of ADEP1. However, when ADEP1 was added, ClpP1 as well as ClpP1P2, but not ClpP2, hydrolysed Suc-LY-AMC efficiently.

Accordingly, exchanging wild-type ClpP1 with the catalytic triad knock-out mutant ClpP1$_{S113A}$ completely abolished Suc-LY-AMC degradation in combination with wild-type ClpP2 or ClpP2$_{S131A}$, whereas ClpP1P2$_{S131A}$ exhibited similar peptidolytic activities compared to wild-type ClpP1P2. Applying the hydrophobic pocket mutant proteins ClpP1$_{hp}$ and ClpP2$_{hp}$ in combination with wild-type ClpP1 or ClpP2 revealed that ADEP1 failed to activate ClpP1$_{hp}$ or ClpP1$_{hp}$P2, whereas exchanging ClpP2 by ClpP2$_{hp}$ did not change the peptidolytic activity of ClpP1ClpP2$_{hp}$ compared to wild-type ClpP1P2.

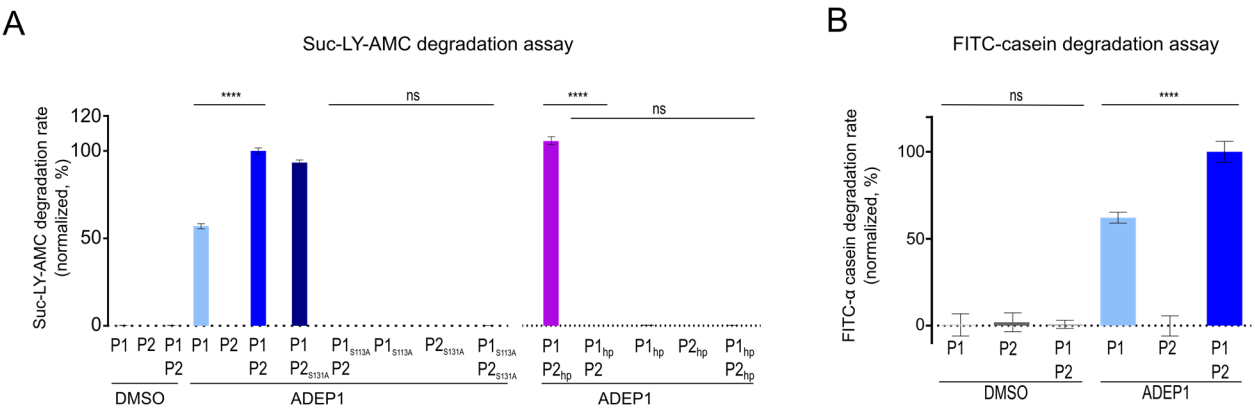

Figure 3.13: **The natural product ADEP1 was utilised to activate ShClp1 and ShClpP2 in *in vitro* substrate degradation experiments. A:** Wild-type ShClpP1 and ShClpP2 were tested independently (4 µM) or in combination (2 + 2 µM) together with the catalytic triad knock-out mutant proteins ShClpP1$_{S113A}$ and ShClpP2$_{S131A}$ to degrade the fluorescently-labeled dipeptide Suc-LY-AMC (100 µM) in the absence and presence of ADEP1 (10 µM). For testing the hydrophobic pocket mutant proteins ShClpP1$_{hp}$ and ShClpP2$_{hp}$ in combination with wild-type ShClpP1 and ShClpP2, 8 µM or 4 + 4 µM in single or combined samples were used in the presence of 30 µM ADEP1. The degradation assay employing the hydrophobic pocket mutants ShClpP1$_{hp}$ and ShClpP2$_{hp}$ was performed with ShClpP2 and ShClpP2$_{ATG2}$ side by side in combination with ShClpP1 or ShClpP1$_{hp}$. The simplified assay is shown here, whereas the complete bar chart is presented in the appendix, see Figure 6.6. **B**: The proteolytic activity of ShClpP1 (10 µM), ShClpP2 (10 µM) and ShClpP1P2 (5 + 5 µM) was analysed in the absence and presence of the ClpP activator ADEP1 (30 µM). **A + B**: Time-dependent increase of fluorescence was monitored (RFUs). Mean of initial slopes are represented (normalized in %). Statistics were calculated with one way ANOVA using three biological comprising three technical replicates. P-values: ns > 0.05; ****≤ 0.0001. Error bars indicate corresponding standard deviations.

These results strongly indicate that ADEP1 preferably binds to the apical surface of ClpP1, whereas ClpP2 seems to be an ADEP-insensitive peptidase. Of note, ClpP1P2, ClpP1P2$_{S131A}$ and ClpP1P2$_{hp}$ exhibited superior peptidolytic activity compared to ClpP1.

Accordingly, FITC-casein degradation assays in the absence and presence of ADEP1 showed similar results. While ClpP1, ClpP2 and ClpP1P2 failed to hydrolyse FITC-casein in the absence of ADEP1, ClpP1 as well as ClpP1P2, but not ClpP2, degraded fluorogenic casein after ADEP1 addition. Conclusively, ADEP1 is able to activate the *Streptomyces* ClpP1P2 proteolytic core to degrade short peptides and the model protein FITC-casein in a Clp-ATPase-independent manner.

3.1.9 Analysis of the oligomeric states of ShClpP1 and ShClpP2 in the absence and presence of ADEP1

As it was seen in the previous chapter, ClpP1 could be activated to degrade the fluorogenic model substrate FITC-casein by the addition of ADEP1, dysregulating the protease complex by turning the strictly controlled Clp-ATPase-dependent peptidase ClpP into an un-controlled, Clp-ATPase-independent protease. In contrast, ADEP1 failed to activate ClpP2 for the degradation of short dipeptides as well as proteins, strongly suggesting that ClpP2 is an ADEP-insensitive peptidase. As a following step, the oligomeric behaviour of both ClpP isoforms in the presence and absence of ADEP1 was analysed, illustrating its ability to assemble ClpP into its active tetradecameric state. Therefor, 80 µM of native ClpP1 or ClpP2 were mixed with and without ADEP1 and applied to the size exclusion chromatography column (Fig. 3.14).

In the absence of ADEP1, ClpP1 mostly eluted as heptameric and lower oligomeric states, presumably dimers and trimers (black curve). However, after ADEP1 addition (red curve), ClpP1 assembled into higher oligomeric species, presumably tetradecamers (calculated size: ~ 305.2 kDa). Interestingly, lower oligomeric states could still be observed after the addition of ADEP1, yet in low abundance. While a surplus of ADEP1 was used in this experiment, the oligomeric behaviour of ClpP1 in the presence of equal concentrations of ClpP1 and ADEP1 was tested as well, resulting in a similar assembly of ClpP1 homo-tetradecamers, see Figure 6.7 in the appendix.

In addition, $ClpP1_{hp}$ was analysed via size exclusion chromatograpy with and without the addition of ADEP1, see Figure 6.7 in the appendix. Similarily to $ClpP1_{hp}$ in the absence of ADEP1, $ClpP1_{hp}$ eluted mostly as heptameric species and failed to assemble into homo-tetradecamers in the presence of ADEP1, Fig. 6.7.

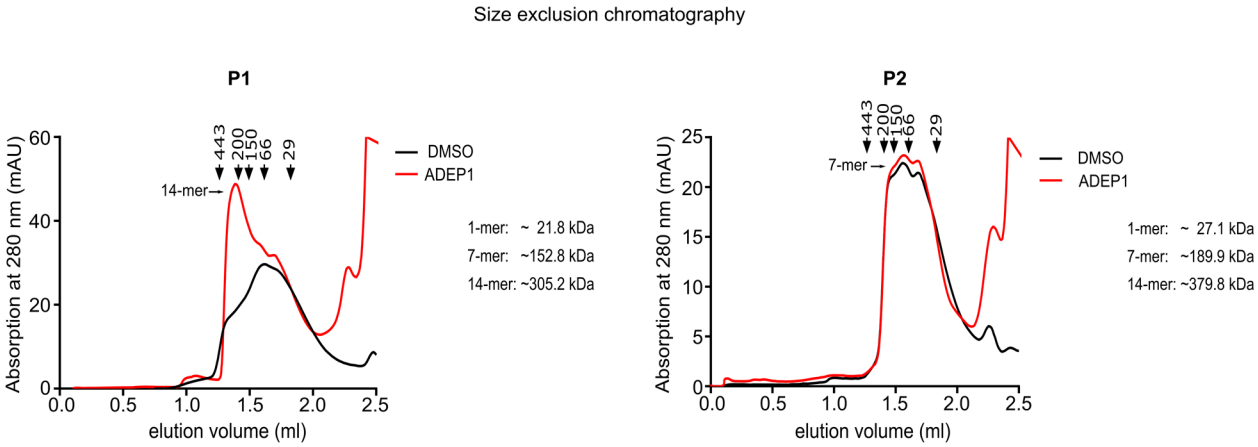

Figure 3.14: **Size exclusion chromatography of native ShClpP1 (80 µM) and ShClpP2 (80 µM) in the presence and absence of the natural product ADEP1 (200 µM)**. The column Superdex^{TM} 200 Increase 3.2 300 was used to analyse the oligomeric behaviour of ShClpP1 and ShClpP2 with and without the addition of ADEP1.

Furthermore, ADEP1 failed to assemble ClpP2 into tetradecamers (calculated size: ~379.8 kDa) which still eluted mostly as heptameric species after ADEP1 addition, similar to the elution behaviour without ADEP1 (black curve), strongly implying that ClpP2 might be an ADEP-insensitive peptidase, whereas the ADEP1-triggered peptido- and proteolytic activity of ClpP1 can be explained by the oligomerisation of catalytically active ClpP1 homo-tetradecamers. Additionally, a mixed ClpP1P2 sample with and without ADEP1 was applied to the gel filtration column, employing $ClpP2_{His}$ in combination with native ClpP1. While His_6-tagged ClpP2 exclusively displayed heptameric species on native Tris-Glycine gels, see Figure 3.9, the C-terminally His_6-tagged ClpP2 protein eluted in oligomeric species of ~670 kDa in size which could not be detected anymore in the presence of ClpP1 and ADEP1. Tetradecameric species could be observed in a ClpP1P2 sample in the presence of ADEP1 which eluted earlier (after 1.35 ml) than ADEP-induced ClpP1 homo-tetradecamers (after 1.39 ml), demonstrating the formation of ADEP-bound ClpP1P2 heteromeric complexes, see Figure 6.8 in the appendix.

3.1.10 Analysis of ShClpP1 and ShClpP2 processing in association with ShClp-ATPases as well as in the absence and presence of ADEP1

In the course of Clp-ATPase-mediated substrate degradation experiments, a processing reaction of both ClpP isoforms could be observed, however depending on certain conditions applied (Fig. 3.15). Focusing on the assembly of physiologically active Clp protease complexes and employing the unfoldase ClpX together with ClpP1, ClpP2 or a mixture of ClpP1P2, it was described above that neither ClpXP1, nor ClpXP2 exhibited proteolytic activity. Accordingly, a processing reaction of ClpP1 and ClpP2 could only be observed in samples consisting of both ClpP isoforms as indicated in blue (ClpP1) and green (ClpP2) asterisks in Figure 3.15.

Strikingly, the processing of ClpP2 seemed to happen almost directly after starting the reaction, whereas a faint processed band of ClpP1 could only be detected after 60 min. Applying the hydrophobic pocket mutant proteins $ClpP1_{hp}$ and $ClpP2_{hp}$, a potential role of ClpX binding on ClpP1 and ClpP2 processing was analysed. Surprisingly, employing the hydrophobic pocket mutant proteins $ClpP1_{hp}$ and $ClpP2_{hp}$ in different combinations with wild-type ClpP1 and ClpP2 did not change the processing pattern of ClpP2, however, ClpP1 processing was abolished in samples where wild-type ClpP2 was exchanged by $ClpP2_{hp}$, strongly indicating that ClpP1 processing is induced by the binding of ClpX to the interaction surface of ClpP2 (Fig. 3.15 A and Fig. 6.3 in the appendix). As shown above, the natural antibiotic ADEP1 is able to confer Clp-ATPase-independent protease activity to ClpP1 and ClpP1P2 complexes, see Figure 3.13 B. Next, potential effects of ADEP1 on ClpP1 and ClpP2 processing were analysed using DMSO as control. While ClpP2 processing strictly depended on the presence of ClpP1 in the absence or presence of ADEP1, ClpP1 was observed to be self-processed in the presence of ADEP1, further confirming ClpP1 to be an ADEP-sensitive peptidase. Remarkably, ClpP1 as well as ClpP2 processing seemed to be even stimulated after ADEP1 addition to mixed ClpP1P2 samples. The catalytic triad knock-out mutant proteins $ClpP1_{S113A}$ and $ClpP2_{S131A}$ were applied in combination with wild-type ClpP1 and ClpP2 as well, demonstrating that ClpP1 is the sole propeptide processor of itself and ClpP2. Exchanging wild-type ClpP1 by $ClpP1_{S113A}$ completely abolished ClpP1 and ClpP2 processing

whereas ClpP1P2$_{S131A}$ displayed a processing pattern comparable to wild-type ClpP1P2, see Figure 3.15 C.

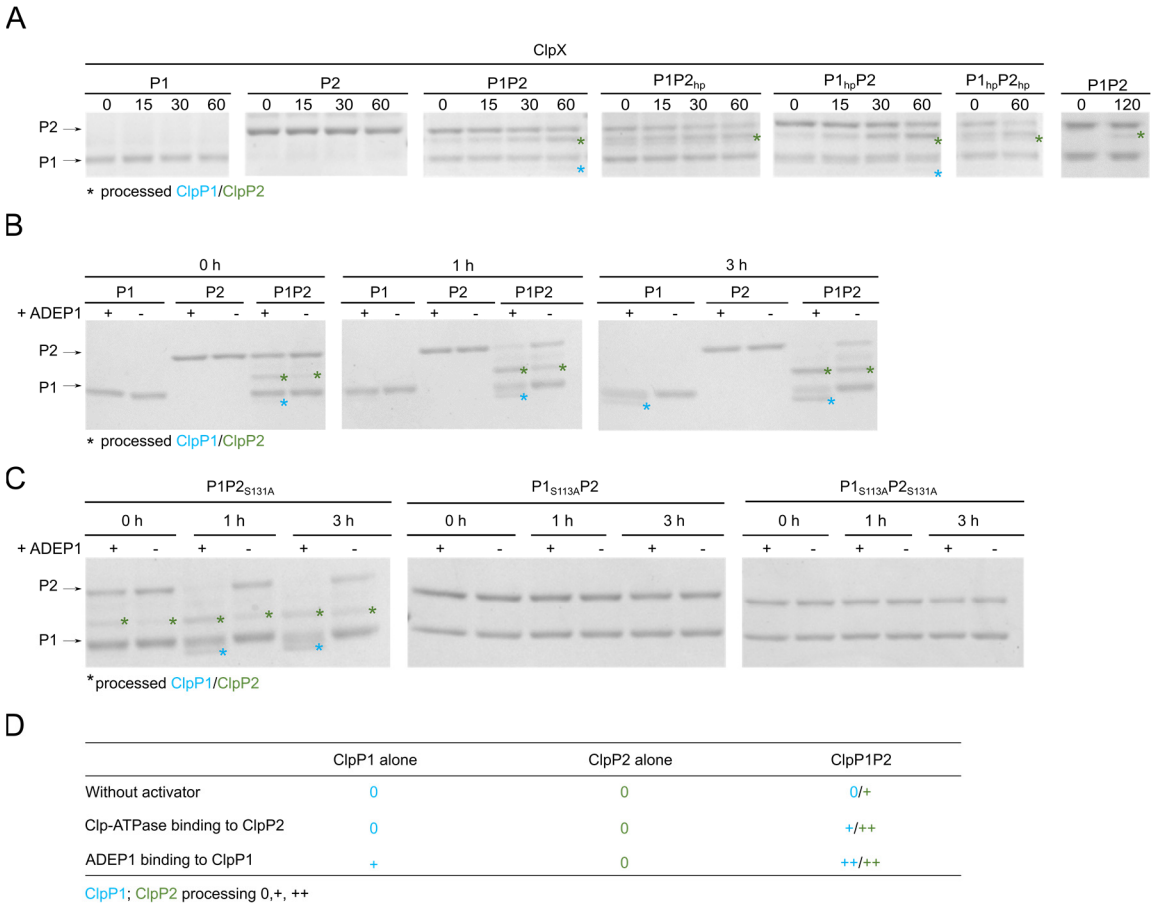

Figure 3.15: **Processing of ShClpP1 and ShClpP2 during ShClpX-mediated degradation of ShClgR as well as in the absence and presence of ADEP1. A**: Processing reactions observed during ShClpX-mediated substrate degradation employing ShClpP1, ShClpP2, ShClpP1P2 as well as the hydrophobic pocket mutant proteins ShClpP1$_{hp}$ and ShClpP2$_{hp}$ in combination with wild-type ShClpP1 and ShClpP2. Here, wild-type ShClpP2$_{ATG2}$ is shown. The complete assay with ShClpP2 and ShClpP2$_{ATG2}$ side by side is shown in the appendix, see Figure 6.3 A. Furthermore, the dependence of ShClpP1 processing on the interaction of ShClpX with ShClpP2 is further visualised in Fig. 6.3 B in the appendix. **B**: Processing of ShClpP1 (2 µM), ShClpP2 (2 µM) and ShClpP1P2 (2 + 2 µM) in the presence and absence of ADEP1 (10 µM). **C**: The catalytic triad knock-out mutant proteins ShClpP1$_{S113A}$ and ShClpP2$_{S131A}$ were applied in combination with wild-type ShClpP1 and ShClpP2 (2 µM each). All experiments were performed at 30°C and samples were taken after different time points and loaded on 12% Bis-Tris gels. The gels are exemplary for at least three biological replicates. **D**: Overview of processing reactions.

In cooperation with the working group of Prof. Stephan Sieber, TU munich, the processing sites of ClpP1 and ClpP2 could be identified by intact protein mass spectrometry to be located

between the amino acids G24/P25 for ClpP1 (sequence starting with PSIGGGL) and S33/R34 for ClpP2 (sequence starting with RYIIPR), see Figure 6.4 in the appendix. Furthermore, the processing site of $ClpP2_{ATG2}$ could be confirmed as the same processing site for full-length ClpP2, see Figure 6.5 in the appendix. Intact protein mass spectrometry was performed by Dr. Markus Lakemeyer, see chapter 11.

In order to exclude the formation of proteolytically active ClpP1 and ClpP2 homo-tetradecamers after the processing reaction was completed, truncated versions of ClpP1 and ClpP2 (named ClpP1* and ClpP2*) were cloned, purified and applied in a ClpC1-dependent FITC-casein degradation experiment. The cloned constructs started with the processing site, thus being equivalent to the mature processed products. The purification of ClpP1* and ClpP2* can be seen in Figure 6.1 in the appendix.

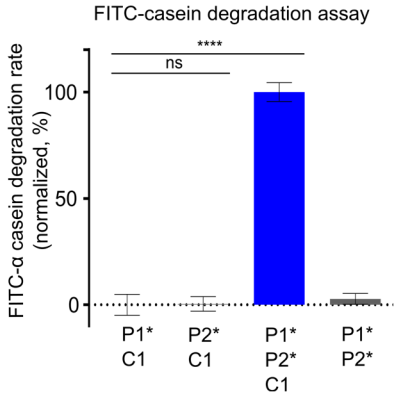

Figure 3.16: **ShClpC1-dependent degradation of fluorogenic casein (6 µM) by ShClpP1*, ShClpP2* and ShClpP1*P2*.** 8 µM of ShClpP1*, ShClpP2* or 4 + 4 µM of ClpP1*P2* were employed in combination with 4 µM ClpC1**.** Hydrolysis of FITC-casein was monitored as an increase of fluorescence intensity over time. Mean of initial slopes are given. Statistics were performed with one-way ANOVA using three biological comprising three technical replicates. P-values: P-values: ns > 0.05; ****≤ 0.0001. Error bars indicate corresponding standard deviations.

Figure 3.16 illustrates that neither ClpC1P1* nor ClpC1P2* exhibited proteolytic activity. However, when mixed together, ClpP1*P2* rapidly hydrolysed fluorogenic casein in association with ClpC1, further emphasising that ClpP1 and ClpP2 processing is not a prerequisite for the formation of proteolytically active ClpP1 and ClpP2 homo-tetradecamers.

3.1.11 ShClpP1P2: competition assays, applying ADEP1 and the Clp-ATPases ShClpX, ShClpC1 and ShClpC2 in substrate degradation experiments

All experiments performed up to that point provided evidence that *Streptomyces* ClpP1 and ClpP2 form heteromeric ClpP1P2 complexes, which can be proteolytically activated by asymmetrical binding of the Clp-ATPases to ClpP2 or ADEP1 binding to ClpP1. Studies on ADEP mechanisms of action in other bacteria such as *Escherichia coli*, *Staphylococcus aureus*, *Bacillus subtilis*, *Mycobacterium tuberculosis* or *Chlamydia trachomatis* illustrated that Clp-ATPase binding to the proteolytic core ClpP is prevented after ADEP addition, abolishing ATPase-mediated substrate hydrolysis, consequently leading to the inhibition of natural functions of the Clp protease (Kirstein et al., 2009, Gersch et al., 2015, Amor et al., 2016, Famulla et al., 2016, Pan et al., 2019). To explore potential effects of ADEP on the Clp-ATPase mediated degradation of substrates by *Streptomyces* ClpP1P2, competition assays were performed employing ClpP1P2 in association with ClpX, ClpC1 or ClpC2 to degrade a set of different substrates in the absence or presence of ADEP1 (Fig. 3.17).

First, ClpX-mediated ClgR and PopR degradation experiments were performed with wild-type ClpP1 and ClpP2 in combination with the hydrophobic pocket mutant proteins $ClpP1_{hp}$ and $ClpP2_{hp}$, see Figure 3.17. Intriguingly, adding ADEP1 to the reaction mixture did not lead to the inhibition of ClgR and PopR degradation by ClpXP1P2, contrariwise it led to a slightly stimulated substrate degradation. Nevertheless, exchanging wild-type ClpP2 by the hydrophobic pocket mutant $ClpP2_{hp}$ completely abrogated ClgR and PopR degradation, demonstrating that ClpX binding to ClpP2 remained a prerequisite for substrate degradation, even in the presence of a surplus of ADEP1. Furthermore, ClpP1P2 without the addition of ClpX in the absence or presence of ADEP1 failed to hydrolyse ClgR and PopR, excluding a Clp-ATPase-independent, ADEP-induced degradation (Fig. 3.17 A).

As a next step, the effects of ADEP on the ClpX-mediated degradation of substrates by ClpP1P2 were analysed in detail. Therefor, green fluorescent protein (GFP) was chosen as substrate with an attached C-terminal ssrA-tag, which is a common degron recognised by Clp-ATPases, resulting in subsequent hydrolysis of the fusion protein that can be monitored via a decreasing fluorescence signal over time (Gottesman et al., 1998, Flynn et al., 2001).

Fig. 3.17 B presents the ClpX-dependent degradation of GFP-ssrA by ClpP1P2. In the absence of ClpX, ClpP1P2 did not degrade GFP-ssrA and ADEP addition did not change this. However, the addition of ClpX to ClpP1P2 led to an efficient degradation of GFP-ssrA over time (pink curve), which could be stimulated significantly by ADEP1 (red curve).

Accordingly, ADEP1 stimulated the ClpC1-dependent degradation of fluorogenic casein by ClpP1P2, see Figure 3.17 C. However, ADEP1 induced a ClpC1-independent degradation of fluorogenic casein by ClpP1P2 as well but significantly less efficient compared to the ClpC1-dependent degradation of the model substrate. In addition, the ClpC2-dependent and independent degradation of ß-casein by ClpP1P2 in the absence and presence of ADEP1 was explored, employing the hydrophobic pocket mutant proteins $ClpP1_{hp}$ and $ClpP2_{hp}$. Similarly, ADEP1 stimulated the ClpC2-mediated degradation of ß-casein compared to the DMSO control and induced a ClpC2-independent hydrolysis of ß-casein by the mixed proteolytic core (Fig. 3.17 D). Of note, while in the absence of ADEP1 the ClpC2-mediated degradation of ß-casein could be inhibited applying the hydrophobic pocket mutant $ClpP2_{hp}$ in combination with wild-type ClpP1, casein degradation could be solely abolished in the presence of ADEP1 employing both hydrophobic pocket mutant proteins $ClpP1_{hp}$ and $ClpP2_{hp}$, thereby abrogating ADEP binding to the heptameric ring of ClpP1. Remarkably, adding ADEP1 to ClpC2P1P2 led not only to the degradation of ß-casein, but to the degradation of ClpC2 as well, after the model substrate was digested completely, implying ClpC2 as a new target for ADEP-activated ClpP1P2 in streptomycetes.

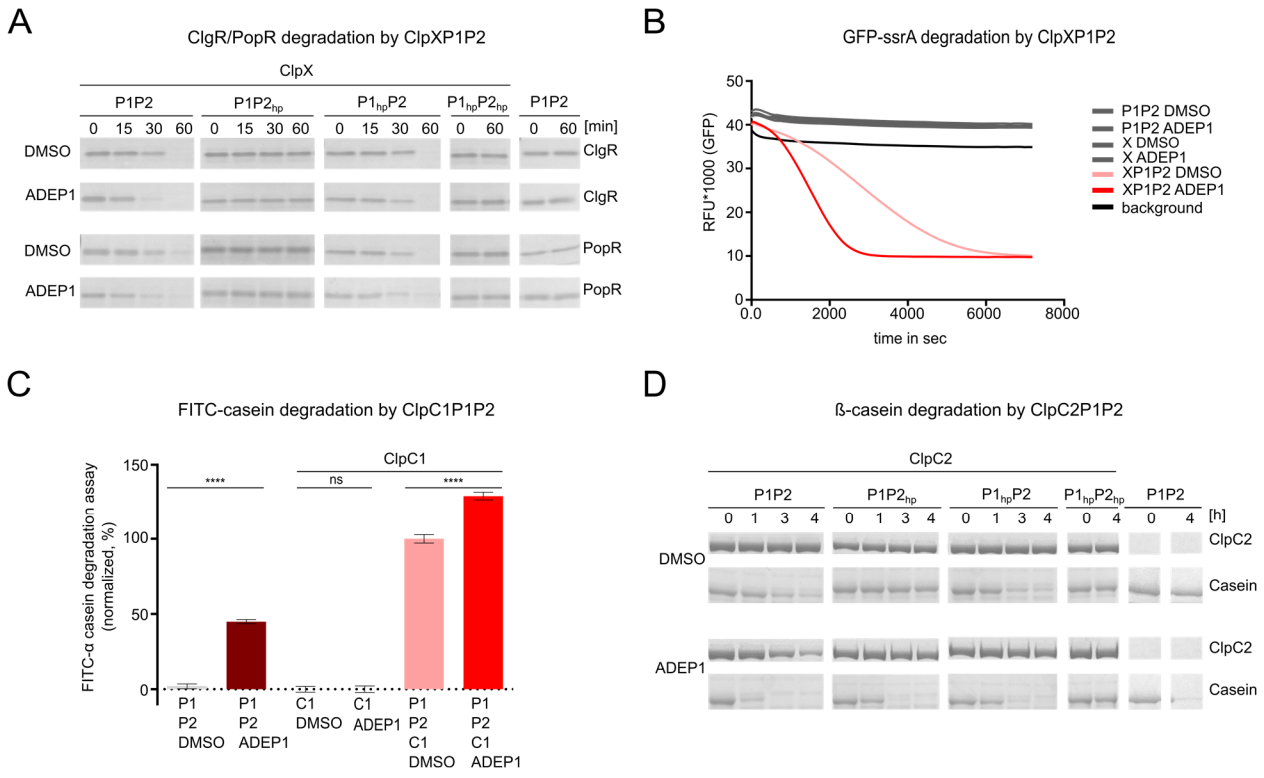

Figure 3.17: **ADEP stimulates *Streptomyces* ClpP1P2 for accelerated, yet Clp-ATPase-mediated proteolysis. A:** ADEP led to a stimulated, ShClpX-mediated degradation of ShClgR and ShPopR by ShClpP1P2. Additionally, the hydrophobic pocket mutant proteins ShClpP1$_{hp}$ and ShClpP2$_{hp}$ were employed in combination with wild-type ShClpP1 and ShClpP2 as well. For this assay, ShClpP2 and ShClpP2$_{ATG2}$ were applied side by side together with ShClpP1 or ShClpP1$_{hp}$. Here, the simplified degradation experiment, comprising ShClpP2$_{ATG2}$, is shown. The complete assay is presented in the appendix, see Figure 6.6. 1.5 µM of ShClpP1, ShClpP2 and ShClpX were used to degrade 3 µM ShClgR or ShPopR in the absence or presence of 30 µM ADEP1. The experiment was performed at 30°C and samples were loaded on 12 % Bis-Tris gels for subsequent analysis. The presented gel is exemplary for at least three independent biological replicates. **B**: GFP-ssrA (0.36 µM) degradation by ShClpXP1P2 (3 µM each) in the absence and presence of a surplus of ADEP1 (30 µM). Time-dependent decrease in fluorescence intensity (RFUs) is shown. The experiment is exemplary for at least three individual biological replicates. **C**: ShClpC1-dependent (4 µM) and independent degradation of fluorogenic casein by ShClpP1P2 (4 + 4 µM) in the absence and presence of ADEP1 (30 µM). Time dependent increase in fluorescence intensity was monitored. Mean of initial slopes are given (normalized in %). Statistics were calculated with one-way ANOVA using three biological comprising three technical replicates. P-values: P-values: ns > 0.05; ****≤ 0.0001. Error bars indicate corresponding standard deviations. **D**: ß-casein (10 µM) degradation by ShClpP1P2 (1.5 + 1.5 µM) in combination with the hydrophobic pocket mutant proteins ShClpP1$_{hp}$ and ShClpP2$_{hp}$ in association with the unfoldase ShClpC1 (1.5 µM) in the absence and presence of ADEP1 (30 µM). This experiment was performed employing ShClpP2 and ShClpP2$_{ATG2}$ side by side in combination with ShClpP1 or ShClpP1$_{hp}$. The complete gel is presented in the appendix, see Figure 6.6. The experiment was conducted at 30°C and samples

were taken and loaded on 12 % Bis-Tris gels. The presented gel is exemplary for three individually obtained biological replicates.

Furthermore, previous results demonstrated that ClpC1P1P2 failed to degrade the natural substrate PopR within the time course of four hours. However, regarding the ADEP-induced accelerated degradation of substrates by ClpC1P1P2, the degradation experiment was repeated using a surplus of ADEP1, with DMSO as control, see Figure 3.18.

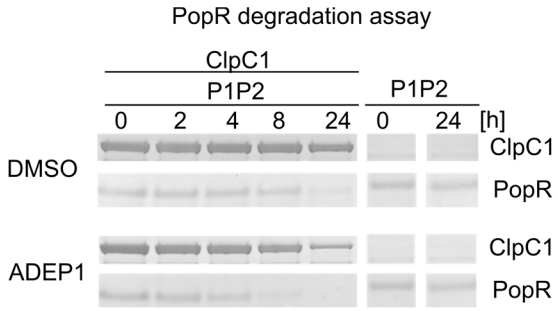

Figure 3.18: **ShClpC1-dependent degradation of ShPopR by ShClpP1P2 in the absence and presence of ADEP1.** 1.5 µM ShClpP1, ShClpP2 and ShClpC2 were applied to degrade 3 µM ShPopR in *in vitro* substrate degradation experiments. The presented SDS-PAGE gel is exemplary for three biological replicates.

As expected, ADEP1 caused a stimulated degradation of the natural substrate PopR by ClpP1P2. As a control, ClpP1P2 without ClpC1 failed to degrade PopR in the absence or presence of ADEP1. Remarkably, an ADEP1-induced hydrolysis of ClpC1 by ClpP1P2 could be observed as well, similarly to the ADEP-induced degradation of ClpC2, however, within a prolonged time period of 24 h.

Conclusively, all degradation experiments demonstrate that ADEP1 has a strong effect on *Streptomyces* ClpXP1P2, ClpC1P1P2 and ClpC2P1P2 complexes, leading to an accelerated degradation of natural and model substrates. This observation can be explained by a concomitant binding of ADEP1 and the Clp-ATPases to opposite sites of the heteromeric ClpP1P2 complex. Contrariwise, in all bacteria analysed so far, ADEP binding to the proteolytic core ClpP resulted in the inhibition of Clp-ATPase/ClpP interactions, inhibiting the physiological function of the caseinolytic protease Clp and revealing a new and unprecedented ADEP mode of action in *Streptomyces* (Kirstein et al., 2009, Gersch et al., 2015, Amor et al., 2016, Famulla et al., 2016, Pan et al., 2019).

3.1.12 *In vitro* substrate degradation experiments employing the mutant proteins ShClpP1$_{Y76S}$ and ShClpP2$_{S94Y}$

In the course of constructing the hydrophobic pocket mutant proteins ClpP1$_{hp}$ (Y74V, Y76V and Y98V) and ClpP2$_{hp}$ (S94A, Y96V, Y116V), it became apparent that the exchanged amino acid residues of ClpP1 and ClpP2 only differ in S94 of ClpP2, see Figure 3.10. Regarding ClpP2 as the exclusive interaction partner for the Clp-ATPases ClpX, ClpC1 and ClpC2 and its ADEP-insensitivity, questions emerged, if S94 might be essential for either one or both of those distinct features. However, the ADEP-sensitive ClpP from *B. subtilis* comprises a serine residue at the respective position (see Figure 3.10), which is known to be involved in ADEP1 binding (Lee et al., 2010), indicating that S94 in ShClpP2 might not contribute to its ADEP-insensitivity. Nevertheless, to answer this question, S94 of ClpP2 was replaced by a tyrosine residue, resulting in identical amino acid residues of wild-type Clp1 and ClpP2$_{S94Y}$ at this position. Similarly, Y76 of ClpP1, which corresponds to S94 of ClpP2 at the respective position, was replaced by a serine residue, yielding the mutant protein ClpP1$_{Y76S}$. The purification of ClpP1$_{Y76S}$ and ClpP2$_{S94Y\text{-}ATG2}$ can bee seen in Figure 6.2 in the appendix. Besides, *clpP2$_{S94Y\text{-}ATG2}$* was expressed from the putative second start codon. However, for the sake of simplicity, ClpP2$_{S94Y\text{-}ATG2}$ is only referred to as ClpP2$_{S94Y}$. As a following step, *in vitro* substrate degradation experiments were performed, employing the fluorogenic dipeptide Suc-LY-AMC or fluorogenic casein as substrate and ADEP1 or the Clp-ATPase ClpC1 as ClpP activator.

Surprisingly, applying ClpP1$_{Y76S}$ and ClpP2$_{S94Y}$ in combination with wild-type ClpP1 and ClpP2 in Suc-LY-AMC degradation assays after ADEP1 addition revealed a stimulated peptidolytic activity of ClpP1 in complex with ClpP2$_{S94Y}$ which was even higher compared to wild-type ClpP1P2, Fig. 3.19 A. Of note, ClpP2$_{S94Y}$ alone did not exhibit peptidolytic activity, suggesting that S94 is not a key switch turning an ADEP-insensitive peptidase into an ADEP-sensitive ClpP resulting in detectable ADEP-induced peptidolytic activity. In contrast, while the peptidolytic activity of wild-type ClpP1 could be accelerated in complex with either wild-type ClpP2 or ClpP2$_{S94Y}$, the ADEP-activated peptidolytic activity of ClpP1$_{Y76S}$ could not be stimulated anymore by the addition of wild-type ClpP2 and was significantly reduced compared to wild-type ClpP1P2 strongly suggesting a decreased ADEP binding to ClpP1$_{Y76S}$ in comparison to wild-type ClpP1. In line with

these results exhibited ClpP1$_{Y76S}$ alone a significantly decreased ADEP-induced peptidolytic activity as well compared to wild-type ClpP1.

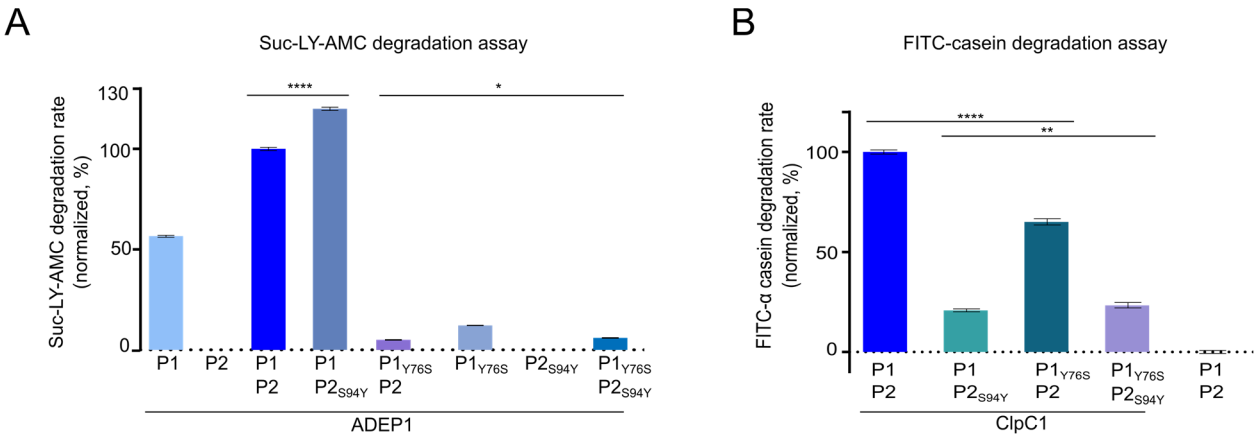

Figure 3.19: ***In vitro* degradation assays applying ShClpP1, ShClpP2 in combination with ShClpP1$_{Y76S}$ and ShClpP2$_{S94Y}$ adding ADEP1 as ClpP activator or the unfoldase ShClpC1 for the degradation of Suc-LY-AMC (A) or fluorogenic casein (B).** The Suc-LY-AMC degradation assay was conducted using 4 µM ShClpP1/ClpP2 or 2 + 2 µM ShClpP1P2 wild-type or mutant proteins in the absence or presence of 10 µM ADEP1. In the ShClpC1-mediated (4 µM) FITC-casein (6 µM) degradation assay 4 µM of ShClpP1 and ShClpP2 wild-type and mutant proteins were utilised. In both assays, wild-type ShClpP2$_{ATG2}$ is presented here in combination with ShClpP2$_{S94Y}$. The complete assay employing ClpP2 and ClpP2$_{ATG2}$ side by side is shown in the appendix, see Figure 6.6. Degradation of Suc-LY-AMC and FITC-casein was monitored as a time-dependent increase in fluorescence intensity. Means of initial slopes are given. Statistics were performed with one way ANOVA employing at least two biological replicates. P-values: ns > 0.05; * ≤ 0.05; ** ≤ 0.01; ***≤ 0.001; ****≤ 0.0001. Error bars indicate corresponding standard deviations.

Next, proteolytic activities of ClpP1$_{Y76S}$ and ClpP2$_{S94Y}$ in combination with wild-type ClpP1 and ClpP2 in ClpC1-dependent FITC-casein degradation assays were analysed. While the peptidolytic activity of ClpP1P2$_{S94Y}$ compared to ClpP1P2 was even higher, employing ADEP1 as ClpP activator, the proteolytic activity of ClpP1P2$_{S94Y}$ was significantly decreased in ClpC1-mediated FITC-casein degradation assays compared to wild-type ClpP1P2, strongly implying that S94 might be essential for ClpC1-ClpP2 interactions. Remarkably, replacing Y76 by a serine residue on the apical surface of ClpP1 led to an impaired ClpC1-dependent proteolytic activity in complex with wild-type ClpP2. As a next step, the oligomeric behaviour of ClpP1$_{Y76S}$ in the presence and absence of ADEP1, separately or combined with wild-type ClpP2, was investigated in BS3 cross-linking experiments, see Figure 3.20. Exchanging the tyrosine residue Y76 of ClpP1 by a serine residue reduced the

capacity of ADEP1 to induce ClpP1$_{Y76S}$ homo-tetradecamers as well as ClpP1$_{Y76S}$ClpP2 hetero-tetradecamers. A feasible explanation is a decreased ADEP affinity for the mutated ClpP1 protein.

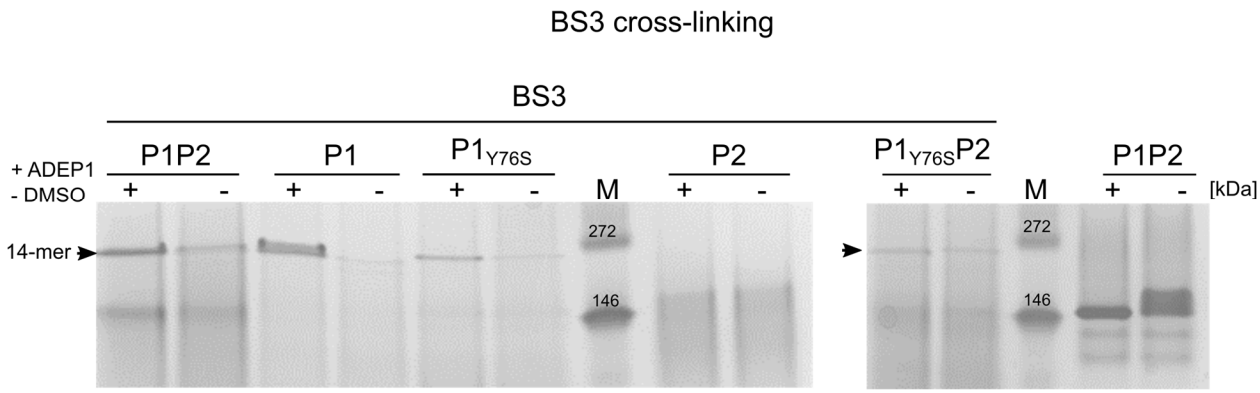

Figure 3.20: **BS3 cross-linking employing wild-type ClpP1 or the mutant protein ShClpP1$_{Y76S}$ in combination with wild-type ShClpP2 in the presence and absence of ADEP1.** 10 µM of each protein was used together with 50 × BS3 of the total ClpP concentration (10 or 20 µM respectively) with and without the addition of 30 µM ADEP1. 30 µl of each sample was applied to a 4-12 % Tris-Glycine gel. The experiment was performed with at least two biological replicates.

Of note, comparing wild-type ClpP1 and ClpP1$_{Y76S}$ in the absence of ADEP1 suggests a similar oligomeric behaviour of both proteins, pointing towards a decreased ADEP-sensitivity of the mutant protein ClpP1$_{Y76S}$ rather than an impaired oligomeric behaviour even in the absence of ADEP1.

By employing higher ClpP concentrations in comparison to the cross-linking experiment seen in Figure 3.9 B, a minor fraction of ClpP1 tetradecamers in a sample consisting of ClpP1 alone could be detected even in the absence of ADEP1, which was significantly lower compared to the mixed ClpP1P2 sample without ADEP1. However, without the addition of the chemical cross-linker BS3, ClpP1P2 combined in the presence and absence of ADEP1 did not assemble tetradecameric states on a native 4-12% Tris-Glycine gel, see Figure 3.20.

3.2 *In vitro* analysis of the ADEP resistance mechanism of *S. hawaiiensis* NRRL 15010

To elucidate the ADEP resistance mechanism of *S. hawaiiensis in vitro*, two different *clpP$_{ADEP}$* constructs were cloned, resulting in the expression of full-length ClpP$_{ADEP}$ and ClpP$_{ADEP\text{-}short}$, the latter with a reduced N-terminus, comprising the amino acid residues 16-206. Previous *in vivo* experiments, which were performed by Dr. Dhana Thomy, had revealed that ClpP$_{ADEP}$ is processed, similar to ClpP1 and ClpP2 (Thomy, 2019). However, full-length ClpP$_{ADEP}$ was never processed neither by itself nor by another peptidase like ClpP1 or ClpP2 in *in vitro* experiments. In addition, ClpP$_{ADEP}$ did not exhibit catalytic activity in *in vitro* degradation experiments. Therefore, the processed version of ClpP$_{ADEP}$ was considered to be the activated form of this Clp peptidase. Besides, protein sequence homologies between ClpP$_{ADEP}$ and the respective Clp peptidases ClpP1-ClpP5 from *S. hawaiiensis* were analysed. As it is seen in table 3.1, ClpP$_{ADEP}$ shares the highest sequence identity with ClpP1, followed by ClpP3, ClpP2, ClpP4 and ClpP5 with the lowest sequence identity, indicated in percentage.

Table 3.1: **Amino acid sequence identities of ClpP$_{ADEP}$ to ClpP1-ClpP5 from *S. hawaiiensis***. Amino acid sequence identities were calculated using Blastp (https://blast.ncbi.nlm.nih.gov /Blast.cgi?PAGE=Proteins) and are indicated in [%]. Query cover defines the percentage of a sequence aligned to another sequence.

	ClpP$_{ADEP}$	
	sequence identity	query cover
ClpP1	73.99 %	83 %
ClpP2	50.00 %	80 %
ClpP3	59.77 %	83 %
ClpP4	45.61 %	82 %
ClpP5	44.97 %	90 %

Considering the fact that a processing reaction of ClpP$_{ADEP}$ never occurred *in vitro*, a shorter, truncated version of ClpP$_{ADEP}$ was purified. However, since the exact processing site of ClpP$_{ADEP}$ is not known, a potential processing site was chosen by analysing previously identified processing sites of streptomycetes and mycobacterial ClpP proteins (Viala and Mazodier, 2002, Benaroudj et al., 2011). Figure 3.21 displays a part of the amino acid sequence alignment of the respective ClpP proteins with known processing sites of ScClpP1, ScClpP2 (Viala and Mazodier, 2002),

ShClpP1, ShClpP2 (this study), MtClpP1 and MtClpP2 (Benaroudj et al., 2011) marked in red boxes and the chosen potential processing site of $ClpP_{ADEP}$ indicated in yellow.

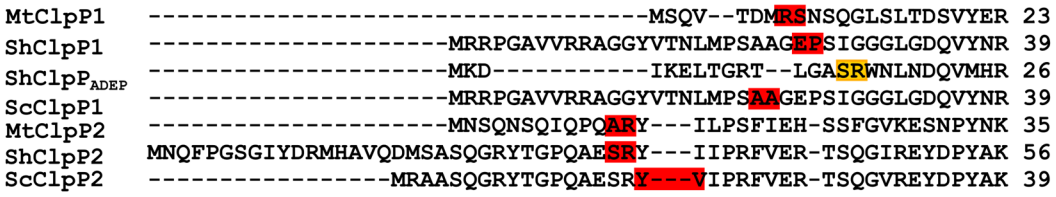

Figure 3.21: **Amino acid sequence sequence alignment of ClpP homologues from *S. coelicolor*, *S. hawaiiensis* and *M. tuberculosis* (Viala and Mazodier, 2002, Benaroudj et al., 2011).** According to the known processing sites of homologous ClpP proteins, a potential processing site of $ShClpP_{ADEP}$ was chosen, which is framed in yellow. The amino acid sequence alignment was performed with the online tool clustal Ω (https ://www.ebi.ac.uk/Tools/msa/clustalo/) with ClpP proteins from *S. coelicolor* ATCC BAA-471 (GCA_000203835.1), *S. hawaiiensis* NRRL 15010 (CP021978.1) and *M. tuberculosis* ATCC 25618 (NC_000962.3).

Strikingly, four out of six identified processing sites of the analysed ClpP proteins contain a combination of alanine, arginine or serine residues. Therefore, a potential processing site for $ClpP_{ADEP}$ was chosen between S15 and R16 and the respective *clpP$_{ADEP}$* gene was cloned with an attached C-terminal His_6-tag. The purification of $ClpP_{ADEP}$ and $ClpP_{ADEP\text{-}short}$ is described in the following chapter.

3.2.1 Purification of $ShClpP_{ADEP}$ (full-length and truncated version)

Both *clpP$_{ADEP}$* genes, expressing the full-length or truncated version of $ClpP_{ADEP}$, were inserted into the pET22b vector with an attached C-terminal Histidine-tag, respectively. Heterologous expression of $ClpP_{ADEP}$ and $ClpP_{ADEP\text{-}short}$ was performed utilising the BL21 derivative SG1146a. $ClpP_{ADEP}$ expression was induced with 0.08 mM IPTG in 8 L LB media for 4 h at 25 °C. For purifying $ClpP_{ADEP\text{-}short}$, the protein expression was conducted for ~ 16 h at 20°C in 4 L TB media and induced with 0.1 mM IPTG. In the case of full-length $ClpP_{ADEP}$, the elution fractions were pooled and further purified by size exclusion chromatography. Therefor, the protein solution was applied to the Superdex^{TM} 200 10 300 column and eluted in activity buffer (50 mM HEPES, 150 mM KCl, 20 mM MgCl, 10 % glycerin, pH 7.5). Fractions 18-20 were pooled and the volume of protein solution was reduced using Thermo protein concentrators. Figure 3.22 presents the size exclusion

chromatography of $ClpP_{ADEP}$ and the immobilised nickel ion affinity chromatography of $ClpP_{ADEP\text{-}short}$ using the same purification protocol as described in 2.2.14.5.

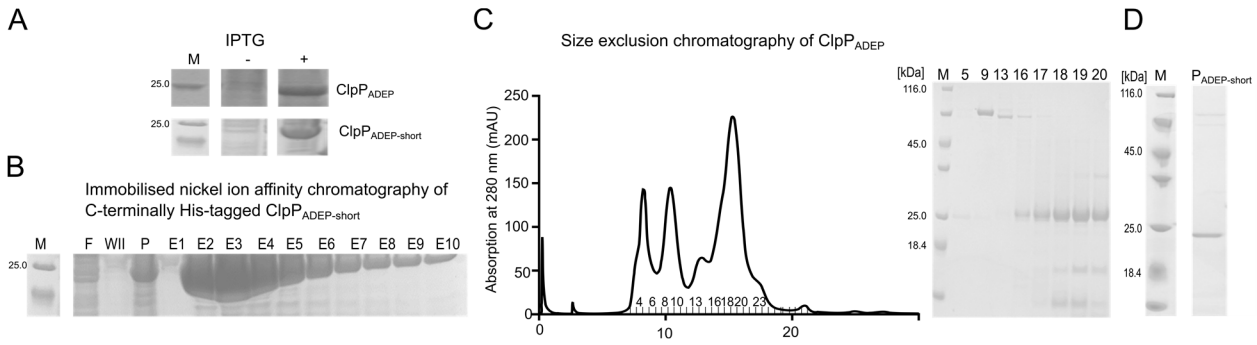

Figure 3.22: **Size exclusion chromatography of $ShClpP_{ADEP}$ and immobilised nickel ion affinity chromatography of $ClpP_{ADEP\text{-}short}$. A**: The expression of $ShClpP_{ADEP}$ and $ShClpP_{ADEP\text{-}short}$ was tested for 4 h at 37°C, induced with 1 mM IPTG and whole cell extracts were loaded on 12 % Bis-Tris gels. **B:** Samples were collected during the nickel ion affinity chromatography of $ShClpP_{ADEP\text{-}short}$ including the flow-through (F), wash II, pellet after centrifugation (P) and elution fractions E1-E10 and loaded on 12 % Bis-Tris gels. **C**: A nickel ion affinity chromatography was performed of full-length $ClpP_{ADEP}$ followed by an additional size exclusion chromatography of the pooled elution fractions employing the Superdex^{TM} 200 10 300 column. Protein elution was monitored at A_{280} nm and samples of the respective fractions, which were collected during the size exclusion chromatography, were analysed via SDS-PAGE. No markers had been applied to the column since this column was used for purification purposes only and the oligomeric behaviour of full-length $ClpP_{ADEP}$ was tested utilising the Superdex^{TM} 200 Increase 3.2 300 described in chapter 2.2.15 **D**: In addition, 2 µM of purified $ClpP_{ADEP\text{-}short}$ was loaded on a 12% Bis-Tris gel.

It is noteworthy to mention that both, $ClpP_{ADEP}$ and $ClpP_{ADEP\text{-}short}$, formed inclusion bodies in the cells with low amounts of soluble protein in the supernatant after cell disruption and centrifugation. However, high protein amounts of $ClpP_{ADEP\text{-}short}$ could be achieved at least three times, whereas other protein purification attempts yielded only low protein amounts.

As a following step, the oligomeric behaviour of $ClpP_{ADEP}$ was analysed in the absence and presence of ADEP1 to confirm its ADEP-insensitivity as it was previously demonstrated by the heterologous expression of *$clpP_{ADEP}$* in *S. lividans* (Thomy et al., 2019), see chapter 1.7 and Figure 1.17.

3.2.2 Analysis of the oligomeric behaviour of full-length ShClpP$_{ADEP}$ in the presence and absence of ADEP1

To investigate the oligomeric behaviour of ClpP$_{ADEP}$ in the absence and presence of ADEP1, analytical size exclusion chromatography of full-length ClpP$_{ADEP}$ was performed using the Superdex^{TM} 200 Increase 3.2 300 column in activity buffer pH 7.5. In the absence of ADEP1 (black curve), ClpP$_{ADEP}$ formed lower oligomeric states, presumably mostly monomers and dimers and adding the natural product ADEP1 did not lead to the assembly into higher oligomeric states (red curve), as observed for ClpP1 (Fig. 3.14). Similarly to ClpP2, the protein did not change its oligomeric behaviour after ADEP1 addition, confirming that ClpP$_{ADEP}$ is indeed an ADEP-insensitive peptidase (Fig. 3.23).

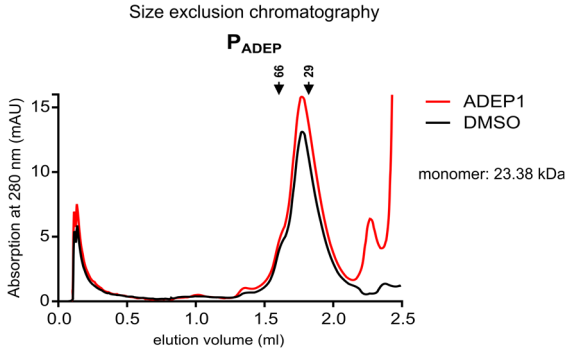

Figure 3.23: **Size exclusion chromatography of full-length ShClpP$_{ADEP}$ using the Superdex^{TM} 200 Increase 3.2 300 column.** The oligomeric behaviour of ShClpP$_{ADEP}$ (50 µM) was analysed in the absence (black curve) and presence (red curve) of ADEP1 (80 µM). The experiment was performed in two biological replicates.

The experiments shown in chapter 3.1.8 and 3.1.9 led to the conclusion that ADEP1 confers a Clp-ATPase-independent proteolytic activity to the ClpP1P2 heteromeric complex with ClpP1 as the preferred target for ADEP1 binding, whereas ClpP2 never exhibited peptido-and proteolytic activity in the presence of ADEP1. These results indicated that the ADEP-sensitive ClpP1 has to be inactivated by ClpP$_{ADEP}$ in order to protect the cells from their own antibiotic.

As a following step, interaction studies were performed using ClpP$_{ADEP\text{-}short}$ in combination with the ADEP-sensitive ClpP1. Given that the truncated version of ClpP$_{ADEP}$, namely ClpP$_{ADEP\text{-}short}$, was used in all following experiments and for the sake of simplicity, ClpP$_{ADEP\text{-}short}$ hereinafter referred to as ClpP$_{ADEP}$.

3.2.3 Pull-down experiment of ShClpP1 with His_6-tagged $ShClpP_{ADEP}$

To investigate $ClpP_{ADEP}$-ClpP1 interactions, a pull-down experiment with purified proteins was conducted, employing native ClpP1 and Histidine-tagged $ClpP_{ADEP}$. Therefor, samples consisting of either ClpP1 or $ClpP_{ADEP}$ as well as a mixture of ClpP1 and $ClpP_{ADEP}$ were incubated for 1 h at 4°C in activity buffer pH 7.5 and subsequently applied to a previously prepared nickel ion affinity chromatography column for the elution of His_6-tagged $ClpP_{ADEP}$. Samples were taken from the flow-through, the washing steps and the elution fractions and analysed via SDS-PAGE. The detailed protocol is described in chapter 2.2.21.3.

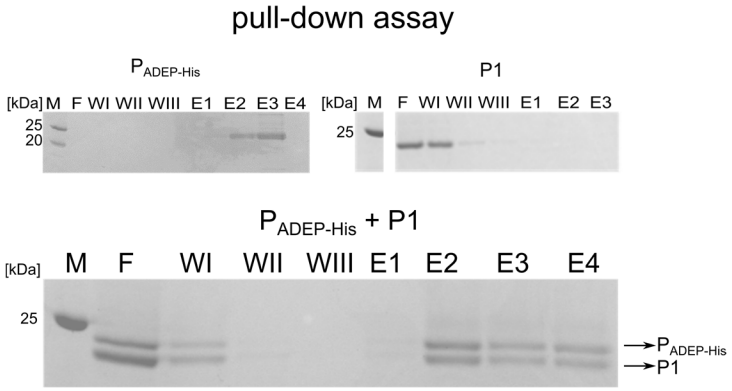

Figure 3.24: **Pull-down assay applying native ShClpP1 with Histidine-tagged $ShClpP_{ADEP}$.** 8 µM of native ShClpP1 and His_6-tagged $ShClpP_{ADEP}$ were incubated separately as well as combined for 1 h at 4 °C and subsequently loaded on a nickel ion affinity chromatography column. The column was washed repeatedly using 500 µl lysis and wash buffer and $ShClpP_{ADEP}$ was eluted in four steps consisting of 50 µl elution buffer, each. Samples of the flow-through (F), the washing steps (WI, WII and WIII), and the elution fractions were loaded on an SDS-PAGE gel. The SDS-PAGE gel is exemplary for three biological replicates.

While native ClpP1 could be washed off of the Ni-NTA column when incubated separately, $ClpP_{ADEP\text{-}His}$ alone was detected exclusively in the elution fractions E2 and E3, see Figure 3.24. However, when $ClpP_{ADEP\text{-}His}$ and ClpP1 were mixed together, as documented on a 12 % SDS-gel, native ClpP1 co-eluted with $ClpP_{ADEP\text{-}His}$, suggesting stabile interactions between both ClpP isoforms. Interestingly, portions of $ClpP_{ADEP\text{-}His}$ could be detected in the flow-through and wash I in combination with ClpP1, whereas when incubated separately, the protein could be detected exclusively in the elution fractions, indicating a decreased susceptibility of the C-terminal Histidine-tag of $ClpP_{ADEP}$ in complex with ClpP1.

3.2.4 ShClpP$_{ADEP}$ + ShClpP1: analysis of the oligomeric state via size exclusion chromatography

As it was shown in the previous chapter, ClpP$_{ADEP}$ interacts with the ADEP-sensitive ClpP1, even in the absence of ADEP1. For this reason, interactions between ClpP$_{ADEP}$ and ClpP1 were analysed in detail, employing analytical size exclusion chromatography to examine the oligomeric state of a mixture of ClpP$_{ADEP}$ + ClpP1. In a first experiment Fig. 3.25 A, a combination of ClpP$_{ADEP}$ and ClpP1 was incubated for 24 h at 4°C without the addition of ADEP1. Additionally, a sample consisting of ClpP1 alone, after a pre-incubation time of 24 h at 4°C, was incubated with a surplus of ADEP1 to induce the formation of homo-tetradecamers as reference.

While ClpP1 assembled into a homo-tetradecamer in the presence of ADEP1, ClpP$_{ADEP}$P1 eluted mostly as dimers and/or trimers in high abundance as well as higher oligomeric states in low abundance without the addition of ADEP1, see Figure 3.25 A. As a following step, the formation of ClpP1 homo-tetradecamers was investigated in a ClpP$_{ADEP}$ + ClpP1 sample after ADEP1 addition. Figure 3.25 B illustrates that even in the presence of ADEP1, ClpP$_{ADEP}$P1 mainly eluted as dimers and/or trimers, preventing the assembly of ClpP1 homo-tetradecamers. Surprisingly, inhibiting the formation of ClpP1 homo-tetradecamers by ClpP$_{ADEP}$ required a pro-longed pre-incubation time between ClpP$_{ADEP}$ and ClpP1. To further investigate this result, pre-incubation times were varied from two to seven hours at 4°C, before ADEP1 was added to the protein mixtures and applied to the gel filtration column. Compared to ClpP1 (without pre-incubation at 4°C but after ADEP1 addition), a ClpP$_{ADEP}$ + ClpP1 sample, which was pre-incubated for 2 h at 4°C, already revealed a slight decrease in the assembly of ClpP1 homo-tetradecamers after ADEP1 addition with dimers and trimers in high abundance. Increasing the incubation time to seven hours at 4°C demonstrated a distinct peak, indicating an increased formation of lower oligomeric complexes comprising a combination of ClpP$_{ADEP}$P1 proteins.

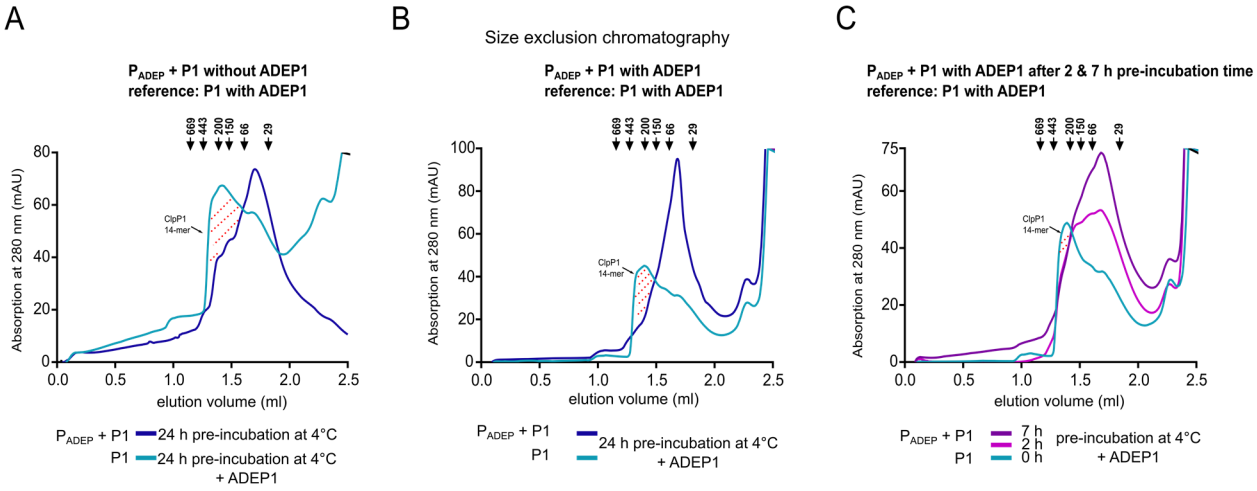

Figure 3.25: **Size exclusion chromatography of ShClpP$_{ADEP}$ + ShClpP1 and ShClpP1 alone, pre-incubated for different time periods at 4°C in the absence or presence of ADEP1. A**: A sample of ShClpP$_{ADEP}$ + ShClpP1 was pre-incubated for 24 h at 4 °C and applied to the gel filtration column without the addition of ADEP1. As reference, ADEP1 was added to ShClpP1 to induce the assembly of homo-tetradecamers after the protein was pre-incubated for 24 h at 4°C. 80 µM of ShClpP$_{ADEP}$ and/or ShClpP1 was used in the absence and presence of ADEP1 (320 µM). **B**: ShClpP$_{ADEP}$ + ShClpP1 (80 µM each) as ShClpP1 (80 µM) alone, were pre-incubated for 24 °C at 4°C before a surplus of ADEP1 (320 µM) was added to the samples for 30 min at 30°C. **C**: ShClpP$_{ADEP}$ + ShClpP1 (80 + 80 µM) samples were pre-incubated for two and seven hours at 4°C, before adding a surplus of ADEP1 (320 µM) for 30 min at 30°C. As reference, ADEP1 was added directly to ShClpP1 (without pre-incubation at 4°C) to induce the formation of homo-tetradecamers. The experiments were performed in three biological replicates.

As a control, ClpP$_{ADEP}$ was incubated for 24 h at 4°C and applied to the gel filtration column without the addition of ADEP1, see Figure 3.26. Compared to the oligomeric behaviour of full-length ClpP$_{ADEP}$, see Figure 3.23, which eluted exclusively in lower oligomeric states, the truncated version of ClpP$_{ADEP}$ presented a broad range of oligomeric species in equal abundance presumably monomers, dimers (calculated size of dimers: 43.5 kDa) and heptameric states (calculated size: ~152. 4 kDa), see Figure 3.26.

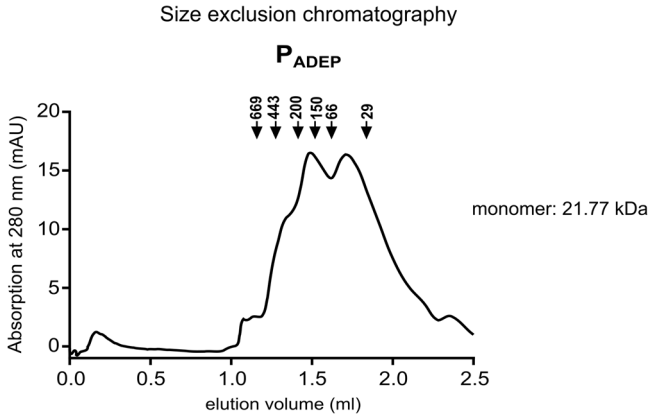

Figure 3.26: **Size exclusion chromatography of ShClpP$_{ADEP}$ (80 µM) after pre-incubation for 24 h at 4°C.** The experiment was performed in two biological replicates.

3.2.5 *In vitro* substrate degradation experiments using the natural product ADEP1 as ShClpP1 activator in the presence and absence of ShClpP$_{ADEP}$

The analysis of the oligomeric state of ClpP$_{ADEP}$P1 revealed a significant reduction in the ADEP1-induced formation of ClpP1 homo-tetradecamers in the presence of ClpP$_{ADEP}$. Additonally, it was speculated, if the formation of ClpP$_{ADEP}$P1 complexes might inhibit the interaction of ClpP1 with its partner Clp peptidase ClpP2, monitored in substrate degradation experiments utilising ADEP1 as ClpP activator. For this purpose, the fluorogenic dipeptide Suc-LY-AMC as well as the model substrate ß-casein were employed, investigating possible effects of ClpP$_{ADEP}$ on the ADEP-induced degradation of those model substrates by ClpP1P2. First, equal concentrations of ClpP1, ClpP2 and ClpP$_{ADEP}$ were tested in substrate degradation experiments as well as a ratio of 1:1:4 of ClpP1, ClpP2 and ClpP$_{ADEP}$. Similarly, a ratio of 4:1:1 of ClpP1, ClpP2 and ClpP$_{ADEP}$ was tested in substrate degradation experiments, whereas the concentration of ClpP2 was not varied but, remained the same. Surplus amounts of ClpP$_{ADEP}$ or ClpP1 are indicated in bold. As a positive control, a mixture of ClpP1P2 was used without the addition of ClpP$_{ADEP}$, see Figure 3.27.

The ADEP-induced dysregulation of the *Streptomyces* ClpP1P2 proteolytic core could be inhibited effectively in the presence of ClpP$_{ADEP}$, as it is demonstrated in *in vitro* degradation experiments employing the fluorescently labeled dipeptide Suc-LY-AMC (A) and ß-casein (B) as substrates.

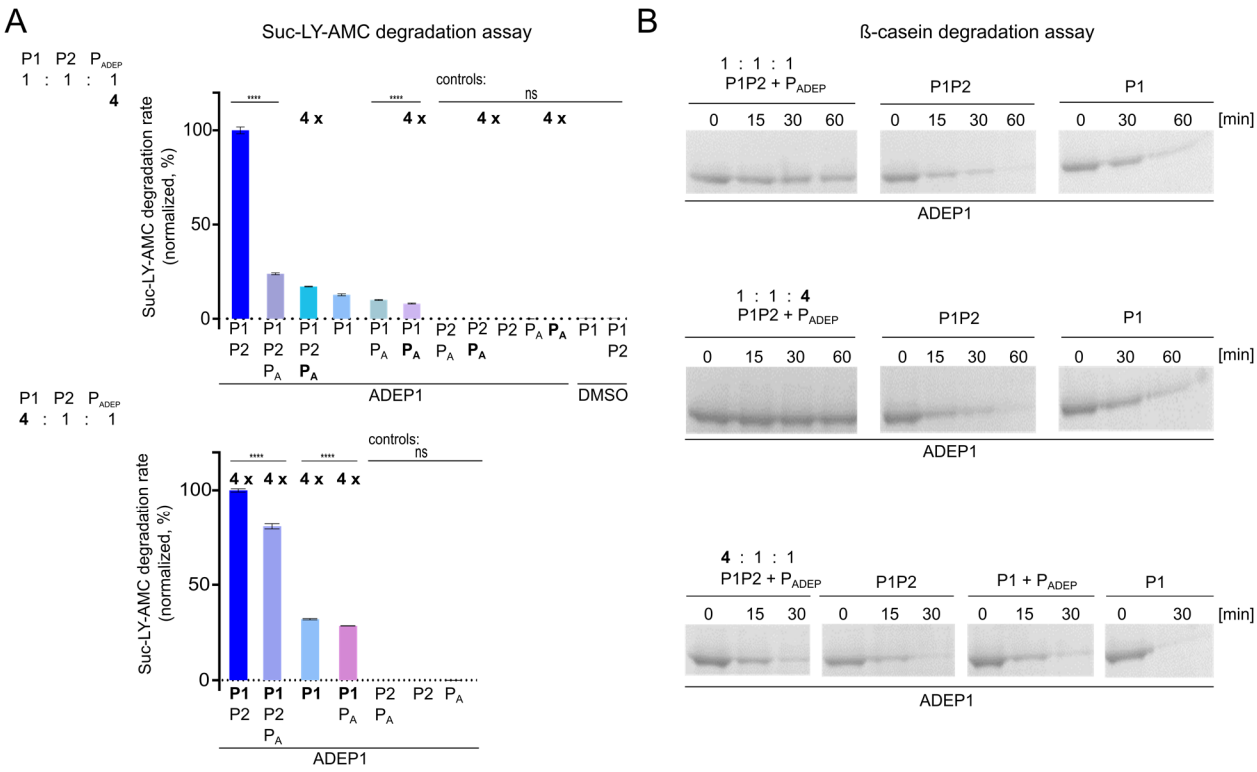

Figure 3.27: **ADEP1-induced degradation of Suc-LY-AMC (A) and ß-casein (B) by ShClpP1P2 or ShClpP1 in the presence and absence of ShClpP$_{ADEP}$. A:** First, equal concentrations of ShClpP1, ShClpP2 and ShClpP$_{ADEP}$ (2 µM each) were tested in peptide degradation experiments as well as a ratio of 1:1:4 of ShClpP1, ShClpP2 and ShClpP$_{ADEP}$. Similarly, a surplus of ShClpP1 was added to ShClpP2 and ShClpP$_{ADEP}$, whereas the concentration of ShClpP2 was not varied, but remained the same in all experiments. Surplus amounts of ShClpP1 or ShClpP$_{ADEP}$ are indicated in bold. 30 µM ADEP1 was added to the samples, respectively. As a control, ShClpP1P2 and ShClpP1 were tested in the absence of ADEP1 after the addition of DMSO. Mean of initial slopes are given. Statistics were performed with one way ANOVA using two biological replicates comprising three technical replicates, respectively. P-values: p values: ns > 0.05; ****≤ 0.0001. Error bars indicate corresponding standard deviations. All samples were incubated for 24 h at 4 °C, before ADEP1 and the substrate Suc-LY-AMC were added. **B**: Equal concentrations of ShClpP1, ShClpP2 and ShClpP$_{ADEP}$ (2 µM each) were used for the degradation of ß-casein (10 µM). In addition, a surplus of ShClpP$_{ADEP}$ was added to ShClpP1 and ShClpP2 and tested for the degradation of ß-casein. Furthermore, a ratio of 4:1:1 of ShClpP1, ShClpP2 and ShClpP$_{ADEP}$ was tested in ß-casein degradation experiments, whereas the concentration of ShClpP2 remained the same. After the samples were pre-incubated for 24 h at 4°C, 30 µM ADEP1 and the substrate ß-casein were added to start the reaction. The experiments were performed at 30°C, samples were taken and analysed via SDS-PAGE. The presented data are exemplary for at least three individual biological replicates.

Remarkably, adding ClpP$_{ADEP}$ to ClpP1 and ClpP2 in a ratio of 1:1:1 inhibited the ADEP-induced degradation of Suc-LY-AMC and ß-casein by ADEP-activated ClpP1P2 nearly as effective as the

addition of a surplus of $ClpP_{ADEP}$ to the reaction mixture. Furthermore, the inhibition of the ADEP1-induced degradation of Suc-LY-AMC and ß-casein could be reversed by adding a surplus of ClpP1 to ClpP2 and $ClpP_{ADEP}$.

However, the inactivating effect of $ClpP_{ADEP}$ could only be monitored effectively on the ADEP-induced ClpP1P2 proteolytic core instead of ClpP1 homo-tetradecamers, since the catalytic activity of ClpP1 increased by forming heteromeric complexes with ClpP2. Of note, $ClpP_{ADEP}$, ClpP2 and a mixture of $ClpP_{ADEP}$P2 were tested, using different protein concentrations in *in vitro* Suc-LY-AMC degradation assays as well, which exhibited no peptidolytic activities after ADEP1 addition, confirming both Clp peptidases to be ADEP-insensitive, see Figure 3.27 A.

Furthermore, previous experiments demonstrated an ADEP1-induced stimulated self-processing of ClpP1 in the presence of ClpP2, see Figure 3.15. Consequently, it was investigated if $ClpP_{ADEP}$ might inhibit the ADEP1-induced stimulated self-processing of ClpP1 in the presence of ClpP2, thus strongly suggesting a decreased formation of ClpP1P2 hetero-tetradecamers. In addition, analysing the oligomeric state of a mixture of ClpP1 + ClpP2 + $ClpP_{ADEP}$ in comparison to ClpP1 + ClpP2, after a pre-incubation time of 24 h at 4°C and ADEP1 addition, displayed a reduced amount of tetradecamers, further pointing towards an inhibited tetradecamer formation of ClpP1P2 in the presence of $ClpP_{ADEP}$, see appendix Figure 6.10.

Figure 3.28 illustrates the processing of ClpP1 in the course of the ADEP-induced degradation of ß-casein by ClpP1P2 in the presence of $ClpP_{ADEP}$, which is presented in Figure 3.27 B. As previously described, all samples were pre-incubated for 24 h at 4°C, before the reaction was started by adding ADEP1 and ß-casein. As controls, two samples were collected, first before the samples were incubated for 24 h at 4°C (time point 0) and a second sample immediately after the reaction was started by adding ADEP and the substrate, indicated by a dot (time point 0.), see Figure 3.28. Remarkably, $ClpP_{ADEP}$ inhibited the ADEP-induced processing of ClpP1 effectively, even by the use of equal concentrations of ClpP1 and ClpP2 and $ClpP_{ADEP}$, see Figure 3.28 A. Processed ClpP1 is indicated by a blue asterisk. A complete inhibition of the ADEP1-induced ClpP1 processing reaction could be achieved by adding a surplus of $ClpP_{ADEP}$ (8 µM) to ClpP1 and ClpP2 (2 µM each).

Of note, the inhibition of the ADEP-induced processing reaction of ClpP1 could be reversed by applying a surplus of ClpP1 to ClpP2 and $ClpP_{ADEP}$ as it is seen in Figure 3.28 C.

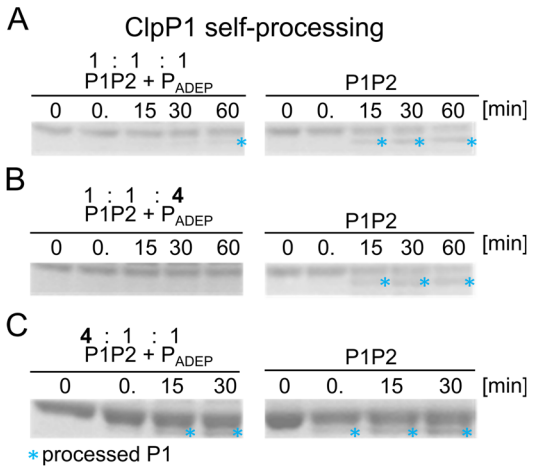

Figure 3.28: **The ADEP-induced processing reaction of ShClpP1 is inhibited in the presence of ShClpP2 after the addition of $ShClpP_{ADEP}$ in the course of the *in vitro* ß-casein degradation assay, which is shown in Figure 3.30**. **A**: Equal concentrations of ShClpP1, ShClpP2 and $ShClpP_{ADEP}$ were applied (2 µM each) in combination with 30 µM ADEP1. **B**: 2 µM ShClpP1, 2 µM ShClpP2 and 8 µM $ClpP_{ADEP}$ were employed in combination with 30 µM ADEP1. **C**: 8 µM ShClpP1, 2 µM ShClpP2 and 2 µM $ClpP_{ADEP}$ were applied in combination with 30 µM ADEP1. The presented data are exemplary for at least three independent biological replicates.

To sum up, gel filtration experiments of $ClpP_{ADEP}$ in combination with ClpP1 revealed the formation of lower oligomeric complexes in the absence and presence of ADEP1, preventing the ADEP-induced formation of ClpP1 homo-tetradecamers. Furthermore, $ClpP_{ADEP}$P1 complexes inhibited not only the formation of ClpP1 homo-tetradecamers but the ADEP-induced degradation of Suc-LY-AMC and ß-casein by ClpP1P2 as well. In addition, it is noteworthy to mention that an impaired functional interaction between ClpP1 and ClpP2 by $ClpP_{ADEP}$ could be monitored in the course of ClpP1 self-processing. Without the addition of $ClpP_{ADEP}$, ClpP1 self-processing was stimulated in combination with ClpP2 as it is seen in Figure 3.15 in the presence of ADEP1. However, the stimulated self-processing of ClpP1 could be efficiently inhibited by the addition of $ClpP_{ADEP}$ despite the presence of ClpP2, see Figure 3.28.

3.2.6 Reconstitution of proteolytically active Clp complexes employing ShClpP$_{ADEP}$ and ShClpP2

In the last two chapters, it was shown that ClpP$_{ADEP}$ interacts with ClpP1, thereby inhibiting the formation of ClpP1 homo-tetradecamers, impairing functional interactions between ClpP1 and ClpP2. Nevertheless, ClpP is essential for cell viability in streptomycetes (Viala et al., 2000) and the inhibition of the physiological function of ClpP1P2 has to be compensated. Given that ClpP$_{ADEP}$ and ClpP2 are both ADEP-insensitive peptidases, the formation of a ClpP$_{ADEP}$P2 complex was investigated, which could potentially function as an ADEP-insensitive replacement of the ADEP-inducible ClpP1P2 complex. Therefor, *in vitro* degradation experiments were conducted, using ClpP$_{ADEP}$ and ClpP2 in association with ClpX for the degradation of the natural substrates ClgR and PopR and the ATPase ClpC1 to hydrolyse the model substrate ß-casein.

In vitro degradation experiments employing ClpX or ClpC1 in combination with either ClpP$_{ADEP}$ or ClpP2 failed to degrade the two natural substrates ClgR and PopR as well as ß-casein, Figure 3.29. However, ClpP$_{ADEP}$ in combination with ClpP2 led to the ClpX-mediated hydrolysis of ClgR and PopR as well as to the ClpC1-mediated digestion of ß-casein, yet less efficiently compared to ClpXP1P2 and ClpC1P1P2, see Figure 3.7. Nevertheless, both degradation experiments strongly suggest the formation of a ClpP$_{ADEP}$P2 hetero-tetradecamer. Additionally, control experiments applying ClpP$_{ADEP}$P2 without the addition of ClpX or ClpC1 confirmed the dependence of a Clp-ATPase-mediated degradation of ClgR, PopR and ß-casein. Furthermore, different ratios of the Clp-ATPase ClpC1 compared to the total ClpP concentration were tested, employing 5 µM or 2.5 µM ClpC1 together with 2.5 µM of each ClpP$_{ADEP}$ and ClpP2 proteins for the degradation of ß-casein. Figure 6.9 in the appendix demonstrates that the degradation of ß-casein by ClpP$_{ADEP}$P2 was comparable despite different ClpC1 concentrations.

Although the ADEP-insensitivity of ClpP$_{ADEP}$ and ClpP2 could already be confirmed via size exclusion chromatography, a ClpC1-dependent degradation of ß-casein was performed in the presence and absence of ADEP1, revealing no effect on the ClpC1-mediated degradation of ß-casein, see Figure 3.29 C.

Furthermore, $ClpP_{ADEP}$ in combination with either ClpP2 or $ClpP2_{ATG2}$ was tested side by side in a ClpC1-dependent ß-casein degradation assay, resulting in similar proteolytic activities of $ClpC1P_{ADEP}P2$ and $ClpC1P_{ADEP}P2_{ATG2}$, as documented via SDS-PAGE, see Figure 3.29 D.

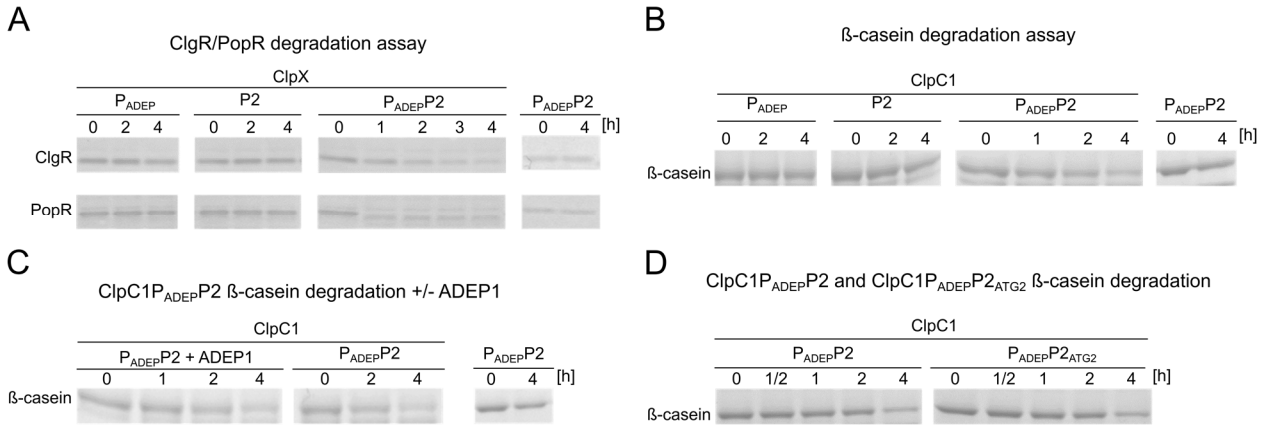

Figure 3.29: **ShClpX- and ShClpC1-mediated degradation of ShClgR, ShPopR (A) and ß-casein (B) by $ShClpP_{ADEP}$, ShClpP2 and $ShClpP_{ADEP}P2$. In addition the degradation of ß-casein by $ShClpC1P_{ADEP}P2$ was analysed in the absence and presence of ADEP1 (C). The degradation of ß-casein by $ShClpP_{ADEP}$ in combination with either ShClpP2 or $ShClpP2_{ATG2}$ was tested in ClpC1-mediated ß-casein degradation experiments (D).** The experiments were conducted at 30°C and samples were taken after different time points and analysed via SDS-PAGE. **A**: $ShClpP_{ADEP}$ (5 µM), ShClpP2 (5 µM) and a combination of $ShClpP_{ADEP}P2$ (2.5 + 2.5 µM) were employed to degrade the natural substrates ShClgR (2 µM) or ShPopR (2 µM) in association with the unfoldase ShClpX (2.5 µM). **B**: $ShClpP_{ADEP}$ (5 µM), ShClpP2 (5 µM) and $ShClpP_{ADEP}P2$ (2.5 + 2.5 µM) were applied in combination with ClpC1 (5 µM) to degrade the model substrate ß-casein (10 µM). **C** : Additionally, a ShClpC1-mediated ß-casein (10 µM) degradation by $ShClpP_{ADEP}P2$ was performed in the absence and presence of ADEP1 (30 µM), employing 2.5 µM of $ClpP_{ADEP}$, ShClpP2 and ShClpC1. **D**: $ShClpP_{ADEP}$ in combination with ShClpP2 or $ShClpP2_{ATG2}$ (2.5 µM each) was used to degrade ß-casein (10 µM) in association with ShClpC1 (2.5 µM).

In the course of the ClpC1-dependent ß-casein degradation by $ClpP_{ADEP}P2$, processing of ClpP2 could be observed, revealing a different processing pattern compared to the processing of ClpP2 by ClpP1. While ClpP2 is processed by ClpP1 resulting in a mature protein that starts with the following sequence RYIIPR, processing of ClpP2 in the presence of $ClpP_{ADEP}$ resulted in a slightly bigger protein, comparable to the size of $ClpP2_{ATG2}$, namely $ClpP2_{intermediate}$, see Figure 3.30.

Remarkably, while ClpP2 processing by ClpP1 is independent of the presence of a Clp-ATPase, processing of ClpP2 in the presence of Clp_{ADEP} could only be observed when ClpC1 was added to the sample, strongly implying a Clp-ATPase-dependent processing of ClpP2 in combination with

$ClpP_{ADEP}$. Control experiments employing $ClpP_{ADEP}P2$ without the addition of ClpC1 support this suggestion, Fig. 3.30 A. It is noteworthy to mention that N-terminal processing of ClpP2 after $ClpP_{ADEP}$ addition could only be observed applying full-length ClpP2 instead of $ClpP2_{ATG2}$, starting from the putative second start codon.

Furthermore, ClpP2 processing in combination with $ClpP_{ADEP}$ or ClpP1 was analysed in detail. Therefor, a Clp-ATPase mediated substrate degradation experiment applying ClpP1P2 and $ClpP_{ADEP}P2$ was performed and processed ClpP2 and $ClpP_{ADEP}$ could be detected specifically via Western blot experiments. Differences in the processing pattern of ClpP2 in combination with ClpP1 or $ClpP_{ADEP}$ became apparent after specific detection with anti-His antibodies, see Figure 3.30 B.

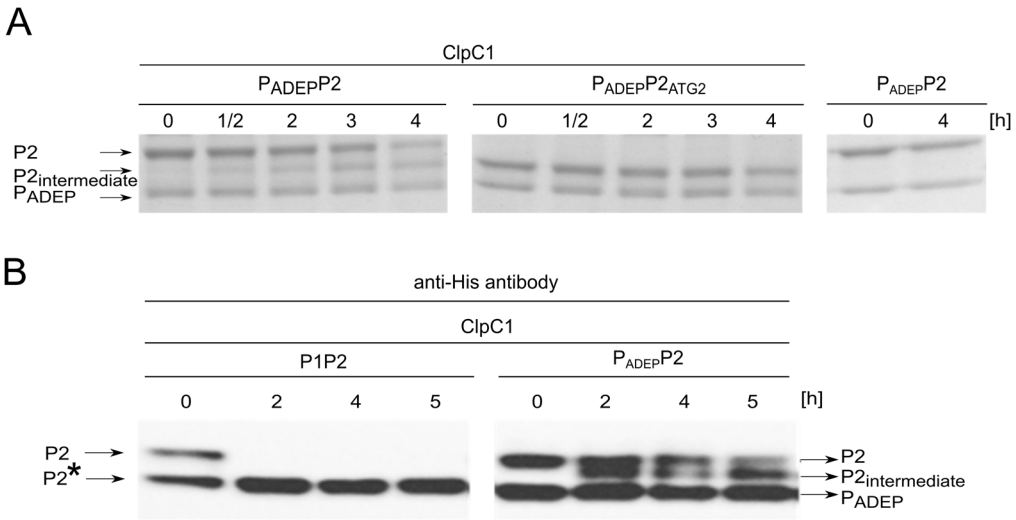

Figure 3.30: **Processing of ShClpP2 in combination with $ShClpP_{ADEP}$ in the course of the ShClpC1-mediated ß-casein degradation side by side with $ShClpP_{ADEP}P2_{ATG2}$. Processing of ShClpP2 in the presence of $ClpP_{ADEP}$ deviates from the processing pattern of ClpP2 after ClpP1 addition, analysed via immunoblotting. (A):** Processing of ShClpP2 in the course of ShClpC1-dependent (2.5 µM) ß-casein (10 µM) degradation, applying 2.5 µM of each $ShClpP_{ADEP}$, ShClpP2 or $ShClpP2_{ATG2}$. The experiment was performed at 30°C and samples were loaded on a 12% Bis-Tris gel. **(B)**: Processing of ShClpP2 in combination with ShClpP1 or $ShClpP_{ADEP}$ in the course of the ClpC1-mediated degradation of ClgR. The processing was documented via immunoblotting employing anti-His antibodies. Data shown are exemplary for three independent biological replicates.

While only ClpP2 could be detected via anti-His-antibodies in combination with native ClpP1, C-terminally His_6-tagged $ClpP_{ADEP}$ could be detected in addition when combined with ClpP2. One

can observe that ClpP2 was processed efficiently and completely after two hours in combination with ClpP1, whereas ClpP2 processing in combination with $ClpP_{ADEP}$ was significantly slower, see Figure 3.30 B. Furthermore, processed ClpP2 in combination with $ClpP_{ADEP}$ appeared slightly bigger on SDS-PAGE gels, named $ClpP2_{intermediate}$, compared to processed ClpP2 (ClpP2*) by ClpP1.

In vitro substrate degradation experiments strongly indicate the formation of a $ClpP_{ADEP}P2$ heteromeric complex, resulting in the hydrolysis of the natural substrates ClgR and PopR in association with the ATPase ClpX and the model substrate ß-casein in association with ClpC1.

As a following step, the catalytic triad knock-out mutant $ClpP2_{S131A}$ as well as the hydrophobic pocket mutant $ClpP2_{hp}$ were applied in combination with wild-type $ClpP_{ADEP}$ in ClpC1-dependent ß-casein degradation experiments to investigate the catalytic activity and Clp-ATPase/ClpP interactions of the $ClpP_{ADEP}P2$ heteromeric complex, respectively.

While the proteolytic activtiy of $ClpP_{ADEP}P2_{S131A}$ was comparable to wild-type $ClpP_{ADEP}P2$, the hydrophobic pocket mutant protein $ClpP2_{hp}$ completely abolished ß-casein degradation, implying that ClpP2 in combination with $ClpP_{ADEP}$ did not exhibit catalytic activity and functions as the exclusive interaction partner for the Clp-ATPase ClpC1, similar to the physiological function ClpP2 fulfils in the ClpP1P2 heteromeric complex, see Figure 3.31 and Figure 3.12. Furthermore, these results indicate that $ClpP_{ADEP}$ replaces ClpP1 in the heteromeric, ADEP inducible ClpP1P2 complex, adopting its distinct functions as propeptide processor which confers proteolytic activity to the ADEP-insensitive $ClpP_{ADEP}P2$ complex.

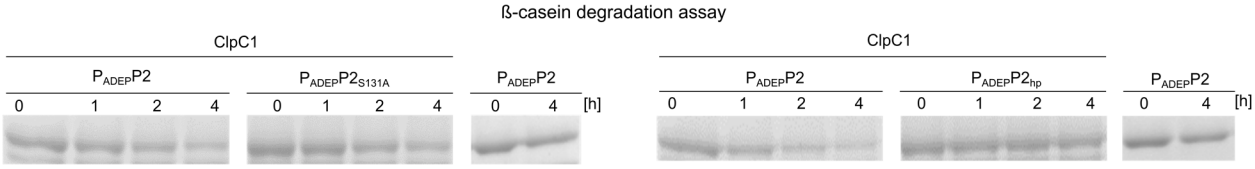

Figure 3.31: **ShClpC1-dependent ß-casein degradation by $ShClpP_{ADEP}P2$, in combination with the catalytic triad knock-out mutant protein $ShClpP2_{S131A}$ and the hydrophobic pocket mutant protein $ShClpP2_{hp}$.** ShClpP2, $ShClpP2_{S131A}$ and $ShClpP2_{hp}$ were applied in combination with $ShClpP_{ADEP}$ (2.5 µM of each) in association with ShClpC1 (5 µM) to digest ß-casein (10 µM).

4. Discussion

4.1 ClpP1P2 of *S. hawaiiensis*: a Clp protease complex consisting of two ClpP isoforms with defined functional roles

Streptomycetes are well-known for their complex life cycle and the production of various secondary metabolites, including clinical valuable antibiotics. Their life cycle undergoes two major stages, the development of a substrate mycelium out of branching germ tubes and subsequently the formation of a reproductive aerial mycelium, which disperses through spores (Flärdh and Buttner, 2009). Those spores are largely dormant and can survive long periods of time (Hopwood, 2007). The production of secondary metabolites is often initiated by nutrient starvation and tightly coupled with the morphological differentiation of streptomycetes (Flärdh and Buttner, 2009). Regulated proteolysis, namely the activation or inactivation of specific regulators, is often indispensable for the execution of such complex developmental programmes. The caseinolytic protease Clp is an essential compartmentalised degradation machinery in *Streptomyces* and involved in morphological differentiation (de Crecy-Lagard et al., 1999, Viala and Mazodier, 2003, Guyet et al., 2013, Wolanski et al., 2011, Guyet et al., 2014). In contrast to most other bacteria, Clp is indispensable for the survival of streptomycetes (Viala et al., 2000) and its importance seems to reflect on its increased complexity, mostly harbouring up to five *clpP* genes organised in one monocistronic and two bicistronic operons (de Crecy-Lagard et al., 1999, Viala et al., 2000). All five ClpP homologues could potentially contribute to the physiological function ClpP has to fulfil in streptomycetes. However, whole cell studies in *S. lividans* provided first insights into the working mode of the complex Clp system in *Streptomyces*. Mazodier and colleagues found out that the presence of ClpP1 and ClpP2 represses the expression of ClpP3 and ClpP4 in *Streptomyces lividans* wild type and that both ClpP isoforms, ClpP1 and ClpP2, are necessary for the degradation of substrates (Viala and Mazodier, 2002, Bellier et al., 2006). Besides, the construction of a Δ*clpP1* knock-out mutant demonstrated that ClpP3 and ClpP4 can be expressed in the absence of ClpP1 and function as a back-up system in case of a dysfunction of the housekeeping Clp system (Viala and Mazodier, 2002). While ClpP3 and ClpP4 replace ClpP1

and ClpP2 as a fail-safe mechanism, ClpP5 cannot compensate the physiological function of either ClpP1P2 or ClpP3P4 (Gominet et al., 2011).

This study focuses on the housekeeping Clp system of *Streptomyces*, providing insights into the molecular composition of the ClpP1P2 proteolytic core from *Streptomyces hawaiiensis* and sheds light on the functional differentiation of both ClpP1 and ClpP2 homologues. Investigating ClpP1 and ClpP2 via *in vitro* reconstitution revealed the formation of a heteromeric ClpP1P2 complex, instead of homomeric tetradecamers, composed of either ClpP1 or ClpP2. Both ClpP homologues possess distinct but complementary functions regarding substrate hydrolysis in heteromeric ClpP1P2 complexes. *In vitro* substrate degradation experiments employing catalytic triad knock-out and hydrophobic patch mutant proteins provided evidence that ClpP1 confers catalytic activity to the proteolytic core, while ClpP2 exclusively interacts with the Clp-ATPases ClpX, ClpC1 and ClpC2 to allow access of natural protein substrates, such as ClgR and PopR, to the proteolytic chamber. Cross-linking as well as gel filtration experiments corroborate the formation of ClpP1P2 heteromeric complexes out of two homo-heptameric ClpP1 and ClpP2 rings instead of hetero-heptameric rings composed of both ClpP isoforms. When incubated separately, ClpP1, like ClpP2, displayed mostly heptameric species on native 4-12% Tris-Glycine gels after the addition of the chemical cross-linker BS3, whereas in combination, tetradecamers could be detected. In addition, native ClpP1 and ClpP2 assembled into heptameric species in high abundance when applied separately on the gel filtration column. Furthermore, size exclusion chromatography of native ClpP1 and His-tagged ClpP2 combined in the presence of ADEP1 revealed a tetradecamer with a distinct retention volume compared to a ClpP1 homo-tetradecamer, strongly suggesting the formation of a heteromeric ClpP1P2 complex, Fig. 6.8 in the appendix.

Experiments applying the hydrophobic pocket mutant protein $ClpP2_{hp}$ in combination with wild-type ClpP1 fully abrogated substrate degradation in association with ClpX, ClpC1 or ClpC2. Those hydrophobic pockets on the apical surface of ClpP are important for the interaction with the (I/L/V)-G-(F/L) loops of the Clp-ATPases (Kim et al., 2001). In this context, Martin *et al.* explored Clp-ATPase/ClpP interactions by analysing the number of IGF loops required for sufficient substrate degradation. It was demonstrated that even the loss of a single IGF-loop reduced the affinity of EcClpX to EcClpP ~50 fold (Martin et al., 2007). Therefore, the binding of all six IGF-

loops is required for functional substrate degradation by the Clp protease. In the current work, mutating the hydrophobic pockets of *Streptomyces* ClpP1 did not impair substrate degradation, strongly pointing towards the formation of a mixed ClpP1P2 tetradecamer out of two homo-heptameric ClpP1 and ClpP2 rings.

Furthermore, the assembly of two homo-heptameric ClpP1 and ClpP2 rings in *Streptomyces* correlates with the composition of the proteolytic core ClpP from *L. monocytogenes* (Dahmen et al., 2015, Gatsogiannis et al., 2019) and the closely related *M. tuberculosis* (Akopian et al., 2012, Raju et al., 2012, Leodolter et al., 2015) in which ClpP1 and ClpP2 form hetero-tetradecamers composed of homo-heptameric rings with ClpP2 as the sole interaction partner for the Clp-ATPases ClpX and ClpC1 in *M. tuberculosis* and ClpX in *L. monocytogenes*. Remarkably, in contrast to *S. hawaiiensis*, in which ClpP1 exclusively confers peptido-and proteolytic activity to the mixed ClpP1P2 complex, in *L. monocytogenes* and *M. tuberculosis* both ClpP1 and ClpP2 peptidases contribute to the catalytic activity of mixed LmClpP1P2 and MtClpP1P2 complexes (Dahmen et al., 2015, Akopian et al., 2012).

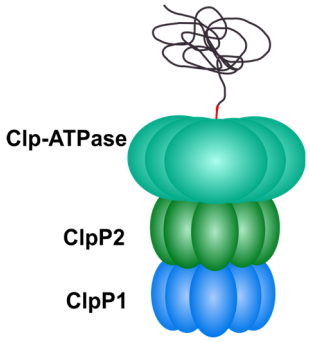

Figure 4.1: **The housekeeping Clp protease from *S. hawaiiensis* consists of a heteromeric ClpP1P2 proteolytic core and either the Clp-ATPase ClpX, ClpC1 or ClpC2, which recognise, unfold and thread substrates into the proteolytic chamber under ATP consumption via the homo-heptameric ring of ClpP2**. Enzymatic activity of the complex is conferred by the catalytic triads of ClpP1 for peptide and protein hydrolysis.

Almost two decades ago, whole cell experiments employing ClpP1 and ClpP2 from *S. coelicolor* revealed an N-terminal processing of both ClpP isoforms, which was detected via immunoblotting. These Western blot experiments indicated a cross-processing of ClpP1 and ClpP2 since mature ClpP proteins could only be observed when both ClpP homologues were present in the cell (Viala and Mazodier, 2002).

However, the current *in vitro* study of ClpP1 and ClpP2 from S. *hawaiiensis* revealed ClpP1 as the main propeptide processor for itself and ClpP2. Nevertheless, major differences were observed between the self-processing of ClpP1 and the processing of ClpP2 by ClpP1. While ClpP2 was processed by ClpP1 in buffer without the addition of a Clp-ATPase, ClpP1 processed itself only in combination with ClpP2 upon Clp-ATPase binding to ClpP2, Fig. 3.15.

Furthermore, it is apparent that in ClpX-mediated ClgR and PopR degradation experiments, processed ClpP1 could only be detected clearly on SDS-gels after the substrates were already completely degraded, in contrast to the processing of ClpP2, which occurred almost immediately after all ingredients were added to start the reaction. Of note, in contrast to the processing of ClpP1, ClpP2 is processed by ClpP1 even without the addition of a Clp-ATPase, Fig. 3.15. One can speculate that the removal of the N-terminal propeptide of ClpP2 is essential for the functionality of the ClpP1P2 protease complex in contrast to the self-processing of ClpP1. Differences concerning the processing of ClpP1 and ClpP2 seem to reflect on the functional roles they have to fulfil in the heteromeric ClpP1P2 complex. Kessel *et al*. visualised EcClpXP complexes by negative stain electron microscopy and investigated the translocation of substrates. Electron micrographs visualised that the propeptides occupied the catalytic chamber of ClpP and thus limited the entry of substrates (Kessel et al., 1995). In contrast to other ClpP proteins, such as ClpP from *B. subtilis*, ClpP1 and ClpP2 from *S. hawaiiensis* and *S. lividans* comprise an extended N-terminus, see Fig. 3.10. Considering that ClpX, ClpC1 and ClpC2 exclusively bind to ClpP2 and substrates enter the proteolytic chamber via the axial pore of ClpP2, it seems plausible that the propeptides of ClpP2 have to be cleaved off to allow the substrates to enter.

Although ClpP1 and ClpP2 differ in their functional roles significantly, there are clear indications that conformational changes in one heptameric ring result in a concerted conformational change of both ClpP rings. This assumption is supported by two different observations: First, the binding of ClpX to ClpP2 in ClgR and PopR substrate degradation experiments initiated the self-processing of the opposing heptameric ring of ClpP1. Second, the proteolytic activity of ClpP1, which emerged only after tetradecamer formation with the catalytically inactive ClpP2, was activated by the binding of ClpX to the interaction surface of ClpP2. Inter-ring communication has been investigated before on the Clp protease system of *E. coli*. There, studies on EcClpAP protease

complexes using asymmetric ClpP particles composed of one active and one catalytically inactive ring demonstrated that ClpA activity could be stimulated regardless of whether ClpA bound to the catalytically inactive ring or the opposing ring, indicating a concerted conformational change of both rings (Maglica et al., 2009). It has been investigated before that Clp-ATPase activity of ClpA is stimulated by an allosteric activation across the Clp-ATPase/ClpP interface. The only requirement was the presence of proteolytically active ClpP proteins while the presence of substrates was not necessary (Maurizi, 1991, Hinnerwisch et al., 2005).

ADEP1, the ClpP-interfering natural product, is produced by the *Streptomyes* genus, representing the progenitor of a promising new class of acyldepsipeptide antibiotics (Sass and Brötz-Oesterhelt, 2013, Malik and Brötz-Oesterhelt, 2017, Thomy et al., 2019). However, although the mechanism of ADEP action has been investigated in some detail in major target bacteria, effects of ADEP on the housekeeping Clp protease of the producer genus *Streptomces* have been largely elusive.

Whole cell studies in *S. lividans* provided first indications on the effects ADEP exerts on the different ClpP isoforms ClpP1 and ClpP2. First, a Δ*clpP1* knock-out mutant conferred ADEP resistance in *S. lividans*. Second, investigations on spontaneous ADEP-resistant mutants revealed that all strains carrying mutations in the *clpP1P2* operon solely affected *clpP1* but not *clpP2*. Third, complementing a Δ*clpP1* knock-out strain with only *clpP2* did not restore ADEP-sensitivity, strongly implying that ClpP1 is an ADEP-sensitive ClpP, whereas ClpP2 seemed to be ADEP-insensitive (Gominet et al., 2011).

Investigating the effect of ADEP1 on *Streptomyces* ClpP on the molecular level provided further insights into the way how ADEP1 influences the functionality of the house keeping Clp protease system. Studying the oligomeric behaviour of ClpP1 and ClpP2 and performing substrate degradation experiments with ADEP1 as ClpP activator, confirmed that ClpP1 is indeed an ADEP-sensitive Clp peptidase, since it formed homo-tetradecamers upon ADEP1 addition and exhibited a Clp-ATPase-independent peptido- as well as proteolytic activity. In contrast, ClpP2 did not assemble homo-tetradecamers after ADEP1 addition and was peptido- as well as proteolytically inactive under the conditions applied here, implying that ClpP2 is an ADEP-insensitive ClpP, Fig.

3.13 and 3.14. Remarkably, a mixture of ClpP1 and ClpP2 exhibited a two-fold higher peptido- and proteolytic activity compared to ClpP1 alone upon ADEP1 addition, strongly suggesting an allosteric activation of the catalytic triads of ClpP1 in complex with ClpP2.

Furthermore, effects of ADEP1 on ClpP1 and ClpP2 processing were analysed in detail. ClpP1 self-processing was induced upon ADEP1 addition and did not require the presence of ClpP2, while ClpP2 processing still depended on the presence of ClpP1. However, a stimulated processing of ClpP1 and ClpP2 in the presence of ADEP1 could be observed compared to the DMSO control. Remarkably, even upon ADEP1 addition, processing of ClpP2 happened first, before the self-processing of ClpP1 took place.

Hence, the stimulated self-processing of ClpP1 and the accelerated processing of ClpP2 by ClpP1 in the presence of ADEP1 could be explained by the binding of ADEP to ClpP1. An explanation for the boost of its catalytic activity could be an optimised alignment of the catalytic triads of ClpP1 in complex with ClpP2 and after binding of ADEP (Gersch et al., 2015).

In vitro and *in vivo* studies on ClpP from various organisms in concert with ADEP led to a detailed understanding of the ADEP mode of action. Two different mechanisms have to be considered, and which of the two is responsible for bacterial death depends on the species investigated. First, ADEP binding to the proteolytic core ClpP displaces the Clp-ATPases, thereby inhibiting the physiological function of the Clp protease including natural substrate hydrolysis (Kirstein et al., 2009, Gersch et al., 2015, Amor et al., 2016, Famulla et al., 2016, Pan et al., 2019). Second, ADEP binding induces the opening of the ClpP entrance pores and allosterically activates the catalytic centers, leading to un-controlled proteolysis of non-native substrates (Lee et al., 2010, Li et al., 2010, Sass et al., 2011, Alexopoulos et al., 2013, Gersch et al., 2015, Pan et al., 2019, Silber et al., 2020b). The latter mechanism of ADEP action leads to bacterial killing in species, bearing non-essential ClpP proteins like *B. subtilis* or *S. aureus* (Brötz-Oesterhelt et al., 2005a, Sass et al., 2011, Mayer et al., 2019, Silber et al., 2020a, Silber et al., 2020b). On the contrary, the Clp protease is indispensable for viability in *M. tuberculosis* (Raju et al., 2012, Raju et al., 2014) and the ADEP-induced inhibition of the natural functions of the Clp protease leads to cell death in mycobacteria (Famulla et al., 2016). Given that the Clp protease is essential for viability in streptomycetes (Viala

et al., 2000), one might speculate that the ADEP mode of killing in this genus results from a mechanism of Clp protease inhibition, similarly to *M. tuberculosis*.

Surprisingly, the addition of ADEP1 to the *Streptomyces* Clp protease complex did not lead to a displacement of the Clp-ATPases ClpX, ClpC1 or ClpC2 in substrate degradation experiments, but even led to accelerated Clp-ATPase-dependent substrate hydrolysis, revealing a concomitant binding of the Clp-ATPases ClpX, ClpC1 or ClpC2 and ADEP1 to the heteromeric ClpP1P2 complex.

4.2 ShClpX/C1/C2-P1P2: Concomitant binding of ADEP1 and Clp-ATPases leads to an accelerated degradation of substrates revealing a novel ADEP mode of action

The heteromeric ClpP1P2 complex of *S. hawaiiensis* represents the first discovered Clp complex with asymmetrical binding of ADEP1 and the Clp-ATPases, leading to an accelerated Clp-ATPase mediated proteolysis. ADEP1 stimulated the ClpX-mediated degradation of the two natural substrates ClgR and PopR as well as the model substrate GFP-ssrA (see Figure 3.17) significantly, presenting a novel, third mechanism of ADEP action. The Clp-ATPases ClpC1 and ClpC2 were also degraded by the ADEP-activated Clp protease *in vitro*. The *in vitro* studies conducted during this PhD project employing the unfoldase ClpC1 in combination with ClpP1P2 in prolonged PopR substrate degradation experiments, revealed ClpC1 as substrate for ClpP1P2 exclusively upon ADEP1 addition and only after PopR was completely degraded. Similarly, an ADEP-induced degradation of ClpC2 by ClpP1P2 in ß-casein degradation experiments could be detected after four hours, when the model substrate was fully digested. In *S. lividans*, it could be observed that ClpC1 accumulated in a Δ*clpP1P2* knock-out mutant, strongly suggesting a ClpP1P2-dependent degradation of ClpC1 (Bellier et al., 2006). However, it is important to mention that in *S. lividans* ClpC1 is suggested to be a substrate of ClpP1P2 without the presence of ADEP, whereas in the ADEP-producer *S. hawaiiensis*, ClpC1 and ClpC2 could only be confirmed *in vitro* as substrates of ADEP-activated ClpP1P2.

How could the accelerated substrate degradation by the *Streptomyces* Clp protease in the presence of ADEP1 be explained?

As it was described previously in chapter 1.5, ADEP exerts conformational control over the ClpP barrel by stabilising the active extended conformation, thereby activating its catalytic triads allosterically, leading to un-regulated substrate degradation (Gersch et al., 2015). Additionally, ADEP opens the entrance pores of ClpP, allowing nascent polypeptide chains and loosely folded proteins to enter the proteolytic chamber (Brötz-Oesterhelt et al., 2005b, Kirstein et al., 2009, Lee et al., 2010, Li et al., 2010). In the ADEP-bound state, the axial pores of BsClpP were not only widened but the N-terminal loops of the peptidase were found to be pointing upwards, allowing un-controlled access to the internal degradation chamber of ClpP (Lee et al., 2010, Malik and Brötz-Oesterhelt, 2017).

Furthermore, three different studies utilising EcClpP, SaClpP and MtClpP1P2 highlight that ADEP exerts conformational control not only on the binding surface of the peptidase, but over the complete tetradecameric barrel regardless of its composition out of only one or two different ClpP isoforms. First, studies on the flexibility of EcClpP with and without ADEP1 showed less flexibility of ADEP-bound EcClpP especially in the handle region of the barrel compared to EcClpP without ADEP1. In this experiment, EcClpP was incubated in a deuterated solution with and without ADEP1 and the exchange of hydrogen/deuterium was monitored via mass spectrometry, indicating an increased rigidity of the handle region of ADEP-bound EcClpP (Sowole et al., 2013). Second, the thermal stability of SaClpP was analysed in thermal shift assays using a temperature range from 20 to 80°C in the presence and absence of the synthetic derivative ADEP7 which revealed a significant increase of the melting temperature of ADEP-bound SaClpP, suggesting a strong folding stability in the presence of ADEP7 (Gersch et al., 2015). Third, a remarkable example for ADEP gaining conformational control over ClpP is the crystal structure of MtClpP1P2. Interestingly, the binding of the synthetic derivative ADEP2 to MtClpP2 led not only to the pore opening of MtClpP2 but to the concerted pore opening of both rings, MtClpP1 and MtClpP2, dysregulating the entity of the protease complex. More precisely, ADEP2 induced the formation of ß-hairpins of the N-terminal loops of MtClpP2 directly and of MtClpP1 indirectly, executing conformational control over a distance of ~90 Å (Schmitz et al., 2014). Although substrate degradation is mediated by the interaction between the Clp-ATPases ClpX, ClpC1 or ClpC2 and the ADEP-insensitive ClpP2 in *S. hawaiiensis*, substrate degradation is stimulated indirectly, by

the binding of ADEP1 to the opposing ring of ClpP1, strongly indicating that ADEP1 exerts conformational control not only on the heptameric ring of ClpP1 but on the entire protease complex. Therefore, it is most likely that binding of ADEP1 to ShClpP1 leads to the concerted pore opening of both ShClpP1 and ShClpP2 rings, as is was observed previously for MtClpP1P2 (Schmitz et al., 2014).

Additionally, all ClpP-ADEP bound crystal structures from different organisms were captured in the active extended conformation in contrast to apo-ClpP, which could be crystallised in the active extended, inactive compact and inactive compressed state, suggesting that ADEP shifts the equilibrium between the active extended and transiently adopted inactive states towards the extended conformation (Malik and Brötz-Oesterhelt, 2017).

Considering all information gained so far, it is most likely that ADEP1 induces the assembly of ClpP1P2 hetero-tetradecamers and the opening of the entrance pores of ClpP1 and potentially ClpP2, with the N-terminal loops located in the “up-conformation”, as it was described for ADEP-bound BsClpP (Lee et al., 2010). Furthermore, ADEP-binding to ClpP1 probably leads to the stabilisation of the proteolytic core in the extended active conformation, thereby exerting conformational control over the entity of ClpX/C1/C2-P1P2 protease complexes of *S. hawaiiensis*.

If ADEP1 shifts the equilibrium of the ClpP1P2 heteromeric complex to the extended conformation, questions arise, how ADEP1 binding to ClpP1 affects Clp-ATPase/ClpP dynamics, which are necessary for a functional substrate degradation cycle.

Gribun *et al*. suggested that the flexibility of the IGF/IGL loops of EcClpX/ClpA and the axial loops of EcClpP are necessary for maintaining Clp-ATPase/ClpP interactions during conformational changes of EcClpP, which are required for a functional substrate degradation cycle (Gribun et al., 2005). In accordance with Gribun *et al.*, Malik & Brötz-Oesterhelt proposed that the weak and partial binding of Clp-ATPases to ClpP might have evolved to sustain ClpP dynamics, which are relevant for the physiological function of the protease complex (Malik and Brötz-Oesterhelt, 2017). Furthermore, cryo-EM structures of LmClpXP visualised highly flexible interactions between the symmetry mismatched partners ClpX and ClpP leading to a further hypothesis about potential rotational movements of ClpX during substrate degradation (Gatsogiannis et al., 2019).

In addition, cryo-EM structures of substrate bound ClpXP from *Neisseria meningitis* concluded a model for ClpXP interactions involving rotations of the Clp-ATPase ClpX on the apical surface of the peptidase ClpP to enable substrate hydrolysis (Ripstein et al., 2020).

Given that ADEP1 accelerates the degradation of natural and model substrates by the *Streptomyces* Clp protease, degradation products have to be released efficiently, which is in the absence of ADEP assumed to take place by adopting transiently inactive states of ClpP (Kimber et al., 2010). However, ADEP is known to stabilise the extended active conformational state and it can be speculated that ADEP1 compensates the necessity of conformational changes within the tetradecameric barrel by the opened entrance pore of ClpP1, thereby allowing exit of cleaved substrates. It has been shown before that ADEP-activated EcClpP degrades model substrates like casein with reduced processivity compared to EcClpAP, resulting in the accumulation of intermediate degradation products (Kirstein et al., 2009). Li *et al*. suggested that partially cleaved substrates can diffuse away through the opened entrance pore of EcClpP, whereas the binding of EcClp-ATPases to EcClpP prevent the escape of degradation intermediates (Li et al., 2010). Similarly, casein degradation experiments by ADEP-activated ClpP1P2 from *S. hawaiiensis* clearly display an accumulation of intermediate degradation products on SDS-PAGE gels (see Figure 6.11 in the appendix). Without ADEP, the degradation of substrates by the Clp protease is tightly controlled and assures that no intermediate degradation products can exit the proteolytic chamber, indicating that its accumulation by ADEP-activated ClpP might cause serious damage in the cells.

Since ADEP affects ClpP extensively, causing a stabilisation of the active extended state, an allosteric activation of the catalytic triads and the opening of the entrance pore (Lee et al., 2010, Li et al., 2010, Gersch et al., 2015), it seems plausible that the accelerated degradation of substrates by ADEP-activated *Streptomyces* Clp complexes represents a combination of different effects ADEP1 exerts on ClpX/C1/C2-P1P2 complexes. Not only the stabilisation of the active extended conformation of ClpP1P2 complexes and an allosteric activation of the catalytic triads are considered to cause major effects on the Clp-ATPase-mediated degradation of substrates, but the opened entrance pores of ClpP1 and/or ClpP2 as well. While an opened entrance pore of

ClpP1 might ensure the release of degradation products, an opened entrance pore of ClpP2 could facilitate the Clp-ATPase-mediated translocation of substrates.

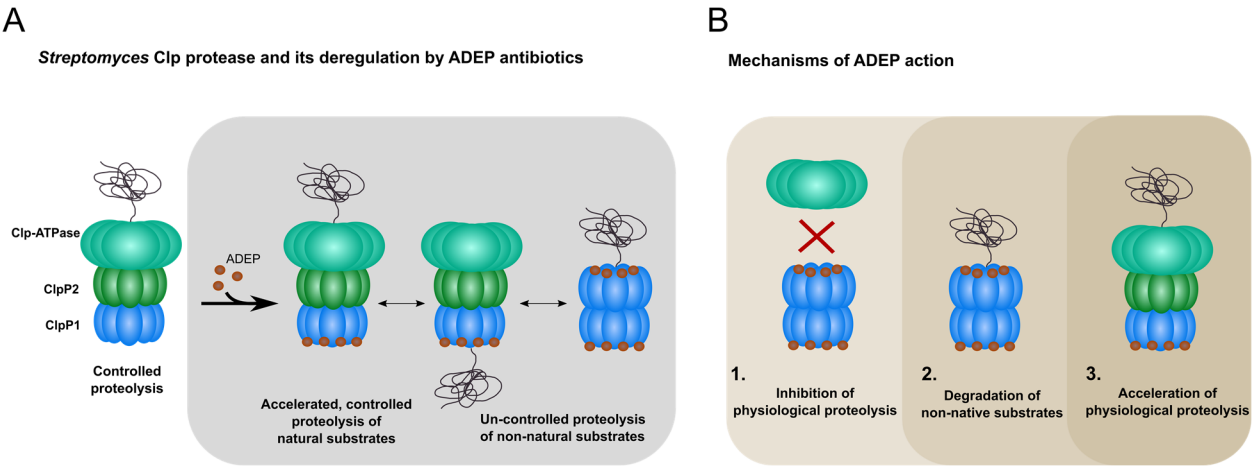

Figure 4.2: **ADEP mechanisms of action**. **A**: Model of the housekeeping Clp protease in *Streptomyces*. The proteolytic core consists of a mixed ClpP1P2 complex that interacts with the Clp-ATPases ClpX, ClpC1 or ClpC2 via the heptameric ring of ClpP2. Enzymatic activity is conferred by the catalytic triads of ClpP1 for the hydrolysis of peptides and proteins. The Clp-ATPases ClpX, ClpC1 or ClpC2 bind to the hydrophobic pockets of ClpP2, thereby unfolding and translocating substrates into the proteolytic chamber of ClpP1P2 under ATP consumption. Simultaneously, ADEP1 binds to ClpP1, stabilising the heteromeric proteolytic core in the extended conformation, resulting in accelerated hydrolysis of natural substrates, which gain access to the proteolytic chamber via ClpP2. While the physiological function of the Clp protease is still maintained upon ADEP1 addition, even accelerated, ADEP1 triggers the assembly of ClpP1 homo-tetradecamers and ClpP1P2 hetero-tetradecamers, leading to un-regulated proteolysis on non-native substrates which might represent the ADEP mode of killing in *Streptomyces*. Additionally, the accelerated degradation of native substrates by the Clp protease might also negatively affect the cells through protein imbalance. **B**: Mechanism of ADEP-action. It was previously described, that ADEP leads to the inhibition of the physiological function of the Clp protease by abrogating Clp-ATPase/ClpP interactions (1) as well as to un-controlled degradation of non-native substrates (2) by ADEP-activated ClpP. This study reveals a third, novel ADEP mode of action in the genus *Streptomyces*, resulting in accelerated degradation of natural Clp protease substrates (3).

With ClpP2 as exclusive interaction partner for the Clp-ATPases and its ADEP-insensitivity, the physiological function of the *Streptomyces* Clp protease is still maintained in the presence of ADEP. In principle, the accelerated degradation of natural substrates by ADEP-bound ClpC1/C2/X-P1P2 has to be considered to cause serious damage to the cells, affecting the dynamics of regulatory processes by e.g., a stimulated hydrolysis of transcriptional regulators such as ClgR

leading to protein imbalance. However, despite such a probable imbalance, there is accumulated evidence indicating that accelerated degradation of natural substrates by the *Streptomyces* Clp protease may contribute to, but is not the primary cause of ADEP-induced bacterial killing of ADEP-sensitive *Streptomyces* species, such as *S. lividans*. Complementing a *S. lividans clpP1P2* knock-out strain with only the ADEP-sensitive ClpP1 leads to cell-death (Thomy, 2019), demonstrating that the un-controlled degradation of proteins gaining access through the opened entrance pores of ADEP-activated ClpP1 homo-tetradecamers is sufficient for causing cell-death. Therefore, an ATPase-independent degradation of non-native substrates by ADEP1-activated ClpP1 in ClpP1P2 heteromeric protease complexes and/ or ClpP1 homo-tetradecamers has to be considered to be the primary ADEP mode of killing in *Streptomyces.*

4.3 ShClpP$_{ADEP}$: a dual mode of resistance

Almost one decade ago, Mazodier and colleagues investigated the ADEP-sensitivity of *Streptomyces* ClpP proteins in whole cell studies and considered a target substitution as resistance mechanism against ADEP in the producer strain *S. hawaiiensis*. Specifically, they explored ClpP3P4 as an ADEP-insensitive replacement of the housekeeping protease ClpP1P2. By constructing a Δ*clpP1* knock-out mutant in *S. lividans,* they observed that expression of ClpP3P4 conferred ADEP resistance, strongly indicating that ClpP3 might be an ADEP-insensitive ClpP (Gominet et al., 2011). When investigating *S. hawaiiensis* via immunoblotting with specific anti-ClpP1 and anti-ClpP3 antibodies, they detected ClpP1 instead of ClpP3, eliminating a potential target substitution by ClpP3P4 as resistance mechanism in the ADEP producer strain (Gominet et al., 2011). Recently, Thomy and co-workers discovered an additional *clpP* gene located in close vicinity to the ADEP biosynthetic gene cluster whose expression mediates ADEP resistance (Thomy et al., 2019). However, the mechanism of ADEP resistance has not been investigated on a molecular level. As in the study of Dhana Thomy, *clpP1*, *clpP2* and *clpP$_{ADEP}$* were expressed in *S. hawaiiensis* under the conditions tested, but not *clpP3* and *clpP4* (Thomy, 2019), I focused my PhD project on the three expressed ClpP variants and investigated their interactions on a molecular level. The results indicate a dual mode of resistance to protect the bacterial cell against

ADEP. Pull-down experiments in combination with size exclusion chromatography demonstrated that $ClpP_{ADEP}$ interacts with ClpP1, thereby inhibiting the ADEP-induced assembly of ClpP1 homo-tetradecamers. The $ClpP_{ADEP}P1$ complexes formed consisted of lower oligomeric species, presumably dimers and/or trimers. By sequestering ClpP1 in a complex, $ClpP_{ADEP}$ prevented not only the ADEP-induced assembly of ClpP1 homo-tetradecamers, but the interaction of ClpP1 with its partner peptidase ClpP2 as well, and thereby the formation of mixed heteromeric ClpP1P2 complexes. The inhibition of the ADEP-induced formation of ClpP1P2 tetradecamers by $ClpP_{ADEP}$ was demonstrated by performing *in vitro* degradation experiments with model substrates such as the fluorogenic di-peptide Suc-LY-AMC and the protein ß-casein which both serve as substrates of ADEP-activated ClpP1P2. Adding $ClpP_{ADEP}$ to ClpP1P2 led to a significant decrease of the ADEP-induced, Clp-ATPase-independent degradation of Suc-LY-AMC and ß-casein. Hence, these results clearly indicate that $ClpP_{ADEP}$ is able to inhibit the peptio-and proteolytic activity of ADEP-induced ClpP1P2.

However, ClpP is essential for cell viability in *Streptomyces* (Viala et al., 2000) and the physiological function of the Clp complex has to be maintained. Therefore, we investigated as a following step if a potential target substitution might not be mediated by ClpP3P4, but by $ClpP_{ADEP}P2$. *In vitro* substrate degradation experiments were conducted using $ClpP_{ADEP}P2$ and employing the Clp-ATPases ClpX and ClpC1 for the degradation of ClgR, PopR and the model substrate ß-casein. Those experiments confirmed the formation of a physiologically active $ClpP_{ADEP}P2$ complex in association with either ClpX or ClpC1. In addition, substrate degradation experiments employing the catalytic triad knock-out mutant $ClpP2_{S131A}$ and the hydrophobic pocket mutant $ClpP2_{hp}$ in combination with wild-type $ClpP_{ADEP}$, strongly imply that $ClpP_{ADEP}$ performs the catalytic function in a $ClpP_{ADEP}P2$ heteromeric complex, whereas ClpP2 is the sole interaction partner for the Clp-ATPases, similar to the function ClpP2 possesses in the heteromeric ClpP1P2 complex.

In addition, comparing protein sequences of ClpP1-5 with $ClpP_{ADEP}$ revealed the highest sequence identity to ClpP1 (71.89 % sequence identity), followed by ClpP3 (59.77 % sequence identity).

Based on these findings, a model for the $ClpP_{ADEP}$ dual mode of resistance in the ADEP producer strain *S. hawaiiensis* NRRL 15010 is illustrated in Figure 4.3.

To inhibit un-controlled proteolysis by ADEP-bound ClpP1 homo-tetradecamers as well as ClpP1P2 hetero-tetradecamers with or without a Clp-ATPase bound to ClpP2, $ClpP_{ADEP}$ interacts with the ADEP-sensitive ClpP1 and forms lower oligomeric complexes. Additionally, the $ClpP_{ADEP}P2$ heteromeric complex replaces physiological functions of the housekeeping protease, (i.e., the proteolytic core ClpP1P2 in association with ClpX, ClpC1 or ClpC2), Fig. 4.3. In addition, it is important to mention that investigations of the $ClpP_{ADEP}$ mode of resistance on the molecular level do not allow conclusions if the $ClpP_{ADEP}P2$ complex can replace all physiological functions of the housekeeping Clp protease.

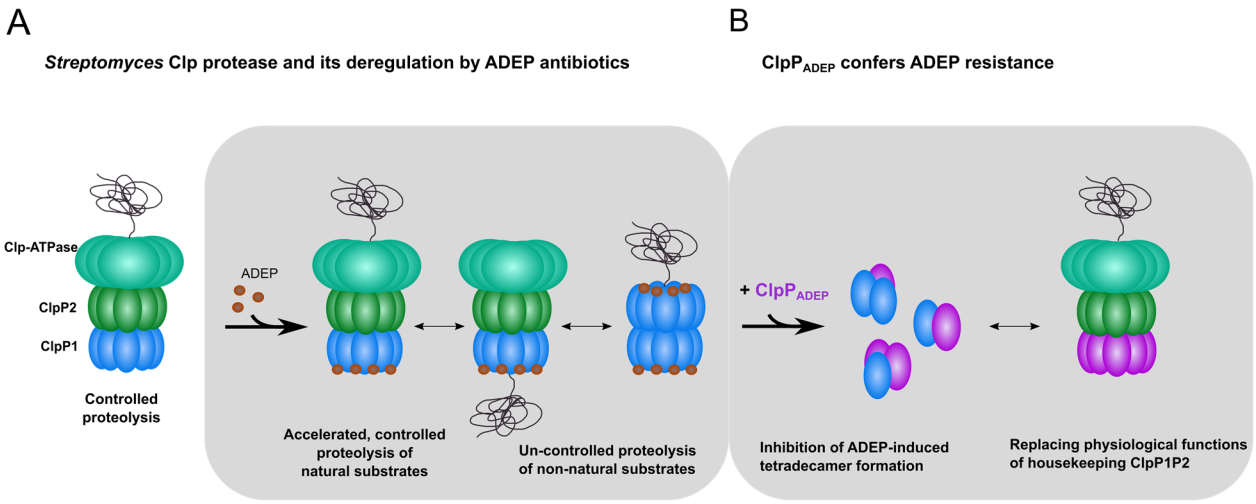

Figure 4.3: **Model of the $ClpP_{ADEP}$ dual mode of resistance in the ADEP producer strain *S. hawaiiensis* NRRL 15010. A**: ADEP1 binding to heteromeric ClpP protease complexes in *Streptomyces* leads to accelerated Clp-ATPase-mediated degradation of natural substrates. In addition, un-controlled proteolysis of non-natural substrates by ADEP-activated ClpP1 homo-tetradecamers as well as heteromeric ClpP1P2 tetradecamers can occur, presumably resulting in cell death in ADEP sensitive *Streptomyces* species. **B**: $ClpP_{ADEP}$ inhibits the formation of ClpP1 homo-tetradecamers and ClpP1P2 hetero-tetradecamers by the formation of $ClpP_{ADEP}P1$ complexes. Furthermore, to replace the physiological functions of the housekeeping Clp protease ClpP1P2, $ClpP_{ADEP}$ forms a physiologically active complex with the ADEP-insensitive ClpP2 for the Clp-ATPase-dependent degradation of natural substrates.

Among the Clp peptidases of various organisms studied to date, $ClpP_{ADEP}$ is the first described member of the Clp family, which simultaneously functions as a Clp peptidase and as a resistance factor.

Considering known resistance mechanisms of producer strains of different antibiotics, three major mechanisms can be specified. First, modifying the target inside the cell represents one option to protect the cells from suicide as it is realised by the producer of erythromycin (*Saccharopolyspora erythrea*), an antibiotic that targets bacterial ribosomes, resulting in inhibition of protein biosynthesis (Brock and Brock, 1959, Golkar et al., 2018). In *S. erythrea, ermE* which encodes a 23S rRNA methylase, protects the ribosomes by N^6-dimethylation of the 23S rRNA at a single adenine resulting in inhibition of erythromycin binding (Thompson et al., 1982). Another mechanism by which producer strains can protect themselves from their own antibiotic is actively exporting the molecule out of the cell, as it occurs in *Streptomyces aureofaciens*, the producer strain of the protein biosynthesis inhibitor tetracycline (Duggar, 1948, Dairi et al., 1995, Grossman, 2016). A third strategy conferring self-protection, is to keep the antibiotic in an inactive state as long as it is in the producer strain by, for example the attachment of a protecting group to the molecule as long as the unfinished product moves along the biosynthetic pathway. Exemplary is streptomycin, which is phosphorylated in the bacterial cell of the producer strain *S. griseus* (Miller and Walker, 1969). As soon as the biosynthesis of the molecule is finished, streptomycin is dephosphorylated and the active molecule exported (Miller and Walker, 1970).

The discovery of an additional sixth *clpP* gene downstream of the ADEP-biosynthetic gene cluster in *S. hawaiiensis* (Thomy et al., 2019) indicated a new, yet undiscovered mechanism of antibiotic resistance involving a Clp peptidase, a mechanism that was unravelled in the current PhD project. Nevertheless, even after having understood now how $ClpP_{ADEP}$ works, the principle question remains why a sixth Clp peptidase is necessary at all to obtain ADEP resistance, instead of merely inactivating the *clpP1* gene by mutation, thereby utilising the ADEP-insensitive ClpP3P4 as a target substitution or evolving an ADEP-insensitive ClpP1 by ADEP binding-site mutation, yielding an ADEP-insensitive ClpP1P2 housekeeping protease.

Concerning the first option, whole cell studies with *S. lividans* and *S. coelicolor* employing *ΔclpP1* deletion mutants, i.e., strains that express ClpP3P4, depicted the inhibition of the formation of aerial mycelium, also known as *bald* phenotype and the formation of accelerated aerial mycelium in strains (*S. lividans*, *S. albus*, *S. coelicolor*) overexpressing *clpP1P2* genes (de Crecy-Lagard et al., 1999, Viala et al., 2000). Furthermore, AdpA, which activates *clpP1clpP2* expression, controls genes encoding key regulators of cell differentiation, such as aerial growth (Wolanski et al., 2011). The fact that *Δ clpP1* mutants fail to form an aerial mycelium (de Crecy-Lagard et al., 1999, Viala et al., 2000) and that *clpP2clpP2* are induced by the pleitropic regulator AdpA (Guyet et al., 2013, Guyet et al., 2014), further emphasises the importance of ClpP1P2 for cell differentiation. In *S. coelicolor*, the AdpA level reaches its maximum during the early stage of aerial mycelium formation (36 h) and remains constant during 48 to 60 h followed by a rapid decrease (Wolanski et al., 2011). These observations indicate that the physiological function of the housekeeping Clp protease ClpP1P2, which seems to be involved in cell cycle differentiation (de Crecy-Lagard et al., 1999, Wolanski et al., 2011, Guyet et al., 2013, Guyet et al., 2014), cannot be fully replaced by the back-up Clp protease ClpP3P4. Also, a decreased fitness/ stress tolerance of the bacterial cell was reported as the *ΔclpP1* mutant was described as thermosensitive and to grow poorly at 37°C (de Crecy-Lagard et al., 1999). In addition, a knock-out of *clpX* in *S. lividans* led to a conditional *bald* phenotype, indicating that ClpX is necessary for cell differentiation on certain media (Viala and Mazodier, 2003). McCormick and Flärdh hypothesised, that BldD, an important transcriptional regulator for cell differentiation, might be a substrate of ClpXP in *Streptomyces* (McCormick and Flärdh, 2012).

Regarding the second possibility, modifying the target ClpP1 to evolve an ADEP-insensitive house-keeping protease, the current *in vitro* degradation experiments employing the mutant proteins $ClpP1_{Y76S}$ and $ClpP2_{S94Y}$ may provide potential explanations. Corresponding to the three conserved aromatic amino acid residues within the hydrophobic pocket of EcClpP, the respective amino acid residues of ClpP1 and ClpP2 were mutated, yielding the hydrophobic pocket mutant proteins $ClpP1_{hp}$ and $ClpP2_{hp}$, which only differ in the first of these three conserved amino acid residues. While ClpP1 comprises three tyrosine residues at the respective positions, ClpP2 harbours a serine and two tyrosine residues. $ClpP1_{Y76S}$ alone or in combination with wild-type

ClpP2 revealed a dramatic decrease in the ADEP-induced degradation of the fluorogenic dipeptide Suc-LY-AMC compared to wild-type ClpP1 and ClpP1P2. Investigating the oligomeric state of ClpP1, ClpP2 and the mutant protein ClpP1$_{Y76S}$ on a native PAGE in the presence and absence of ADEP1 and the chemical cross-linker BS3 strongly indicate a significant decrease in the ADEP-induced assembly of ClpP1$_{Y76S}$ tetradecamers compared to wild-type ClpP1, see Figure 3.20. Additionally, a significant decrease in the proteolytic activity of ClpP1$_{Y76S}$P2 compared to wild-type ClpP1P2 in ClpC1-mediated FITC-casein degradation experiments could be observed. These findings strongly imply that single amino acid substitutions, which lead to a decreased ADEP-sensitivity, could have unfavourable effects concerning the maintenance of the physiological function of the Clp protease. Studying a set of spontaneous ADEP-resistant ClpP proteins in Firmicutes followed by a detailed biochemical characterisation revealed defects in ClpP oligomerisation or Clp-ATPase/ClpP interactions, demonstrating that all studied ClpP proteins, which carried single amino acid mutations, were functionally impaired (Malik et al., 2020). Malik and Brötz-Oesterhelt previously described the Clp peptidase ClpP as a clockwork where each cogwheel is tightly interconnected and mutations of single amino acid residues can affect the structural organisation of the complete macromolecule (Malik and Brötz-Oesterhelt, 2017). Therefore, a sixth Clp peptidase, which inactivates ClpP1 and simultaneously replaces its function in a heteromeric ClpP$_{ADEP}$P2 complex seems to be for *Streptomyces* the most suitable resistance mechanism by which *Streptomyces* cells can best maintain their biological fitness.

However, the particular amino acid residues which are responsible for the ADEP-insensitivity of ClpP$_{ADEP}$ and ClpP2 are still elusive. Therefore, amino acid (aa) sequences of BsClpP, ShClpP$_{ADEP}$, ShClpP2 and the ADEP-sensitive ShClpP1 were aligned. Amino acid residues in BsClpP, which are known to be involved in ADEP1 binding (Lee et al., 2010), are illustrated along with the corresponding amino acid residues of ShClpP$_{ADEP}$ and ShClpP2 in Figure 4.4. Numbers in Figure 4.4 A correspond to the position of the respective amino acid residue in BsClpP. Amino acid alterations in ShClpP$_{ADEP}$ and ShClpP2, which are considered to disturb ADEP1 binding according to their physicochemical properties compared to corresponding amino acid residues in BsClpP, are marked in red. Furthermore, individual changes in either ShClpP$_{ADEP}$ or ShClpP2 are marked

in dark red and yellow. Of note, amino acid alterations in ShClpP$_{ADEP}$ and ShClpP2 which are present in the ADEP-sensitive ClpP1 as well, were not considered to confer ADEP-insensitivity.

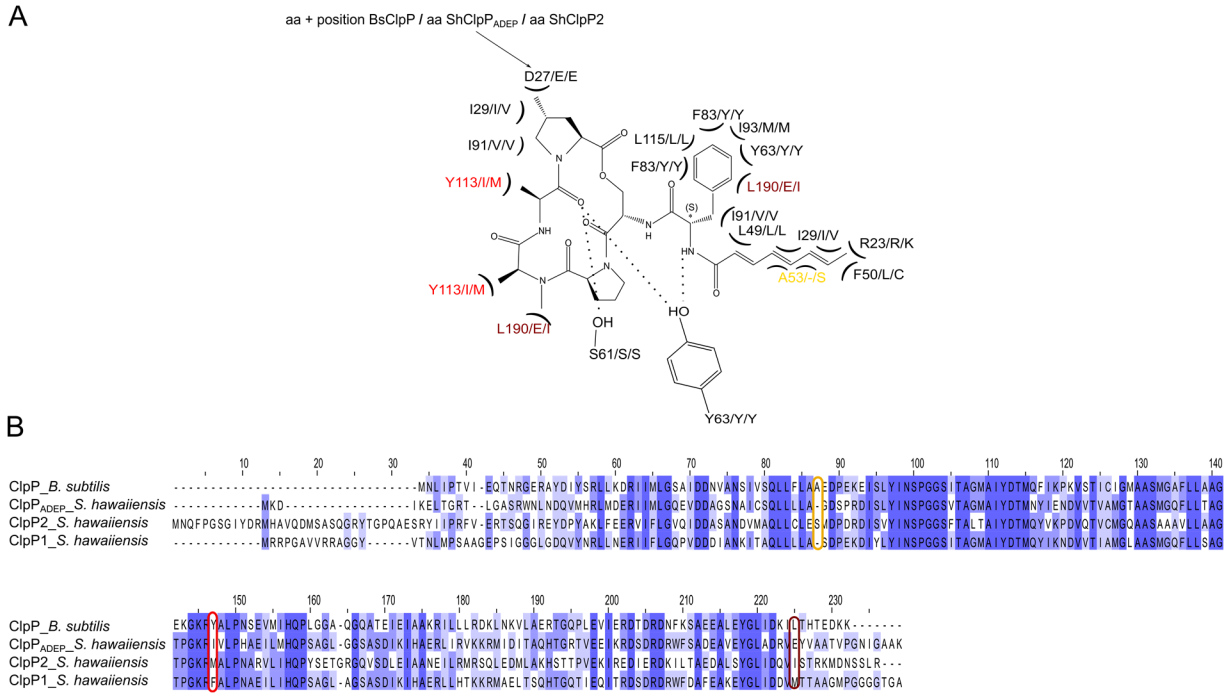

Figure 4.4: **Amino acid residues of BsClpP which are known to be involved in ADEP1 binding (Lee et al., 2010) and corresponding amino acid residues of ShClpP$_{ADEP}$ and ShClpP2 are illustrated. A:** Numbers shown here include the initiating methionine. The first position corresponds to amino acid residues in BsClpP, which are known to be involved in ADEP1 binding and the second and third position correspond to amino acid residues in ShClpP$_{ADEP}$ and ShClpP2. Hydrophobic interactions with the molecule ADEP1 are indicated by brackets and hydrogen bonds by dotted lines. Significant changes according to the physicochemical properties of the respective amino acid residue in both ShClpP$_{ADEP}$ and ShClpP2 are indicated in red, whereas individual changes in either ShClpP$_{ADEP}$ or ShClpP2 are indicated in dark red and yellow. **B:** Amino acid sequence alignment of ShClpP1, ShClpP2 and ShClpP$_{ADEP}$ from *S. hawaiiensis* and ClpP from *B. subtilis*. The alignment was generated using protein sequences of *S. hawaiiensis* NRRL 15010 (CP021978.1) and *B. subtilis* strain 168 (NC_000964.3) with the online tool clustalΩ (https ://www.ebi. ac.uk/Tools/msa/clustalo/). ClpP sequence identities were computed using Jalview Software (Waterhouse et al., 2009). In each column, the percentage of amino acid residues that agree with the consensus sequence are visualised from dark blue (> 80 %) to marine (> 60 %) to pale blue (> 40 %). Amino acid sequence alterations, which are shown in A, are indicated correspondingly as boxes.

Strikingly, there are only a few changes in the composition of the respective amino acid residues in ShClpP$_{ADEP}$ and ShClpP2, which could be considered to disturb ADEP1 binding. First, the aromatic, hydrophilic tyrosine residue in BsClpP (Y113) is replaced by both hydrophobic iso-

leucine and methionine residues in ShClpP$_{ADEP}$ and ShClpP2, respectively (marked in red). Specifically Y113 in BsClpP is known to strongly interact with ADEP1, as it forms multiple hydrophobic interactions (Lee et al., 2010). The ADEP-sensitive ClpP1 comprises a hydrophobic, aromatic phenylalanine residue at the corresponding position. Furthermore, the hydrophobic leucine residue (L190) in BsClpP is replaced by a hydrophilic, negatively charged glutamate residue in ShClpP$_{ADEP}$ (marked in dark red) and the hydrophobic alanine residue (A53) in BsClpP is exchanged by a hydrophilic serine residue in ShClpP2 (marked in yellow), see Figure 4.4 and table 4.1.

Table 4.1: **Alterations in ShClpP$_{ADEP}$ and ShClpP2 corresponding to known amino acid residues involved in ADEP1 binding in BsClpP (Lee et al., 2010)**

BsClpP	ShClpP$_{ADEP}$	ShClpP2
Y113	I115	M142
L190	E193	
A53		S86

In contrast to the hydrophobic leucine residue L190 in BsClpP, ShClpP$_{ADEP}$ harbours a hydrophilic, charged glutamate residue at the corresponding position which is likely to hamper ADEP1 binding. In BsClpP, the analysis of spontaneous ADEP-resistant clones revealed a mutant which harbours an hydrophilic serine residue instead of the original hydrophobic leucine residue at position 190 and showed a significant increase in the miniminal inhibitory concentration (MIC) against ADEP1 (Malik et al., 2020). In *S. aureus*, the same position was also found to be mutated in the ClpP peptidase of a spontaneous ADEP-resistant mutant. In this mutant, the methionine residue was exchanged by a tyrosine residue leading to a reduced ADEP-sensitivity (Malik et al., 2020).

Collectively, the data described in this thesis represent a detailed characterisation of the complex *Streptomyces* Clp system on the molecular level, highlighting a novel, third ADEP mode of action on the heteromeric ClpX/C1/C2-ClpP1P2 complex. In addition, the ClpP$_{ADEP}$ mode of resistance of the ADEP producer *Streptomyces hawaiiensis* NRRL 15010 was unrevalled, revealing a new mechanism of producer strain survival.

5. Outlook

Strikingly, regarding the formation of physiologically active $ClpP_{ADEP}P2$ protease complexes in ClpX and ClpC1-mediated substrate degradation experiments, substrate degradation was remarkably slower compared to ClpX or ClpC1-mediated substrate degradation by ClpP1P2. However, a potential reason for a less efficient substrate degradation by $ClpP_{ADEP}P2$ could be the missing induction of $ClpP_{ADEP}$ processing *in vitro,* which was observed in *in vivo* experiments by Dr. Dhana Thomy from our group (Thomy, 2019). In contrast to ClpP1, $ClpP_{ADEP}$ never processed itself *in vitro*, nor was it processed by another peptidase such as ClpP1 in different combinations with natural substrates and its partner Clp-ATPases ClpX, ClpC1 or ClpC2 with or without ADEP1 addition. Therefore, the factor which induces $ClpP_{ADEP}$ processing is still unknown. However, by choosing a potential processing site and working with a shortened, recombinant $ClpP_{ADEP}$ *in vitro* improved the situation as the processing of $ClpP_{ADEP}$ induced assembly of $ClpP_{ADEP}$ into heptameric species, whereas full-length $ClpP_{ADEP}$ displayed exclusively monomers. Nevertheless, the shortened $ClpP_{ADEP}$ exhibited proteolytic activity far weaker than its ADEP-sensitive homologue ClpP1, which could be due to an impaired folding of the protein due to the missing processing reaction and/or because of the expression of the shortened protein starting from a potentially incorrect processing site. Impaired folding of $ClpP_{ADEP}$ could potentially also be responsible for slower processing of ClpP2 and delayed complex formation with ClpP1. Given that the factor which induces $ClpP_{ADEP}$ processing is not known, the correct processing site of $ClpP_{ADEP}$ could in principle be analysed via intact protein mass spectrometry after isolating processed $ClpP_{ADEP}$ out of *Streptomyces* cells. However, this is challenging since protein amounts of $ClpP_{ADEP}$ isolated from *Streptomyces* are low and the protein has to be purified for intact protein mass spectrometry. Nevertheless, by analysing the correct processing site of $ClpP_{ADEP}$, the protein could be purified heterologously in *E. coli* cells and its catalytic activity could be tested in combination with ClpP2 and its partner Clp-ATPases in substrate degradation experiments. Considering the challenging protein purification of $ClpP_{ADEP}$ due to the formation of inclusion bodies in the cells, the expression of the protein starting from the correct processing site could improve the solubility of $ClpP_{ADEP}$ as well. As a following step, $ClpP_{ADEP}$ mutant proteins could be constructed such as catalytic triad knock-out and hydrophobic pocket mutants to analyse its

catalytic activity in combination with ClpP2 as well as Clp-ATPase/ClpP interactions. Regarding the complex formation of $ClpP_{ADEP}$ and ClpP2, BS3 cross-linking experiments and/or pull-down assays could be performed to study the interaction between these two ClpP variants in detail.

Furthermore, the ADEP-sensitivity of ClpP1 could be analysed using isothermal titration calorimetry (ITC), thereby gaining in-depth knowledge of ADEP1 affinity to ClpP1 compared to other ADEP-sensitive Clp peptidases from other organisms such as *E. coli* or *B. subtilis*.

In addition, according to known amino acid residues in BsClpP which are involved in ADEP1 binding (Lee et al., 2010), an amino acid sequence alignment of BsClpP, ShClpP2, $ShClpP_{ADEP}$ and the ADEP-sensitive ShClpP1 revealed amino acid residue alterations which could potentially affect ADEP1 binding (see Figure 4.4). As a following step, mutant proteins of $ShClpP_{ADEP}$ and ShClpP2 could be constructed in which the respective amino acid residues, which are listed in table 4.1, could be exchanged by the corresponding amino acid residue of the ADEP-sensitive BsClpP. Subsequently, the ADEP-sensitivity of those mutant proteins could be tested via size exclusion chromatography, native-PAGE and activity assays.

Additionally, the mutant proteins $ClpP1_{Y76S}$ and $ClpP2_{S94Y}$ could be analysed in more detail considering their oligomeric behaviour in the presence and absence of ADEP1 via size exclusion chromatography and isothermal titration calorimetry could be conducted investigating potential differences concerning their susceptibility towards ADEP1 compared to wild-type ClpP1 and ClpP2 proteins. To complete the set of *Streptomyes* Clp complexes to be investigated in *in vitro* reconstitution experiments, ClpP3 and ClpP4 could be reconstituted and analysed in substrate degradation experiments as well, employing ADEP1 and/or the Clp-ATPases as Clp activator. Perceiving ClpP3P4 function as a fail-safe mechanism in *Streptomyces lividans* (Viala and Mazodier, 2002), it would be interesting to analyse if ClpP3 and ClpP4 form a heteromeric complex similar to ClpP1P2 with ClpP3 conferring catalytic activity and ClpP4 as the exclusive interaction partner for the Clp-ATPases. Therefor, catalytic triad knock-out mutant and hydrophobic pocket mutant proteins of the two ClpP isoforms ClpP3 and ClpP4 could be constructed accordingly. In addition, and considering the fact that ClpP5 shows a non-typical spacing in its catalytic triad, see chapter 1.7 figure 1.19, it should be tested if this Clp protein

exhibits enzymatic activity in concert with a partner Clp-ATPase in substrate degradation experiments. In whole cell experiments, a mutant of *S. lividans* with the *clpP1P2* and *clpP3P4* genes deleted could not be achieved, demonstrating that *clpP5* was not able to replace the physiological function of ClpP (Viala et al., 2000) further emphasising that ClpP5 might not function as a Clp peptidase.

The results presented in this work revealed the composition of the *Streptomyces* housekeeping Clp protease and provided insights into the mechanism how $ClpP_{ADEP}$ functions as a resistance factor in the ADEP producer strain *Streptomyces hawaiiensis* NRRL 15010 on the molecular level. The achieved knowledge forms the foundation for future work on the complex ClpP system of *Streptomyces in vitro*.

6. Appendix

6.1 Further protein purifications and experiments

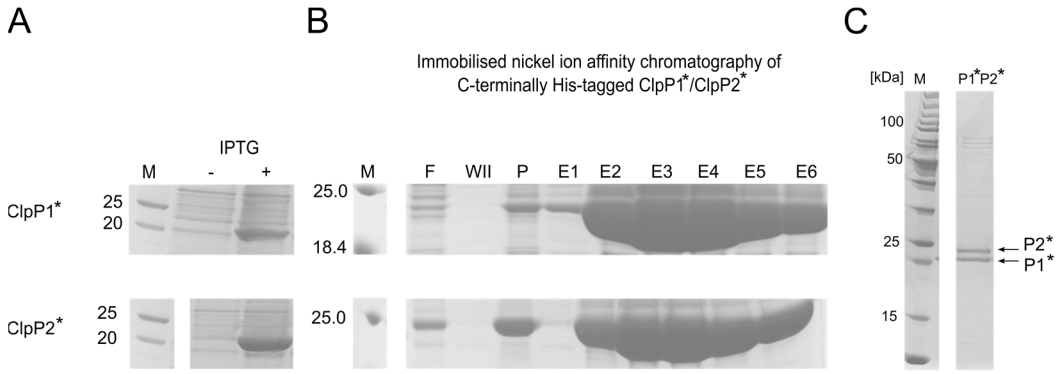

Figure 6.1: **Nickel ion affinity chromatography of ShClpP1* and ShClpP2***. **A:** The expression of ShClpP1* and ShClpP2* was induced by the addition of 1 mM IPTG for 4 h at 37°C. Subsequently, an un-induced and induced sample was loaded on a 12% Bis-Tris gel and analysed via SDS-PAGE. **B**: Nickel ion affinity chromatography of C-terminally His_6-tagged ClpP1* and ClpP2* was performed. Samples of the flow-through (F), WII (wash II), pellet after centrifugation (P) and elution fractions E1-E6 were loaded on 12 % Bis-Tris gels. **C**: Additionally, purified ShClpP1* and ShClpP2* were analysed via SDS-PAGE.

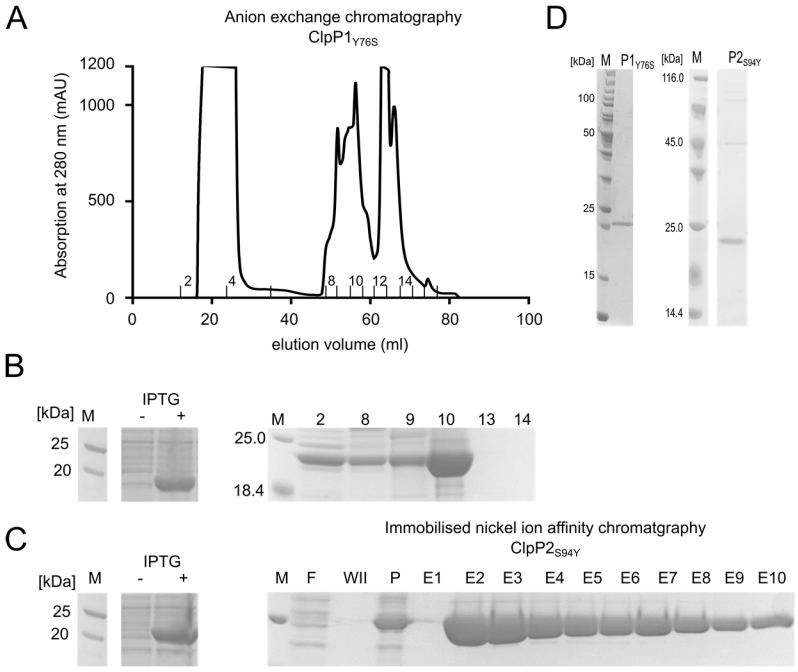

Figure 6.2: **Anion exchange chromatography of native ShClpP1$_{Y76S}$ employing an HiTrap™ Q XL column (GE Healthcare) and nickel ion affinity chromatography of C-terminally His-tagged ShClpP2$_{S94Y}$. A:** Elution of the ShClpP1$_{Y76S}$ protein was observed by recording the absoption

spectrum at 280 nm. **B**: The expression of ShClpP1$_{Y76S}$ was induced by the addition of 1 mM IPTG and carried out for 4 h at 37°C. Subsequently, an un-induced and induced sample was taken and analysed via SDS-PAGE. In addition, samples of the fractions which were collected during the anion exchange chromatography of ShClpP1$_{Y76S}$ were applied on 12% Bis-Tris gels as well. **C**: Analysis of ShClpP2$_{S94Y}$ expression and immobilised nickel ion affinity chromatography. The expression of ShClpP2$_{S94Y}$ was induced by the addition of 1 mM IPTG for 4 h at 37°C and the expression of the respective protein was analysed via SDS-PAGE. To isolate the ShClpP2$_{S94Y}$ mutant protein, a nickel ion affinity chromatography was carried out applying samples of the flow-through (F), the wash II (wash II) and the elution fractions E1-E10 on a 12 % Bis-Tris-gel. **D**: Purified ShClpP1$_{Y76S}$ and ShClpP2$_{S94Y}$ were analysed via SDS-PAGE.

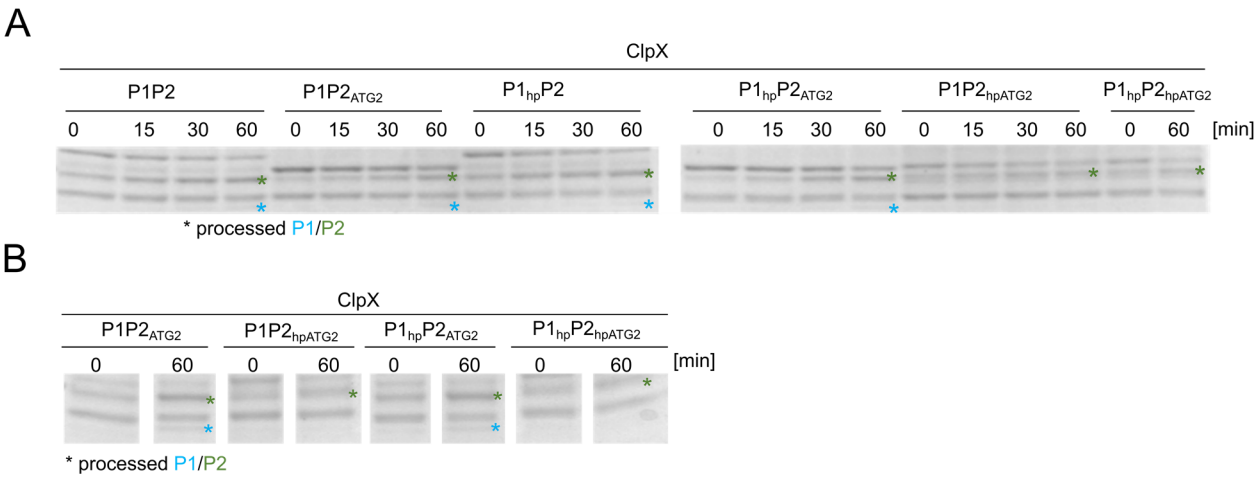

Figure 6.3: **ShClpP1P2 versus ShClpP1P2$_{ATG2}$ processing in the course of the ShClpX-mediated degradation of ShClgR. ShClpP1 processing depends on the interaction of ShClpX with ShClpP2 A:** Both ShClpP2 and ShClpP2$_{ATG2}$ proteins are processed similarily by ClpP1 resulting in a shortened mature ShClpP2 protein. **B**: In order to visualise the dependence of ShClpP1 processing on the interaction of ShClpX with ShClpP2 more clearly, processing reactions of ShClpP1, ShClpP2 and the corresponding hydrophobic pocket mutants are presented, which could be observed during ShClpX-mediated degradation experiments, employing ShClgR as substrate.

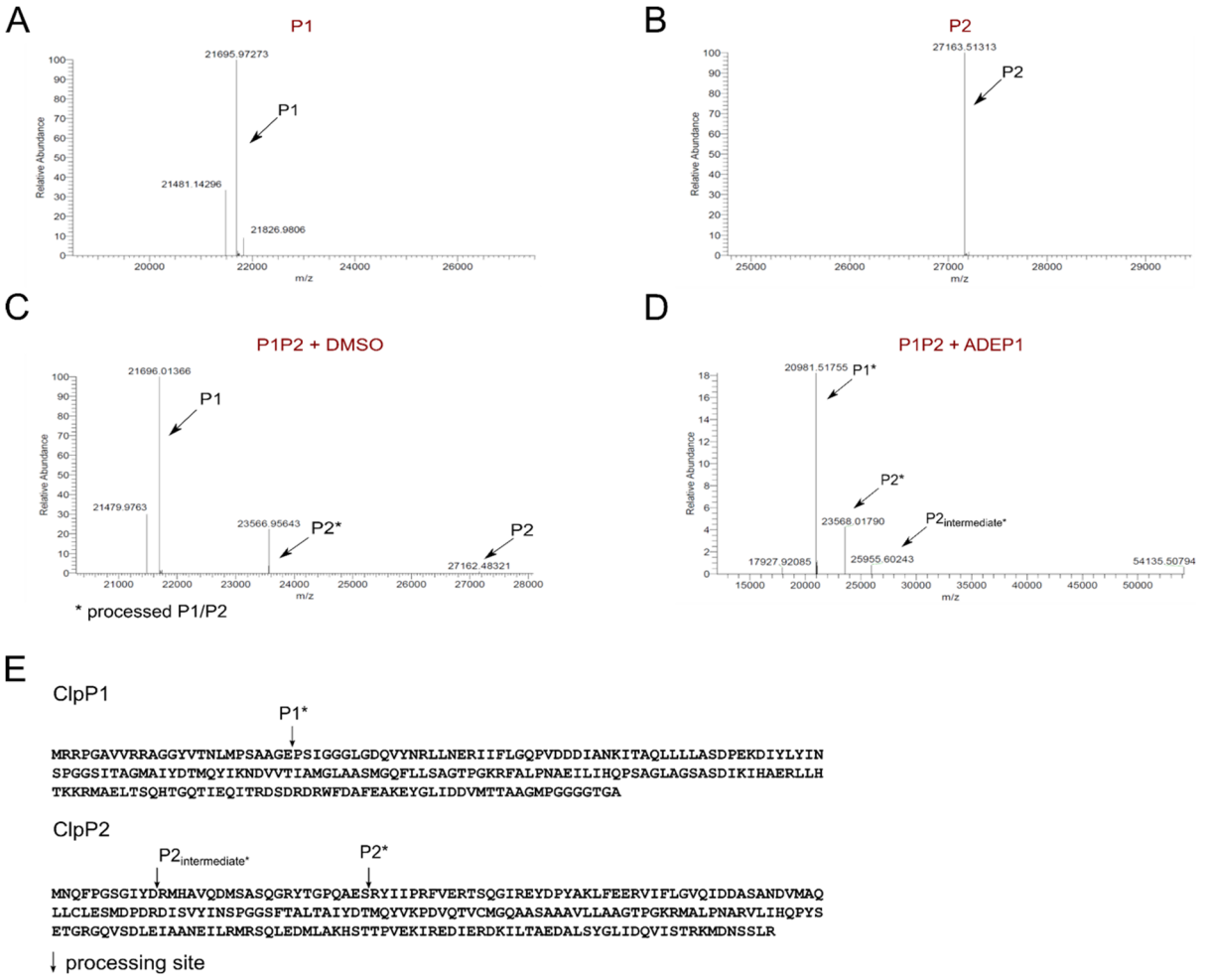

Figure 6.4: **Intact protein mass spectrometry of ShClpP1 and ShClpP2, including full-length and processed ClpP variants.**

A-D. Intact protein mass spectrometry was carried out by Dr. Markus Lakemeyer, AG Sieber, TU munich of (A) ShClpP1 alone, (B) ShClpP2 alone, (C) ShClpP1 + ShClpP2 + DMSO, and (D) ShClpP1 + ShClpP2 + ADEP1, confirming that ShClpP2 is processed by ShClpP1 in the absence and presence of ADEP1 (indicated by P2*), whereas ShClpP1 is self-processed only in the presence of ADEP1 (indicated by ShP1*). In addition, these data illustrate that ShClpP2 is processed with one intermediate processing step, finally resulting in mature ShClpP2*. **E.** Amino acid sequences of ShClpP1 and ShClpP2. The suggested processing sites according to intact protein mass spectrometry are indicated. ShClpP2 is first processed between amino acids D11 and R12, resulting in an intermediately processed ShClpP2 ($P2_{intermediate}$*) that starts with the amino acids RMHAVQ. The second processing site of ShClpP2 is located between amino acids S33 and R34, yielding the mature ShClpP2 (P2*) protein that starts with the amino acid sequence RYIIPR. Furthermore, the detected mass for processed ShClpP1 indicates the processing site to be located between the amino acids G24 and P25, which could only be detected in the presence of ADEP1.

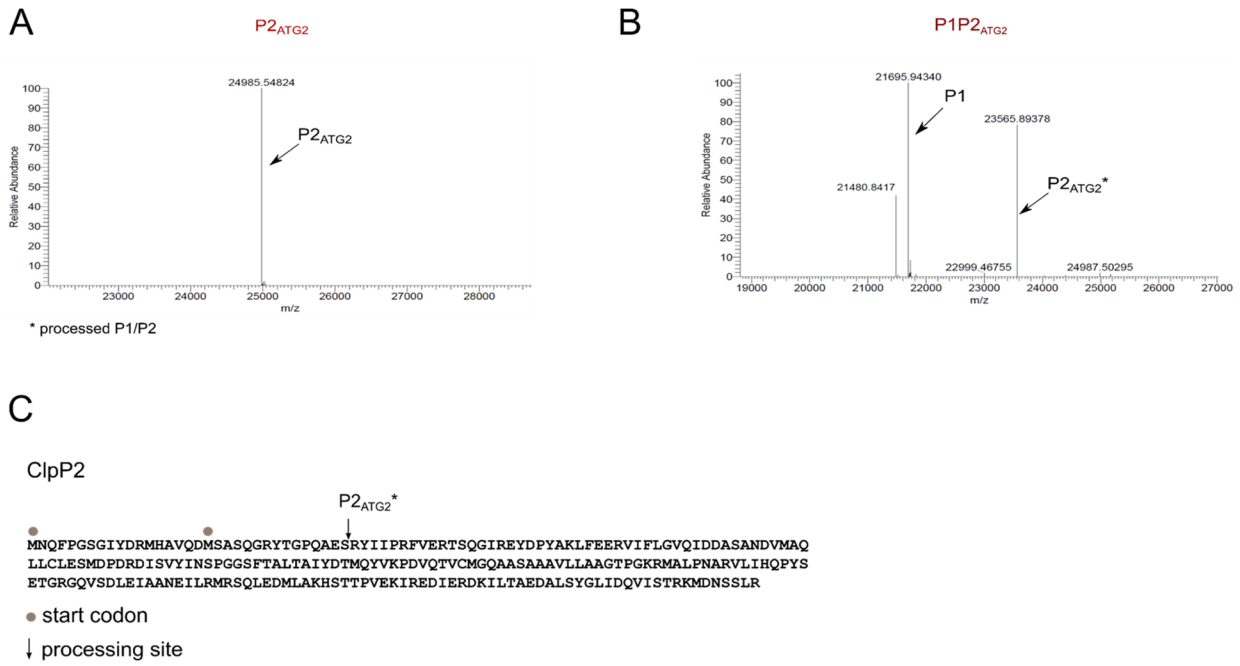

Figure 6.5: **Intact protein mass spectrometry of full-length ShClpP2$_{ATG2}$ including mature ShClpP2$_{ATG2}$* which was processed after the addition of ShClpP1, performed by Dr. Markus Lakemeyer, AG Sieber, TU munich. A + B:** Intact protein mass spectrometry of (A) ShClpP2$_{ATG2}$ and (B) ShClpP1 + ShClpP2$_{ATG2}$ confirm the same processing site of ShClpP2$_{ATG2}$ as full-length ShClpP2, yielding the same mature ShClpP2$_{ATG2}$* protein that starts with RYIIPR. **C.** Amino acid sequence of ShClpP2 illustrating the first and putative second start codon (red dots) as well as the resulting processing site concluded from intact protein mass spectrometry. The detected mass for processed ClpP2$_{ATG2}$* indicates the same processing site between the amino acids S33 and R34, resulting in a protein that starts with RYIIPR, similar to processed ShClpP2*.

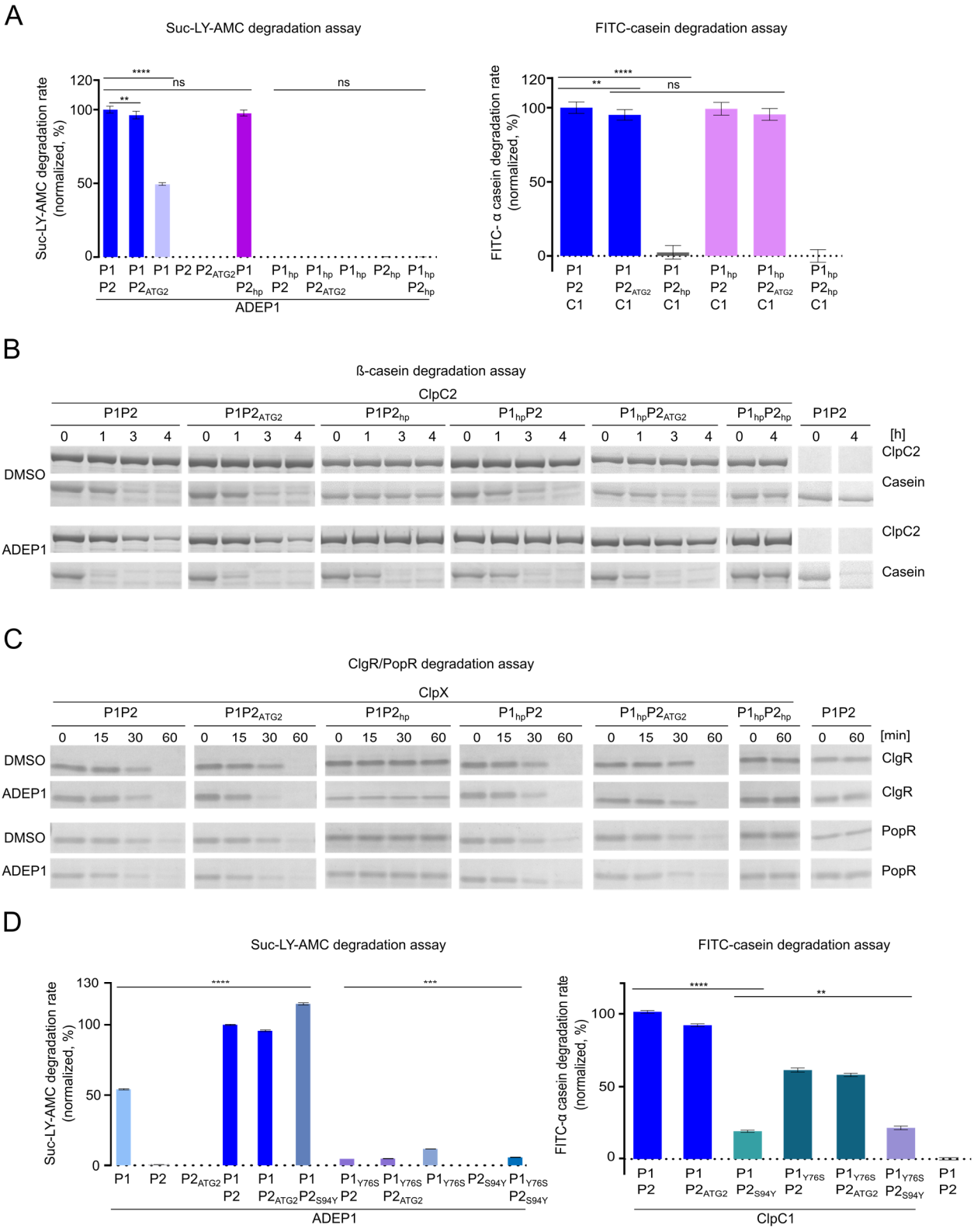

Figure 6.6: **Peptidase and protease activities of ShClpP2 compared to ShClpP2$_{ATG2}$.**

A. Suc-LY-AMC (left) and FITC-casein (right) degradation experiments illustrate peptiolytic and proteolytic activities of ShClpP2 compared to ShClpP2$_{ATG2}$, separately or combined with ShClpP1. ClpP wild-type and mutant proteins were employed as indicated. These data confirm the role of ShClpP1 in ADEP-induced Clp-ATPase mediated proteolysis as well as of ShClpP2 for Clp-ATPase binding. Additionally, ShClpP2 and ShClpP2$_{ATG2}$ exhibited comparable activites in both substrate degradation assays. **B-C.** *In vitro* ShClpC2 and ShClpX-mediated substrate degradation of ß-casein, ShClgR or ShPopR by purified ClpP proteins in the presence and absence of ADEP1 is shown. Confirming the results shown above, employing either ShClpP2 or ShClpP2$_{ATG2}$ in combination with ShClpP1 (wild-type or mutant proteins) resulted in comparable proteolytic activities. Of note, accelerated substrate degradation after ADEP1 addition could be observed in samples utilising ShClpP2$_{ATG2}$ as well. All assays were performed at least in biological triplicates and representative SDS-PAGE images are shown. DMSO was used in control reactions. **D:** *In vitro* substrate degradation experiments employing the mutant proteins ShClpP1$_{Y76S}$ and ShClpP2$_{S94Y-ATG2-His}$ in combination with wild-type ShClpP1, ShClpP2 as well as ShClpP2$_{ATG2}$ for the ADEP-induced hydrolysis of the fluorogenic di-peptide Suc-LY-AMC (left) and the ShClpC1-mediated degradation of fluorogenic casein (right). Wild-type ShClpP2 compared to ShClpP2$_{ATG2}$ in combination with ShClpP1 (wild-type or ShClpP1$_{Y76S}$) resulted in comparable peptio-and proteolytic activities. **A + D**: Hydrolysis of Suc-LY-AMC and FITC-casein was recorded as an increase in fluorescence intensity (RFUs) over time. Mean of initial slopes (normalized in %) are shown. Statistics were performed with one-way ANOVA using at least two biological replicates comprising multiple technical replicates. P-values: ns > 0.05; * ≤ 0.05; ** ≤ 0.01; *** ≤ 0.001; **** ≤ 0.0001. Error bars indicate corresponding standard deviations.

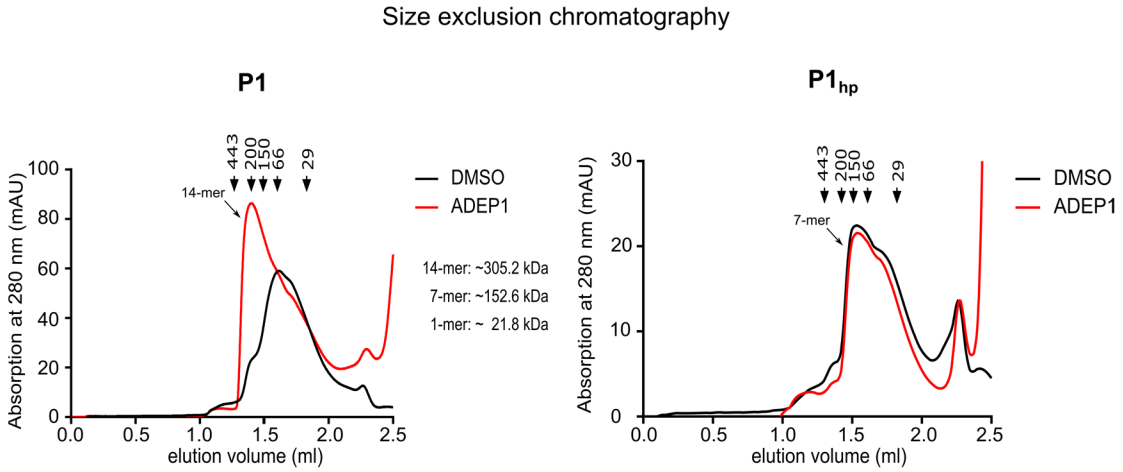

Figure 6.7: **Analytical size exclusion chromatography of native, wild-type ShClpP1 (left) and native ShClpP1$_{hp}$ (right) in the presence and absence of ADEP1 utilising the Superdex^{TM} 200 Increase 3.2 300 column (GE Healthcare).** While equal concentrations of the Clp peptidase and ADEP1 were used (150 µM each) for wild-type ShClpP1, the oligomeric behaviour of the mutant protein ShClpP1$_{hp}$ (80µ) was investigated applying a surplus of ADEP1 (150 µM). Wild-type

ShClpP1 assembled tetradecameric species in high abundance even in the presence of equal concentrations of ShClpP1 and ADEP1. Samples were incubated with ADEP1 or DMSO for 30 min at 30°C prior to the sample application. In contrast, the hydrophobic pocket mutant ShClpP1$_{hp}$ did not assemble into a tetradecamer even in the presence of a surplus of ADEP1, confirming the ADEP-insensitivity of ShClpP1$_{hp}$. Samples comprising the mutant protein ShClpP1$_{hp}$ were incubated with ADEP1 or DMSO for 60 min at 30°C prior to the sample application. The experiments were performed in at least two biological replicates.

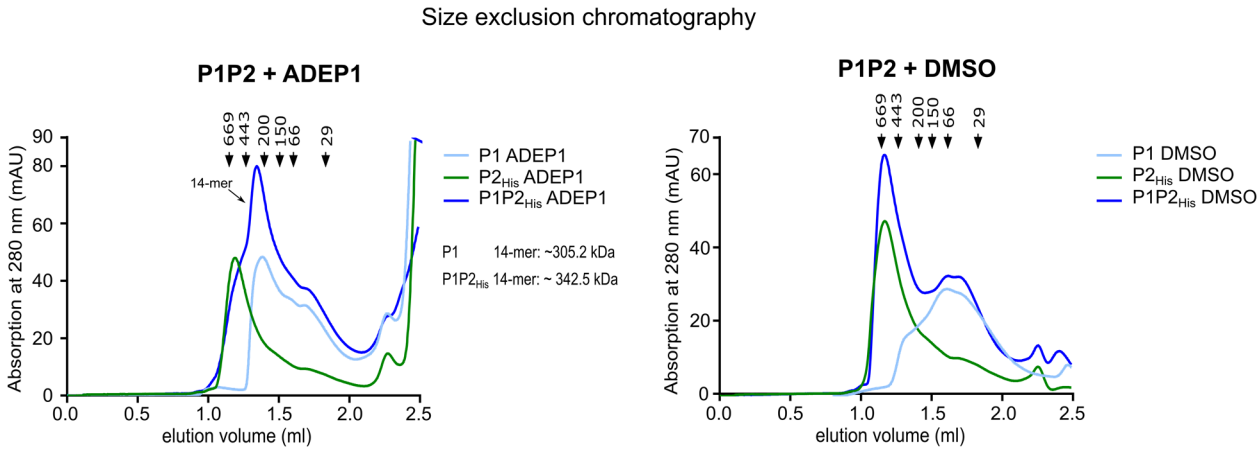

Figure 6.8: **Analytical size exclusion chromatography of mixed ShClpP1P2$_{His}$ (90 µM each) compared to native ShClpP1 (90 µM) and C-terminally His$_6$-tagged ShClpP2 (90µM) which were applied separately to the Superdex^{TM} 200 Increase 3.2 300 gel filtration column in the presence and absence of ADEP1 (200 µM).** Whereas ShClpP2$_{His}$ alone appeared as heptameric states on a native-PAGE, large oligomeric species comprising the size of approximately two tetradecameric complexes (~670 kDa) could be detected in the presence and absence of ADEP1 on the gel filtration column. In contrast, native ShClpP1 eluted mostly as heptameric and lower oligomeric states in the absence of ADEP1, but assembled homo-tetradecameric species after ADEP1 addition. Combining the ClpP isoforms ShClpP1 and ShClpP2$_{His}$ did not change their oligomeric behaviour compared to ShClpP1 or ShClpP2$_{His}$, which were applied separately on the gel filtration column in the absence of ADEP1. However, after ADEP1 addition, tetradecameric species could be detected in a mixed ShClpP1P2$_{His}$ sample, which eluted slightly earlier (after 1.35 ml) than ClpP1 homo-tetradecamers (after 1.39 ml) in the presence of ADEP1, strongly indicating the formation of a heteromeric ShClpP1P2 complex. Samples were incubated for 2 h at 30°C after the addition of ADEP1, prior to the sample application. The experiments are exemplary for at least two biological replicates.

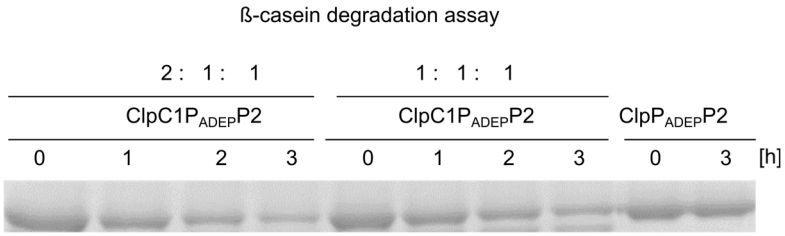

Figure 6.9: **ShClpC1-mediated ß-casein degradation by ShClpP$_{ADEP}$P2 employing different ShClpC1 concentrations (5 µM or 2.5 µM), yielding a ratio of 2:1:1 or 1:1:1 of ShClpC1, ShClpP$_{ADEP}$ and ShClpP2.** Increasing the concentration of ShClpC1 in combination with ShClpP$_{ADEP}$P2 did not stimulate the degradation of ß-casein over time compared to the digestion of casein by ShClpC1P$_{ADEP}$P2 applying equal concentrations of ShClpC1, ShClpP$_{ADEP}$ and ShClpP2 (2.5 µM each). The gel is exemplary for three biological replicates.

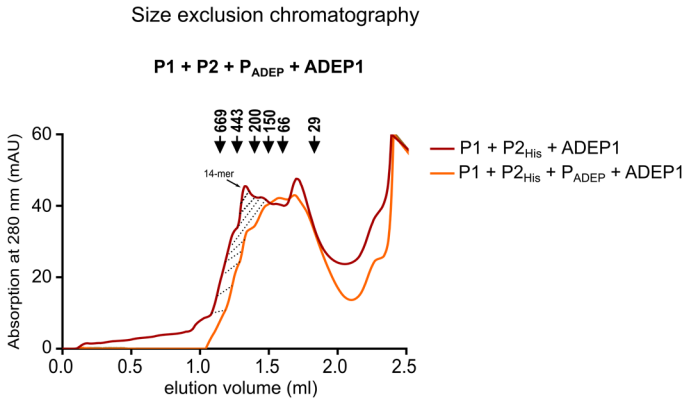

Figure 6.10: **Analytical size exclusion chromatography of ShCpP1 + ShClpP2 + ShClpP$_{ADEP}$ compared to ShClpP1 + ShClpP2 (80 µM each) after ADEP1 addition (320 µM) utilising the Superdex^{TM} 200 3.2 300 gel filtration column.** After the samples were pre-incubated for 24 h at 4°C, ADEP was added and incubated for 30 min at 30°C prior to the sample application. Experiments were performed in at least two biological replicates.

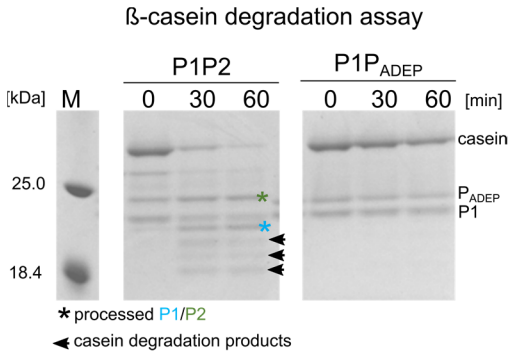

Figure 6.11: **ß-casein degradation by ADEP1-activated ShClpP1P2**. 2 µM of ShClpP1 and ShClpP2 were utilised to digest 10 µM ß-casein in the presence of 30 µM ADEP1. As a negative control, ShClpP$_{ADEP}$ in combination with ShClpP1 (2 µM each) were utilised to digest 10 µM casein after ADEP1 addition (30 µM ADEP1). The SDS-gel is exemplary for at least three biological replicates.

6.2 Nucleotide sequences

6.2.1 pET11a constructs

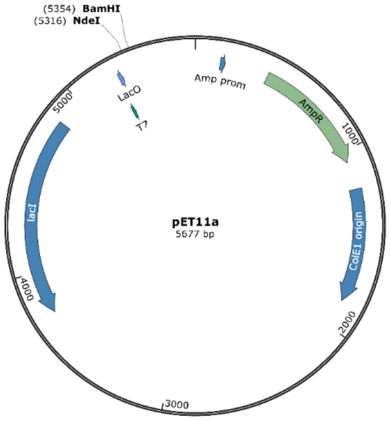

Figure 6.12: **pET11a vector map.**

Nucleotide sequence of the pET11a vector with used resitriction sites in bold and underlined:

ttcttgaagacgaaagggcctcgtgatacgcctatttttataggttaatgtcatgataataatggtttcttagacgtcaggtggcacttttcggggaaatgtgcgcggaa
cccctatttgtttatttttctaaatacattcaaatatgtatccgctcatgagacaataaccctgataaatgcttcaataatattgaaaaaggaagagtatgagtattcaac
atttccgtgtcgcccttattccctttttgcggcattttgccttcctgtttttgctcacccagaaacgctggtgaaagtaaaagatgctgaagatcagttgggtgcacgagt
gggttacatcgaactggatctcaacagcggtaagatccttgagagttttcgccccgaagaacgttttccaatgatgagcacttttaaagttctgctatgtggcgcggtat
tatcccgtgttgacgccgggcaagagcaactcggtcgccgcatacactattctcagaatgacttggttgagtactcaccagtcacagaaaagcatcttacggatggcat
gacagtaagagaattatgcagtgctgccataaccatgagtgataacactgcggccaacttacttctgacaacgatcggaggaccgaaggagctaaccgcttttttgca
caacatgggggatcatgtaactcgccttgatcgttgggaaccggagctgaatgaagccataccaaacgacgagcgtgacaccacgatgcctgcagcaatggcaaca
acgttgcgcaaactattaactggcgaactacttactctagcttcccggcaacaattaatagactggatggaggcggataaagttgcaggaccacttctgcgctcggccc
ttccggctggctggtttattgctgataaatctggagccggtgagcgtgggtctcgcggtatcattgcagcactggggccagatggtaagccctcccgtatcgtagttatc
tacacgacggggagtcaggcaactatggatgaacgaaatagacagatcgctgagataggtgcctcactgattaagcattggtaactgtcagaccaagtttactcatat
atactttagattgatttaaaacttcatttttaatttaaaaggatctaggtgaagatccttttgataatctcatgaccaaaatcccttaacgtgagttttcgttccactgagc
gtcagaccccgtagaaaagatcaaaggatcttcttgagatcctttttttctgcgcgtaatctgctgcttgcaaacaaaaaaaccaccgctaccagcggtggtttgtttgc
cggatcaagagctaccaactctttttccgaaggtaactggcttcagcagagcgcagataccaaatactgtccttctagtgtagccgtagttaggccaccacttcaagaa
ctctgtagcaccgcctacatacctcgctctgctaatcctgttaccagtggctgctgccagtggcgataagtcgtgtcttaccgggttggactcaagacgatagttaccgg
ataaggcgcagcggtcgggctgaacgggggttcgtgcacacagcccagcttggagcgaacgacctacaccgaactgagatacctacagcgtgagctatgagaaa
gcgccacgcttcccgaagggagaaaggcggacaggtatccggtaagcggcagggtcggaacaggagagcgcacgagggagcttccagggggaaacgcctggtat
ctttatagtcctgtcgggtttcgccacctctgacttgagcgtcgatttttgtgatgctcgtcaggggggcggagcctatggaaaaacgccagcaacgcggcctttttacg
gttcctggccttttgctggccttttgctcacatgttctttcctgcgttatcccctgattctgtggataaccgtattaccgcctttgagtgagctgataccgctcgccgcagcc
gaacgaccgagcgcagcgagtcagtgagcgaggaagcggaagagcgcctgatgcggtattttctccttacgcatctgtgcggtatttcacaccgcatatatggtgcac
tctcagtacaatctgctctgatgccgcatagttaagccagtatacactccgctatcgctacgtgactgggtcatggctgcgccccgacacccgccaacacccgctgacg
cgccctgacgggcttgtctgctcccggcatccgcttacagacaagctgtgaccgtctccgggagctgcatgtgtcagaggttttcaccgtcatcaccgaaacgcgcgag
gcagctgcggtaaagctcatcagcgtggtcgtgaagcgattcacagatgtctgcctgttcatccgcgtccagctcgttgagtttctccagaagcgttaatgtctggcttct
gataaagcgggccatgttaagggcggttttttcctgtttggtcactgatgcctccgtgtaagggggatttctgttcatgggggtaatgataccgatgaaacgagagagg
atgctcacgatacgggttactgatgatgaacatgcccggttactggaacgttgtgagggtaaacaactggcggtatggatgcggcgggaccagagaaaaatcactca
gggtcaatgccagcgcttcgttaatacagatgtaggtgttccacagggtagccagcagcatcctgcgatgcagatccggaacataatggtgcagggcgctgacttccg
cgtttccagactttacgaaacacggaaaccgaagaccattcatgttgttgctcaggtcgcagacgttttgcagcagcagtcgcttcacgttcgctcgcgtatcggtgatt
cattctgctaaccagtaaggcaaccccgccagcctagccgggtcctcaacgacaggagcacgatcatgcgcacccgtggccaggacccaacgctgcccgagatgcg
ccgcgtgcggctgctggagatggcggacgcgatggatatgttctgccaagggttggtttgcgcattcacagttctccgcaagaattgattggctccaattcttggagtgg
tgaatccgttagcgaggtgccgccggcttccattcaggtcgaggtggcccggctccatgcaccgcgacgcaacgcggggaggcagacaaggtatagggcggcgcct
acaatccatgccaacccgttccatgtgctcgccgaggcggcataaatcgccgtgacgatcagcggtccagtgatcgaagttaggctggtaagagccgcgagcgatcct
tgaagctgtccctgatggtcgtcatctacctgcctggacagcatggcctgcaacgcgggcatcccgatgccgccggaagcgagaagaatcataatggggaaggccat

ccagcctcgcgtcgcgaacgccagcaagacgtagcccagcgcgtcggccgccatgccggcgataatggcctgcttctcgccgaaacgtttggtggcgggaccagtga
cgaaggcttgagcgagggcgtgcaagattccgaataccgcaagcgacaggccgatcatcgtcgcgctccagcgaaagcggtcctcgccgaaaatgacccagagcgc
tgccggcacctgtcctacgagttgcatgataaagaagacagtcataagtgcggcgacgatagtcatgccccgcgcccaccggaaggagctgactgggttgaaggctc
tcaagggcatcggtcgagatcccggtgcctaatgagtgagctaacttacattaattgcgttgcgctcactgcccgctttccagtcgggaaacctgtcgtgccagctgcat
taatgaatcggccaacgcgcggggagaggcggtttgcgtattgggcgccagggtggtttttcttttcaccagtgagacgggcaacagctgattgcccttcaccgcctgg
ccctgagagagttgcagcaagcggtccacgctggtttgccccagcaggcgaaaatcctgtttgatggtggttaacggcgggatataacatgagctgtcttcggtatcgt
cgtatcccactaccgagatatccgcaccaacgcgcagcccggactcggtaatggcgcgcattgcgcccagcgccatctgatcgttggcaaccagcatcgcagtggga
acgatgccctcattcagcatttgcatggtttgttgaaaaccggacatggcactccagtcgccttcccgttccgctatcggctgaatttgattgcgagtgagatatttatgc
cagccagccagacgcagacgcgccgagacagaacttaatgggcccgctaacagcgcgatttgctggtgacccaatgcgaccagatgctccacgcccagtcgcgtac
cgtcttcatgggagaaaataatactgttgatgggtgtctggtcagagacatcaagaaataacgccggaacattagtgcaggcagcttccacagcaatggcatcctggt
catccagcggatagttaatgatcagcccactgacgcgttgcgcgagaagattgtgcaccgccgctttacaggcttcgacgccgcttcgttctaccatcgacaccaccac
gctggcacccagttgatcggcgcgagatttaatcgccgcgacaatttgcgacggcgcgtgcagggccagactggaggtggcaacgccaatcagcaacgactgtttgc
ccgccagttgttgtgccacgcggttgggaatgtaattcagctccgccatcgccgcttccacttttttcccgcgttttcgcagaaacgtggctggcctggttcaccacgcggg
aaacggtctgataagagacaccggcatactctgcgacatcgtataacgttactggtttcacattcaccaccctgaattgactctcttccgggcgctatcatgccataccg
cgaaaggttttgcgccattcgatggtgtccgggatctcgacgctctcccttatgcgactcctgcattaggaagcagcccagtagtaggttgaggccgttgagcaccgcc
gccgcaaggaatggtgcatgcaaggagatggcgcccaacagtcccccggccacggggcctgccaccatacccacgccgaaacaagcgctcatgagcccgaagtgg
cgagcccgatcttccccatcggtgatgtcggcgatataggcgccagcaaccgcacctgtggcgccggtgatgccggccacgatgcgtccggcgtagaggatcgagat
ctcgatcccgcgaaattaatacgactcactataggggaattgtgagcggataacaattcccctctagaaataattttgtttaactttaagaaggagatata**catatg**gc
tagcatgactggtggacagcaaatgggtcgc**ggatcc**ggctgctaacaaagcccgaaaggaagctgagttggctgctgccaccgctgagcaataactagcataacc
ccttggggcctctaaacgggtcttgaggggttttttgctgaaaggaggaactatatccggatatcccgcaagaggcccggcagtaccggcataaccaagcctatgcct
acagcatccagggtgacggtgccgaggatgacgatgagcgcattgttagatttcatacacggtgcctgactgcgttagcaatttaactgtgataaactaccgcattaaa
gcttatcgatgataagctgtcaaacatgagaa

6.2.1.1 pET11aShclpP1$_{ATG2}$

catatgacgaatctgatgccctcagccgccggcgagccttccatcggtggtggcctcggtgaccaggtctacaaccggctgctcaacgagcggatcatcttcctcggcc
agccggtcgacgacgacatcgcgaacaagatcaccgcacagttgctgctccttgcctccgacccggagaaggacatctacctgtacatcaacagccccggcggttcg
atcacggcgggcatggcgatctacgacaccatgcagtacatcaagaacgacgtggtgaccatcgccatgggcctggcagcctcgatgggccagttcctgctcagcgc
gggcaccccggcaagcgcttcgcgctgccgaacgccgagattctgatccatcagccctccgccggcctcgccggctcggcctcggacatcaagatccacgccgagc
ggctgctgcacaccaagaagcgcatggccgagctgacctcccagcacaccggccagacgatcgagcagatcacccgcgactcggaccgcgaccgctggttcgacgc
cttcgaggccaaggagtacggcctcatcgacgacgtgatgacgacggccgccggtatgccgggcggcggcggcaccggggcctga**ggatcc**

6.2.1.2 pET11aShclpP2

catatgaaccagttccccggcagcgggatctacgaccgtatgcacgccgtgcaggacatgagcgcctcccagggccgctacaccggcccgcaggccgagtcccgcta
catcattccccgcttcgtcgagcgcacctcccagggcatccgcgagtacgacccgtacgcgaagctcttcgaggagcgcgtgatcttcctcggcgtccagatcgacgac
gcctccgccaacgacgtcatggcacagctgctgtgcctggagtcgatggaccccgaccgtgacatctcggtgtacatcaacagccccggcggctccttcacggcgctc
accgcgatctacgacacgatgcagtacgtgaagccggacgtccagacggtctgcatgggccaggcggcctccgccgccgccgtcctgctggccgccggtacgccggg
caagcgcatggccctgccgaacgcgcgtgtgctgatccaccagccgtacagcgagaccggccgcggtcaggtctccgacctggagatcgccgcgaacgagatcctgc
ggatgcgctcgcagctggaggacatgctggccaagcactccaccacgccggtcgagaagatccgcgaggacatcgagcgcgacaagatcctcacggccgaggacg
cgctgagctacggcctgatcgaccaggtcatcagcacccggaagatggacaactcgagcctgcgctga**ggatcc**

6.2.1.3 pET11aShclpP2$_{ATG2}$

catatgagcgcctcccagggccgctacaccggcccgcaggccgagtcccgctacatcattccccgcttcgtcgagcgcacctcccagggcatccgcgagtacgacccg
tacgcgaagctcttcgaggagcgcgtgatcttcctcggcgtccagatcgacgacgcctccgccaacgacgtcatggcacagctgctgtgcctggagtcgatggacccc
gaccgtgacatctcggtgtacatcaacagccccggcggctccttcacggcgctcaccgcgatctacgacacgatgcagtacgtgaagccggacgtccagacggtctgc
atgggccaggcggcctccgccgccgccgtcctgctggccgccggtacgccgggcaagcgcatggccctgccgaacgcgcgtgtgctgatccaccagccgtacagcga
gaccggccgcggtcaggtctccgacctggagatcgccgcgaacgagatcctgcggatgcgctcgcagctggaggacatgctggccaagcactccaccacgccggtc
gagaagatccgcgaggacatcgagcgcgacaagatcctcacggccgaggacgcgctgagctacggcctgatcgaccaggtcatcagcacccggaagatggacaac
tcgagcctgcgctga**ggatcc**

6.2.1.4 pET11aShclgR$_{\text{-N-His6}}$

catatgcaccaccaccaccaccacattctgctccgtcgcctgctgggtgacgtgctgcgtcggcagcgccagcgccagggccgtactctgcgcgaagtctcctcgtccg
cccgagtctcactcggctatctctccgaggtggagcgggggcagaaggaggcttcctccgagctgctctccgccatctgcgacgcgctggacgtacggatgtccgagc
tcatgcgggaagtgagcgacgagctcgccctcgccgagctggcccagtctgctgcggccacccccagcgagcctgtacacacgccggttcgctcgatgctgggctccg
tgtcggtggccggtgtgccaccggaacgggtgaccatcaaggcgcctgccgaagcagtggacgtcgtcgccgcgtga**ggatcc**

6.2.1.5 pET11aShpopR$_{\text{-N-His6}}$

Catatgcaccaccaccaccaccacaccagccacctgccgaacgaagcccgagtcatcccgctgcgcccgcacggcgcgcgtcccaccggcgcaccgccgcgccagg
cgccgccggccccgccgtgaaggagccgctgtggcgggacctggtgggcgacgtcctgcgccgtgaacgcctcgcgcaggagcgcacgttgaaggacgtcgccga
cgaggcgcggatctccatgccctacctctccgaggtggagcgcggccgcaaggaggcctcctccgaggtcctcgcggccgccgcccacgccctcggactgaacctcg
gcgacctgctgacgagggcgcagggcgaactgacccgcgtcacgtcgcgctacgcgggcggcagccgccgcggggcggccacctcgtcgcacgacggaatgtgcct
ggccgcctga**ggatcc**

6.2.1.6 pET11aShclpP1$_{hp}$

catatgacgaatctgatgccctcagccgccggcgagccttccatcggtggtggcctcggtgaccaggtctacaaccggctgctcaacgagcggatcatcttcctcggcc
agccggtcgacgacgacatcgcgaacaagatcaccgcacagttgctgctccttgcctccgacccggagaaggacatc**gt**cctg**gt**catcaacagccccggcggttcg
atcacggcgggcatggcgatctacgacaccatgcag**gt**catcaagaacgacgtggtgaccatcgccatgggcctggcagcctcgatgggccagttcctgctcagcgc
gggcacccccggcaagcgcttcgcgctgccgaacgccgagattctgatccatcagccctccgccggcctcgccggctcggcctcggacatcaagatccacgccgagc
ggctgctgcacaccaagaagcgcatggccgagctgacctcccagcacaccggccagacgatcgagcagatcacccgcgactcggaccgcgaccgctggttcgacgc
cttcgaggccaaggagtacggcctcatcgacgacgtgatgacgacggccgccggtatgccgggcggcggcggcaccggggcctga**ggatcc**

A site directed mutagenesis was performed, utilising pET11aShclpP1 as template. The exchanged nucleotides are bold and marked in yellow.

6.2.1.7 pET11aShclpP1$_{Y76SATG2\text{-}His6}$

catatgacgaatctgatgccctcagccgccggcgagccttccatcggtggtggcctcggtgaccaggtctacaaccggctgctcaacgagcggatcatcttcctcggcc
agccggtcgacgacgacatcgcgaacaagatcaccgcacagttgctgctccttgcctccgacccggagaaggacatct**c**cctgtacatcaacagccccggcggttcg
atcacggcgggcatggcgatctacgacaccatgcagtacatcaagaacgacgtggtgaccatcgccatgggcctggcagcctcgatgggccagttcctgctcagcgc
gggcacccccggcaagcgcttcgcgctgccgaacgccgagattctgatccatcagccctccgccggcctcgccggctcggcctcggacatcaagatccacgccgagc
ggctgctgcacaccaagaagcgcatggccgagctgacctcccagcacaccggccagacgatcgagcagatcacccgcgactcggaccgcgaccgctggttcgacgc
cttcgaggccaaggagtacggcctcatcgacgacgtgatgacgacggccgccggtatgccgggcggcggcggcaccggggcctga**ggatcc**

6.2.2 pET22b constructs

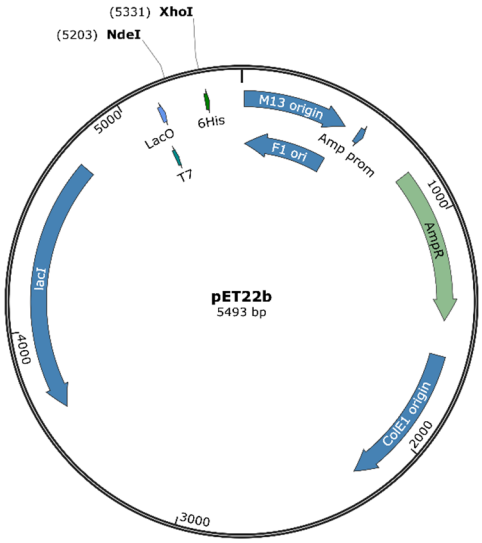

Figure 6.13: **pET22b vector map.**

Nucleotide sequence of the pET22b vector with used resitriction sites in bold and underlined:

tggcgaatgggacgcgccctgtagcggcgcattaagcgcggcgggtgtggtggttacgcgcagcgtgaccgctacacttgccagcgccctagcgcccgctcctttcgc
tttcttcccttcctttctcgccacgttcgccggctttccccgtcaagctctaaatcgggggctccctttagggttcgatttagtgctttacggcacctcgaccccaaaaaa
cttgattagggtgatggttcacgtagtgggccatcgccctgatagacggtttttcgccctttgacgttggagtccacgttctttaatagtggactcttgttccaaactggaa
caacactcaaccctatctcggtctattcttttgatttataagggattttgccgatttcggcctattggttaaaaaatgagctgatttaacaaaaatttaacgcgaattttaa
caaaatattaacgtttacaatttcaggtggcacttttcggggaaatgtgcgcggaacccctatttgtttatttttctaaatacattcaaatatgtatccgctcatgagaca
ataaccctgataaatgcttcaataatattgaaaaaggaagagtatgagtattcaacatttccgtgtcgcccttattcccttttttgcggcattttgccttcctgtttttgctc
acccagaaacgctggtgaaagtaaaagatgctgaagatcagttgggtgcacgagtgggttacatcgaactggatctcaacagcggtaagatccttgagagttttcgc
cccgaagaacgttttccaatgatgagcacttttaaagttctgctatgtggcgcggtattatcccgtattgacgccgggcaagagcaactcggtcgccgcatacactattc
tcagaatgacttggttgagtactcaccagtcacagaaaagcatcttacggatggcatgacagtaagagaattatgcagtgctgccataaccatgagtgataacactgc
ggccaacttacttctgacaacgatcggaggaccgaaggagctaaccgcttttttgcacaacatgggggatcatgtaactcgccttgatcgttgggaaccggagctgaa
tgaagccataccaaacgacgagcgtgacaccacgatgcctgcagcaatggcaacaacgttgcgcaaactattaactggcgaactacttactctagcttcccggcaac
aattaatagactggatggaggcggataaagttgcaggaccacttctgcgctcggcccttccggctggctggtttattgctgataaatctggagccggtgagcgtgggtc
tcgcggtatcattgcagcactggggccagatggtaagccctcccgtatcgtagttatctacacgacggggagtcaggcaactatggatgaacgaaatagacagatcg
ctgagataggtgcctcactgattaagcattggtaactgtcagaccaagtttactcatatatactttagattgatttaaaacttcatttttaatttaaaaggatctaggtga
agatccttttgataatctcatgaccaaaatcccttaacgtgagttttcgttccactgagcgtcagaccccgtagaaaagatcaaaggatcttcttgagatcctttttttct
gcgcgtaatctgctgcttgcaaacaaaaaaaccaccgctaccagcggtggtttgtttgccggatcaagagctaccaactcttttccgaaggtaactggcttcagcaga
gcgcagataccaaatactgtccttctagtgtagccgtagttaggccaccacttcaagaactctgtagcaccgcctacatacctcgctctgctaatcctgttaccagtggc
tgctgccagtggcgataagtcgtgtcttaccgggttggactcaagacgatagttaccggataaggcgcagcggtcgggctgaacgggggttcgtgcacacagccca
gcttggagcgaacgacctacaccgaactgagatacctacagcgtgagctatgagaaagcgccacgcttcccgaagggagaaaggcggacaggtatccggtaagcg
gcagggtcggaacaggagagcgcacgagggagcttccagggggaaacgcctggtatctttatagtcctgtcgggtttcgccacctctgacttgagcgtcgatttttgtg
atgctcgtcaggggggcggagcctatggaaaaacgccagcaacgcggccttttacggttcctggccttttgctggccttttgctcacatgttctttcctgcgttatcccct
gattctgtggataaccgtattaccgcctttgagtgagctgataccgctcgccgcagccgaacgaccgagcgcagcgagtcagtgagcgaggaagcggaagagcgcct
gatgcggtattttctccttacgcatctgtgcggtatttcacaccgcatatatggtgcactctcagtacaatctgctctgatgccgcatagttaagccagtatacactccgct
atcgctacgtgactgggtcatggctgcgccccgacacccgccaacacccgctgacgcgccctgacgggcttgtctgctcccggcatccgcttacagacaagctgtgac
cgtctccgggagctgcatgtgtcagaggttttcaccgtcatcaccgaaacgcgcgaggcagctgcggtaaagctcatcagcgtggtcgtgaagcgattcacagatgtc

tgcctgttcatccgcgtccagctcgttgagtttctccagaagcgttaatgtctggcttctgataaagcgggccatgttaagggcggttttttcctgtttggtcactgatgcct
ccgtgtaaggggatttctgttcatgggggtaatgataccgatgaaacgagagaggatgctcacgatacgggttactgatgatgaacatgcccggttactggaacgtt
gtgagggtaaacaactggcggtatggatgcggcgggaccagagaaaaatcactcagggtcaatgccagcgcttcgttaatacagatgtaggtgttccacagggtagc
cagcagcatcctgcgatgcagatccggaacataatggtgcagggcgctgacttccgcgtttccagactttacgaaacacggaaaccgaagaccattcatgttgttgct
caggtcgcagacgttttgcagcagcagtcgcttcacgttcgctcgcgtatcggtgattcattctgctaaccagtaaggcaaccccgccagcctagccgggtcctcaacg
acaggagcacgatcatgcgcacccgtggggccgccatgccggcgataatggcctgcttctcgccgaaacgtttggtggcgggaccagtgacgaaggcttgagcgagg
gcgtgcaagattccgaataccgcaagcgacaggccgatcatcgtcgcgctccagcgaaagcggtcctcgccgaaaatgacccagagcgctgccggcacctgtcctac
gagttgcatgataaagaagacagtcataagtgcggcgacgatagtcatgccccgcgcccaccggaaggagctgactgggttgaaggctctcaagggcatcggtcga
gatcccggtgcctaatgagtgagctaacttacattaattgcgttgcgctcactgcccgctttccagtcgggaaacctgtcgtgccagctgcattaatgaatcggccaacg
cgcggggagaggcggtttgcgtattgggcgccagggtggttttttcttttcaccagtgagacgggcaacagctgattgcccttcaccgcctggccctgagagagttgcag
caagcggtccacgctggtttgccccagcaggcgaaaatcctgtttgatggtggttaacggcgggatataacatgagctgtcttcggtatcgtcgtatcccactaccgag
atatccgcaccaacgcgcagcccggactcggtaatggcgcgcattgcgcccagcgccatctgatcgttggcaaccagcatcgcagtgggaacgatgccctcattcagc
atttgcatggtttgttgaaaaccggacatggcactccagtcgccttcccgttccgctatcggctgaatttgattgcgagtgagatatttatgccagccagccagacgcag
acgcgccgagacagaacttaatgggcccgctaacagcgcgatttgctggtgacccaatgcgaccagatgctccacgcccagtcgcgtaccgtcttcatgggagaaaa
taatactgttgatgggtgtctggtcagagacatcaagaaataacgccggaacattagtgcaggcagcttccacagcaatggcatcctggtcatccagcggatagttaa
tgatcagcccactgacgcgttgcgcgagaagattgtgcaccgccgctttacaggcttcgacgccgcttcgttctaccatcgacaccaccacgctggcacccagttgatc
ggcgcgagatttaatcgccgcgacaatttgcgacggcgcgtgcagggccagactggaggtggcaacgccaatcagcaacgactgtttgcccgccagttgttgtgcca
cgcggttgggaatgtaattcagctccgccatcgccgcttccacttttcccgcgttttcgcagaaacgtggctggcctggttcaccacgcgggaaacggtctgataagag
acaccggcatactctgcgacatcgtataacgttactggtttcacattcaccaccctgaattgactctcttccgggcgctatcatgccataccgcgaaaggttttgcgccat
tcgatggtgtccgggatctcgacgctctcccttatgcgactcctgcattaggaagcagcccagtagtaggttgaggccgttgagcaccgccgccgcaaggaatggtgc
atgcaaggagatggcgcccaacagtccccggccacggggcctgccaccatacccacgccgaaacaagcgctcatgagcccgaagtggcgagcccgatcttcccca
tcggtgatgtcggcgatataggcgccagcaaccgcacctgtggcgccggtgatgccggccacgatgcgtccggcgtagaggatcgagatctcgatcccgcgaaatta
atacgactcactataggggaattgtgagcggataacaattcccctctagaaataattttgtttaactttaagaaggagatata**catatg**aaatacctgctgccgaccgc
tgctgctggtctgctgctcctcgctgcccagccggcgatggccatggatatcggaattaattcggatccgaattcgagctccgtcgacaagcttgcggccgca**ctcgag**
caccaccaccaccaccactgagatccggctgctaacaaagcccgaaaggaagctgagttggctgctgccaccgctgagcaataactagcataaccccttggggcctc
taaacgggtcttgaggggttttttgctgaaaggaggaactatatccggat

6.2.2.1 pET22bShclpP1$_{ATG2\text{-}His6}$

catatgacgaatctgatgccctcagccgccggcgagccttccatcggtggtggcctcggtgaccaggtctacaaccggctgctcaacgagcggatcatcttcctcggcc
agccggtcgacgacgacatcgcgaacaagatcaccgcacagttgctgctccttgcctccgacccggagaaggacatctacctgtacatcaacagccccggcggttcg
atcacggcgggcatggcgatctacgacaccatgcagtacatcaagaacgacgtggtgaccatcgccatgggcctggcagcctcgatgggccagttcctgctcagcgc
gggcacccccggcaagcgcttcgcgctgccgaacgccgagattctgatccatcagccctccgccggcctcgccggctcggcctcggacatcaagatccacgccgagc
ggctgctgcacaccaagaagcgcatggccgagctgacctcccagcacaccggccagacgatcgagcagatcacccgcgactcggaccgcgaccgctggttcgacgc
cttcgaggccaaggagtacggcctcatcgacgacgtgatgacgacggccgccggtatgccgggcggcggcggcaccgggggcc**ctcgag**caccaccaccaccaccac
tga

6.2.2.2 pET22bShclpP1*$_{\text{-}His6}$

catatgccttccatcggtggtggcctcggtgaccaggtctacaaccggctgctcaacgagcggatcatcttcctcggccagccggtcgacgacgacatcgcgaacaag
atcaccgcacagttgctgctccttgcctccgacccggagaaggacatctacctgtacatcaacagccccggcggttcgatcacggcgggcatggcgatctacgacacc
atgcagtacatcaagaacgacgtggtgaccatcgccatgggcctggcagcctcgatgggccagttcctgctcagcgcgggcacccccggcaagcgcttcgcgctgcc
gaacgccgagattctgatccatcagccctccgccggcctcgccggctcggcctcggacatcaagatccacgccgagcggctgctgcacaccaagaagcgcatggccg
agctgacctcccagcacaccggccagacgatcgagcagatcacccgcgactcggaccgcgaccgctggttcgacgccttcgaggccaaggagtacggcctcatcga
cgacgtgatgacgacggccgccggtatgccgggcggcggcggcaccggggcc**ctcgag**caccaccaccaccaccactga

6.2.2.3 pET22bShclpC2$_{\text{-}His6}$

This construct was cloned by Denjiel Latifovic.

catatgagcagcggcttcaccagcccggagggctacggctcggatcccttcggagaattcctcgcacgcttcttcggcggaccgcgtcccggtccccggcagatcgat
ctcgggcggctgctcagtcagccggcccgggagctcgtccgcggcgccgcccagtacgccgccgagcacggcagccgggacctcgacacgcagcatctgctgcggg
cggcgctcgccaccgagcccacccgcaccctgctcagcaaggccggcgcgaatcccgactcactggcgtcgcagatcgacgaccggtcgggacccgcccagcacac
gccggacgacgctcccccacccaccgccctctccctcaccccggccgccaagcgggccctgctggacgcgcacgacatggcccgggcccgcggctacggctacatcg
gcccggagcacgtgctgagcgccctggcgtcgaaccccgactcggccgccgggcacatcctcaacgcggcccgcttcgccccctccgaaccgcccgaggcgccggag
atgccccagtccgagcgcccgcgcccgacgaacacgcccaccctcgacaagtacggccgtgacctcaccgagctggcccggcagggccggatcgacccggtgatcg
gccgggacgaggagatcgagcagaccgtcgaggtcctctcccggcgcggcaagaacaacccggtgctcatcggtgacgcgggcgtcggcaagacggccatcgtgg
aggggctggcgcagcgcatctccgaggcggacgtgcccgacgtgctgatcgggcgccgcgtggtcgccctggacctgacgggagtggtcgcgggcacccgctaccg
gggtgacttcgaggagcggatgaacaacatcgtgggcgagatccgcgcccactccgaccagctgatcatcttcatcgacgagctgcacacggtcgtgggcgccgggt
ccggtggcggcgacggcagctcgatggacgccggcaacatcctcaagccggccctggcccggggcgagctgcacatcgtgggcgccaccacgctggaggagtaccg
ccggatcgagaaggacgcggcgctggcccgccgcttccagccgatcatggtgccggagccgaccgccgcggacgcgatcgagatcctgcgcggcctgcaggaccgc
tacgaggcccaccaccaggtccgctacaccgacgaggccctggtcacggccgtggagctgtcggaccgctacctcaccgcccgccgtctgcccgacaaggcgatcga
cctgatcgaccaggccggtgcccgggtgcggctgcgggcccggaccaagggcacggacgtgcgggccctggagcgggagctggagcagctgacccgggacaagga
ccaggcggtcgcggacgagagttacgagcaagccacccagttgcgcgaccggatcgtggacgtgaagcagcggatcaccgcggccggcggcgatggcgaggtcga
cgagggccaggacctggtggtcggggccgaggcgatcgccgaggtggtgtcccggcagaccggcatcccggtcagcagcctcacccaggaggagaaggaccgtttg
ctgggcctggaggagcatctgcaccagcgggtggtcggccaggacgaggccgtgcgggtcgtctcggacgcggtgctgcgctcccgcgccgggctcgcgtctcccga
ccggccgatcggcagtttcctgttcctcggcccgacgggcgtcggcaagaccgaactggcccgggcgctcgccgaggccctgttcggcagcgaggaccgcatggtcc
gcctcgacatgagcgagtaccaggagcggcacaccgtcagccggctgatcggcgcccgcccggttacgtcggccacgaggaggcgggccagctcaccgaggtcgt
gcgccgccacccgtactcgctgctcctgctggacgaggtggagaaggcccacccggacgtcttcaacatcctgctccaggtcctcgacgacggccggctgaccgactc
gcagggccgcacggtggacttcagcaacacggtcatcgtgatgacgagcaacctcggctccgaggcgatcacccgccggggcgccacgacgggcttcgcggcgggc
ggcgccgacgcggacgaggaggcccgccgcgagcagatcctgcgcccgctgcgcgagcacttccgccccgagttcctcaaccgcatcgacgagatcgtcgtcttccg
ccagctcaccacggagcaactgcgccggatcaccaacctcctgctggaccgcacccgctccctggtgcagagcaagggcgtcacggtgaccttcaccgaccgggcgg
tggagtggctggccgagcgcggttaccaaccggagtacggcgcccgcccgctccgccgcacgatccagcgcgaggtggacaacgagctgtcacgactgctgctgga
cggcagggtggaggagaacggccgggtgacggtggacgtggaggacggccatctcgcgttcagtaccgtgccccga**ctcgag**caccaccaccaccaccaccactga

6.2.2.4 pET22bShclpP1$_{S113A}$

catatgacgaatctgatgccctcagccgccggcgagccttccatcggtggtggcctcggtgaccaggtctacaaccggctgctcaacgagcggatcatcttcctcggcc
agccggtcgacgacgacatcgcgaacaagatcaccgcacagttgctgctccttgcctccgacccggagaaggacatctacctgtacatcaacagccccggcggttcg
atcacggcgggcatggcgatctacgacaccatgcagtacatcaagaacgacgtggtgaccatcgccatgggcctggcagcc**g**cgatgggccagttcctgctcagcgc
gggcacccccggcaagcgcttcgcgctgccgaacgccgagattctgatccatcagccctccgccggcctcgccggctcggcctcggacatcaagatccacgccgagc
ggctgctgcacaccaagaagcgcatggccgagctgacctcccagcacaccggccagacgatcgagcagatcacccgcgactcggaccgcgaccgctggttcgacgc
cttcgaggccaaggagtacggcctcatcgacgacgtgatgacgacggccgccggtatgccgggcggcggcggcaccgggggcc**ctcgag**caccaccaccaccaccac
tga

A site directed mutagenesis was performed, utilising pET22bShclpP1$_{-His}$ as template. The exchanged nucleotide is bold and marked in yellow.

6.2.2.5 pET22bShclpP$_{ADEP-His6}$

Catatgaaggacattaaggaactgacgggtcgcaccctcggcgcatcacggtggaacctgaacgaccaggtaatgcatcgcctcatggacgagcgtattattatgct
gggtcaagaggtcgatgacgccggaagcaatgcgatttgctcgcaactgcttctgttggcaggagattcccctcgcgacatcagcctttatatcaactcaccgggtggg
tccgtcaccgcgggaatggctatctacgacaccatgaactacatcgagaacgatgtagtcacagtagcgatggggaccgcagcctcgatgggccaattcctcctgact
gcgggcaccccaggcaagcgcatcgttctgcctcatgcggaaatcctcatgcaccagccctctgccggtctcggcggctctgccagtgacatcaagattcatgccgag
cgactcattcgtgtcaaaaagcgcatgattgacatcacggctcagcacaccggacggactgtcgaggagattaagcgggattcagaccgcgacaggtggttctccgc
tgacgaagcagtcgagtacggcctcgccgacagggttgaatatgtagccgctaccgttcctggcaatatcggggcagcgaag**ctcgag**caccaccaccaccaccact
ga

6.2.2.6 pET22bShclpP$_{ADEP\text{-}short\text{-}His}$

catatgcggtggaacctgaacgaccaggtaatgcatcgcctcatggacgagcgtattattatgctgggtcaagaggtcgatgacgccggaagcaatgcgatttgctcg
caactgcttctgttggcaggagattcccctcgcgacatcagcctttatatcaactcaccgggtgggtccgtcaccgcgggaatggctatctacgacaccatgaactaca
tcgagaacgatgtagtcacagtagcgatggggaccgcagcctcgatgggccaattcctcctgactgcgggcaccccaggcaagcgcatcgttctgcctcatgcggaa
atcctcatgcaccagccctctgccggtctcggcggctctgccagtgacatcaagattcatgccgagcgactcattcgtgtcaaaaagcgcatgattgacatcacggctc
agcacaccggacggactgtcgaggagattaagcgggattcagaccgcgacaggtggttctccgctgacgaagcagtcgagtacggcctcgccgacagggttgaata
tgtagccgctaccgttcctggcaatatcggggcagcgaag**ctcgag**caccaccaccaccaccactga

6.2.3 pET22b*_Nco_I constructs

This vector was constructed by Janna Hauser, in which the *Xho*I restriction site was exchanged by a *Nco*I restriction site utilising pET22b as template.

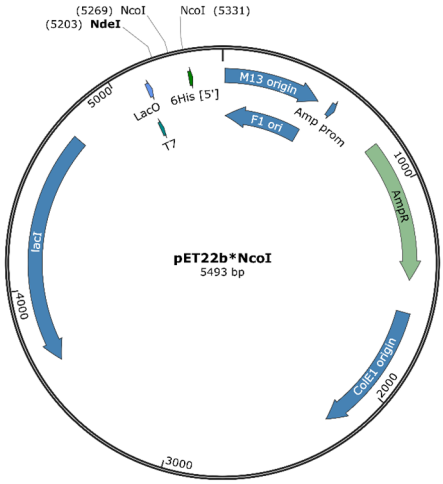

Figure 6.14: **pET22b*_Nco_I vector map.**

Nucleotide sequence of the pET22b*_Nco_I vector with used resitriction sites in bold and underlined:

tggcgaatgggacgcgccctgtagcggcgcattaagcgcggcgggtgtggtggttacgcgcagcgtgaccgctacacttgccagcgccctagcgcccgctcctttcgc
tttcttcccttcctttctcgccacgttcgccggctttccccgtcaagctctaaatcgggggctccctttagggttccgatttagtgctttacggcacctcgaccccaaaaaa
cttgattagggtgatggttcacgtagtgggccatcgccctgatagacggtttttcgccctttgacgttggagtccacgttctttaatagtggactcttgttccaaactggaa
caacactcaaccctatctcggtctattcttttgatttataagggattttgccgatttcggcctattggttaaaaaatgagctgatttaacaaaaatttaacgcgaattttaa
caaaatattaacgtttacaatttcaggtggcacttttcggggaaatgtgcgcggaacccctatttgtttatttttctaaatacattcaaatatgtatccgctcatgagaca
ataaccctgataaatgcttcaataatattgaaaaaggaagagtatgagtattcaacatttccgtgtcgcccttattcccttttttgcggcattttgccttcctgtttttgctc
acccagaaacgctggtgaaagtaaaagatgctgaagatcagttgggtgcacgagtgggttacatcgaactggatctcaacagcggtaagatccttgagagttttcgc
cccgaagaacgttttccaatgatgagcacttttaaagttctgctatgtggcgcggtattatcccgtattgacgccgggcaagagcaactcggtcgccgcatacactattc
tcagaatgacttggttgagtactcaccagtcacagaaaagcatcttacggatggcatgacagtaagagaattatgcagtgctgccataaccatgagtgataacactgc
ggccaacttacttctgacaacgatcggaggaccgaaggagctaaccgcttttttgcacaacatgggggatcatgtaactcgccttgatcgttgggaaccggagctgaa
tgaagccataccaaacgacgagcgtgacaccacgatgcctgcagcaatggcaacaacgttgcgcaaactattaactggcgaactacttactctagcttcccggcaac
aattaatagactggatggaggcggataaagttgcaggaccacttctgcgctcggcccttccggctggctggtttattgctgataaatctggagccggtgagcgtgggtc
tcgcggtatcattgcagcactggggccagatggtaagccctcccgtatcgtagttatctacacgacggggagtcaggcaactatggatgaacgaaatagacagatcg
ctgagataggtgcctcactgattaagcattggtaactgtcagaccaagtttactcatatatactttagattgatttaaaacttcatttttaatttaaaaggatctaggtga

agatccttttgataatctcatgaccaaaatcccttaacgtgagttttcgttccactgagcgtcagaccccgtagaaaagatcaaaggatcttcttgagatccttttttttct
gcgcgtaatctgctgcttgcaaacaaaaaaaccaccgctaccagcggtggtttgtttgccggatcaagagctaccaactctttttccgaaggtaactggcttcagcaga
gcgcagataccaaatactgtccttctagtgtagccgtagttaggccaccacttcaagaactctgtagcaccgcctacatacctcgctctgctaatcctgttaccagtggc
tgctgccagtggcgataagtcgtgtcttaccgggttggactcaagacgatagttaccggataaggcgcagcggtcgggctgaacgggggttcgtgcacacagccca
gcttggagcgaacgacctacaccgaactgagatacctacagcgtgagctatgagaaagcgccacgcttcccgaagggagaaaggcggacaggtatccggtaagcg
gcagggtcggaacaggagagcgcacgagggagcttccagggggaaacgcctggtatctttatagtcctgtcgggtttcgccacctctgacttgagcgtcgatttttgtg
atgctcgtcaggggggcggagcctatggaaaaacgccagcaacgcggccttttacggttcctggccttttgctggccttttgctcacatgttctttcctgcgttatcccct
gattctgtggataaccgtattaccgcctttgagtgagctgataccgctcgccgcagccgaacgaccgagcgcagcgagtcagtgagcgaggaagcggaagagcgcct
gatgcggtattttctccttacgcatctgtgcggtatttcacaccgcatatatggtgcactctcagtacaatctgctctgatgccgcatagttaagccagtatacactccgct
atcgctacgtgactgggtcatggctgcgccccgacacccgccaacacccgctgacgcgccctgacgggcttgtctgctcccggcatccgcttacagacaagctgtgac
cgtctccgggagctgcatgtgtcagaggttttcaccgtcatcaccgaaacgcgcgaggcagctgcggtaaagctcatcagcgtggtcgtgaagcgattcacagatgtc
tgcctgttcatccgcgtccagctcgttgagtttctccagaagcgttaatgtctggcttctgataaagcgggccatgttaagggcggttttttcctgtttggtcactgatgcct
ccgtgtaaggggatttctgttcatgggggtaatgataccgatgaaacgagagaggatgctcacgatacgggttactgatgatgaacatgcccggttactggaacgtt
gtgagggtaaacaactggcggtatggatgcggcgggaccagagaaaaatcactcagggtcaatgccagcgcttcgttaatacagatgtaggtgttccacagggtagc
cagcagcatcctgcgatgcagatccggaacataatggtgcagggcgctgacttccgcgtttccagactttacgaaacacggaaaccgaagaccattcatgttgttgct
caggtcgcagacgttttgcagcagcagtcgcttcacgttcgctcgcgtatcggtgattcattctgctaaccagtaaggcaaccccgccagcctagccgggtcctcaacg
acaggagcacgatcatgcgcacccgtggggccgccatgccggcgataatggcctgcttctcgccgaaacgtttggtggcgggaccagtgacgaaggcttgagcgagg
gcgtgcaagattccgaataccgcaagcgacaggccgatcatcgtcgcgctccagcgaaagcggtcctcgccgaaaatgacccagagcgctgccggcacctgtcctac
gagttgcatgataaagaagacagtcataagtgcggcgacgatagtcatgccccgcgcccaccggaaggagctgactgggttgaaggctctcaagggcatcggtcga
gatcccggtgcctaatgagtgagctaacttacattaattgcgttgcgctcactgcccgctttccagtcgggaaacctgtcgtgccagctgcattaatgaatcggccaacg
cgcggggagaggcggtttgcgtattgggcgccagggtggttttttcttttcaccagtgagacgggcaacagctgattgcccttcaccgcctggccctgagagagttgcag
caagcggtccacgctggtttgccccagcaggcgaaaatcctgtttgatggtggttaacggcgggatataacatgagctgtcttcggtatcgtcgtatcccactaccgag
atatccgcaccaacgcgcagcccggactcggtaatggcgcgcattgcgcccagcgccatctgatcgttggcaaccagcatcgcagtgggaacgatgccctcattcagc
atttgcatggtttgttgaaaaccggacatggcactccagtcgccttcccgttccgctatcggctgaatttgattgcgagtgagatatttatgccagccagccagacgcag
acgcgccgagacagaacttaatgggcccgctaacagcgcgatttgctggtgacccaatgcgaccagatgctccacgcccagtcgcgtaccgtcttcatgggagaaaa
taatactgttgatgggtgtctggtcagagacatcaagaaataacgccggaacattagtgcaggcagcttccacagcaatggcatcctggtcatccagcggatagttaa
tgatcagcccactgacgcgttgcgcgagaagattgtgcaccgccgctttacaggcttcgacgccgcttcgttctaccatcgacaccaccacgctggcacccagttgatc
ggcgcgagatttaatcgccgcgacaatttgcgacggcgcgtgcagggccagactggaggtggcaacgccaatcagcaacgactgtttgcccgccagttgttgtgcca
cgcggttgggaatgtaattcagctccgccatcgccgcttccacttttcccgcgttttcgcagaaacgtggctggcctggttcaccacgcgggaaacggtctgataagag
acaccggcatactctgcgacatcgtataacgttactggtttcacattcaccaccctgaattgactctcttccgggcgctatcatgccataccgcgaaaggttttgcgccat
tcgatggtgtccgggatctcgacgctctcccttatgcgactcctgcattaggaagcagcccagtagtaggttgaggccgttgagcaccgccgccgcaaggaatggtgc
atgcaaggagatggcgcccaacagtccccggccacggggcctgccaccatacccacgccgaaacaagcgctcatgagcccgaagtggcgagcccgatcttcccca
tcggtgatgtcggcgatataggcgccagcaaccgcacctgtggcgccggtgatgccggccacgatgcgtccggcgtagaggatcgagatctcgatcccgcgaaatta
atacgactcactatagggaattgtgagcggataacaattcccctctagaaataattttgtttaactttaagaaggagatata**catatg**aaatacctgctgccgaccgc
tgctgctggtctgctgctcctcgctgcccagccggcgatggccatggatatcggaattaattcggatccgaattcgagctccgtcgacaagcttgcggccgca**ccatgg**
caccaccaccaccaccactgagatccggctgctaacaaagcccgaaaggaagctgagttggctgctgccaccgctgagcaataactagcataacccccttggggcctc
taaacgggtcttgaggggttttttgctgaaaggaggaactatatccggat

6.2.3.1 pET22b*_Nco_I-ShclpP2$_{\text{-His6}}$

catatgaaccagttccccggcagcgggatctacgaccgtatgcacgccgtgcaggacatgagcgcctcccagggccgctacaccggcccgcaggccgagtcccgcta
catcattccccgcttcgtcgagcgcacctcccagggcatccgcgagtacgacccgtacgcgaagctcttcgaggagcgcgtgatcttcctcggcgtccagatcgacgac
gcctccgccaacgacgtcatggcacagctgctgtgcctggagtcgatggaccccgaccgtgacatctcggtgtacatcaacagccccggcggctccttcacggcgctc
accgcgatctacgacacgatgcagtacgtgaagccggacgtccagacggtctgcatgggccaggcggcctccgccgccgccgtcctgctggccgccggtacgccggg
caagcgcatggccctgccgaacgcgcgtgtgctgatccaccagccgtacagcgagaccggccgcggtcaggtctccgacctggagatcgccgcgaacgagatcctgc
ggatgcgctcgcagctggaggacatgctggccaagcactccaccacgccggtcgagaagatccgcgaggacatcgagcgcgacaagatcctcacggccgaggacg
cgctgagctacggcctgatcgaccaggtcatcagcacccggaagatggacaactcgagcctgcgc**ccatgg**caccaccaccaccaccactga

6.2.3.2 pET22b*_Nco_I-ShclpP2$_{ATG2\text{-}His6}$

catatgagcgcctcccagggccgctacaccggcccgcaggccgagtcccgctacatcattccccgcttcgtcgagcgcacctcccagggcatccgcgagtacgacccg
tacgcgaagctcttcgaggagcgcgtgatcttcctcggcgtccagatcgacgacgcctccgccaacgacgtcatggcacagctgctgtgcctggagtcgatggacccc
gaccgtgacatctcggtgtacatcaacagccccggcggctccttcacggcgctcaccgcgatctacgacacgatgcagtacgtgaagccggacgtccagacggtctgc
atgggccaggcggcctccgccgccgccgtcctgctggccgccggtacgccgggcaagcgcatggccctgccgaacgcgcgtgtgctgatccaccagccgtacagcga
gaccggccgcggtcaggtctccgacctggagatcgccgcgaacgagatcctgcggatgcgctcgcagctggaggacatgctggccaagcactccaccacgccggtc
gagaagatccgcgaggacatcgagcgcgacaagatcctcacggccgaggacgcgctgagctacggcctgatcgaccaggtcatcagcacccggaagatggacaac
tcgagcctgcgc**ccatgg**caccaccaccaccaccactga

6.2.3.3 pET22b*_Nco_I-ShclpP2*$_{\text{-}His6}$

catatgcgctacatcattccccgcttcgtcgagcgcacctcccagggcatccgcgagtacgacccgtacgcgaagctcttcgaggagcgcgtgatcttcctcggcgtcc
agatcgacgacgcctccgccaacgacgtcatggcacagctgctgtgcctggagtcgatggaccccgaccgtgacatctcggtgtacatcaacagccccggcggctcct
tcacggcgctcaccgcgatctacgacacgatgcagtacgtgaagccggacgtccagacggtctgcatgggccaggcggcctccgccgccgccgtcctgctggccgcc
ggtacgccgggcaagcgcatggccctgccgaacgcgcgtgtgctgatccaccagccgtacagcgagaccggccgcggtcaggtctccgacctggagatcgccgcga
acgagatcctgcggatgcgctcgcagctggaggacatgctggccaagcactccaccacgccggtcgagaagatccgcgaggacatcgagcgcgacaagatcctcac
ggccgaggacgcgctgagctacggcctgatcgaccaggtcatcagcacccggaagatggacaactcgagcctgcgc**ccatgg**caccaccaccaccaccactga

6.2.3.4 pET22b*_Nco_I-ShclpX$_{\text{-}His6}$

This construct was cloned by Janna Hauser.

catatggcacgcatcggtgacggcggcgatctgctcaagtgctcgttctgcggcaagagccagaagcaggtcaagaagctcatcgcagggcccggtgtgtacatctg
cgacgagtgcatcgacctctgcaacgagatcatcgaggaagaactcgctgagaccagcgaggtccgctgggaggagctcccgaagcctcgtgagatctacgagttcc
tcgagggctatgtggtcggccaggaggccgccaagaaggccctctccgtagcggtgtacaaccactacaagcgagtccaggccggcgagaacggcggggcgaacg
gccgcgacgacgccatcgagttggcgaagtccaacatcctgctcctcggccccacgggctccggcaagaccctcctcgcgcagaccctcgcgcgcatgctgaacgtcc
ccttcgcgatcgccgacgccacggccctcacggaggcgggatacgtcggcgaggacgtcgagaacatcctgctcaagctgatccaggcggccgattacgacgtcaag
aaggccgagaccgggatcatctacatcgacgagatcgacaaggtcgcgaggaagagtgaaaaacccctcgatcacgcgggaagtatcgggcgagggcgtccagcag
gcgctgctgaagatcctggagggcaccaccgcctcggtcccgccgcagggcggccgtaagcacccccaccaggagttcatccagatcgacacgacgaacgtgctgtt
catcgtgggcggcgccttctccgggctggagaagatcatcgagtcccgggccggtgccaagggcatcggcttcggcgcgcagatccgctccaagcgcgagatggagt
ccaaggaccagttccaggaggtcatgccggaggatttggtcaagttcggcatgatccccgagttcatcggccgcctcccggtcatcacctcggtccacaacctcgacc
gcgaggcgctgctccagatcctggtcgagccgcgcaacgcgctcgtcaagcagtacgagcgcctcttcgaactcgacggcgtggagctggacttcgagcgcgaggcc
ctcgaggcgatcgccgaccaggccatcctccgccagaccggcgcgcgcggcctgcgcgccatcatggaggaggtcctccagggcgtgatgtacgaggtcccgtcccg
caaggacgtggcccgggtcgtcatcacggcggacgtcgtccagtcgaacgtcaacccgacgctgatcccgcgggatgcgcggggacgtgggccgggggagcagaa
gacggcc**ccatgg**caccaccaccaccaccactga

6.2.3.5 pET22b*_Nco_I-ShclpC1$_{\text{-}His6}$

This construct was cloned by Janna Hauser.

catatgttcgagaggttcaccgaccgcgcgcggcgggttgtcgtcctggctcaggaagaagcccggatgctcaaccacaactacatcggcactgagcacatcctcctg
ggcctgatccacgagggtgaaggtgtcgccgccaaggcccttgagagcctcgggatttcgctcgaggcggtccgccagcaggtggaggagatcatcggccagggcc
agcaggccccgtccggccacatccccttcaccccccgtgccaagaaggtcctggagctgtcgctccgggaggcccttcagctgggccacaactacatcggcacggag
cacatcctgctcggcctgatccgcgagggcgagggcgtcgccgcccaggtcctcgtcaagctgggcgcagatctgaaccgcgtgcggcagcaggtcatccagctgctc
tccggttaccagggcaaggagaccgccaccgccggcggtcctgccgagggcacccccctccacgtccctggtcctcgaccagttcggccggaacctcacccaggccgc
tcgtgagtccaagctcgacccggtcatcgggcgcgagaaggagatcgagcgggtcatgcaggtgctgtcccgccgtacgaagaacaacccggtgctgatcggtgag
cccggcgtcggcaagaccgccgtcgtcgagggcctcgctcaggccatcgtcaagggcgaggtgcccgagaccctcaaggacaagcacctctacaccctggacctcg
gcgccctggtcgccggctcccgctaccgcggtgacttcgaggagcgcctgaagaaggtcctcaaggagatccgcacccgcggcgacatcatcctgttcatcgacgag
ctgcacacgctggtcggtgcgggtgccgccgagggcgccatcgacgcggcttccatcctgaagccgatgctggcccgcggtgagctccagaccatcggtgccaccac
gctggacgagtaccgcaagcacctggagaaggacgccgccctcgagcgccgcttccagcccatccaggtcgcggagccgtccctgccgcacacgatcgagatcctca

agggtctgcgggaccggtacgaggcccaccaccgcgtttccatcacggacgaggcgctggtccaggccgccaccctggccgaccggtacatctcggaccgcttcctgc
cggacaaggcgatcgacctgatcgacgaggccggctcgaggatgcgcatccgccggatgaccgcgccgccggacctgcgcgagttcgacgagaagatcgccggcgt
ccgccgcgacaaggagtccgcgatcgactcgcaggacttcgagaaggccgcctccctgcgcgacaaggagaagcagctcctggccgccaaggccaagcgggagaa
ggagtggaaggccggcgacatggacgtcgtcgccgaggtcgacggcgagctgatcgccgaggtcctcgccacggcgaccggcatcccggtcttcaagctgaccgag
gaggagtcctcgcgtctgctgcgcatggaggacgagctccacaagcgggtgatcggccaggtcgacgccgtcaaggcgctgtcgaaggcgatccgccgtacgcgtgc
cggtctgaaggaccccaagcgccccggtggctcgttcatcttcgccggcccgtccggtgtcggtaagaccgagctgtccaaggcgctcgccgaattcctcttcggcgac
gaggacgcgctgatctccctcgacatgtcggagttcagcgagaagcacacggtctcgcgtctcttcggttcgcccccggctacgtgggctacgaggagggcggccag
ctcaccgagaaggtccgccgcaagccgttctcggtcgtcctgttcgacgaggtcgagaaggcccacccggacatcttcaactcgctgctgcagatcctggaggacggt
cgcctgacggactcccagggccgggtcgtggacttcaagaacacggtcatcatcatgacgaccaacctcggcacccgggacatctccaagggcttcaacctgggcttc
gcggcccagggcgacaccaagtccaactacgagcgcatgaagaacaaggtctcggacgagctcaagcagcacttccggcccgagttcctcaaccgcgtcgacgacg
tggtcgtcttcccgcagctcagccaggccgacatcctcaagatcgtcgacctgatgatcgacaaggtggacgagcgcctgaaggaccgggacatgggcatcgagctc
tcgtcgtccgccaaggagctgctgtccaagaagggctacgacccggtgctgggtgcgcgtccgctgcgtcgcaccatccagcgcgagatcgaggactcgctgtcgga
gaagatcctcttcggcgagctgcgccccggtcacatcgtggtcgtcgacacggagggcgagggcgagaccaagaccttcaccttccgcggcgaggagaaggcggct
cttccggacgtcccgccgatcgagcaggcggccggcggctcgggcccgaacctgagcaaggacgcc**ccatgg**caccaccaccaccaccaccactga

6.2.3.6 pET22b*_Nco_I-ShclpP2$_{S131A}$

catatgaaccagttccccggcagcgggatctacgaccgtatgcacgccgtgcaggacatgagcgcctcccagggccgctacaccggcccgcaggccgagtcccgcta
catcattccccgcttcgtcgagcgcacctcccagggcatccgcgagtacgacccgtacgcgaagctcttcgaggagcgcgtgatcttcctcggcgtccagatcgacgac
gcctccgccaacgacgtcatggcacagctgctgtgcctggagtcgatggaccccgaccgtgacatctcggtgtacatcaacagccccggcggctccttcacggcgctc
accgcgatctacgacacgatgcagtacgtgaagccggacgtccagacggtctgcatgggccaggcggccgccgccgccgtcctgctggccgccggtacgccgg
gcaagcgcatggccctgccgaacgcgcgtgtgctgatccaccagccgtacagcgagaccggccgcggtcaggtctccgacctggagatcgccgcgaacgagatcct
gcggatgcgctcgcagctggaggacatgctggccaagcactccaccacgccggtcgagaagatccgcgaggacatcgagcgcgacaagatcctcacggccgagga
cgcgctgagctacggcctgatcgaccaggtcatcagcacccggaagatggacaactcgagcctgcgc**ccatgg**caccaccaccaccaccactga

A site directed mutagenesis was performed, utilising pET22b*_Nco_I-ShclpP2$_{-His}$ as template. The exchanged nucleotide is bold and marked in yellow.

6.2.3.7 pET22b*_Nco_I-shclpP2$_{S131A-ATG2}$

catatgagcgcctcccagggccgctacaccggcccgcaggccgagtcccgctacatcattccccgcttcgtcgagcgcacctcccagggcatccgcgagtacgacccg
tacgcgaagctcttcgaggagcgcgtgatcttcctcggcgtccagatcgacgacgcctccgccaacgacgtcatggcacagctgctgtgcctggagtcgatggacccc
gaccgtgacatctcggtgtacatcaacagccccggcggctccttcacggcgctcaccgcgatctacgacacgatgcagtacgtgaagccggacgtccagacggtctgc
atgggccaggcggccgccgccgccgtcctgctggccgccggtacgccgggcaagcgcatggccctgccgaacgcgcgtgtgctgatccaccagccgtacagcga
gaccggccgcggtcaggtctccgacctggagatcgccgcgaacgagatcctgcggatgcgctcgcagctggaggacatgctggccaagcactccaccacgccggtc
gagaagatccgcgaggacatcgagcgcgacaagatcctcacggccgaggacgcgctgagctacggcctgatcgaccaggtcatcagcacccggaagatggacaac
tcgagcctgcgc**ccatgg**caccaccaccaccaccactga

A site directed mutagenesis was performed, utilising pET22b*_Nco_I-ShclpP2$_{ATG2--His}$ as template. The exchanged nucleotide is bold and marked in yellow.

6.2.3.8 pET22b*_Nco_I-ShclpP2$_{hp}$

catatgagcgcctcccagggccgctacaccggcccgcaggccgagtcccgctacatcattccccgcttcgtcgagcgcacctcccagggcatccgcgagtacgacccg
tacgcgaagctcttcgaggagcgcgtgatcttcctcggcgtccagatcgacgacgcctccgccaacgacgtcatggcacagctgctgtgcctggagtcgatggacccc
gaccgtgacatc**g**cggtg**gt**catcaacagccccggcggctccttcacggcgctcaccgcgatcta**t**gacacgatgcag**gt**cgtgaagccggacgtccagacggtctg
catgggccaggcggcctccgccgccgccgtcctgctggccgccggtacgccgggcaagcgcatggccctgccgaacgcgcgtgtgctgatccaccagccgtacagcg

agaccggccgcggtcaggtctccgacctggagatcgccgcgaacgagatcctgcggatgcgctcgcagctggaggacatgctggccaagcactccaccacgccggt
cgagaagatccgcgaggacatcgagcgcgacaagatcctcacggccgaggacgcgctgagctacggcctgatcgaccaggtcatcagcacccggaagatggacaa
ctcgagcctgcgc**ccatgg**caccaccaccaccaccactga

A site directed mutagenesis was performed, utilising pET22b*_Nco_I-ShclpP2$_{ATG2\text{--}His}$ as template. The exchanged nucleotides are bold and marked in yellow and a silent mutation is marked in green.

6.2.3.9 pET22b*_Nco_I-ShclpP2$_{S94YATG2\text{-}His6}$

catatgagcgcctcccagggccgctacaccggcccgcaggccgagtcccgctacatcattccccgcttcgtcgagcgcacctcccagggcatccgcgagtacgacccg
tacgcgaagctcttcgaggagcgcgtgatcttcctcggcgtccagatcgacgacgcctccgccaacgacgtcatggcacagctgctgtgcctggagtcgatggacccc
gaccgtgacatct**ac**gtgtacatcaacagccccggcggctccttcacggcgctcaccgcgatctacgacacgatgcagtacgtgaagccggacgtccagacggtctgc
atgggccaggcggcctccgccgccgccgtcctgctggccgccggtacgccgggcaagcgcatggccctgccgaacgcgcgtgtgctgatccaccagccgtacagcga
gaccggccgcggtcaggtctccgacctggagatcgccgcgaacgagatcctgcggatgcgctcgcagctggaggacatgctggccaagcactccaccacgccggtc
gagaagatccgcgaggacatcgagcgcgacaagatcctcacggccgaggacgcgctgagctacggcctgatcgaccaggtcatcagcacccggaagatggacaac
tcgagcctgcgc**ccatgg**caccaccaccaccaccactga

A site directed mutagenesis was performed, utilising pET22b*_Nco_I-ShclpP2$_{ATG2\text{--}His}$ as template. The exchanged nucleotides are bold and marked in yellow.

6.2.4 petDUET construct

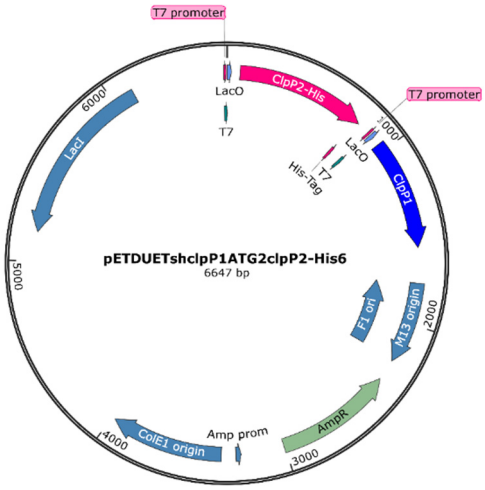

Figure 6.15: **The pETDUETShclpP1$_{ATG2}$clpP2$_{\text{-}His6}$ vector map.**

Sequence of the pETDUETShclpP1$_{ATG2}$clpP2$_{\text{-}His6}$ construct. Restriction sites are underlined. The *ShclpP1$_{ATG2}$* nucleotide sequence is coloured in green, whereas the *ShclpP2$_{\text{-}His6}$* sequence is marked in blue.

ggggaattgtgagcggataacaattcccctctagaaataattttgtttaactttaagaaggagatata**ccatgG**GAAACCAGTTcCCCGGCAGCgGGATCT
ACGACCGTATGCACGCCGTGCAGGACATGAGCGCCTCCCAGGGCCGCTACACCGGCCCGCAGGCCGAGTCCCGCTACATCATT
CCCCGCTTCGTCGAGCGCACCTCCCAGGGCATCCGCGAGTACGACCCGTACGCGAAGCTCTTCGAGGAGCGCGTGATCTTCCT
CGGCGTCCAGATCGACGACGCCTCCGCCAACGACGTCATGGCACAGCTGCTGTGCCTGGAGTCGATGGACCCCGACCGTGAC

APPENDIX

ATCTCGGTGTACATCAACAGCCCCGGCGGCTCCTTCACGGCGCTCACCGCGATCTACGACACGATGCAGTACGTGAAGCCGGA
CGTCCAGACGGTCTGCATGGGCCAGGCGGCCTCCGCCGCCGCCGTCCTGCTGGCCGCCGGTACGCCGGGCAAGCGCATGGCC
CTGCCGAACGCGCGTGTGCTGATCCACCAGCCGTACAGCGAGACCGGCCGCGGTCAGGTCTCCGACCTGGAGATCGCCGCGA
ACGAGATCCTGCGGATGCGCTCGCAGCTGGAGGACATGCTGGCCAAGCACTCCACCACGCCGGTCGAGAAGATCCGCGAGGA
CATCGAGCGCGACAAGATCCTCACGGCCGAGGACGCGCTGAGCTACGGCCTGATCGACCAGGTCATCAGCACCCGGAAGATG
GACAACTCGAGCCTGCGCCACCACCACCACCACCACTGA**Aagctt**gcggccgcataatgcttaagtcgaacagaaagtaatcgtattgtacacggc
cgcataatcgaaattaatacgactcactataggggaattgtgagcggataacaattccccatcttagtatattagttaagtataagaaggagatata**cataTG**ACG
AATCTGATGCCCTCAGCCGCCGGCGAGCCTTCCATCGGTGGTGGCCTCGGTGACCAGGTCTACAACCGGCTGCTCAACGAGCG
GATCATCTTCCTCGGCCAGCCGGTCGACGACGACATCGCGAACAAGATCACCGCACAGTTGCTGCTCCTTGCCTCCGACCCGG
AGAAGGACATCTACCTGTACATCAACAGCCCCGGCGGTTCGATCACGGCGGGCATGGCGATCTACGACACCATGCAGTACATC
AAGAACGACGTGGTGACCATCGCCATGGGCCTGGCAGCCTCGATGGGCCAGTTCCTGCTCAGCGCGGGCACCCCCGGCAAGC
GCTTCGCGCTGCCGAACGCCGAGATTCTGATCCATCAGCCCTCCGCCGGCCTCGCCGGCTCGGCCTCGGACATCAAGATCCAC
GCCGAGCGGCTGCTGCACACCAAGAAGCGCATGGCCGAGCTGACCTCCCAGCACACCGGCCAGACGATCGAGCAGATCACCC
GCGACTCGGACCGCGACCGCTGGTTCGACGCCTTCGAGGCCAAGGAGTACGGCCTCATCGACGACGTGATGACGACGGCCGC
CGGTATGCCGGGCGGCGGCGGCACCGGGGCCTGA**Ggtacc**ctcgagtctggtaaagaaaccgctgctgcgaaatttgaacgccagcacatggact
cgtctactagcgcagcttaattaacctaggctgctgccaccgctgagcaataactagcataacccctttggggcctctaaacgggtcttgaggggttttttgctgaaagg
aggaactatatccggattggcgaatgggacgcgccctgtagcggcgcattaagcgcggcgggtgtggtggttacgcgcagcgtgaccgctacacttgccagcgccct
agcgcccgctcctttcgctttcttcccttcctttctcgccacgttcgccggctttccccgtcaagctctaaatcgggggctccctttagggttccgatttagtgctttacggca
cctcgaccccaaaaaacttgattagggtgatggttcacgtagtgggccatcgccctgatagacggtttttcgcccttgacgttggagtccacgttctttaatagtggact
cttgttccaaactggaacaacactcaaccctatctcggtctattcttttgatttataagggattttgccgatttcggcctattggttaaaaaatgagctgatttaacaaaaa
tttaacgcgaattttaacaaaatattaacgtttacaatttctggcggcacgatggcatgagattatcaaaaaggatcttcacctagatccttttaaattaaaaatgaagt
tttaaatcaatctaaagtatatatgagtaaacttggtctgacagttaccaatgcttaatcagtgaggcacctatctcagcgatctgtctatttcgttcatccatagttgcct
gactccccgtcgtgtagataactacgatacgggagggcttaccatctggccccagtgctgcaatgataccgcgagacccacgctcaccggctccagatttatcagcaa
taaaccagccagccggaagggccgagcgcagaagtggtcctgcaactttatccgcctccatccagtctattaattgttgccgggaagctagagtaagtagttcgccag
ttaatagtttgcgcaacgttgttgccattgctacaggcatcgtggtgtcacgctcgtcgtttggtatggcttcattcagctccggttcccaacgatcaaggcgagttacat
gatccccatgttgtgcaaaaaagcggttagctccttcggtcctccgatcgttgtcagaagtaagttggccgcagtgttatcactcatggttatggcagcactgcataat
tctcttactgtcatgccatccgtaagatgcttttctgtgactggtgagtactcaaccaagtcattctgagaatagtgtatgcggcgaccgagttgctcttgcccggcgtca
atacgggataataccgcgccacatagcagaactttaaaagtgctcatcattggaaaacgttcttcggggcgaaaactctcaaggatcttaccgctgttgagatccagtt
cgatgtaacccactcgtgcacccaactgatcttcagcatcttttactttcaccagcgtttctgggtgagcaaaaacaggaaggcaaaatgccgcaaaaaagggaataa
gggcgacacggaaatgttgaatactcatactcttccttttttcaatcatgattgaagcatttatcagggttattgtctcatgagcggatacatatttgaatgtatttagaaa
aataaacaaataggtcatgaccaaaatcccttaacgtgagttttcgttccactgagcgtcagaccccgtagaaaagatcaaaggatcttcttgagatccttttttttctgc
gcgtaatctgctgcttgcaaacaaaaaaaccaccgctaccagcggtggtttgtttgccggatcaagagctaccaactctttttccgaaggtaactggcttcagcagagc
gcagataccaaatactgtccttctagtgtagccgtagttaggccaccacttcaagaactctgtagcaccgcctacatacctcgctctgctaatcctgttaccagtggctg
ctgccagtggcgataagtcgtgtcttaccgggttggactcaagacgatagttaccggataaggcgcagcggtcgggctgaacgggggggttcgtgcacacagcccagc
ttggagcgaacgacctacaccgaactgagatacctacagcgtgagctatgagaaagcgccacgcttcccgaagggagaaaggcggacaggtatccggtaagcggc
agggtcggaacaggagagcgcacgagggagcttccagggggaaacgcctggtatctttatagtcctgtcgggtttcgccacctctgacttgagcgtcgatttttgtgat
gctcgtcaggggggcggagcctatggaaaaacgccagcaacgcggccttttacggttcctggccttttgctggccttttgctcacatgttctttcctgcgttatcccctga
ttctgtggataaccgtattaccgcctttgagtgagctgataccgctcgccgcagccgaacgaccgagcgcagcgagtcagtgagcgaggaagcggaagagcgcctga
tgcggtattttctccttacgcatctgtgcggtatttcacaccgcatatatggtgcactctcagtacaatctgctctgatgccgcatagttaagccagtatacactccgctat
cgctacgtgactgggtcatggctgcgccccgacacccgccaacacccgctgacgcgccctgacgggcttgtctgctcccggcatccgcttacagacaagctgtgaccg
tctccgggagctgcatgtgtcagaggttttcaccgtcatcaccgaaacgcgcgaggcagctgcggtaaagctcatcagcgtggtcgtgaagcgattcacagatgtctg
cctgttcatccgcgtccagctcgttgagtttctccagaagcgttaatgtctggcttctgataaagcgggccatgttaagggcggttttttcctgtttggtcactgatgcctcc
gtgtaagggggatttctgttcatgggggtaatgataccgatgaaacgagagaggatgctcacgatacgggttactgatgatgaacatgcccggttactggaacgttgt
gagggtaaacaactggcggtatggatgcggcgggaccagagaaaaatcactcagggtcaatgccagcgcttcgttaatacagatgtaggtgttccacagggtagcc
agcagcatcctgcgatgcagatccggaacataatggtgcagggcgctgacttccgcgtttccagactttacgaaacacggaaaccgaagaccattcatgttgttgctc
aggtcgcagacgttttgcagcagcagtcgcttcacgttcgctcgcgtatcggtgattcattctgctaaccagtaaggcaaccccgccagcctagccgggtcctcaacga
caggagcacgatcatgctagtcatgccccgcgcccaccggaaggagctgactgggttgaaggctctcaagggcatcggtcgagatcccggtgcctaatgagtgagct
aacttacattaattgcgttgcgctcactgcccgctttccagtcgggaaacctgtcgtgccagctgcattaatgaatcggccaacgcgcggggagaggcggtttgcgtatt
gggcgccagggtggtttttctttcaccagtgagacgggcaacagctgattgcccttcaccgcctggccctgagagagttgcagcaagcggtccacgctggtttgcccc

agcaggcgaaaatcctgtttgatggtggttaacggcgggatataacatgagctgtcttcggtatcgtcgtatcccactaccgagatgtccgcaccaacgcgcagcccg
gactcggtaatggcgcgcattgcgcccagcgccatctgatcgttggcaaccagcatcgcagtgggaacgatgccctcattcagcatttgcatggtttgttgaaaaccgg
acatggcactccagtcgccttcccgttccgctatcggctgaatttgattgcgagtgagatatttatgccagccagccagacgcagacgcgccgagacagaacttaatgg
gcccgctaacagcgcgatttgctggtgacccaatgcgaccagatgctccacgcccagtcgcgtaccgtcttcatgggagaaaataatactgttgatgggtgtctggtca
gagacatcaagaaataacgccggaacattagtgcaggcagcttccacagcaatggcatcctggtcatccagcggatagttaatgatcagcccactgacgcgttgcgc
gagaagattgtgcaccgccgctttacaggcttcgacgccgcttcgttctaccatcgacaccaccacgctggcacccagttgatcggcgcgagatttaatcgccgcgaca
atttgcgacggcgcgtgcagggccagactggaggtggcaacgccaatcagcaacgactgtttgcccgccagttgttgtgccacgcggttgggaatgtaattcagctcc
gccatcgccgcttccactttttcccgcgttttcgcagaaacgtggctggcctggttcaccacgcgggaaacggtctgataagagacaccggcatactctgcgacatcgt
ataacgttactggtttcacattcaccaccctgaattgactctcttccgggcgctatcatgccataccgcgaaaggttttgcgccattcgatggtgtccgggatctcgacgc
tctcccttatgcgactcctgcattaggaagcagcccagtagtaggttgaggccgttgagcaccgccgccgcaaggaatggtgcatgcaaggagatggcgcccaacag
tccccccggccacggggcctgccaccatacccacgccgaaacaagcgctcatgagcccgaagtggcgagcccgatcttccccatcggtgatgtcggcgatataggcgc
cagcaaccgcacctgtggcgccggtgatgccggccacgatgcgtccggcgtagaggatcgagatcgatctcgatcccgcgaaattaatacgactcactata

6.3 Amino acid sequences

6.3.1 ShClpP1

MRRPGAVVRRAGGYVTNLMPSAAGEPSIGGGLGDQVYNRLLNERIIFLGQPVDDDIANKITAQLLLLASDPEKDIYLYIN
SPGGSITAGMAIYDTMQYIKNDVVTIAMGLAASMGQFLLSAGTPGKRFALPNAEILIHQPSAGLAGSASDIKIHAERLLH
TKKRMAELTSQHTGQTIEQITRDSDRDRWFDAFEAKEYGLIDDVMTTAAGMPGGGGTGA

6.3.2 ShClpP2

MNQFPGSGIYDRMHAVQDMSASQGRYTGPQAESRYIIPRFVERTSQGIREYDPYAKLFEERVIFLGVQIDDASANDVM
AQLLCLESMDPDRDISVYINSPGGSFTALTAIYDTMQYVKPDVQTVCMGQAASAAAVLLAAGTPGKRMALPNARVLIH
QPYSETGRGQVSDLEIAANEILRMRSQLEDMLAKHSTTPVEKIREDIERDKILTAEDALSYGLIDQVISTRKMDNSSLR

6.3.3 ShClpX

MARIGDGGDLLKCSFCGKSQKQVKKLIAGPGVYICDECIDLCNEIIEEELAETSEVRWEELPKPREIYEFLEGYVVGQEAAK
KALSVAVYNHYKRVQAGENGGANGRDDAIELAKSNILLLGPTGSGKTLLAQTLARMetLNVPFAIADATALTEAGYVGE
DVENILLKLIQAADYDVKKAETGIIYIDEIDKVARKSENPSITREVSGEGVQQALLKILEGTTASVPPQGGRKHPHQEFIQID
TTNVLFIVGGAFSGLEKIIESRAGAKGIGFGAQIRSKREMetESKDQFQEVMetPEDLVKFGMetIPEFIGRLPVITSVHNL
DREALLQILVEPRNALVKQYERLFELDGVELDFEREALEAIADQAILRQTGARGLRAIMetEEVLQGVMYEVPSRKDVAR
VVITADVVQSNVNPTLIPRDARGRGPGEQKTA

6.3.4 ShClpC1

MFERFTDRARRVVVLAQEEARMLNHNYIGTEHILLGLIHEGEGVAAKALESLGISLEAVRQQVEEIIGQGQQAPSGHIPF
TPRAKKVLELSLREALQLGHNYIGTEHILLGLIREGEGVAAQVLVKLGADLNRVRQQVIQLLSGYQGKETATAGGPAEGT
PSTSLVLDQFGRNLTQAARESKLDPVIGREKEIERVMQVLSRRTKNNPVLIGEPGVGKTAVVEGLAQAIVKGEVPETLKD
KHLYTLDLGALVAGSRYRGDFEERLKKVLKEIRTRGDIILFIDELHTLVGAGAAEGAIDAASILKPMLARGELQTIGATTLDE
YRKHLEKDAALERRFQPIQVAEPSLPHTIEILKGLRDRYEAHHRVSITDEALVQAATLADRYISDRFLPDKAIDLIDEAGSM
RIRRMTAPPDLREFDEKIAGVRRDKESAIDSQDFEKAASLRDKEKQLLAAKAKREKEWKAGDMDVVAEVDGELIAEVLA
TATGIPVFKLTEEESSRLLRMEDELHKRVIGQVDAVKALSKAIRRTRAGLKDPKRPGGSFIFAGPSGVGKTELSKALAEFLF
GDEDALISLDMSEFSEKHTVSRLFGSPPGYVGYEEGGQLTEKVRRKPFSVVLFDEVEKAHPDIFNSLLQILEDGRLTDSQG
RVVDFKNTVIIMTTNLGTRDISKGFNLGFAAQGDTKSNYERMKNKVSDELKQHFRPEFLNRVDDVVVFPQLSQADILKI

VDLMIDKVDERLKDRDMGIELSSSAKELLSKKGYDPVLGARPLRRTIQREIEDSLSEKILFGELRPGHIVVVDTEGEGETKT
FTFRGEEKAALPDVPPIEQAAGGSGPNLSKDA

6.3.5 ShClpC2

MSSGFTSPEGYGSDPFGEFLARFFGGPRPGPRQIDLGRLLSQPARELVRGAAQYAAEHGSRDLDTQHLLRAALATEPTR
TLLSKAGANPDSLASQIDDRSGPAQHTPDDAPPPTALSLTPAAKRALLDAHDMARARGYGYIGPEHVLSALASNPDSAA
GHILNAARFAPSEPPEAPEMPQSERPRPTNTPTLDKYGRDLTELARQGRIDPVIGRDEEIEQTVEVLSRRGKNNPVLIGD
AGVGKTAIVEGLAQRISEADVPDVLIGRRVVALDLTGVVAGTRYRGDFEERMNNIVGEIRAHSDQLIIFIDELHTVVGAG
SGGGDGSSMDAGNILKPALARGELHIVGATTLEEYRRIEKDAALARRFQPIMVPEPTAADAIEILRGLQDRYEAHHQVRY
TDEALVTAVELSDRYLTARRLPDKAIDLIDQAGARVRLRARTKGTDVRALERELEQLTRDKDQAVADESYEQATQLRDRI
VDVKQRITAAGGDGEVDEGQDLVVGAEAIAEVVSRQTGIPVSSLTQEEKDRLLGLEEHLHQRVVGQDEAVRVVSDAVL
RSRAGLASPDRPIGSFLFLGPTGVGKTELARALAEALFGSEDRMVRLDMSEYQERHTVSRLIGAPPGYVGHEEAGQLTE
VVRRHPYSLLLLDEVEKAHPDVFNILLQVLDDGRLTDSQGRTVDFSNTVIVMTSNLGSEAITRRGATTGFAAGGADADE
EARREQILRPLREHFRPEFLNRIDEIVVFRQLTTEQLRRITNLLLDRTRSLVQSKGVTVTFTDRAVEWLAERGYQPEYGAR
PLRRTIQREVDNELSRLLLDGRVEENGRVTVDVEDGHLAFSTVPR

6.3.6 ShClgR

MILLRRLLGDVLRRQRQRQGRTLREVSSSARVSLGYLSEVERGQKEASSELLSAICDALDVRMSELMREVSDE
LALAELAQSAAATPSEPVHTPVRSMLGSVSVAGVPPERVTIKAPAEAVDVVAA

6.3.7 ShPopR

MTSHLPNEARVIPLRPHGARPTGAPPRQAPPAPAVKEPLWRDLVGDVLRRERLAQERTLKDVADEARISMPYLSEVER
GRKEASSEVLAAAAHALGLNLRISMPYLSEVERGRKEASSEVLAAAAHALGLNLGDLLTRAQGELTRVTSRYAGGS
RRGAATSSHDGMCLAA

6.3.8 ShClpP$_{ADEP}$

MKDIKELTGRTLGASRWNLNDQVMHRLMDERIIMLGQEVDDAGSNAICSQLLLLAGDSPRDISLYINSPGGSVTAGM
AIYDTMNYIENDVVTVAMGTAASMGQFLLTAGTPGKRIVLPHAEILMHQPSAGLGGSASDIKIHAERLIRVKKRMIDITA
QHTGRTVEEIKRDSDRDRWFSADEAVEYGLADRVEYVAATVPGNIGAAK

7. Abbreviations

°C	degree celcius
µ	micro (10^{-6})
A	Ampere
AAA+	ATPases associated with diverse cellular activities
ADEPs	Acyldepsipeptides
Aa	amino acid residue
ATP	Adenosine triphosphate
Approx.	approximately
BLAST	basic local alignment search tool
bp	Base pair

ABBREVIATIONS

BSA	Bovine Serum albumin
BsClpP	ClpP from *Bacillus subtilis*
ClgR	*clpP* and *lon* gene regulator
Clp	caseinolytic protease
ClpP	Clp peptidase
CdClpP	ClpP from *Clostridium difficile*
CtClpP	ClpP from *Chlamydia trachomatis*
DMSO	Dimethyl sulfoxide
DNA	Deoxyribonucleic acid
dNTP	Deoxyribonucleotide triphosphate
DTT	1,4-Dithiothreitol
EDTA	Ethylenediamine tetraacetic acid
EcClpP	ClpP from *E. coli*
EM	electron microscopy
g	relative centrifugal force (RCF)
gDNA	genomic DNA
h	hours
HEPES	4-(2-hydroxyethyl)-1-piperazineethanesulfonic acid
His_6	histidin-Tag comprising 6 histidin residues
HRP	Horseradish peroxidase
IPTG	Isopropyl-β-D-thiogalactopyranoside
l	litre
ITC	isothermal titration calorimetry
LB	lysogeny broth
LmClpP	ClpP from *Listeria monocytogenes*
m	milli (10^{-3})
M	Molarity (molar concentration) [mol/L]
min	Minute
MIC	Minimal inhibitory concentration
mol	amount of substance (6,022 10^{23} particles)
MOPS	3-(*N*-Morpholino)propane sulfonic acid
mRNA	messenger RNA
MSA	Multiple Sequence Alignment
MtClpP	ClpP from *Mycobacterium tuberculosis*
n	nano (10^{-9})
NCBI	national center for biotechnology information
n.d.	not determined
Ni-NTA	nickel nitrilotriacetic acid
NmClpP	ClpP from *Neisseria meningitis*
OD_{600}	Optical density measured at 600 nm
PaClpP	ClpP from *Pseudomonas aeroginosa*
PBS	phosphate buffered saline
PBST	PBS with 0,1% Tween 20
PCR	polymerase chain reaction
PDB	protein data bank
pH (Latin: pontentia hydrogenii)	measurement of hydrogen ion concentration in a liquid solution

pI	isoelectric point
PopR	*clpP3* operon regulator
p.a.	pro analysis (analytical-grade)
rpm	revolutions per minute
RT	room temperature
s	second
SaClpP	ClpP from *Staphylococcus aureus*
SDS-PAGE	sodium dodecyl sulfate polyacrylamide gel electrophoresis
ShClpP	ClpP from *Streptomyces hawaiiensis*
TAE	Tris-Acetate-EDTA
TB	teriffic broth
Tris	Tris(hydroxymethyl)aminomethane
V	Voltage

Amino acids:

Amino acid name	3-letter abbreviation	1-letter abbreviation
Alanine	Ala	A
Arginine	Arg	R
Asparagine	Asn	N
Aspartic acid	Asp	D
Cysteine	Cys	C
Glutamine	Gln	Q
Glutamate (Glutamic acid)	Glu	E
Glycine	Gly	G
Histidine	His	H
Isoleucine	Ile	I
Leucine	Leu	L
Lysine	Lys	K
Methionine	Met	M
Phenylalanine	Phe	F
Proline	Pro	P
Serine	Ser	S
Threonine	Thr	T
Tryptophan	Trp	W
Tyrosine	Tyr	Y
Valine	Val	V

8. Literature

Akopian, T., Kandror, O., Raju, R. M., Unnikrishnan, M., Rubin, E. J. & Goldberg, A. L. (2012). The active ClpP protease from M. tuberculosis is a complex composed of a heptameric ClpP1 and a ClpP2 ring. *EMBO J,* 31, 1529-41 doi:10.1038/emboj.2012.5.

Alexopoulos, J., Ahsan, B., Homchaudhuri, L., Husain, N., Cheng, Y. Q. & Ortega, J. (2013). Structural determinants stabilizing the axial channel of ClpP for substrate translocation. *Mol Microbiol,* 90, 167-80 doi:10.1111/mmi.12356.

Amor, A. J., Schmitz, K. R., Sello, J. K., Baker, T. A. & Sauer, R. T. (2016). Highly Dynamic Interactions Maintain Kinetic Stability of the ClpXP Protease During the ATP-Fueled Mechanical Cycle. *ACS Chem Biol,* 11, 1552-60 doi:10.1021/acschembio.6b00083.

Baker, T. A. & Sauer, R. T. (2012). ClpXP, an ATP-powered unfolding and protein-degradation machine. *Biochim Biophys Acta,* 1823, 15-28 doi:10.1016/j.bbamcr.2011.06.007.

Banecki, B., Wawrzynow, A., Puzewicz, J., Georgopoulos, C. & Zylicz, M. (2001). Structure-function analysis of the zinc-binding region of the ClpX molecular chaperone. *J Biol Chem,* 276, 18843-8 doi:10.1074/jbc.M007507200.

Bellier, A., Gominet, M. & Mazodier, P. (2006). Post-translational control of the Streptomyces lividans ClgR regulon by ClpP. *Microbiology,* 152, 1021-7 doi:10.1099/mic.0.28564-0.

Bellier, A. & Mazodier, P. (2004). ClgR, a novel regulator of clp and lon expression in Streptomyces. *J Bacteriol,* 186, 3238-48

Benaroudj, N., Raynal, B., Miot, M. & Ortiz-Lombardia, M. (2011). Assembly and proteolytic processing of mycobacterial ClpP1 and ClpP2. *BMC Biochem,* 12, 61 doi:10.1186/1471-2091-12-61.

Bertani, G. (1951). Studies on lysogenesis. I. The mode of phage liberation by lysogenic Escherichia coli. *J Bacteriol,* 62, 293-300 doi:10.1128/jb.62.3.293-300.1951.

Bewley, M. C., Graziano, V., Griffin, K. & Flanagan, J. M. (2006). The asymmetry in the mature amino-terminus of ClpP facilitates a local symmetry match in ClpAP and ClpXP complexes. *J Struct Biol,* 153, 113-28 doi:10.1016/j.jsb.2005.09.011.

Bradford, M. M. (1976). A rapid and sensitive method for the quantitation of microgram quantities of protein utilizing the principle of protein-dye binding. *Anal Biochem,* 72, 248-54 doi:10.1006/abio.1976.9999.

Brock, T. D. & Brock, M. L. (1959). Similarity in mode of action of chloramphenicol and erythromycin. *Biochim Biophys Acta,* 33, 274-5 doi:10.1016/0006-3002(59)90535-9.

Brötz-Oesterhelt, H., Bandow, J. E. & Labischinski, H. (2005a). Bacterial proteomics and its role in antibacterial drug discovery. *Mass Spectrom Rev,* 24, 549-65 doi:10.1002/mas.20030.

Brötz-Oesterhelt, H., Beyer, D., Kroll, H. P., Endermann, R., Ladel, C., Schroeder, W., Hinzen, B., Raddatz, S., Paulsen, H., Henninger, K., Bandow, J. E., Sahl, H. G. & Labischinski, H. (2005b). Dysregulation of bacterial proteolytic machinery by a new class of antibiotics. *Nat Med,* 11, 1082-7 doi:10.1038/nm1306.

Brötz-Oesterhelt, H. & Sass, P. (2014). Bacterial caseinolytic proteases as novel targets for antibacterial treatment. *Int J Med Microbiol,* 304, 23-30 doi:10.1016/j.ijmm.2013.09.001.

Burton, R. E., Siddiqui, S. M., Kim, Y. I., Baker, T. A. & Sauer, R. T. (2001). Effects of protein stability and structure on substrate processing by the ClpXP unfolding and degradation machine. *EMBO J,* 20, 3092-100 doi:10.1093/emboj/20.12.3092.

Champness, W. C. (1988). New loci required for Streptomyces coelicolor morphological and physiological differentiation. *J Bacteriol,* 170, 1168-74 doi:10.1128/jb.170.3.1168-1174.1988.

Compton, S. J. & Jones, C. G. (1985). Mechanism of dye response and interference in the Bradford protein assay. *Anal Biochem,* 151, 369-74 doi:10.1016/0003-2697(85)90190-3.

Conlon, B. P., Nakayasu, E. S., Fleck, L. E., Lafleur, M. D., Isabella, V. M., Coleman, K., Leonard, S. N., Smith, R. D., Adkins, J. N. & Lewis, K. (2013). Activated ClpP kills persisters and eradicates a chronic biofilm infection. *Nature,* 503, 365-70 doi:10.1038/nature12790.

Cordova, J. C., Olivares, A. O., Shin, Y., Stinson, B. M., Calmat, S., Schmitz, K. R., Aubin-Tam, M. E., Baker, T. A., Lang, M. J. & Sauer, R. T. (2014). Stochastic but highly coordinated protein unfolding and translocation by the ClpXP proteolytic machine. *Cell,* 158, 647-58 doi:10.1016/j.cell.2014.05.043.

Dahmen, M., Vielberg, M. T., Groll, M. & Sieber, S. A. (2015). Structure and mechanism of the caseinolytic protease ClpP1/2 heterocomplex from Listeria monocytogenes. *Angew Chem Int Ed Engl,* 54, 3598-602 doi:10.1002/anie.201409325.

Dairi, T., Aisaka, K., Katsumata, R. & Hasegawa, M. (1995). A self-defense gene homologous to tetracycline effluxing gene essential for antibiotic production in Streptomyces aureofaciens. *Biosci Biotechnol Biochem,* 59, 1835-41 doi:10.1271/bbb.59.1835.

De Crecy-Lagard, V., Servant-Moisson, P., Viala, J., Grandvalet, C. & Mazodier, P. (1999). Alteration of the synthesis of the Clp ATP-dependent protease affects morphological and physiological differentiation in Streptomyces. *Mol Microbiol,* 32, 505-17

Donaldson, L. W., Wojtyra, U. & Houry, W. A. (2003). Solution structure of the dimeric zinc binding domain of the chaperone ClpX. *J Biol Chem,* 278, 48991-6 doi:10.1074/jbc.M307826200.

Duggar, B. M. (1948). Aureomycin; a product of the continuing search for new antibiotics. *Ann N Y Acad Sci,* 51, 177-81 doi:10.1111/j.1749-6632.1948.tb27262.x.

Erzberger, J. P. & Berger, J. M. (2006). Evolutionary relationships and structural mechanisms of AAA+ proteins. *Annu Rev Biophys Biomol Struct,* 35, 93-114 doi:10.1146/annurev.biophys.35.040405.101933.

Famulla, K., Sass, P., Malik, I., Akopian, T., Kandror, O., Alber, M., Hinzen, B., Ruebsamen-Schaeff, H., Kalscheuer, R., Goldberg, A. L. & Brötz-Oesterhelt, H. (2016). Acyldepsipeptide antibiotics kill mycobacteria by preventing the physiological functions of the ClpP1P2 protease. *Mol Microbiol,* 101, 194-209 doi:10.1111/mmi.13362.

Fazekas De St Groth, S., Webster, R. G. & Datyner, A. (1963). Two new staining procedures for quantitative estimation of proteins on electrophoretic strips. *Biochim Biophys Acta,* 71, 377-91 doi:10.1016/0006-3002(63)91092-8.

Fei, X., Bell, T. A., Jenni, S., Stinson, B. M., Baker, T. A., Harrison, S. C. & Sauer, R. T. (2020). Structures of the ATP-fueled ClpXP proteolytic machine bound to protein substrate. *Elife,* 9 doi:10.7554/eLife.52774.

Flärdh, K. & Buttner, M. J. (2009). Streptomyces morphogenetics: dissecting differentiation in a filamentous bacterium. *Nat Rev Microbiol,* 7, 36-49 doi:10.1038/nrmicro1968.

Flynn, J. M., Levchenko, I., Seidel, M., Wickner, S. H., Sauer, R. T. & Baker, T. A. (2001). Overlapping recognition determinants within the ssrA degradation tag allow modulation of proteolysis. *Proc Natl Acad Sci U S A,* 98, 10584-9 doi:10.1073/pnas.191375298.

Flynn, J. M., Neher, S. B., Kim, Y. I., Sauer, R. T. & Baker, T. A. (2003). Proteomic discovery of cellular substrates of the ClpXP protease reveals five classes of ClpX-recognition signals. *Mol Cell,* 11, 671-83 doi:10.1016/s1097-2765(03)00060-1.

Frees, D., Gerth, U. & Ingmer, H. (2014). Clp chaperones and proteases are central in stress survival, virulence and antibiotic resistance of Staphylococcus aureus. *Int J Med Microbiol,* 304, 142-9 doi:10.1016/j.ijmm.2013.11.009.

Frees, D., Qazi, S. N., Hill, P. J. & Ingmer, H. (2003). Alternative roles of ClpX and ClpP in Staphylococcus aureus stress tolerance and virulence. *Mol Microbiol,* 48, 1565-78 doi:10.1046/j.1365-2958.2003.03524.x.

Fux, A., Korotkov, V. S., Schneider, M., Antes, I. & Sieber, S. A. (2019). Chemical Cross-Linking Enables Drafting ClpXP Proximity Maps and Taking Snapshots of In Situ Interaction Networks. *Cell Chem Biol,* 26, 48-59.e7 doi:10.1016/j.chembiol.2018.10.007.

Gatsogiannis, C., Balogh, D., Merino, F., Sieber, S. A. & Raunser, S. (2019). Cryo-EM structure of the ClpXP protein degradation machinery. *Nat Struct Mol Biol,* 26, 946-954 doi:10.1038/s41594-019-0304-0.

Geiger, S. R., Bottcher, T., Sieber, S. A. & Cramer, P. (2011). A conformational switch underlies ClpP protease function. *Angew Chem Int Ed Engl,* 50, 5749-52 doi:10.1002/anie.201100666.

Gersch, M., Famulla, K., Dahmen, M., Gobl, C., Malik, I., Richter, K., Korotkov, V. S., Sass, P., Rubsamen-Schaeff, H., Madl, T., Brötz-Oesterhelt, H. & Sieber, S. A. (2015). AAA+ chaperones and acyldepsipeptides activate the ClpP protease via conformational control. *Nat Commun,* 6, 6320 doi:10.1038/ncomms7320.

Gersch, M., List, A., Groll, M. & Sieber, S. A. (2012). Insights into structural network responsible for oligomerization and activity of bacterial virulence regulator caseinolytic protease P (ClpP) protein. *J Biol Chem,* 287, 9484-94 doi:10.1074/jbc.M111.336222.

Gerth, U., Kirstein, J., Mostertz, J., Waldminghaus, T., Miethke, M., Kock, H. & Hecker, M. (2004). Fine-tuning in regulation of Clp protein content in Bacillus subtilis. *J Bacteriol,* 186, 179-91 doi:10.1128/jb.186.1.179-191.2004.

Glynn, S. E., Martin, A., Nager, A. R., Baker, T. A. & Sauer, R. T. (2009). Structures of asymmetric ClpX hexamers reveal nucleotide-dependent motions in a AAA+ protein-unfolding machine. *Cell,* 139, 744-56 doi:10.1016/j.cell.2009.09.034.

Goldberg, A. L., Moerschell, R. P., Chung, C. H. & Maurizi, M. R. (1994). ATP-dependent protease La (lon) from Escherichia coli. *Methods Enzymol,* 244, 350-75 doi:10.1016/0076-6879(94)44027-1.

Golkar, T., Zieliński, M. & Berghuis, A. M. (2018). Look and Outlook on Enzyme-Mediated Macrolide Resistance. *Front Microbiol,* 9, 1942 doi:10.3389/fmicb.2018.01942.

Gominet, M., Seghezzi, N. & Mazodier, P. (2011). Acyl depsipeptide (ADEP) resistance in Streptomyces. *Microbiology,* 157, 2226-34 doi:10.1099/mic.0.048454-0.

Gottesman, S., Roche, E., Zhou, Y. & Sauer, R. T. (1998). The ClpXP and ClpAP proteases degrade proteins with carboxy-terminal peptide tails added by the SsrA-tagging system. *Genes Dev,* 12, 1338-47

Gribun, A., Kimber, M. S., Ching, R., Sprangers, R., Fiebig, K. M. & Houry, W. A. (2005). The ClpP double ring tetradecameric protease exhibits plastic ring-ring interactions, and the N termini of its subunits form flexible loops that are essential for ClpXP and ClpAP complex formation. *J Biol Chem,* 280, 16185-96 doi:10.1074/jbc.M414124200.

Grimaud, R., Kessel, M., Beuron, F., Steven, A. C. & Maurizi, M. R. (1998). Enzymatic and structural similarities between the Escherichia coli ATP-dependent proteases, ClpXP and ClpAP. *J Biol Chem,* 273, 12476-81

Grossman, T. H. (2016). Tetracycline Antibiotics and Resistance. *Cold Spring Harb Perspect Med,* 6, a025387 doi:10.1101/cshperspect.a025387.

Guyet, A., Benaroudj, N., Proux, C., Gominet, M., Coppee, J. Y. & Mazodier, P. (2014). Identified members of the Streptomyces lividans AdpA regulon involved in differentiation and secondary metabolism. *BMC Microbiol,* 14, 81 doi:10.1186/1471-2180-14-81.

Guyet, A., Gominet, M., Benaroudj, N. & Mazodier, P. (2013). Regulation of the clpP1clpP2 operon by the pleiotropic regulator AdpA in Streptomyces lividans. *Arch Microbiol,* 195, 831-41 doi:10.1007/s00203-013-0918-2.

Hall, B. M., Breidenstein, E. B. M., De La Fuente-Nunez, C., Reffuveille, F., Mawla, G. D., Hancock, R. E. W. & Baker, T. A. (2017). Two Isoforms of Clp Peptidase in Pseudomonas aeruginosa Control Distinct Aspects of Cellular Physiology. *J Bacteriol,* 199 doi:10.1128/jb.00568-16.

Haslberger, T., Bukau, B. & Mogk, A. (2010). Towards a unifying mechanism for ClpB/Hsp104-mediated protein disaggregation and prion propagation. *Biochem Cell Biol,* 88, 63-75 doi:10.1139/o09-118.

Hersch, G. L., Burton, R. E., Bolon, D. N., Baker, T. A. & Sauer, R. T. (2005). Asymmetric interactions of ATP with the AAA+ ClpX6 unfoldase: allosteric control of a protein machine. *Cell,* 121, 1017-27 doi:10.1016/j.cell.2005.05.024.

Hinnerwisch, J., Reid, B. G., Fenton, W. A. & Horwich, A. L. (2005). Roles of the N-domains of the ClpA unfoldase in binding substrate proteins and in stable complex formation with the ClpP protease. *J Biol Chem,* 280, 40838-44 doi:10.1074/jbc.M507879200.

Hinzen, B., Raddatz, S., Paulsen, H., Lampe, T., Schumacher, A., Habich, D., Hellwig, V., Benet-Buchholz, J., Endermann, R., Labischinski, H. & Brötz-Oesterhelt, H. (2006). Medicinal chemistry optimization of acyldepsipeptides of the enopeptin class antibiotics. *ChemMedChem,* 1, 689-93 doi:10.1002/cmdc.200600055.

Hopwood, D. A. (2007). *Streptomyces in Nature and Medicine: The Antibiotic Makers,* New York, Oxford Univ. Press

Ingmer, H., Vogensen, F. K., Hammer, K. & Kilstrup, M. (1999). Disruption and analysis of the clpB, clpC, and clpE genes in Lactococcus lactis: ClpE, a new Clp family in gram-positive bacteria. *J Bacteriol,* 181, 2075-83 doi:10.1128/jb.181.7.2075-2083.1999.

Ingvarsson, H., Mate, M. J., Hogbom, M., Portnoi, D., Benaroudj, N., Alzari, P. M., Ortiz-Lombardia, M. & Unge, T. (2007). Insights into the inter-ring plasticity of caseinolytic proteases from the X-ray structure of Mycobacterium tuberculosis ClpP1. *Acta Crystallogr D Biol Crystallogr,* 63, 249-59 doi:10.1107/s0907444906050530.

Joshi, S. A., Baker, T. A. & Sauer, R. T. (2003). C-terminal domain mutations in ClpX uncouple substrate binding from an engagement step required for unfolding. *Mol Microbiol,* 48, 67-76 doi:10.1046/j.1365-2958.2003.03424.x.

Joshi, S. A., Hersch, G. L., Baker, T. A. & Sauer, R. T. (2004). Communication between ClpX and ClpP during substrate processing and degradation. *Nat Struct Mol Biol,* 11, 404-11 doi:10.1038/nsmb752.

Kenniston, J. A., Burton, R. E., Siddiqui, S. M., Baker, T. A. & Sauer, R. T. (2004). Effects of local protein stability and the geometric position of the substrate degradation tag on the efficiency of ClpXP denaturation and degradation. *J Struct Biol,* 146, 130-40 doi:10.1016/j.jsb.2003.10.023.

Kessel, M., Maurizi, M. R., Kim, B., Kocsis, E., Trus, B. L., Singh, S. K. & Steven, A. C. (1995). Homology in structural organization between E. coli ClpAP protease and the eukaryotic 26 S proteasome. *J Mol Biol,* 250, 587-94 doi:10.1006/jmbi.1995.0400.

Kim, D. Y. & Kim, K. K. (2003). Crystal structure of ClpX molecular chaperone from Helicobacter pylori. *J Biol Chem,* 278, 50664-70 doi:10.1074/jbc.M305882200.

Kim, M. S., Hahn, M. Y., Cho, Y., Cho, S. N. & Roe, J. H. (2009). Positive and negative feedback regulatory loops of thiol-oxidative stress response mediated by an unstable isoform of sigmaR in actinomycetes. *Mol Microbiol,* 73, 815-25 doi:10.1111/j.1365-2958.2009.06824.x.

Kim, Y. I., Levchenko, I., Fraczkowska, K., Woodruff, R. V., Sauer, R. T. & Baker, T. A. (2001). Molecular determinants of complex formation between Clp/Hsp100 ATPases and the ClpP peptidase. *Nat Struct Biol,* 8, 230-3 doi:10.1038/84967.

Kimber, M. S., Yu, A. Y., Borg, M., Leung, E., Chan, H. S. & Houry, W. A. (2010). Structural and theoretical studies indicate that the cylindrical protease ClpP samples extended and compact conformations. *Structure,* 18, 798-808 doi:10.1016/j.str.2010.04.008.

Kirstein, J., Hoffmann, A., Lilie, H., Schmidt, R., Rubsamen-Waigmann, H., Brötz-Oesterhelt, H., Mogk, A. & Turgay, K. (2009). The antibiotic ADEP reprogrammes ClpP, switching it from a regulated to an uncontrolled protease. *EMBO Mol Med,* 1, 37-49 doi:10.1002/emmm.200900002.

Kock, H., Gerth, U. & Hecker, M. (2004). The ClpP peptidase is the major determinant of bulk protein turnover in Bacillus subtilis. *J Bacteriol,* 186, 5856-64 doi:10.1128/jb.186.17.5856-5864.2004.

Lavey, N. P., Shadid, T., Ballard, J. D. & Duerfeldt, A. S. (2019). Clostridium difficile ClpP Homologues are Capable of Uncoupled Activity and Exhibit Different Levels of Susceptibility to Acyldepsipeptide Modulation. *ACS Infect Dis,* 5, 79-89 doi:10.1021/acsinfecdis.8b00199.

Lee, B. G., Kim, M. K. & Song, H. K. (2011). Structural insights into the conformational diversity of ClpP from Bacillus subtilis. *Mol Cells,* 32, 589-95 doi:10.1007/s10059-011-0197-1.

Lee, B. G., Park, E. Y., Lee, K. E., Jeon, H., Sung, K. H., Paulsen, H., Rubsamen-Schaeff, H., Brötz-Oesterhelt, H. & Song, H. K. (2010). Structures of ClpP in complex with acyldepsipeptide antibiotics reveal its activation mechanism. *Nat Struct Mol Biol,* 17, 471-8 doi:10.1038/nsmb.1787.

Leodolter, J., Warweg, J. & Weber-Ban, E. (2015). The Mycobacterium tuberculosis ClpP1P2 Protease Interacts Asymmetrically with Its ATPase Partners ClpX and ClpC1. *PLoS One,* 10, e0125345 doi:10.1371/journal.pone.0125345.

Li, D. H., Chung, Y. S., Gloyd, M., Joseph, E., Ghirlando, R., Wright, G. D., Cheng, Y. Q., Maurizi, M. R., Guarne, A. & Ortega, J. (2010). Acyldepsipeptide antibiotics induce the formation of a structured axial channel in ClpP: A model for the ClpX/ClpA-bound state of ClpP. *Chem Biol,* 17, 959-69 doi:10.1016/j.chembiol.2010.07.008.

Liu, K., Ologbenla, A. & Houry, W. A. (2014). Dynamics of the ClpP serine protease: a model for self-compartmentalized proteases. *Crit Rev Biochem Mol Biol,* 49, 400-12 doi:10.3109/10409238.2014.925421.

Maglica, Z., Kolygo, K. & Weber-Ban, E. (2009). Optimal efficiency of ClpAP and ClpXP chaperone-proteases is achieved by architectural symmetry. *Structure,* 17, 508-16 doi:10.1016/j.str.2009.02.014.

Malik, I. T. & Brötz-Oesterhelt, H. (2017). Conformational control of the bacterial Clp protease by natural product antibiotics. *Nat Prod Rep,* doi:10.1039/c6np00125d.

Malik, I. T., Pereira, R., Vielberg, M. T., Mayer, C., Straetener, J., Thomy, D., Famulla, K., Castro, H., Sass, P., Groll, M. & Brötz-Oesterhelt, H. (2020). Functional Characterisation of ClpP Mutations Conferring Resistance to Acyldepsipeptide Antibiotics in Firmicutes. *Chembiochem,* 21, 1997-2012 doi:10.1002/cbic.201900787.

Martin, A., Baker, T. A. & Sauer, R. T. (2007). Distinct static and dynamic interactions control ATPase-peptidase communication in a AAA+ protease. *Mol Cell,* 27, 41-52 doi:10.1016/j.molcel.2007.05.024.

Maurizi, M. R. (1991). ATP-promoted interaction between Clp A and Clp P in activation of Clp protease from Escherichia coli. *Biochem Soc Trans,* 19, 719-23 doi:10.1042/bst0190719.

Maurizi, M. R., Clark, W. P., Katayama, Y., Rudikoff, S., Pumphrey, J., Bowers, B. & Gottesman, S. (1990a). Sequence and structure of Clp P, the proteolytic component of the ATP-dependent Clp protease of Escherichia coli. *J Biol Chem,* 265, 12536-45

Maurizi, M. R., Clark, W. P., Kim, S. H. & Gottesman, S. (1990b). Clp P represents a unique family of serine proteases. *J Biol Chem,* 265, 12546-52

Mayer, C., Sass, P. & Brötz-Oesterhelt, H. (2019). Consequences of dosing and timing on the antibacterial effects of ADEP antibiotics. *Int J Med Microbiol,* 309, 151329 doi:10.1016/j.ijmm.2019.151329.

Mccormick, J. R. & Flärdh, K. (2012). Signals and regulators that govern Streptomyces development. *FEMS Microbiol Rev,* 36, 206-31 doi:10.1111/j.1574-6976.2011.00317.x.

Michel, K. H. & Kastner, R. E. (1985). A54556 antibiotics and process for production thereof. *US Pat. 4492650.*

Miller, A. L. & Walker, J. B. (1969). Enzymatic phosphorylation of streptomycin by extracts of streptomycin-producing strains of Streptomyces. *J Bacteriol,* 99, 401-5 doi:10.1128/jb.99.2.401-405.1969.

Miller, A. L. & Walker, J. B. (1970). Accumulation of streptomycin-phosphate in cultures of streptomycin producers grown on a high-phosphate medium. *J Bacteriol,* 104, 8-12 doi:10.1128/jb.104.1.8-12.1970.

Moreno-Cinos, C., Goossens, K., Salado, I. G., Van Der Veken, P., De Winter, H. & Augustyns, K. (2019). ClpP Protease, a Promising Antimicrobial Target. *Int J Mol Sci,* 20 doi:10.3390/ijms20092232.

Msadek, T., Dartois, V., Kunst, F., Herbaud, M. L., Denizot, F. & Rapoport, G. (1998). ClpP of Bacillus subtilis is required for competence development, motility, degradative enzyme synthesis, growth at high temperature and sporulation. *Mol Microbiol,* 27, 899-914 doi:10.1046/j.1365-2958.1998.00735.x.

Neuwald, A. F., Aravind, L., Spouge, J. L. & Koonin, E. V. (1999). AAA+: A class of chaperone-like ATPases associated with the assembly, operation, and disassembly of protein complexes. *Genome Res,* 9, 27-43

Ni, T., Ye, F., Liu, X., Zhang, J., Liu, H., Li, J., Zhang, Y., Sun, Y., Wang, M., Luo, C., Jiang, H., Lan, L., Gan, J., Zhang, A., Zhou, H. & Yang, C. G. (2016). Characterization of Gain-of-Function Mutant Provides New Insights into ClpP Structure. *ACS Chem Biol,* 11, 1964-72 doi:10.1021/acschembio.6b00390.

Olivares, A. O., Baker, T. A. & Sauer, R. T. (2016). Mechanistic insights into bacterial AAA+ proteases and protein-remodelling machines. *Nat Rev Microbiol,* 14, 33-44 doi:10.1038/nrmicro.2015.4.

Paget, M. S., Kang, J. G., Roe, J. H. & Buttner, M. J. (1998). sigmaR, an RNA polymerase sigma factor that modulates expression of the thioredoxin system in response to oxidative stress in Streptomyces coelicolor A3(2). *EMBO J,* 17, 5776-82 doi:10.1093/emboj/17.19.5776.

Pan, S., Malik, I. T., Thomy, D., Henrichfreise, B. & Sass, P. (2019). The functional ClpXP protease of Chlamydia trachomatis requires distinct clpP genes from separate genetic loci. *Sci Rep,* 9, 14129 doi:10.1038/s41598-019-50505-5.

Pope, M. K., Green, B. & Westpheling, J. (1998). The bldB gene encodes a small protein required for morphogenesis, antibiotic production, and catabolite control in Streptomyces coelicolor. *J Bacteriol,* 180, 1556-62

Pope, M. K., Green, B. D. & Westpheling, J. (1996). The bld mutants of Streptomyces coelicolor are defective in the regulation of carbon utilization, morphogenesis and cell--cell signalling. *Mol Microbiol,* 19, 747-56 doi:10.1046/j.1365-2958.1996.414933.x.

Procopio, R. E., Silva, I. R., Martins, M. K., Azevedo, J. L. & Araujo, J. M. (2012). Antibiotics produced by Streptomyces. *Braz J Infect Dis,* 16, 466-71 doi:10.1016/j.bjid.2012.08.014.

Raju, R. M., Jedrychowski, M. P., Wei, J. R., Pinkham, J. T., Park, A. S., O'brien, K., Rehren, G., Schnappinger, D., Gygi, S. P. & Rubin, E. J. (2014). Post-translational regulation via Clp protease is critical for survival of Mycobacterium tuberculosis. *PLoS Pathog,* 10, e1003994 doi:10.1371/journal.ppat.1003994.

Raju, R. M., Unnikrishnan, M., Rubin, D. H., Krishnamoorthy, V., Kandror, O., Akopian, T. N., Goldberg, A. L. & Rubin, E. J. (2012). Mycobacterium tuberculosis ClpP1 and ClpP2 function together in protein degradation and are required for viability in vitro and during infection. *PLoS Pathog,* 8, e1002511 doi:10.1371/journal.ppat.1002511.

Reisner, A. H., Nemes, P. & Bucholtz, C. (1975). The use of Coomassie Brilliant Blue G250 perchloric acid solution for staining in electrophoresis and isoelectric focusing on polyacrylamide gels. *Anal Biochem,* 64, 509-16 doi:10.1016/0003-2697(75)90461-3.

Ripstein, Z. A., Vahidi, S., Houry, W. A., Rubinstein, J. L. & Kay, L. E. (2020). A processive rotary mechanism couples substrate unfolding and proteolysis in the ClpXP degradation machinery. *Elife,* 9 doi:10.7554/eLife.52158.

Sass, P. & Brötz-Oesterhelt, H. (2013). Bacterial cell division as a target for new antibiotics. *Curr Opin Microbiol,* 16, 522-30 doi:10.1016/j.mib.2013.07.006.

Sass, P., Josten, M., Famulla, K., Schiffer, G., Sahl, H. G., Hamoen, L. & Brötz-Oesterhelt, H. (2011). Antibiotic acyldepsipeptides activate ClpP peptidase to degrade the cell division protein FtsZ. *Proc Natl Acad Sci U S A,* 108, 17474-9 doi:10.1073/pnas.1110385108.

Sauer, R. T. & Baker, T. A. (2011). AAA+ proteases: ATP-fueled machines of protein destruction. *Annu Rev Biochem,* 80, 587-612 doi:10.1146/annurev-biochem-060408-172623.

Schiefer, A., Vollmer, J., Lammer, C., Specht, S., Lentz, C., Ruebsamen-Schaeff, H., Brötz-Oesterhelt, H., Hoerauf, A. & Pfarr, K. (2013). The ClpP peptidase of Wolbachia endobacteria is a novel target for drug development against filarial infections. *J Antimicrob Chemother,* 68, 1790-800 doi:10.1093/jac/dkt105.

Schirmer, E. C., Glover, J. R., Singer, M. A. & Lindquist, S. (1996). HSP100/Clp proteins: a common mechanism explains diverse functions. *Trends Biochem Sci,* 21, 289-96

Schmitz, K. R., Carney, D. W., Sello, J. K. & Sauer, R. T. (2014). Crystal structure of Mycobacterium tuberculosis ClpP1P2 suggests a model for peptidase activation by AAA+ partner binding and substrate delivery. *Proc Natl Acad Sci U S A,* 111, E4587-95 doi:10.1073/pnas.1417120111.

Sedmak, J. J. & Grossberg, S. E. (1977). A rapid, sensitive, and versatile assay for protein using Coomassie brilliant blue G250. *Anal Biochem,* 79, 544-52 doi:10.1016/0003-2697(77)90428-6.

Sherrid, A. M., Rustad, T. R., Cangelosi, G. A. & Sherman, D. R. (2010). Characterization of a Clp protease gene regulator and the reaeration response in Mycobacterium tuberculosis. *PLoS One,* 5, e11622 doi:10.1371/journal.pone.0011622.

Silber, N., Matos De Opitz, C. L., Mayer, C. & Sass, P. (2020a). Cell division protein FtsZ: from structure and mechanism to antibiotic target. *Future Microbiol,* 15, 801-831 doi:10.2217/fmb-2019-0348.

Silber, N., Pan, S., Schakermann, S., Mayer, C., Brötz-Oesterhelt, H. & Sass, P. (2020b). Cell Division Protein FtsZ Is Unfolded for N-Terminal Degradation by Antibiotic-Activated ClpP. *mBio,* 11 doi:10.1128/mBio.01006-20.

Smith, C. K., Baker, T. A. & Sauer, R. T. (1999). Lon and Clp family proteases and chaperones share homologous substrate-recognition domains. *Proc Natl Acad Sci U S A,* 96, 6678-82 doi:10.1073/pnas.96.12.6678.

Sowole, M. A., Alexopoulos, J. A., Cheng, Y. Q., Ortega, J. & Konermann, L. (2013). Activation of ClpP protease by ADEP antibiotics: insights from hydrogen exchange mass spectrometry. *J Mol Biol,* 425, 4508-19 doi:10.1016/j.jmb.2013.08.005.

Sprangers, R., Gribun, A., Hwang, P. M., Houry, W. A. & Kay, L. E. (2005). Quantitative NMR spectroscopy of supramolecular complexes: dynamic side pores in ClpP are important for product release. *Proc Natl Acad Sci U S A,* 102, 16678-83 doi:10.1073/pnas.0507370102.

Thermo Fisher Scientific. (2020). *Pierce™ BS3 (bis(sulfosuccinimidyl)suberate) No-Weigh™ Format* [Online]. Available: https://www.thermofisher.com/order/catalog/product/A39266#/A39266 [Accessed 26.10.2020].

Thompson, C. J., Skinner, R. H., Thompson, J., Ward, J. M., Hopwood, D. A. & Cundliffe, E. (1982). Biochemical characterization of resistance determinants cloned from antibiotic-producing streptomycetes. *Journal of bacteriology,* 151, 678-685 doi:10.1128/jb.151.2.678-685.1982.

Thompson, M. W. & Maurizi, M. R. (1994). Activity and specificity of Escherichia coli ClpAP protease in cleaving model peptide substrates. *J Biol Chem,* 269, 18201-8

Thomy, D. (2019). *In vivo-Studien zur ClpP-Maschinerie in Streptomyceten am Beispiel des ADEP-Produzenten Streptomyces hawaiiensis NRRL 15010 und des Modellorganismus Streptomyces lividans.* Dissertation zur Erlangung des Grades eines Doktors der Naturwissenschaften (Dr. rer. nat.), Eberhard Karls Universität Tübingen

Thomy, D., Culp, E., Adamek, M., Cheng, E. Y., Ziemert, N., Wright, G. D., Sass, P. & Brötz-Oesterhelt, H. (2019). The ADEP Biosynthetic Gene Cluster in Streptomyces hawaiiensis NRRL 15010 Reveals an Accessory clpP Gene as a Novel Antibiotic Resistance Factor. *Appl Environ Microbiol,* 85 doi:10.1128/AEM.01292-19.

Viala, J. & Mazodier, P. (2002). ClpP-dependent degradation of PopR allows tightly regulated expression of the clpP3 clpP4 operon in Streptomyces lividans. *Mol Microbiol,* 44, 633-43

Viala, J. & Mazodier, P. (2003). The ATPase ClpX is conditionally involved in the morphological differentiation of Streptomyces lividans. *Mol Genet Genomics,* 268, 563-9 doi:10.1007/s00438-002-0783-1.

Viala, J., Rapoport, G. & Mazodier, P. (2000). The clpP multigenic family in Streptomyces lividans: conditional expression of the clpP3 clpP4 operon is controlled by PopR, a novel transcriptional activator. *Mol Microbiol,* 38, 602-12

Walker, J. E., Saraste, M., Runswick, M. J. & Gay, N. J. (1982). Distantly related sequences in the alpha- and beta-subunits of ATP synthase, myosin, kinases and other ATP-requiring enzymes and a common nucleotide binding fold. *Embo j,* 1, 945-51

Wang, J., Hartling, J. A. & Flanagan, J. M. (1997). The structure of ClpP at 2.3 A resolution suggests a model for ATP-dependent proteolysis. *Cell,* 91, 447-56

Waterhouse, A. M., Procter, J. B., Martin, D. M. A., Clamp, M. & Barton, G. J. (2009). Jalview Version 2—a multiple sequence alignment editor and analysis workbench. *Bioinformatics,* 25, 1189-1191 doi:10.1093/bioinformatics/btp033.

Watve, M. G., Tickoo, R., Jog, M. M. & Bhole, B. D. (2001). How many antibiotics are produced by the genus Streptomyces? *Arch Microbiol,* 176, 386-90 doi:10.1007/s002030100345.

Wendler, P., Ciniawsky, S., Kock, M. & Kube, S. (2012). Structure and function of the AAA+ nucleotide binding pocket. *Biochim Biophys Acta,* 1823, 2-14 doi:10.1016/j.bbamcr.2011.06.014.

Willey, J., Schwedock, J. & Losick, R. (1993). Multiple extracellular signals govern the production of a morphogenetic protein involved in aerial mycelium formation by Streptomyces coelicolor. *Genes Dev,* 7, 895-903 doi:10.1101/gad.7.5.895.

Wojtyra, U. A., Thibault, G., Tuite, A. & Houry, W. A. (2003). The N-terminal zinc binding domain of ClpX is a dimerization domain that modulates the chaperone function. *J Biol Chem,* 278, 48981-90 doi:10.1074/jbc.M307825200.

Wolanski, M., Donczew, R., Kois-Ostrowska, A., Masiewicz, P., Jakimowicz, D. & Zakrzewska-Czerwinska, J. (2011). The level of AdpA directly affects expression of developmental genes in Streptomyces coelicolor. *J Bacteriol,* 193, 6358-65 doi:10.1128/jb.05734-11.

Woo, K. M., Chung, W. J., Ha, D. B., Goldberg, A. L. & Chung, C. H. (1989). Protease Ti from Escherichia coli requires ATP hydrolysis for protein breakdown but not for hydrolysis of small peptides. *J Biol Chem,* 264, 2088-91

World Health Organization (2014). Antimicrobial resistance: global report on surveillance.

Yanisch-Perron, C., Vieira, J. & Messing, J. (1985). Improved M13 phage cloning vectors and host strains: nucleotide sequences of the M13mp18 and pUC19 vectors. *Gene,* 33, 103-19 doi:10.1016/0378-1119(85)90120-9.

Ye, F., Zhang, J., Liu, H., Hilgenfeld, R., Zhang, R., Kong, X., Li, L., Lu, J., Zhang, X., Li, D., Jiang, H., Yang, C. G. & Luo, C. (2013). Helix unfolding/refolding characterizes the functional dynamics of Staphylococcus aureus Clp protease. *J Biol Chem,* 288, 17643-53 doi:10.1074/jbc.M113.452714.

Yu, A. Y. & Houry, W. A. (2007). ClpP: a distinctive family of cylindrical energy-dependent serine proteases. *FEBS Lett,* 581, 3749-57 doi:10.1016/j.febslet.2007.04.076.

Zeiler, E., List, A., Alte, F., Gersch, M., Wachtel, R., Poreba, M., Drag, M., Groll, M. & Sieber, S. A. (2013). Structural and functional insights into caseinolytic proteases reveal an unprecedented regulation

principle of their catalytic triad. *Proc Natl Acad Sci U S A,* 110, 11302-7 doi:10.1073/pnas.1219125110.

Zhao, B. B., Li, X. H., Zeng, Y. L. & Lu, Y. J. (2016). ClpP-deletion impairs the virulence of Legionella pneumophila and the optimal translocation of effector proteins. *BMC Microbiol,* 16, 174 doi:10.1186/s12866-016-0790-8.

9. Publications

Reinhardt, L., Thomy D., Lakemeyer, M., Ortega, J., Sieber, S., Sass, P. & Brötz-Oesterhelt, H. Antibiotic acyldepsipeptides stimulate the *Streptomyces* Clp-ATPase/ClpP complex for accelerated proteolysis. Under revision.

Thomy*, D., **Reinhardt*, L.**, Sass, P. & Brötz-Oesterhelt, H. A ClpP homologue from *Streptomyces hawaiiensis* mediates a novel resistance mechanism against ADEP antibiotics. In preparation. *contributed equally

Illigmann, A., Thoma, Y., Pan, S., **Reinhardt, L.** & Brötz-Oesterhelt, H. (2021). Contribution of the Clp protease to bacterial survival and mitochondrial homoeostasis. *Microb*. *Physiol*. In press.

Moreno-Cinos, C., Sassetti, E., Salado, I. G., Witt, G., Benramdane, S., **Reinhardt, L.**, Cruz, C. D., Joossens, J., Van der Veken, P., Brötz-Oesterhelt, H., Tammela, P., Winterhalter, M., Gribbon, P., Windshügel, B. & Augustyns K. (2019). *α*-Amino Diphenyl Phosphonates as Novel Inhibitors of *Escherichia coli* ClpP protease. *J. Med. Chem.*, 62 (2), 774-797. doi: 10.1021/acs.jmedchem.8b01466

10. Acknowledgements

First of all i would like to thank Prof. Dr. Heike Brötz-Oesterhelt for the opportunity to work in her laboratory in an excellent research environment on this fascinating and very complex project. In addition, I would like to thank Prof. Dr. Heike Brötz-Oesterhelt for her support and feedback during this time and simultaneously giving me the space to work on this project independently. I also want to express my gratitude for giving me the chance to visit many conferences and symposia.

Furthermore, I thank Prof. Dr. Karl Forchhammer for the possibility to be a part of the research training group (RTG 1708), thereby having access to attend courses and symposia and for the opportunity to give and practice talks in a familiar working environment.

Special thanks to Dr. Peter Sass for always having an open door and helping me out with his knowledge and constant support. Espacially I would like to thank Dr. Peter Sass for correcting my paper draft and giving me insights how to prepare figures and papers in great detail. Peter, I learned a lot from you!

Many thanks to the whole "7th floor lab" Dhana, Nadine, Stefan, Astrid and Cruz for funny times and always a good laugh at work and during coffee breaks as well as fruitful discussions on scientific and non-scientific topics. Especially, I would like to thank Dr. Dhana Thomy who worked on the *in vivo* part of this project, for her critical discussions and opinions on this great topic.

Lots of thanks to my dear friend Astrid Illigmann for her constant support and motivation throughout the past years!

For proofreading my thesis, i want to give great thanks to Astrid, Chris, Domenico and Anna.

Additionally, I would like to thank all past and present members of the whole working group for a great time at work and beyond work at Christmas parties, conferences, celebrating birthdays with coffee and cake and great times on the dance floor!

Schließlich möchte ich mich bei meinen Eltern für ihre bedingungslose Unterstützung in all den Jahren bedanken, ebenso bei meiner Schwester Anna, die einfach immer für mich da ist. Außerdem möchte ich mich bei Anna, Henning, Steffen und Domi bedanken, die mir über die Jahre immer ein großer Ausgleich waren!

11. Contribution

Dr. Markus Lakemeyer performed during his time in the working group of Prof. Stephan Sieber, TU munich, intact protein mass spectrometry of the Clp peptidases ClpP1 and ClpP2 from *S. hawaiiensis*. The summarised results can be seen in Figure 6.4 and 6.5 in the appendix.

12. Erklärung

Ich erkläre hiermit, dass ich die zur Promotion eingereichte Arbeit mit dem Titel: *Functional characterisation of the ClpP1P2/Clp-ATPase complex of the ADEP producer Streptomyces hawaiiensis NRRL 15010 in vitro and elucidation of self-resistance mechanism* selbständig verfasst, nur die angegebenen Quellen und Hilfsmittel benutzt und wörtlich oder inhaltlich übernommene Stellen (alternativ: Zitate) als solche gekennzeichnet habe. Ich erkläre, dass die Richtlinien zur Sicherung guter wissenschaftlicher Praxis der Universität Tübingen (Beschluss des Senats vom 25.5.2000) beachtet wurden. Ich versichere an Eides statt, dass diese Angaben wahr sind und dass ich nichts verschwiegen habe. Mir ist bekannt, dass die falsche Abgabe einer Versicherung an Eides statt mit Freiheitsstrafe bis zu drei Jahren oder mit Geldstrafe bestraft wird.

Ort, Datum

Unterschrift